Interaction of HIF and USF Signaling Pathways at Human Genes Flanked by Hypoxia-response Elements and E-box Palindromes

---

Dissertation
zur
Erlangung der naturwissenschaftlichen Doktorwürde
(Dr. sc. nat.)

vorgelegt der
Mathematisch-naturwissenschaftlichen Fakultät

der

Universität Zürich

von

Junmin Hu

aus der V.R. China

Promotionskomitee

Prof. Dr. Max Gassmann (Vorsitz)
Dr. Thomas A. Gorr (Leitung der Dissertation)
Prof. Dr. Michael Hengartner
Dr. Gieri Camenisch

Zürich, 2010

Table of Contents

1 Abbreviations

AhR	Aryl hydrocarbon receptor
ARNT	Aryl hydrocarbon receptor nuclear translocator
bHLH	basic helix loop helix
BNIP3	Bcl2/adenovirus EIB 19kD-interacting protein 3
ChIP	Chromatin immunoprecipitation
CREB	Cyclic-AMP response element
DCT	Dopachrome tautomerase
EGF	Epidermal growth factor
EMSA	Electrophoretic mobility supershift assay
ENO-1	Enolase-1
EPO	Erythropoietin
FIH-1	Factor inhibiting HIF-1
GADD45a	Growth arrest and DNA-damage-inducible, 45alpha
GAPDH	Glyceraldehyde-3-phosphate dehydrogenase
GLUT-1	Glucose transporter-1
HIF-1	Hypoxia inducible factor-1
HRE	Hypoxia response element
LDHA	Lactate dehydrogenase A
L-PK	L-type pyruvate kinase
MC1R	melancortin 1 receptor
MEFs	Mouse embryonic fibroblasts
MITF	microphthalmia-associated transcription factor
MPTP	mitochondrial permeability transition pore
ODD	Oxygen-dependent degradation domain
PAI-1	Plasminogen activator inhibitor type-1
PDK1	Pyruvate dehydrogenase kinase 1
P4Hα(I)	Prolyl-4-hydroxylase α (I)
PHD	Prolyl hydroxylase domain containing
PI3K	Phosphatidylinositol 3-kinase
PGK	Phosphoglycerate kinase
pO_2	Oxygen partial pressure
POMC	Pro-opiomelanocortin
pVHL	Von Hippel-Lindau tumor-suppressor protein
qPCR	real-time quantitative PCR
ROS	Reactive oxygen species
shRNA	short hairpin RNA
TAD	Transactivation domain
TERT	Telomerase reverse transcriptase
TRP-1	Tyrosinase-related-protein 1
TYR	Tyrosinase
USF	Upstream stimulatory factor
VEGF	Vascular endothelial growth factor

2 Summary

Deprivation of oxygen is a main characteristic of solid human tumors. It was discovered in the 90's that a novel transcription factor termed Hypoxia Inducible Factor 1 (HIF-1), α subunit (HIF-1α) gradually accumulated during markedly reduced oxygen partial pressures (pO_2), a state otherwise known as hypoxia. So far, the heterodimeric HIF-1 α/β-complex has been implicated in targeting more than 70 genes involved in cell metabolism, cell cycle and proliferation, apoptosis and angiogenesis. As a consequence, HIF-1 is instrumental in promoting tumor growth and survival in most experimental models. To date, control of the HIF pathway via the O_2-requiring hydroxylations of specific alpha-subunit proline and asparagine residues, leading to the factors' ubiquitylation and proteasome catalyzed degradation and suppressing its interaction with vital co-activator proteins in (re)oxygenated cells, respectively, is relatively well understood. In contrast, much remains to be discovered in regard to critical oxygen-independent controls that also impinge on HIF-1 signaling in tumor cells.

A previous study had documented the binding of HIF-1 to two of three hypoxia response cis-elements (HREs) within the promoter of the globin-2 gene of *Daphnia magna* (phb2), as a strict requirement for the reporter's maximal hypoxic activation in transfected hepatoma (Hep3B) cancer cells. However, binding of an unknown and constitutive transcription factor to the third phb2 motif, a CACGTG E-box palindrome, in human hepatoma cells (Hep3B), significantly weakened the HIF/HRE-mediated hypoxic induction. This observation suggested that CACGTG-complexes might function to fine-tune or inhibit HIF-driven gene responses in cancer cells and prompted a two-fold objective for the present work: *a) was to identify this CACGTG-binding transcription factor in different human cancer cells, and b) to study the co-regulation of human genes through HIF-1 and this CACGTG-mediated signaling pathway in vitro and in vivo.*

As a first step of this PhD thesis, gel supershift and oligonucleotide pull-down assays were used and consistently and reproducibly identified the basic-helix-loop-helix/leucine zipper (bHLH/ZIP) upstream stimulatory factors 1 and 2 (USF1 and 2) as the major phb2 CACGTG binding factors in human hepatoma cells (Hep3B), human cervical carcinoma cells (HeLa) and human breast carcinoma cells (MCF7). Next, a genome-wide computational scan for *human* HRE/E-box promoters, i.e. those containing the CACGTG palindrome adjacent to or overlapping with a HRE, was carried out and retrieved with lactate dehydrogenase A

(LDHA), Bcl2/adenovirus E1B 19kD-interacting protein 3 (BNIP3), 4E-binding protein 1 (4EBP1) and vascular endothelial growth factor C (VEGFC) etc. as known hypoxia targets. Having verified the human-mouse-rat conservation of this HRE/E-box constellation with regard to the following selected HRE/E-box genes, we either received as generous gifts (BNIP3) or generated ourselves (LDHA, 4EBP1 and melanocortin 1 receptor MC1R) HRE/E-box promoter luciferase reporter plasmids, along with HIF-1 (i.e. prolyl hydroxylase domain 2 PHD2) or USF-specific (i.e. tyrosinase TYR) reporter controls, to systematically investigate the interaction of HIF-1 and USF pathways at DNA level.

Of these four HRE/E-box candidate genes only LDHA and BNIP3 reporter revealed a prominent hypoxia-mediated up-regulation in Hep3B, HeLa and MCF7 cells. Towards the co-regulation of LDHA and BNIP3 promoters by HIF-1 and USFs, co-overexpression of HIF-1α and USF plasmids revealed a significant attenuation of the HIF-dependent hypoxic up-regulation of the BNIP3 luciferase reporter by exogenous USF1 and 2a in Hep3B and HeLa cells. Similarly, the endogenous HIF-dependent hypoxic induction of LDHA was significantly reduced by over-expressed USF1 and 2a in MCF7 cells. To further evaluate the specificity of the expression manipulation of either HIF or USF on this regulation of LDHA reporter, a stable USF2a knockdown MCF7 clone was generated by short-hairpin RNA (shRNA) technology while a stable HIF-1α knockdown MCF7 clone was kindly provided to us by Dr. D. Stiehl (group of Prof. R. Wenger, University Zurich).

Luciferase assay in these stable MCF7 knockdown clones revealed a reduction of LDHA promoter activity upon silencing of USF2a transcription cells and an independent transactivation of LDHA promoter by HIF-1 and USF cascades. We also confirmed the competitive effect on the BNIP3 regulation by HIF-1α and USFs signaling in Hep3B cells by transiently silencing HIF-1α, USF1 or USF2a expression through specific siRNAs. The following luciferase assay revealed for the USF1 knockdown a significantly increased hypoxic activity of the BNIP3 promoter reporter.

In vivo binding of HIF and USF within the promoters of LDHA and BNIP3 was shown by chromatin immunoprecipitation (ChIP) assays for Hep3B, HeLa and MCF7 cells. Regarding the BNIP3 promoter, the ChIP assay revealed chief occupancy in deoxygenated cells by HIF-1 along with the weak and constitutive attachment of USF1 and 2a to this DNA. Remarkably, some HIF-1α had successfully escaped proteolytic degradation since we detected it bound, as heterodimer, to the BNIP3 promoter even in normoxic cells. The native LDHA promoter (region: -2533/-2376 from translation start site) was dominated by bound HIF-1 in hypoxic MCF7 cells, while USF1 and USF2a co-occupied this regulatory DNA

during periods of normoxia (Hep3B, MCF7). The latter finding implied upstream stimulatory factors as physiological drivers of aerobic glycolysis in cancer cells (Warburg effect). We also noted that during hypoxia, both USFs maintained their association with this DNA, which offers additional support of the notion that maximal LDHA transcription during low pO_2 arises from the cooperative transcriptional control by HIF-1 and USF1/2a.

Additional gel supershift assays mapped the exact *in vitro* HIF-1 and USF binding sites within the promoter of LDHA to the CACGTG motif (-2465/-2460; HIF-1 and USFs), the CACGTG palindrome at -2367/-2362 (USFs only) and the GACGTG HRE at -2353/-2345 (HIF-1 only). Thus, distinct binding sites in the LDHA promoter might facilitate the independent transactivation of the gene by both signaling pathways. In contrast, HIF-1 and USFs were found to have either identical or overlapping binding locations within the DNA surrounding the -251/-246 HRE in the BNIP3 promoter, again in line with a mutually displacing, competitive mode of interaction at DNA level.

Currently, I am extending this study to human melanoma cells, since in these cells HIF-1 and USF pathways are induced by physiological stimuli, i.e. hypoxia and tanning-response conferring ultraviolet radiation, respectively. This will allow to examine the response of co-regulated BNIP3 and LDHA promoters in melanoma cells that have been subjected to hypoxia plus UV dual stimulation.

3 Zusammenfassung

Eine negative Bilanz zwischen der Sauerstoffversorgung und dem Sauerstoffverbrauch ist ein klinisch signifikantes Charakteristikum der meisten bösartigen Tumore. Die resultierende O_2-Mangelsituation (Hypoxie), die sich lokal im Tumorgewebe ausbilden kann, wird von den Zellen primär durch einen Transkriptionsfaktor registriert. Dieser Hypoxie-induzierbare Faktor 1 (HIF-1) wird bei reduziertem Sauerstoffpartialdruck (pO_2) aktiviert und kann DNA in Form eines, aus einer α und β Untereinheit bestehenden, heterodimeren Komplexes binden. Erwiesenermassen kontrolliert HIF-1 in hypoxischen Zellen die Transkription von mehr als 70 Genen. Das veränderte Abschreiben dieser Zielgene zieht zelluläre Anpassungen innerhalb des Stoffwechsels, Zellzyklus, Apoptose und Angiogenese nach sich. In den meisten Tumormodellen fungiert ein aktiver HIF Signalweg daher als Protagonist von zellulärem Wachstum, Hypoxietoleranz, Metastaseneigung und Therapieresistenz. Dank jüngerer Arbeiten ist die O_2-abhängige Kontrolle von HIF-1 und dem nahe verwandten HIF-2 Komplex relativ gut verstanden. Von zentraler Bedeutung für diese Kontrolle sind enzymatische Hydroxylierungen einzelner Proline und Asparagine in den HIF-1α und HIF-2α Untereinheiten. Als Folge dieser Signale werden bei einem pO_2 Anstieg beide HIF-α Faktoren nicht nur transkriptionell inaktiviert, sondern auch ubiquitinyliert und proteolytisch abgebaut. Diese O_2-verbrauchenden post-translationalen Hydroxylierungen von HIF-1α/-2α bedingen, dass in normoxischen oder re-oxygenierenden Zellen der HIF Signalweg sehr schnell zum Erliegen kommt. Für eine effektivere Bekämpfung von HIF in einem chronisch desoxygenierten Milieu, müssen jedoch auch die Hydroxylierungs-unabhängigen Kontrollen dieses Signalwegs noch eingehender erforscht und therapeutisch einbezogen werden.

Eine frühere Arbeit befasste sich mit der hypoxisch-induzierbaren Expression von Globingenen, insbesondere des hb2 Gens, in dem planktonischen Süsswasserkrebs („Wasserfloh“) *Daphnia magna*. Im Rahmen sogenannter heterologer Transfektionen von humanen Hepatomazellen (Hep3B Zellen) wurde festgestellt, dass die kooperative Bindung von HIF-1 an zwei von drei funktionellen HIF-1 Bindungsstellen (hypoxia-response element, HRE) im Promoter von hb2 (phb2) für die maximale hypoxische Induktion eines vom Promoter abgeleiteten Luziferase (LUZ) Reportergen Plasmids unbedingt erforderlich war. Ein O_2-unabhängiger (konstitutiver) Faktor hingegen interagierte mit der dritten Bindungsstelle, einem CACGTG Palindrom, im phb2/LUZ Konstrukt. Nach seiner Bindung

an das Palindrom war der CACGTG Komplex in der Lage die HIF/HRE-vermittelte Aktivierung des *Daphnia* phb2 Reportergens deutlich zu schwächen. Möglicherweise liegt die Funktion dieses CACGTG-Komplexes in Hep3B Zellen in der Feinregulierung der durch HIF-1 gesteuerten Genaktivität. *Ziel der vorliegenden Arbeit war es daher diesen unbekannten Bindungskomplex in verschiedenen Krebszelllinien zu identifizieren und die Regulation humaner Gene als Folge der Wechselwirkung von HRE- und CACGTG-Komplexen zu untersuchen.*

Zur Identifikation des unbekannten Faktors kamen electrophoretic mobility shift assays (EMSA) und Oligonukleotid Pull-down Techniken zum Einsatz. Upstream Stimulatory Faktor 1 und 2 (USF1, USF2), ihrerseits Mitglieder der bHLH-leucine zipper (bHLH/ZIP) Transkriptionsfaktorfamilie, konnten als die primären, phb2-CACGTG bindende Faktoren in menschlichen Hepatoma- (Hep3B), Zervikalkarzinom- (HeLa) und Brustkarzinomzellen (MCF7) identifiziert werden. Zur weiteren Übertragbarkeit dieser Befunde auf menschliche Tumorzellen, wurde ein bioinformatischer Screen des humanen Genoms durchgeführt, um sogenannte HRE/E-box Genkandidaten zu erfassen. Humane HRE/E-box Gene tragen, phb2-ähnlich, CACGTG-Palindrome und HIF-bindende HREs unmittelbar benachbart in ihrem Promoter. Mehrere bekannte Hypoxie Zielgene waren unter den HRE/E-box Kandidaten, u.a.: Laktat Dehydrogenase A (LDHA), 4E-bindendes Protein 1 (4EBP1) und der vaskuläre endotheliale Wachstumsfaktor C (VEGFC). Die jeweiligen Palindrom und HRE Motive sind in den Promotoren der homologen Mensch-, Maus- und Rattengene sämtlich konserviert und damit von wahrscheinlicher Funktionalität. Nach erfolgter Klonierung dieser HRE/E-box Promotoren als LUZ Plasmide (i. LDHA; ii. 4EBP1; iii. Bcl2/adenovirus E1B 19kD-interagierendes Protein 3, BNIP3; iv. Melanocortin 1 Rezeptor, MC1R), untersuchte eine erste Serie von Reportergen Transfektionen die Hypoxie-vermittelte Induktion sämtlicher HRE/E-box Konstrukte in Hep3B, HeLa und MCF7 Zellen. Niedrige Sauerstoffkonzentrationen (1% O_2/16h) aktivierten von den getesteten Plasmiden lediglich die LDHA und BNIP3 Reporter in allen drei Zelllinien. Bezüglich einer HIF/USF-Ko-Regulation von LDHA- und BNIP3-Promotoren, wurden HIF-1α, USF1 und 2a in Hep3B, HeLa und MCF7 Zellen überexprimiert. Diese Ko-Transfektionen zeigten, dass die HIF-1α-abhängige hypoxische Erhöhung der BNIP3-Promotor-Aktivität signifikant durch exogenes USF1 und USF2a, nicht aber durch USF2b, abgeschwächt wurde. Ferner unterdrückte die Überexpression USF1/2a in MCF7 Zellen die endogene hypoxische Induktion von LDHA.

Um die spezifischen Einflüsse von HIF-1 oder USF1/2a auf ein HRE/E-box Konstrukt unabhängig von Überexpressionen zu prüfen, wurden stabile USF2a und HIF-1α shRNA

knockdown (kd) Klone in MCF7 Zellen generiert. Der MCF7 HIF-1α kd Klon wurde uns freundlicherweise durch Dr. D. Stiehl (Gruppe Prof. Wenger, Univ. Zürich) überlassen. Die folgenden Luziferase-Versuche zeigten, dass die Aktivität des LDHA-Promoters in kd USF2a Klonen unter Normoxie reduziert war und dass die HIF-1 und USF Kaskaden im LDHA-Promoter größtenteils unabhängig voneinander agierten. Umgekehrt bestätigten Versuchsreihen mit transientem (siRNA basierenden) knockdown von HIF-1α, USF1 und USF2a in Hep3B Zellen die Kompetition beider Signalwege auf Ebene des BNIP3-Promoters. Die hypoxische Aktivität des BNIP3 Reportergens war signifikant in Hep3B Zellen erhöht, die mit siRNAs gegen USF1, nicht aber gegen USF2a, transfiziert wurden.

Um sicher zu stellen, dass die HIF-1 und USF1/2a Signalwege auch unter physiologischen Bedingungen auf die Bindungsstellen im LDHA- und BNIP3-Promotor konvergieren, wurden Chromatin Immunopräzipitation- (ChIP) und EMSA-Experimente durchgeführt. Diese Arbeiten zeigten für BNIP3, dass USF1 und 2a schwach und konstitutiv an dieselbe Stelle, die schon als funktionelle HRE erkannt wurde, binden können. Interaktion von HIF-1 mit der BNIP3 HRE war der dominierende Einfluss in hypoxischen Zellen. Allerdings wurde HIF-1, gebunden am BNIP3 Promoter, auch in normoxischen Kernen detektiert. Ferner binden HIF-1, USF1 und USF2a unter physiologischen Bedingungen an den LDHA Promoter (ChIP-Daten). Während die regulatorischen LDHA Elemente unter hohem pO_2 vornehmlich durch USF1/2a besetzt waren, überwog der HIF-1 Besatz in hypoxischen Zellen (MCF7). Die USF Faktoren behielten allerdings ihre Bindung am LDHA Promoter auch unter Hypoxie bei, was gegen eine Verdrängung durch HIF-1 spricht und einen weiteren Nachweis für die unabhängige HIF/USF Bindung an die LDHA Motive liefert. Die EMSA-Versuche zeigten, dass HIF-1 und USF1/2a vornehmlich an ihre eigenen cis-Elemente im LDHA Promoter binden, d.h. hier, relativ zum BNIP3 Gen, nur eine schwache Konkurrenz zwischen HIF/HRE und USF/Palindrom Komplexen vorherrscht. Allem Anschein nach korreliert die Präsenz individueller Bindungsstellen mit der größtenteils unabhängigen Konvergenz von HIF-1 und USF Signalwegen auf das LDHA Gen. Demgegenüber resultiert aus der Konkurrenz von HIF-1 und USFs um eine gemeinsame Bindungssequenz im BNIP3 Promoter die dargestellte negative Wechselwirkung beider Signalwege auf Genebene.

In fortlaufenden Experimenten in humanen Melanoma Zellen wird zurzeit die Ko-Regulation der LDHA- und BNIP3-Expression durch HIF-1 und USFs durch strikt physiologische Stimuli (Hypoxie → HIF-1; UV → USFs) erforscht.

4 Introduction

4.1 Tumor hypoxia

Landmark studies by Gray *et al.* and Thomlinson and Gray in the 1950s established the direct link between radio-sensitivity and oxygen tension in tumor tissue, thereby initiating the area of research around the many aspects of tumorigenesis that are mediated and accelerated by deprivation (hypoxia) or complete lack (anoxia) of oxygen [1, 2]. Generally speaking, hypoxia occurs when the ambient oxygen partial pressure (pO_2) has fallen to or below the level required to maintain minimal aerobe activity in an organism, tissue or cell. It is the cells' own specific critical oxygen threshold (pC) which separates the aerobe-oxyregulated ($pO_2 > pC$) from the anaerobe-oxyconforming ($pO_2 < pC$) physiological state. Thus, cells or tissues are hypoxic at *specific* $pO_2 < pC$ levels of oxygenation and *not* at some stereotypically applicable numerical oxygen concentration. Common responses to such level of oxygen scarcity include the switch from aerobe to anaerobe metabolism, and from oxyregulated (i.e. O_2 consumption rate is more or less constant across a wide range of pO_2) to oxyconforming respiration (i.e. O_2 consumption rate declines in direct proportion with falling pO_2).

During the five decades following Thomlinson's and Gray's pioneering work, radio-biologically effective degrees of hypoxia (i.e. pO_2 measures ≤ 5 mmHg (~0.7% O_2; 7.35 mmHg ≅ 1% O_2) have been firmly documented in most solid tumors, including brain, lung, breast, pancreatic, cervical, prostate, and head and neck cancer [3-6]. In comparison, median pO_2 data of many normal tissues lie between 40-50mmHg and demonstrate excellent homeostatic control when switching from a resting to an actively working physiological state (e.g. skeletal muscle). It is now understood that, as tumors evolve from a single malignant cell into a multi-cellular mass, oxygen tension and nutrient delivery in the tumor microenvironment drops as the passive diffusional capacity of the existing blood supply is surpassed. Assuming typical values for intracapillary oxygen tensions and oxygen consumption rates, the oxygen diffusion distance in tissue approximately corresponds to 150 μm [7]. Up until this 150 μm distance from the nearest capillaries, O_2 diffuses in form of a gradient. Beyond this distance, necrotic cells tend to amass. Thus, tumor hypoxia develops along this gradient due to the mismatch between high oxygen demands of deregulated growth on the one hand and inadequate nutrient supply via abnormal vessels, erratic blood flow and deteriorating diffusion geometry (vessel-necrosis distance > oxygen diffusion radius) on the

other [3-6]. This high demand-low supply imbalance is responsible for the hostile microenvironment in solid tumors, as is characterized by deprivation of oxygen and nutrients (i.e. ischemia), low extra-cellular pH and reduced growth factor availability [8]. Intra-tumoral O_2 depletion is a powerful stimulus of angiogenesis for a large variety of survival responses (next paragraph). As a result of these cellular adaptations to low oxygen levels, presence of tumor hypoxia frequently associates with a decreased efficacy of many conventional therapies and the emergence of a more virulent, metastasis-prone neoplastic variety of cells.

The genetic or epigenetic changes, that enable cancer cells to adapt to hypoxia commonly comprise acquisition of [9]: 1) self-sufficiency from growth factor signals due to over-expression or dysfunction of various growth factor receptors and/or gained insensitivity to anti-proliferative signals; 2) genetic instability with subsequent selection of more aggressive, therapy-resistent cell clones [10]; 3) increased capacity of cell survival and apoptotic evasion via dysregulation of the apoptotic machinery [11]; 4) sustained angiogenesis by altering the balance between pro- and anti-angiogenic signals, and in particular, by exhibiting increased expression of the pro-angiogenic vascular endothelial growth factor (VEGF) [12, 13]; 5) invasive and metastatic behavior owing to the activation of extra-cellular proteases and altered binding specificities of cadherins and intergrins [14, 15]; 6) unlimited replicative and proliferative potential due to telomere maintenance via up-regulated expression of the telomerase components; 7) increased reliance on glucose uptake and glycolytic ATP production via up-regulation of glucose-transporters genes encoding of glycolytic enzymes [16]; and 8) hypoxia tolerance through ability to slow down or arrest ATP costly macromolecular synthesis and cell cycling processes during periods of O_2 and nutrient depletion [17-20].

Several hypoxia-sensitive transcription factors have been described [21], like hypoxia-inducible transcription factor-1,-2 (HIF-1, 2), metal transcription factor-1 (MTF-1) [8], nuclear factor κB (NF-κB) [22], c-Fos and c-Jun (AP-1) [23], E26 transformation-specific sequence-1 (ETS-1) [24], Specificity protein-1 (SP-1) [25, 26], CCAAT enhancer-binding protein β (C/EBPβ) [27, 28] and early growth response-1 (EGR-1) [29-31]. Of these, HIF-1 and -2 are considered key transcriptional regulators of hypoxia-responsive genes in both primary and neoplastically transformed cells. Immunohistochemical studies of tumor biopsies indicate that HIF-1α and -2α are over-expressed in multiple human cancers, malignancies including carcinomas of the lung, colon, brain, prostate, breast, skin and so on. In contrast, in normal and oxygenated tissue, as well as benign, noninvasive growths either of these proteins remains undetectable. Consequentially, many clinical reports of HIF-1/-2 expression levels in

cancers find them to be strong and independent markers for poor treatment and survival prognoses [32-34].

4.2 Hypoxia-inducible factor overview

First documented in 1988, the stimulatory influence of hypoxia on certain genes was decisively shown with the induced synthesis of human erythropoietin (EPO), the hormone which stimulates red blood cell production during periods of diminished oxygen supply [35]. Subsequent work elicited the existence of a hypoxia-inducible enhancer region 3' to the human EPO gene and, furthermore, unearthed the existence of a functional hypoxia-responsive element (HRE) contained within the 3' sequence. The HRE was required for the hypoxia-mediated transcription of EPO [36]. Affinity-chromatography utilizing an immobilized EPO HRE-containing oligonucleotide led Wang and Semenza in 1995 to eventually isolate from human cancer cell extracts the hypoxia-inducible factor-1 (HIF-1) as the EPO-HRE binding protein constituent [37, 38].

4.2.1 Structure of hypoxia-inducible factors

Transducing minutes to hours of hypoxic pO_2 onto the level of DNA is chiefly accomplished by HIFs. In mammalian cells, several hundred potential [39] and more than 70 validated hypoxia-responsive gene targets of HIF have been identified [40]. Across the animal kingdom, HIF signaling is highly conserved down to the smallest molecular details [19, 41, 42]. Considerable progress has also been made in understanding the molecular basis of HIF and its regulation by oxygen [43, 44]. From mammals to teleosts, *Drosophila*, the crustacean *Daphnia magna*, and the nematode *Caenorhabditis elegans*, the HIF complex functions as heterodimer of homologous α-subunits and β-subunits which both belong to the family of basic helix-loop-helix (bHLH)/PER-ARNT-SIM homology (PAS) transcription factors [19, 41, 42]. To date, three different oxygen-dependent HIF α subunits (HIF-1α, -2α and -3α) have been reported in mammals. All three alpha subunits can heterodimerize with the constitutively present HIF β subunit (also known as aryl hydrocarbon receptor nuclear translocator (ARNT)). HIF-α and ARNT factors have similar structural domains, including N-terminal domains required for DNA binding (basic region) and protein-protein interaction (HLH domain and PAS-A and PAS-B repeats). Domains in the central reading frame and towards the C-terminal end are implicated in controlling stability of HIF-1α and -2α subunits (oxygen dependent degradation domain, ODD) and the transactivating competence of the factor (C-terminal transactivation domain, TAD-C). The ODD of HIF-1α/-2α also contains

the so-called N-terminal transactivation domain (TAD-N). HIF-3α and ARNT exhibit only one transactivation domain and due to the lack of ODD-like sequences, both proteins are rendered stable during normoxic conditions (Fig.1) [44].

Regulation of HIF by oxygen occurs, in cultured cells at least, at protein level, primarily through enzymatic hydroxylation of specific α subunit prolyl and asparaginyl residues (Fig. 1). The *in vitro* transcription of HIF-1α/-2α genes usually does not exhibit any significant O_2-dependence. In contrast, some, though not all [45], studies reported a marked induction of HIF-1α mRNA during low pO_2 in several human and mouse tissues [46, 47].

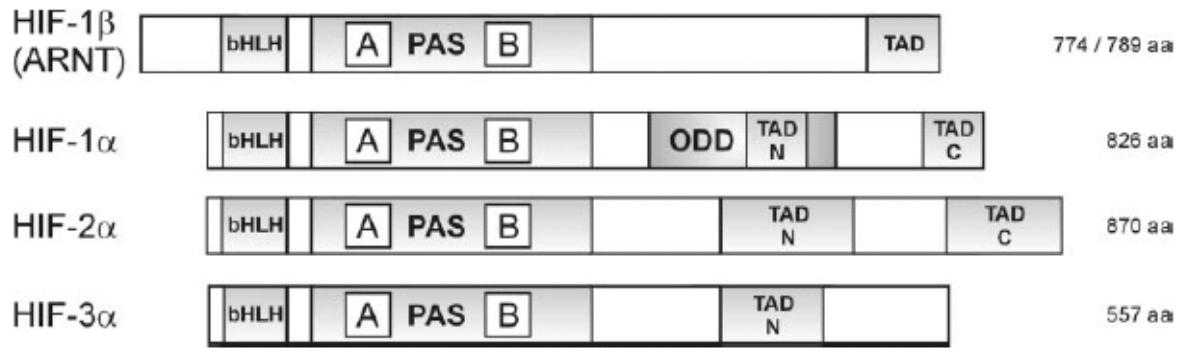

Figure 1 Isoforms of hypoxia-inducible factor (HIF)-1α, 2α, 3α and 1β. bHLH: basic helix-loop-helix; PAS:Per-ARNT-Sim; TAD: transactivation domain; ODD: oxygen-dependent degradation domain. [44]

4.2.2 HIF-1 signaling pathways

At protein level, the most important degradation pathway operates through the hydroxylation of two proline residues embedded in the ODD of HIF-1α and HIF-2α when O_2 is sufficiently available. The efficacy of this control mode is mirrored by the <5 min half-life of HIF-1α upon re-oxygenation [48] and an instantaneous hypoxic induction of the transcription factor [49]. The long sought after HIF oxygen sensors, so-called prolyl hydroxylase domains 1-3 (PHD1-3) dioxygenases, control the abundance of either HIF-α protein during high or rising pO_2. As hallmark achievements in hypoxia research, these three HIF-prolyl hydroxylases were discovered and cloned in 2001 by several leading laboratories [50-53]. According to their data, PHDs catalyze in the presence of oxygen and 2-oxoglutarate, the Fe(II)-dependent hydroxylation of two distinct ODD proline residues, i.e. Pro^{402} and Pro^{564}, in human HIF-1α, and Pro^{405} and Pro^{531} in human HIF-2α (Fig. 2) [43, 54]. Further support of the current sensing paradigm stems from hypoxia-mimicking agents such as iron chelators (e.g. desferrioxamine, DFO) or transition metals such as cobalt. Incubation of cells in non-toxic micromolar concentrations can either scavenge (DFO) or perhaps substitute (Co) the catalytic iron of PHDs, hence resulting in the inhibition of PHD catalysis. PHD activity

can be also inhibited by some physiological substrates such as succinate and fumarate, two components of TCA cycle. Accumulations of succinate and fumarate in tumors with loss-of-function mutations in succinate dehydrogenase (SDH) and fumarate hydratase (FH)- subunits yielded HIF-1 stabilization in a pseudo-hypoxia environment [55, 56]. A reduction in the HIF-1α hydroxylation under hypoxic conditions, and the genetic loss-of-function impact on HIF stability of the *C. elegans* PHD homolog Egl-9 [51], provided the final proof that the PHDs function as HIF oxygen sensors, from "worm to man". The PHD/HIF hypoxia sensing axis is further complemented by the von Hippel Lindau tumor suppressor protein (VHL), whose function lies in recognizing hydroxylated HIF-α subunits and linking them to a proteolytic degradation machinery.

Evidently, prolyl hydroxylation is the oxygen-regulated step governing ubiquitination and proteasomal degradation of HIF-1α/-2α. At center stage of this process is VHL, a component of E3 ubiquitin-ligase complex, which mediates the recruitment of accessory factors, like elongin C, elongin B, cullin 2 and RBX1 to bound (=hydroxylated) HIF-α subunits [57]. The complete E3 ligase assembly will then interact with E1 ubiquitin-activating and E2 ubiquitin-conjugating enzymes, thus mediating ubiquitin-tagging of the index protein (in this case HIF-α) and initiating its subsequent degradation in the 26S proteasome [52, 58, 59]. Consequently, VHL loss of function lesions in renal carcinoma (RCC) or in VHL hereditary cancer syndrome results in an increase in HIF-1α/-2α protein levels in non-hypoxic cells due to the block in the ubiquitylation and proteasomal degradation of either substrate protein [60]. Similarly, proteasomal inhibitors (MG132), a mutation of the ubiquitin-activating enzyme E1, or inhibition of PHDs by pharmacological (e.g. dimethyloxaloylglycine, DMOG) small molecular weight compounds, all cause the stabilization of HIF-α proteins under normoxic or re-oxygenating conditions which switch the inducible pathway into a constitutively active cascade [61, 62].

Additional VHL-mediated HIF-1 degradation is triggered upon acetylation of HIF-1α Lys^{532} which is also located in the ODD domain. Lys^{532} is acetylated by an acetyltransferase called arrest-defective protein 1 (ARD1). This post-translational modification facilitates the interaction of HIF-1α with VHL and leads to HIF-1 degradation. Although activity of ARD1 is not directly affected by oxygen concentration and its catalysis operates in an oxygen-independent manner, it was reported that mRNA and protein level of ARD1 decrease under hypoxia. It suggested that low oxygen might lead to less acetylated HIF-1. To date, however, the relevance of HIF-1α acetylation, and the role of ARD1 in particular, in hypoxic signaling are highly controversial issues [63].

The TAD-C domain is required for the transactivation of HIF-1 or HIF-2 by means of recruiting and interacting with the co-activator p300 and CREB binding protein (p300/CBP) with either alpha subunit. A second O_2-requiring hydroxylation modifies an asparagine within the TAD-C domain of HIF-1α (Asn^{803}) or HIF-2α (Asn^{851}) under aerobic pO_2. This reaction is carried out by the asparaginyl hydroxylase factor inhibiting HIF (FIH). Hydroxylation of the TAD-C Asn residue prevents the recruitment of co-activator and histone acetyltransferase p300/CBP, thereby leading to the suppressed transcriptional activation of HIF target genes under high oxygen [64, 65]. Unlike the proline modification, the hydroxylation of the TAD-C Asn residue catalyzed by FIH in the presence of oxygen culminates in the inhibited transcriptional activity of HIF-1α or -2α without altering the protein levels. It does become clear, however, that oxygen impinges on HIF signaling twofold, by controlling both the abundance and transcriptional activity of the factors sensory alpha subunits.

The fact that HIF's maximal signaling activity specifically occurs during low pO_2 and declines towards both normoxic and anoxic concentrations of oxygen is the combined result of strikingly low oxygen affinities of the PHD and FIH-1 sensor proteins together with a pronounced hypoxia-driven transcriptional induction of some of the sensor genes (i.e. PHD2, PHD3). The *in vitro* and apparent K_M (of short HIF-1α peptide substrates) values for oxygen of ~64 mmHg (FIH-1) and 178 mmHg (average for PHD1-3) imply that HIF hydroxylases operate *in vivo* at pO_2 levels far below their K_M values [66, 67]. Thus, the oxygen affinity of the PHD enzymes actually lies above the concentration of dissolved oxygen in air, which means that the availability of oxygen is predicted to be limiting for activity of HIF hydroxylases over the entire physiological range. The K_M data are therefore consistent with the enzymes function as *bona fide* sensors of graded levels of oxygen. Moreover, the HIF-mediated hypoxic up-regulation of PHD2 and 3 gene expression [68] prepares for the rapid destruction of HIF-α subunits following reoxygenation [69], and enables PHD enzymes, due to their increased protein levels, to stay operative even under low pO_2 conditions [70]. This negative feedback loop not only limits the HIF response but also resets the hypoxia threshold by down-shifting the HIF set point towards further O_2 depletion [70]. Conversely, cells grown in high [O_2] reset their HIF set point upward through the downregulation of PHD genes [71]. Thus, activation of the HIF system can adapt to hypoxia due to its flexible and perhaps tissue-specific O_2 thresholds. These thresholds are adjusted according to the previous cell exposure to low or high [O_2], and, in turn, are responsible to steadily hold the pathway responsive to varying tissue oxygenation.

Despite these various adjustments to extend the oxy-sensory function of HIF prolyl hydroxylases into hypoxia, once the cell faces pO_2 < pC degrees of hypoxia, and of course anoxia, the hydroxylation of prolyl and asparaginyl residues is sufficiently diminished to shift the equilibrium towards the transcriptionally active form of HIF. Due to inhibition of hydroxylation, enough HIF-1α and HIF-2α will escape proteolytic degradation and, following phosphorylation by various kinases and chaperoning through accessory factors, like heat shock protein 90 (HSP90), translocate into the nucleus. Here, the alpha subunits heterodimerize with HIF-1β/ARNT through intermolecular interactions between HLH and PAS domains. Next, the HIF-1/-2 heterodimer interacts with different transcriptional co-activators such as p300/CBP, SRC-1 and TIF2 [72-75] and initiates the hypoxia-triggered control of target gene expression by binding to the HRE(s) mostly from within the 5'or 3' flanks of the gene (Fig. 2).

A complete HIF-mediated transactivation pathway therefore includes HIF-1α/-2α post-translational phosphorylation events, nuclear translocation, heterodimerization with ARNT, recruitment of different co-activators, DNA binding and transcriptional up- or down-regulation of gene expression [76]. There are two main phosphorylation cascades which are known to regulate HIF-1 activity: one is conducted by the rather well characterized pathway of p42/p44 (Erk2/Erk1) mitogen-activated protein kinases (MAPKs) [77, 78]. The other is conducted through phosphatidylinositol (PI)-3-kinase (PI3K) signaling. Activation of PI3K represents an important stimulus of HIF-1α phosphorylation, which, subsequently can lead to an increased HIF-1 protein level [79]. However, PI3K signaling as motor for HIF-1 abundance was recently challenged by Arsham *et al.* [80]. Additionally, several growth factors, most notably insulin-like growth factor-2 (IGF-2) and transforming growth factor-α (TGF-α) are able to initiate autocrine signaling of HIF-1 through enhanced translation of the transcript [81].

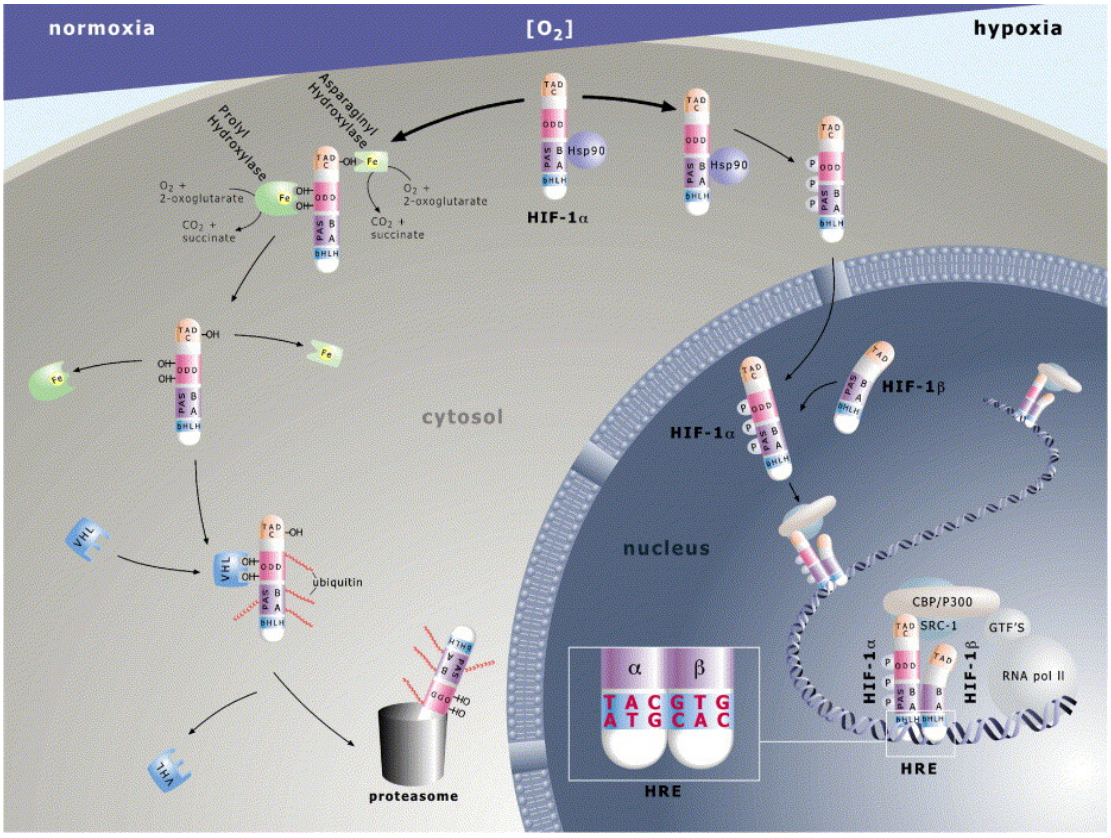

Figure 2 HIF-1 pathway. Under normoxia, hypoxia-inducible factor 1α (HIF-1α) is hydroxylated by prolyl hydroxylases at Pro^{402} and Pro^{564} within the ODD domain of HIF-1α. Subsequently, this hydroxylated HIF-1α is immediately bound by the von Hippel-Lindau tumor-suppression protein (VHL). VHL recruits elongin-B, elongin-C, CUL-2 and RBX-1 to the alpha subunit. This VHL/elongin-complex, together with ubiquitin-activating (E1) and ubiquitin-conjugating (E2) enzymes, mediates the ubiquitination of HIF-1α, resulting in its degradation via the proteasome. During hypoxia, the hydroxylation of HIF-1α is suppressed and HIF-1α becomes stable. This stabilized HIF-1α translocates into the nucleus, dimerizes with HIF-1β, recruits cofactors such as CBP/p300 and binds to hypoxia-responsive elements (HREs) to regulate gene expression in response to hypoxia (taken from [43]).

There are several stimuli known to trigger HIF-1 signaling even in non-hypoxic cells. Firstly, several growth factors, such as insulin, insulin growth factor 1 and 2 (IGF-1 and -2), epidermal growth factor and fibroblast growth factor, are known to stimulate HIF-1 expression which can lead to an enhanced proliferation rate of murine embryonic fibroblasts (MEFs) and embryonic stem (ES) cells [82]. Secondly, stimulation of vascular hormones, such as thrombin, can elevate HIF-1α protein level via the generation of reactive oxygen species (ROS) and the subsequent induction of PAI-1 and VEGF gene expression in human vascular smooth muscle cells (VSMC) [83]. Thirdly, it was also demonstrated that treatment of interleukin-1β (IL-1β) in normoxic human hepatoma cells (HepG2) increased HIF-1 protein level and caused a moderate activation of HIF-1 binding to the HRE of EPO [84]. Lastly, various viral proteins can increase both the stability transcriptional activity of HIF-1 and trigger intensified angiogenesis [85, 86].

4.2.3 HIF-1 target genes

Functional HIF binding sites, or HREs, are composed of mandatory consensus sequence 5'-VNVBRCGTG-3' (V=not T; N= any; B=not A; R=A or G). Through binding to such cis-elements, mammalian HIF-1 is known to control expression of more than 70 validated targets. These genes are involved in regulating oxygen supply, cell metabolism, energy expenditure, angiogenesis, cell growth and apoptosis [40] as summarized in Table 1 below.

Table 1. Selected validated HIF-1 targeted genes.

Gene name	Function	References
Aldolase-A	Glucose metabolism, Glycolysis	[87, 88]
Carbonic anhydrase-9 (CAIX)	pH regulation	[89]
Bcl2/adenovirus E1B 19kD-interacting protein 3 (BNIP3)	Apoptosis	[90]
DEC1/Stra13	Transcriptional regulation	[91]
DEC2	Transcriptional regulation	[91]
Endothelial nitric-oxide synthase (eNOS)	Vasodilation	[92]
Enolase-1	Glucose metabolism, Glycolysis	[87, 88]
Erythropoietin (EPO)	Erythropoiesis, Cell survival	[93, 94]
Glucose transporter-1, and -3 (GLUT-1,-3)	Glucose uptake	[95, 96]
Glyceraldehyde-3-phosphate dehydrogenase (GAPDH)	Glucose metabolism, Glycolysis	[97]
Hexokinase-2 (HK-2)	Glucose metabolism, Glycolysis	[98]
L-type pyruvate kinase (L-PK)	Glucose metabolism, Glycolysis	[99]
Lactate dehydrogenase A (LDHA)	Glucose metabolism, Glycolysis	[100]
Nip like protein X (NIX)	Apoptosis	[101]
Nitric oxide synthase-2 (NOS-2)	Vascular tone, cell survival	[102]
6-Phosphofructokinase-2-kinase/fructose-2,6-biphosphatase	Glucose metabolism	[103]
Plasminogen activator inhibitor-1 (PAI-1)	Angiogenesis, Fibrinolysis	[104]
Prolyl hydroxylase domain 2 (PHD2)	O_2 sensing	[105]
Prolyl-4-hydoxylase α (I) (P4Hα(I))	Collagen metabolism	[106]
Pyruvate dehydrogenase kinase (PDK)	Mitochondrial activity, Respiration	[98]
Telomerase reverse transcriptase (TERT)	Cell proliferation, DNA replication	[107, 108]
Transforming growth factor-α (TGF-α)	Cell proliferation	[109]
Transferrin	Iron transport	[110]
Transferrin receptor	Iron transport	[111, 112]
Vascular endothelial growth factor (VEGF)	Angiogenesis, Cell survival	[113, 114]
VEGF receptor-1 (flt-1)	Angiogenesis	[115]

In mammals, products encoded by these 70 targeted genes can be divided into two main functional categories:

1) improving or maintaining tissue oxygenation via up-regulated angiogenesis, vasodilation and erythropoiesis,
2) switching aerobic to anaerobic substrate consumption and ATP maintenance via increasing glucose uptake and glycolytic flux.

EPO: a major player of erythropoiesis

One example is erythropoiesis, particularly with regard to the functional division of labor between HIF-1 and HIF-2. The glycoprotein hormone erythropoietin regulates the cell mass of erythrocytes and represents a potent stimulus for erythropoiesis. EPO is produced by the fetal liver and the kidney of the adult mammal during hypoxia. While previous findings considered the human EPO gene as being targeted by HIF-1, recent findings point more towards HIF-2 as the main transcriptional driver of EPO transcription. For example, HIF-2, rather than HIF-1, was reported to regulate the hypoxia-mediated expression of liver EPO via preferential binding to EPO 3'enhancer HRE in ChIP assays [116, 117]. Whatever the mechanistic details, induction of EPO mRNA and protein levels will confer a strongly amplified synthesis of red blood cells in the bone marrow [36]. During erythropoiesis, however, the bone marrow also needs more heme. Thus, the iron demand will increase concomitantly with erythrocyte production. To prevent that inadequate iron supply might limit the rate of erythropoiesis, HIF also upregulates a series of genes which facilitate the transport of iron to the bone marrow. This genes include transferrin, the iron transporter in the blood and its receptor [110-112].

VEGF: a key regulator of angiogenesis in tumor

The vascular endothelial growth factor (VEGF) gene is another O_2-sensitive checkpoint to maintain the oxygen carrying capacity and tissue oxygenation during hypoxic and ischemic challenges. Early reports documented that either hypoxia or hypoglycemia were able to up-regulate and stabilize both VEGF mRNA and protein [118-120]. Later, the functional HIF-1 binding site in VEGF's 5' flanking sequence, required for this hypoxia-mediated transcriptional response, was being identified by electrophoretic mobility shift assays (EMSA) together with protein extracts from hypoxic Hep3B cells [113]. Enhanced secretion of VEGF has been implicated in the neovacularization associated with hypoxic states such as myocardial ischemia, stroke or cancer. With regard to malignant pathologies,

considerable evidence points to the strict requirement of angiogenesis for tumor growth and metastasis (reviewed in [12, 13]. For a malignant mass to grow beyond 1-2 mm^3, i.e. ~30 times the size and more of the initial nodule [13], angiogenesis needs to be initiated to counter the increasing diffusion insufficiencies [121, 122]. For solid malignancies, this step is considered to be rate-limiting for further development and spreading [13]. Studies on tumor vasculature have documented that elevated and secreted VEGF concentrations promoter neoangiogensis primarily through endothelial sprouting in pre-existing capillaries. Yet, in contrast to normal vasculature, tumor vasculature is notoriously aberrant in structure with often elongate, tortuous and blind-ending vessels [4], shows sluggish or erratic perfusion (~85% of all tumor capillaries maintain unstable blood flow) [123, 124] and a great degree of heterogeneity in endothelial cell proliferation and pericyte coverage of blood vessels [125]. Moreover, VEGF signaling also induces vascular permeability and facilitates leakage of plasma protein. Although angiogenesis is evoked to improve already failing O_2 supply, the disordered architecture of tumor vasculature often leads to insufficient tumor perfusion. Therefore, cell-autonomous bioenergetic adaptations need to occur as added strategies, to improve the cells' survival odds.

Part A Co-regulatory effect of HIF/USF on human genes containing HRE and E-Box palindromes

5 Background

5.1 HIF and glucose metabolism

To generate ATP as energetic pre-requisite for cell growth, cell motility and macromolecular syntheses, glucose is metabolized in two ways. One way is glycolysis in which glucose is fermented to pyruvate in the cytosol. This linear substrate flux has a net production of 2 moles ATP per mole glucose consumed. The other way is composed of the tricarboxylic acid (TCA) cycle in conjunction with the oxidative phosphorylation of delivered reduction equivalents (NADH) in the electron transport chain (ETC). Both, the cyclical TCA and the linear 4-complex containing ETC reside in the mitochondrium. Oxygen serves as the final electron acceptor in the ETC. The energy released through the exergonic electron transport from the NADH reduction equivalents onto O_2 is temporarily stored in form of an electrochemical proton gradient across the inner mitochondrial membrane. This gradient, in turn, drives ATP synthesis at the ATP synthetase (complex V) for a net production of 36 moles ATP per mole glucose oxidized. During oxygen limitation of the mitochondrial ETC, pyruvate, or rather its decarboxylated C2 acetyl derivative, will no longer be used as initial substrate of the TCA, but instead converted to lactic acid by the cytosolic lactate dehydrogenase A. This reduction does nothing to improve the poor energy balance of fermentative glucose utilization during hypoxic challenges (2 moles ATP net/mole glucose). Due to this inefficient ATP production from anaerobe glycolysis, cells need respond with a much larger throughput of glucose import and glucose-to-lactate breakdown, to at least maintain energy production under anaerobic conditions. This so-called Pasteur effect was first reported by Louis Pasteur in 1861 on yeast cells [126]. Pasteur could show that oxygen inhibited fermentation and that glucose consumption was inversely proportional to oxygen availability, i.e., that glycolysis was positively regulated by hypoxia. Today we know that the elevated substrate flux in hypoxic cells is achieved through the coordinated induction by HIF-1 of whole series of genes encoding glycolytic enzymes [127-131]. In fact, ten of the twelve catalytic steps participating in glycolysis are regulated by HIF-1 (Fig.3). These well characterized HIF-1 target genes include glucose transporter 1 and 3 (GLUT 1 and 3),

involved in glucose uptake [95], aldolase A (ALDA), phosphoglycerate kinase 1, enolase 1 and lactate dehydrogenase A (LDHA) [87, 88, 93, 100]. It was hypothesized that this overwhelming control of the Pasteur effect might well represent HIF's primordial function, which emerged shortly after the transcriptional activity originated in some archetypal metazoan [128]. Similar to angiogenesis, however, the Pasteur effect does not represent the "be all, end all" means of hypoxic adaptations. As serious drawbacks of this defense strategy, high-flux glycolysis can quickly deplete finite stores of fermentable substrate (e.g. glycogen) and amass toxic levels of end products (e.g. H^+ per ATP hydrolysis) in sensitive and hypoxic cells. In the absence of energy expending reductions, anaerobe fermentations fail to meet ATP maintenance demands of ionic and osmotic equilibrium and are thus unable to prevent an ultimately fatal ATP imbalance in central neurons, renal tubular cells or hepatocytes [132-135].

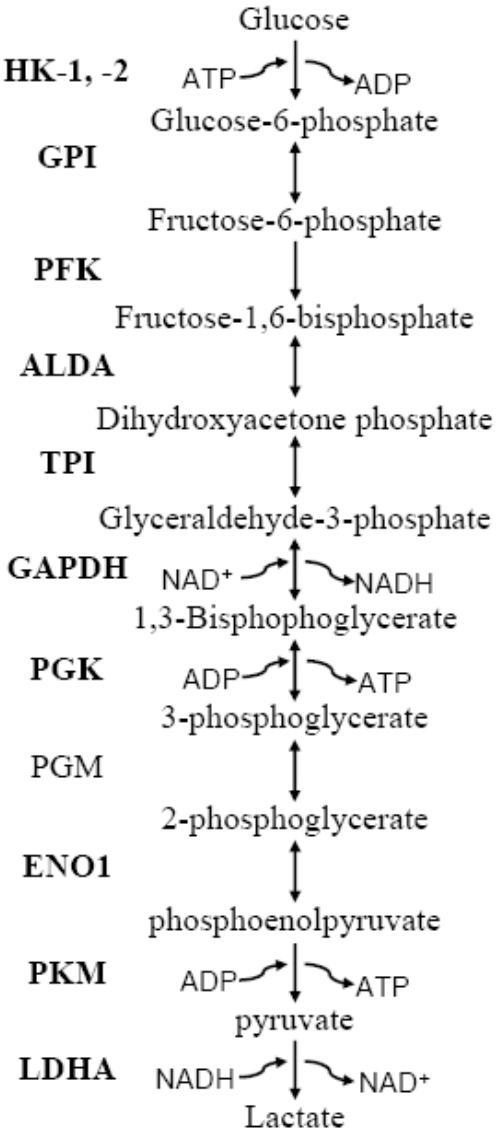

Figure 3 The glycolytic pathway. Enzymes upregulated by HIF-1 are indicated in bold. HK-1,-2: hexokinase type 1 and 2; GPI: glucose phosphate isomerase; PFK: phosphofructokinase; ALDA: aldolase A; TPI: triose phosphate isomerase; GAPDH: glyceraldehydes 3-phosphate dehydrogenase; PGK: phosphoglycerate kinase; PGM: phosphoglycerate mutase; ENO1: enolase 1; PK: pyruvate kinase; LDHA: lactate dehydrogenase A [136]

Many human and animal tumors display, even under aerobic oxygen tensions, a significantly increased rate of glycolytic sugar consumption and lactate build-up [137-140], a phenomenon known as the Warburg effect. When Warburg described prominent aerobic fermentation as unique dedifferentiation-feature of tumor cells some 80 years ago, he saw the tumor's compensatory reprogramming effort to the initial and cancer-causing insult: an irreversible injury of respiration [141, 142]. Warburg had, in essence, associated the mutually antagonistic relationship between glycolysis (= activated) and respiration (= impaired), as formerly formulated by the Pasteur effect (low pO_2 $\Rightarrow$ activated glycolysis $\Rightarrow$ impaired respiration) or Crabtree effect (high glucose concentration $\Rightarrow$ activated glycolysis $\Rightarrow$ impaired respiration), to the genesis of cancer. His discovery has had a very strong impact on the oncological community and, to this day, aerobic up-regulation of glycolysis [139] or a predominantly glycolytic metabolism in general [143], which are regarded as near-universal property of primary and metastatic cancers and remain associated with tumorigenesis. However, it is quite clear now that a strong basal glycolytic capacity, indeed a feature of many tumor types, is neither the cause nor a universal characteristic of malignancies [129, 140]. Rather, it was found that cultured aerobic cancer cells do not exhibit any more glycolytic activity than normal ones, and both cell types alike partition their total normoxic ATP production into equivalent ~80% oxidative and ~20% glycolytic contributions [144, 145]. Furthermore, some studies simply contradicted the existence of a causal link between glycolytic activity and *in vivo* tumorigenesis [146], while others reported that prominent glycolysis only reflects active proliferation [147] and/or exposure to low pO_2 regardless of the cells' cancerous or normal legacy [129]. Thus, cancer cells, on average, are not inherently more glycolytic than normal cells and constitutive high-flux glycolysis is not causally tied to the malignant transformation of cells. Whether the Warburg effect carries diagnostic and therapeutic significance for secondary or metastatic tumor entities remains a matter of debate.

HIF-1 can also coordinate the up-regulated glucose uptake and glycolytic substrate flux with a substantial reduction in mitochondrial activity [148, 149]. As such, HIF-1 is partly responsible to orchestrate the switch from oxyregulated to oxyconforming respiration. Pyruvate dehydrogenase kinase 1 (PDK1), which phosphorylates mitochondrial pyruvate dehydrogenese (PDH) and thus inhibits the complex from using pyruvate to fuel the TCA

cycle, was determined as a direct HIF-1 target gene during $pO_2 \leq pC$ levels of oxygen scarcity. This TCA block was recently shown to actively suppress respiration, redirect both O_2 and glucose utilization towards cytosolic sinks, and rescue cells from hypoxia-induced apoptosis [148-150]. In addition, a study on non-small-cell lung cancers showed that elevated PDK1 expression might reduce PDH expression even in non-hypoxic tumor cells [151]. As outcome of these findings, HIF-1 actively inhibits the oxidative and promotes the fermentative metabolism of glucose under hypoxic conditions.

5.1.1 Interplay between HIF-1 and c-MYC in glycolysis of cancer cells

Besides HIF-1, c-MYC also plays a key role in the regulation of the glycolytic substrate flux. c-MYC, a proto-oncogene, belongs to the family of basic helix-loop-helix (bHLH)/leucine zipper (LZ) transcription factors. It heterodimerizes with other transcription factors like MAX or MAD and binds to the DNA consensus core palindrome: CACGTG. The complex of c-MYC with this palindromic E-box is involved in cell proliferation, differentiation and apoptosis [152-154].

Multiple mechanisms for HIF-1 to counteract c-MYC function in normal cells have been reported. In cancer cells c-MYC is frequently overexpressed. It has been shown that overexpressed c-MYC is able to synergize with HIF-1 in the regulation of genes that alter metabolism and angiogenesis in human cancer. Using human P436-6 Burkitt's lymphoma cells with conditional overexpression of human c-MYC upon tetracycline withdrawal, Kim *et al.* demonstrated that c-MYC and HIF-1 cooperatively enhanced the expression of pyruvate dehydrogenase kinase 1 (PDK1), hexokinase 2 (HK2) and VEGF genes. Furthermore, this HIF-1/c-MYC cooperativity promoted glycolysis (HK2 induction) while slowing respiration and oxidative metabolism (PDK1 induction) in parallel. The authors further surmised that the Warburg phenomenon might result from the cooperation between HIF-1 and overexpressed c-MYC signaling events [98].

Besides such mutually supportive HIF-1/c-MYC interaction, the antagonism between HIF-1 and c-MYC in tumorigenesis has been also evidenced [155]. Displacement of c-MYC by HIF-1 is feasible, since the HIF-1 consensus binding site (5'-G/ACGTG-3') is almost identical with the c-MYC E-box (5'-CACGTG-3'). A study by Koshiji and colleagues showed HIF-1 was found to antagonize c-MYC targeted p21(cip1) gene, encoding a key cyclin-dependent kinase inhibitor. HIF-1α was able to actually activate c-MYC repressed p21 gene transcription by displacing MYC binding from the promoter and consequently triggered cell cycle arrest rather than accelerated proliferation. Additionally, they reported that the HIF-1α could suppress the c-MYC-activated TERT and breast cancer 1 (BRCA1) gene expression

[156]. HIF-1 is also implicated in promoting genetic instability by decreasing the level of MutSα, a MSH2-MSH6 complex recognizing DNA mismatches, via counteracting with c-MYC [157]. Finally, Mazure *et al.* reported that HIF-1 and c-MYC could competitively modulate the activity of the rat α–fetoprotein (afp) gene through targeting the same 5'-CACGTGGG-3' site, located at -3625 to -3619 upstream of the transcription initiate site. In this case, both transcription factors confer opposite effects regarding afp gene regulation: HIF-1 down-regulated, whereas c-MYC up-regulated afp gene transcription in hypoxic human hepatoma cells (HepG2) [158].

5.1.2 Lactate dehydrogenase A (LDHA)

As elaborated above, most of the ATP in cells is produced through the complete oxidation of glucose to CO_2 and H_2O. However, ATP can also be gained via the incomplete breakdown of glucose to pyruvate. Under anaerobic conditions, pyruvate is further reduced to lactate by LDHA, with the necessary electrons coming from NADH. This leaves the oxidized NAD^+ as another product, which in turn, re-fuels the glycolytic pathway as long as a strong incoming flux of glucose demands it. Mammalian lactate dehydrogenase (LDH) is composed of M(uscle) and H(eart) subunits. While the M subunits are encoded by LDHA, H subunits are encoded by LDHB. In this work, we focus on human lactate dehydrogenase A (LDHA), a known HIF-1 target and important player in carcinogenesis. Given the mutually antagonistic relationship between glycolytic and mitochondrial function, silencing of LDHA by short hairpin RNAs was found to stimulated oxidative phosphorylation and to decrease the mitochondrial membrane potential as expected [159]. LDHA is also co-targeted gene by c-MYC and HIF-1. Within the promoter of mouse LDHA there are two conserved functional HIF-1 binding sites (-72 to -65 and -81 to -86; position always given in reference to the transcription initiate site). Works in the mid-90's determined the HRE at -72/-65 to act as a very strong HIF-1 binding site, whereas the HRE at -81/-86 interacted with HIF-1 rather poorly [87, 93]. Later, Shim *et al.* documented that overexpressed c-MYC was able to transactivate the rat LDHA promoter by direct binding to two CACGTG palindrome sequences (-78/-83 and -175/-180), which are highly conserved in the 5' flanks of mouse, rat and human orthologs. Mutation of either of these E-boxes abrogated this c-MYC dependent activation. Additionally, the authors briefly mentioned that overexpression of upstream stimulatory factor (USF), another member of the bHLH/LZ transcription factor family, was also able to bind to both E-boxes and stimulate LDHA promoter activity although only half as efficiently as overexpressed c-MYC [160]. These results indicated that both c-MYC and USF

transcription factors can activate LDHA gene expression and aid in switching cancer cells from oxidative to glycolytic sugar consumption [161].

5.2 HIF-1 and cell survival/apoptosis

5.2.1 Apoptosis and BCL-2 family proteins

Apoptosis (programmed cell death) plays an essential role in development and tissue homeostasis. The characteristics of apoptosis are cell shrinkage, chromatin condensation and DNA fragmentation. Apoptosis is tightly regulated by the activation of the aspartate-specific cysteine protease (caspase) pathway. There are two pathways to activate caspases: one is dependent on mitochondria (receptor-independent), whereas the other starts through the interaction of a death receptor with its ligand (e.g. Fas receptor signaling pathway) [162]. Pro- and anti-apoptotic factors of the BCL-2 family regulate the mitochondrial pathway. BCL-2 was originally discovered as a proto-oncogene in follicular B-cell lymphoma and was later identified as the mammalian homolog to the apoptosis repressor CED-9 in *C. elegans* [163]. To date, various BCL-2 family members have been identified in mammalian cells. All these members contain between one to four BCL-2 homology domains (BH1-4). According to their structure and function, BCL-2 family members are currently classified into 3 categories: 1) anti-apoptotic members, such as BCL-2, BCL-X_L, BCL-W, MCL-1 and A1, which prevent cell death triggered by various stimuli; 2) pro-apoptotic members, such as BAX, BAK, BOK and BCL-X_S, which all inhibit the activity of anti-apoptotic proteins to promote cell death; 3) "BH3-only" pro-apoptotic members including BIM, BIK, BNIP3, BNIP3L with BH3 and transmembrane (TM) domains, in contrast, BID, BAD, NOXA with an unusually short BH3 domain [164, 165].

Once the intrinsic apoptotic pathway is triggered, two pro-apoptotic factors BAX and BAK translocate to the mitochondria to initiate the release of cytochrome c (CYTc) from the intermembrane space into the cytosol. CYTc release leads to mitochondrial changes, such as the opening of the mitochondrial permeability transition pore (MPTP), a reduction of the membrane potential $\Delta\Psi m$ and an increased production of reactive oxygen species (ROS). The main apoptotic pathway resumes upon binding of the liberated CYTc to the apoptotic protease activating factor 1 (APAF-1) in the cytosol. Next, APAF-1 proteolytically cleaves caspase 9, which in turn cleaves and activates caspases 3 and 6, leading to apoptosis [166, 167]. The anti-apoptotic proteins BCL-2 and BCL-X_L prevent CYTc release from mitochondria and, thereby, preserve cell survival whereas pro-apoptotic proteins trigger release of CYTc, MPTP

(pore) opening, caspase activation and initiation of apoptosis. That way, abundance and type of BCL-2 family members determine whether cells will undergo apoptosis or survive exposure to harmful agents or developmental reprogramming decisions.

5.2.2 Bcl2/adenovirus EIB 19kD-interacting protein 3 (BNIP3)

The pro-apoptotic mitochondrial protein BNIP3 was first identified in a yeast two-hybrid screen as interacting partner of the adenovirus E1B19K protein. It contains a single yet atypical BCL-2 homology 3 (BH3) domain together with a transmembrane (TM) domain and thus belongs to the BH3-only subfamily of BCL-2 protein family. As homodimer, BNIP3 predominantly localizes to the outer membrane of mitochondria [164]. The TM domain is required for the mitochondrial localization of BNIP3, the dimerization and the pro-apoptotic activity. Ray *et al.* reported that BNIP3 could heterodimerize with anti-apoptotic factors BCL-2/BCL-X_L via N-terminal regions and TM domain, which also induces cell death [168, 169]. Accumulation and activation of BNIP3 induce a form of cell death that shows features of both necrosis and apoptosis (Fig.4). However, unusually for a BH3-only protein, death occurs independently of the BH3 domain and is critically dependent on a C-terminal transmembrane domain [164]. In hypoxic cells kept at neutral pH, BNIP3 was found loosely attached to mitochondria whereas the protein became more tightly associated with the organelle once hypoxia was accompanied with acidosis. Under these conditions, BNIP3 sparks DNA fragmentation and enhanced formation of the mitochondrial pore transmembrane permeability (MPTP) assembly [170]. The BNIP3-induced necrosis-like cell death is associated with opening of the MPTP, the complete breakdown of the proton electrochemical gradient and the spiking generation of ROS. As such, BNIP3-induced cell death is actually independent of CYTc release from mitochondria, caspase signaling and the nuclear translocation of AIF, a mitochondrial flavoprotein [171].

Besides the induction of apoptotic and necrotic-like cell death pathways, there is mounting evidence that BNIP3 also plays a critical role in the hypoxia-triggered autophagy of cells whereby the protein actually aids in cell survival, not death [172, 173]. To respond to stresses, such as nutrient deprivation and hypoxia, autophagy or “self digestion” is a well-conserved survival strategy across many human cancer cell lines and is *in vivo* considered as a key player of promoting tumor progression [172, 173]. During this “self-digestion”, macromolecules and entire organelles are degraded in autophagosomes followed by regeneration and recycling of the building blocks for upcoming syntheses which process with reduced energy expenditures. Different cells might respond to oxygen deprivation via alternate autophagy pathways and some cascades are able to be proceed even in the absence

of HIF-1 and BNIP3 [174]. Nonetheless, hypoxia has been worked out to spark autophagy in many cells via the HIF-1 mediated induction of BNIP3 and the factors downstream signaling onto the highly conserved coiled-coil BH3-only protein BECLIN-1 [175]. A direct physical interaction between BECLIN-1 and the anti-apoptotic proteins BCL-2 and BCL-X_L normally inhibits autophagy and shifts the fate of dying cells towards the ATP-costly apoptosis [176]. Several recent studies, however, established hypoxic signaling as necessary stimulus to drive cells, through the pronounced and HIF-1 mediated induction of BNIP3 and its homologe BNIP3-like (BNIP3L, also known as NIX), into autophagy by way of releasing BECLIN-1 from the BCL-2/BCL-X_L complexes [172, 177]. BNIP3 and BNIP3L confer this switch due to their direct competition with BECLIN-1/BCL-2 and BECLIN-1/BCL-X_L complexes for the binding of BECLIN-1 [178] (Fig. 4).

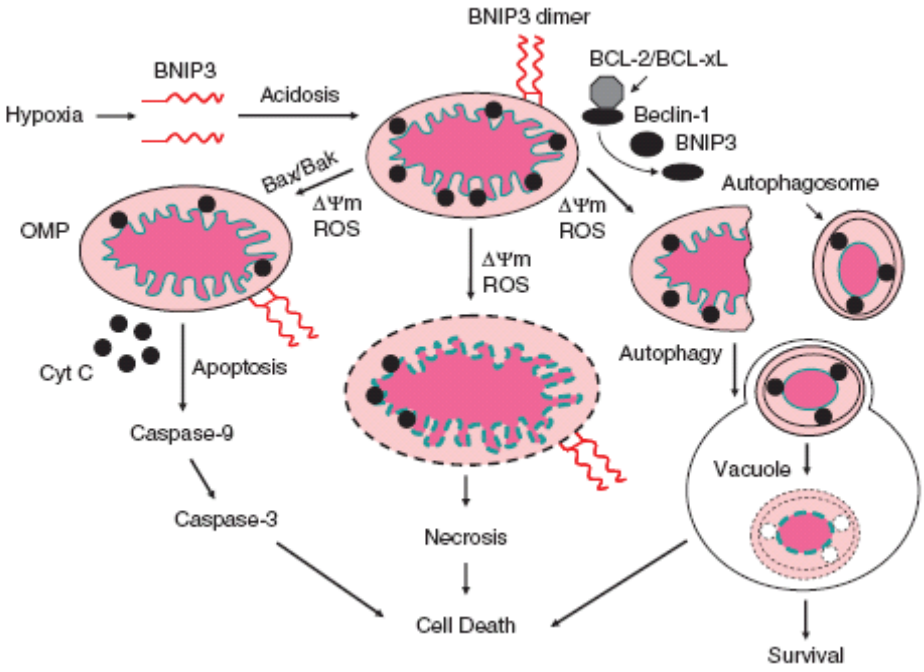

Figure 4 Model for BNIP3-mediated apoptosis and autophagy. BNIP3 is hypoxically induced by HIF-1 and stabilized by acidosis. Subsequently BNIP3 homodimerizes, translocates and integrated into the mitochondrial outer membrane resulting in mitochondrial dysfunction e.g. the loss of $\Delta\psi_m$ and increased production of ROS. Once BNIP3 signaling is activated, cells may undergo three different fates: a) the main apoptosis pathway in which BAX/BAK, CYTc and caspases participate; b) necrosis, characterized through the opening of the MPTP, the collapsing electrochemical gradient across the inner mitochondrial membrane ($\Delta\Psi m$) and the resulting generation of ROS and c) autophagy as a survival mechanism during BECLIN-1 is released from the BCL-2/BCL-X_L complexes [179].

5.2.3 Hypoxia and acidosis: triggers for BNIP3-mediated cell death in human cancer cells

Severe hypoxia is an established stimulus to induce apoptosis by slowing and eventual inhibition of the ETC in the inner mitochondrial membrane. This reduction of electron flux causes a decrease in the membrane potential, subsequent generation of ROS and a declining capacity to produce ATP through the oxidative phosphorylation reactions taking place in the ETC. As mentioned above, hypoxic (pO_2 < pC) cells will also switch from oxyregulated to oxyconforming respiration and from an oxidative to a fermentative (glycolytic) mode of metabolism. This switch results in up-regulated import and consumption rates of glucose and an elevated production of lactic acid (see section 4.2 HIF and glucose metabolism). Together with the pronounced ATP hydrolysis rate (i.e. ATP hydrolysis > ATP production rate) in severely hypoxic cells, dissociation of lactic acid to lactate and protons is the main source of protons during hypoxic stress. Tumor needs to cope with such ensuing acidification and preserve a neutral intracellular pH (pH_i) that is compatible with cell growth and survival (see [180] for review). Acid export leads to a reduction of extracellular pH (pH_e) that it is typical for the tumor microenvironment and commonly associates with a more invasive phenotype. Additionally, substrate flux through the TCA produces a high amount of CO_2 in cancer cells which diffuses through the plasma membrane and contributes to a further fall in pH_e. Hypoxic tumor cells respond to this acidic microenvironment by inducing carbonic anhydrase IX (CAIX), again via HIF-1 transactivation. CAIX catalyzes the reversible hydration of $CO_2 + H_2O \rightarrow HCO_3^- + H^+$ in the extracellular space. The resulting bicarbonate ions are imported by bicarbonate transporters such as anion exchangers (AEs) and the Na^+/HCO_3^- co-transporter and, thus, contribute in neutralizing the intracellular pH, while the CAIX derived protons remain outside only to further aggravate the pericellular acidosis [180].

Outside of cancer, hypoxia and acidosis have also been implicated in ischemic myocard. In cardiac myocytes, it was shown that acidosis was required to induce apoptosis under hypoxia. Kubasiak *et al.* reported that hypoxia, when combined with acidosis, triggers BNIP3-mediated cell death in cardiac myocytes. In contrast, hypoxia alone did not activate cell death in neonatal cardiac myocytes. During the dual insult, hypoxia enhanced the expression of BNIP3 mRNA and protein, whereas acidosis was necessary to stabilize the BNIP3 protein and increase the association of its homodimers with mitochondria [181]. Besides energy deprivation and acidosis, radical formation, in particular, ROS production, contributes to hypoxia induced apoptosis as well. ROS are known to activate caspase-9 in a CYTc independent manner, which causes hypoxic cell death in epithelial cells [182].

When focusing on its pro-apoptotic/pro-autophagic role in cancer, it is worth noticing that BNIP3 protein is highly expressed in some tumors, including breast, lung and cervix cancers, and undetectable in normal tissue [164]. A strict requirement of HIF-1 to induce BNIP3 mRNA and protein levels in O_2-deprived cells (see section 4.2.3 HIF-1 target genes), was substantiated when Sowter *et al.* utilized RCC4 renal clear cell carcinoma cells. RCC4 cells are deficient for VHL, therefore, HIF-1α and HIF-2α are constitutively active. As a result, BNIP3 protein is abundantly expressed even in normoxic RCC4 cells. Reintroduction of VHL into the RCC4 genome led to the typical profile of a normoxic HIF-1α degradation and the subsequent absence of BNIP3 in oxygenated cells [101]. Similarly, treatment of chinese hamster ovary (CHO-K1) cells with "hypoxia mimetics", such as the transition metal $CoCl_2$ and the iron chelator deferoxamine mesylate (DFO) (see section 4.2.1 Structure of hypoxia-inducible factor and section 4.2.2 HIF-1 signaling pathway), was able to induce NIP3 expression [183]. Therefore, BNIP3 has clearly been characterized as HIF-1 controlled hypoxia-induced target gene in cancer. One of two BNIP3 HRE sites (-246 from translation start site) was determined to function as direct HIF-1 binding site by electromobility shift assay [90]. Over-expression of BNIP3 in breast cancer cells (MCF7) induces apoptosis by binding to and inhibiting the anti-apoptotic proteins BCL and BCL-X_L. It has further been reported that hypoxia-induced BNIP3 expression inversely correlates with metastatic potential. Ductal carcinoma in situ (DCIS) of the breast is an early, non-invasive lesion and the prognosis is associated with necrosis and cell death within the tumor. The analysis of DCIS, as well as of benign and invasive breast tissue unearthed the correlation between high expression of BNIP3 and high-grade necrosis in DCIS [184]. Silencing of BNIP3 with siRNA in breast cancer cells was sufficient to evade cell death and enhance metastatic survival [185].

5.2.4 Gaining resistance to apoptotic stimuli

Cells can also acquire resistance to hypoxia-mediated cell death. As first described by Graeber *et al.* [9], hypoxia can select for the expansion of apoptosis-defective cell variants, for example those that acquired loss-of-function mutations in tumor suppressor genes such as p53 (reviewed by [186, 187]). P53 has been implicated in controlling apoptosis of hypoxic cells due to its ability to stimulate BNIP3L via the recruitment of the coactivator CBP (CREB binding protein) [188]. Other than through p53 loss-of-function, acquisition of cell death resistance of hypoxic cells can also process either at mitochondrial or cytosolic compartments. Regarding mitochondria, the translocation of BAX to these organelles can be suppressed, and consequently, less CYTc can be released in resistant cells. Regarding the cytosol, rat kidney proximal tubule cells (RPTC) were found to induce the inhibitor of apoptosis protein 2 (IAP-2)

during anoxia via HIF-1 independent mechanisms [189]. Such increased concentration of IAP-2 in the cytosol can repress the release of CYTc from mitochondria, which again facilitates survival of O_2 depleted cells [190]. Both alterations of the pathway can therefore endow cells to evade incoming apoptotic stimuli.

Another way to escape apoptosis induced by hypoxia and to gain hypoxia tolerance is through inhibiting the expression of BNIP3. Several mechanisms of epigenetic silencing of the BNIP3 gene are known. Various studies on pancreatic cancer showed that hypermethylation of CpG islands in the region of the transcription start site of BNIP3 promoter silenced BNIP3 gene expression in the most pancreatic cancer. This CpG methylation of BNIP3 contributed to resistance to hypoxia-induced cell death in pancreatic cancer cells. Re-expression of BNIP3 by treatment with DNA methyltransferase inhibitor 5-aza-deoxycytidine (5-aza-dc) was able to restore hypoxia-mediated cell death [191-194]. Other studies demonstrated that BNIP3 silencing via DNA methylation occurred not only in pancreatic cancer but also in many colorectal, hematopoietic and gastric cancers. In addition, the authors showed that histone deacetylation also played a role in silencing BNIP3 [195-197]. Beyond epigenetics, several growth factors including epidermal growth factor (EGF) and insulin-like growth factor (IGF) can also protect from BNIP3 induced cell death in hypoxic epithelial cells [90]. On the other hand, BNIP3 protein level was reported to be dramatically increased in breast and lung cancers compared to the equivalent normal tissue. Thus, epigenetic silencing of BNIP3 expression occurs cell-/tissue-type specifically and it remains an open question how BNIP3 silencing influences the phenotype of these tumors.

5.2.5 HIFs' role in apoptosis: crosstalk with p53

HIFs' role in controlling cell death appears multifaceted and cell-type specific. Carmeliet *et al.* reported that HIF-1α induces apoptosis in wild-type (HIF-1α $^{+/+}$) embryonic stem (ES) cells [198], whereas Akakura *et al.* demonstrated boosted survival and proliferation of pancreatic cancer cells under hypoxia and glucose deprivation upon the constitutive expression of HIF-1α and the enhanced expression of the downstream effectors GLUT-1 and aldolase A [199]. HIF-1 can exert control in both p53-independent and p53-dependent ways of apoptosis. p53-independent initiation of apoptosis by hypoxic signals commonly involves BCL-2 family proteins and other unknown factors [138, 200]. The much debated HIF/p53 crosstalk was inspired by early reports in which HIF-1α was thought to function as stabilizer of p53 and, that way, to contribute in the induction programmed cell death [137]. Subsequently, HIF-1α was shown to directly bind to the p53 ubiquitin ligase MDM2 both *in vivo* and *in vitro* and to exert its stability-enhancing effect on p53 [201]. However, other

reports supported a direct interaction of HIF-1α with wildtype, but not tumor derived mutant, p53, whereby the DNA binding region of p53 was in direct contact with the ODD domain of HIF-1α [202]. Whether or not HIF-1 truly underlies the oxygen-regulated induction of p53 has been questioned by Wenger and colleagues, since hypoxia, that activated HIF-1-dependent gene expression as well as HIF-1α protein, induced neither p53-dependent gene expression nor p53 protein [203]. One also has to bear in mind that HIF-1 signaling has evolved to sense hypoxic pO_2, while the p53 pathway commonly engages at a more severe, anoxia approaching, level of O_2 depletion [203, 204]. Thus, under physiological or *in vivo* conditions, the two cascades might complement, rather than overlap, one another to regulate cellular responses under a wider pO_2 spectrum.

5.3 Upstream stimulatory factors (USFs) -- bHLH/LZ transcription factors

5.3.1 Structure and isoforms of USFs

Upstream stimulatory factor (USF)/major late transcription factor (also called MLTF), initially identified from HeLa cell nuclei and purified as heterogeneous complex, consists of two USF isoforms with molecular masses of 43 and 44kDa, that were referred to as USF1 and USF2a, respectively [205, 206]. USF1 and 2a are products of two different genes and each contain a conserved basic helix-loop-helix domain (bHLH) and a leucine zipper (LZ) motif at the C-terminal region. Two transcriptional activation domains, located at the N-terminal region of USF1 (residues 26-39 and 93-156), are required for full activation [207]. The basic region is required to interact with CANNTG E-box core consensus sequence, whereas HLH and LZ motif are involved in factor dimerization. The USF-specific region (USR), located N-terminally from the basic region and highly conserved in USF1 and USF2a, is essential for transcription activation [208, 209]. Several additional domains adjacent to the N-terminus are less conserved in USF1 and USF2a. These regions include domain M, found only in USF1 and domains G and O of USF2a (Fig.5) [210].

A novel splice form of USF1, termed USF1/BD, has been observed. Compared with USF1 wild type, USF1/BD lacks the N-terminal transactivation domain due to the excision of exon 4. USF1/BD is localized in the nucleus, where it heterodimerizes with wild type USF1. Its DNA binding activity, however, repressed the promoter activity of human angiotensinogen gene [211]. Another USF2 splice variant, termed USF2b, can heterodimerize with other USF proteins. As a heterodimer, USF2b can bind to E-boxes but, due to the missing exon 4 with its positive-regulatory domain, fails to activate gene expression. Thus, USF2b contains functional USR and the negative-regulatory domain. It functions as a dominant negative regulator of USF-mediated gene expression [212]. It has been reported that two truncated USF1 and USF2 variants, namely mini-USF1 and mini-USF2, which contain intact dimerization and DNA-binding domain (bHLH/ZIP domain), might result from the use of internal translation initiators [205, 210]. These mini-USF proteins behave as transdominant inhibitors and are expected to down-regulate USF activity [213] (Fig. 5).

Although USF1 and USF2 are ubiquitously expressed, ratios of USF homodimers or heterodimers vary according to cell types [205]. Viollet *et al.* described that USF1/2a heterodimer acts *in vivo* as main constituent of the cells' USF binding activity in rat liver tissues and human cells (hepatoma cells HepG2, megakaryoblastic cells UT7 and cervical cancer cells HeLa) [210].

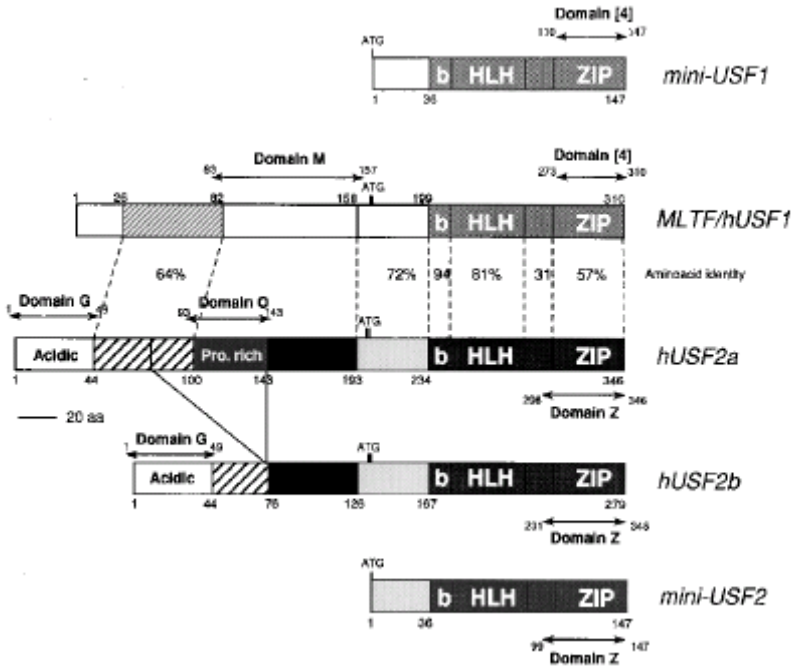

Figure 5 Schematic representation of human USF proteins. The family includes: major late transcription factor (MLTF)/hUSF1, two spliced variants hUSF2a and hUSF2b and two truncated USF species: mini-USF1 and mini-USF2. Percentage indicates the identities among the conserved domains of USF1 and USF2a. Arrows define the sequences encoding specific domains in either USF1 or USF2. bHLH-ZIP: basic helix-loop-helix-leucine zipper [210]

5.3.2 General functions of USFs

USFs are ubiquitously expressed and key regulators of gene regulation networks, including stress and immune responses, control of cell cycle, cell proliferation and glucid-lipid metabolism [214]. USFs modulate gene transcription through direct binding to E-box cis-elements [215] containing the core sequence CANNTG. In most cases, the two central nucleotides NN are either GC or CG. They can seldom be either CA or TG. USFs exert a higher binding affinity for the CACGTG palindrome than the CATGTG motif, the latter also being referred to as M-box. Additionally, the nucleotides flanking the CANNTG core sequence can also contribute to selective recognition of E-box binding protein. Different studies on the binding sites of USF1 regulated promoters suggested that the importance of 3'AC residues are important for USF1 to selectively recognize a CACGTG E-box palindrome [216-218]. Modification within the E-box, including methylation at the CpG site (CACpGTG), may negatively regulate gene expression. Several observations have shown that USF can not only bind to classical E-box elements but also directly to alternative sites, so called pyrimidine-rich initiator elements (5'YYCAYYYYY3') adjacent to the transcription start site in various promoters including those of HIV-1 and Ad-ML. This physical interaction with initiator elements results in a drastic enhancement of basal transcription level [219, 220].

USFs' physical and functional interaction with other general or cell specific transcription factors, such as specificity protein 1 (SP1), polyoma virus enhancer activator 3 (Pea3) and metal-regulatory transcription factor 1 (MTF1) leads to a cooperative transcriptional regulation of several genes including BCL2-associated X protein (BAX), metallothionein-I (MT-1) and deoxycytidine kinase (dCK) [221-223]. In addition, USFs are known to interact with transcription factors of the basal machinery, including TFII-I, TFIIB, TFIID, TFIIE and TATA-binding protein (TBP) associated factor (TAF), upon which a synergistic activation of the TATA-box directed transcription unfolds [218, 224, 225]. To date, different co-factor models for the transcriptional activity of USF in different cell type are considered. Breen and Jordan showed that USF2 activates the mammalian F1F0ATP synthase α–subunit (ATPA) gene through an initiator element in the core promoter and that this USF2 dependent transcriptional activation is mediated by p300 [226]. Activity of the promoter of the human telomerase reverse transcriptase (TERT) gene was enhanced by USF in hTERT positive immortal cells, again due to recruitment of the co-activator p300 [227].

The roles of USFs and USF target genes extend beyond adjustments within the general transcription machinery. To this end, USF-regulated genes have been implicated in the immune response following viral and bacterial infections. Here, USF1 participates in both the humoral-antibody response and the cell-mediated non-specific immune response [212, 228]. Secondly, USFs are involved in controlling cell cycle through the regulated expression of different cyclin and cyclin-dependent kinase (cdk) genes, like CDK4, CYCLN B1 and CDK1 [229, 230]. Thirdly, USFs regulate mediators of cell proliferation like TERT, TGFβ2 and IGF2R [227, 231]. A final important function of USFs lies in the coordinated control of the glucid and lipid metabolism through regulating genes encoding insulin growth factor-binding protein 1 gene (IGFBP1), glucokinase [232, 233], L-pyruvate kinase gene [213] and fatty acid synthase [234].

Different signal transduction pathways may modulate USF1 transcriptional activity including growth factor stimuli, irradiation by ultraviolet (UV) light, heavy metals, oxidative stress, virus infection and DNA damage. For example, phosphorylation of USF1 is required to enhance the factors' transcriptional activity. Several kinase pathways are involved in the phosphorylation of USF1. These cascades include the p38 stress activated kinase pathway [235], the nitrogen-activated protein kinase (MAPK) kinase and tyrosine kinase pathway [236], the protein kinase A and C pathways [237] and the CDK1 pathway [238]. Posttranslational phosphorylation increases USF1 DNA binding activity and allows the modulation of USF mediated gene regulation.

5.3.3 USFs: transcriptional activators and repressors

USFs were originally identified as activator of the adenovirus major late promoter in HeLa cells. Early studies also unravelled these proteins also to act as essential factors for the efficiently enhanced transcription from the adenovirus major promoter via binding to the GGCCACGTGACC sequence located between positions -63 and -52 relative to the transcription start site [218, 239, 240]. Thus, USFs were originally considered as transactivating factors. Unexpectedly, more and more evidence suggested that USFs might act as transcriptional repressors as well. For example, Carter *et al.* reported that overexpressed USF1 could effectively inhibit immunoglobulin heavy chain (IgH) enhancer activity in mouse embryonic fibroblast cells (NIH3T3). According to the authors, this inhibition was correlated with the lack of a strong activation domain within USF1 and absence of other IgH enhancer E-boxes in the vicinity of the μE3 E-box [241]. Additional studies showed that USF1 is able to suppress the transcriptional activity of different genes by competing with positive-transacting factors. In this regard, USF1, in rat liver nuclear extracts, other than the AhR/Arnt (aryl hydrocarbon receptor/aryl hydrocarbon receptor nuclear translocator) complex could *in vitro* constitutively bind to the xenobiotic responsive element (XRE) in the promoter of the rabbit cytochrome gene P450 1A1 (CYP1A1). Overexpression of USF1 antagonized the induction of the rabbit CYP1A1 gene by the AhR/Arnt complex [242]. As possible mechanism of such negative effect on a gene's activity, USF1 and 2a were found to bind to two E-boxes within the promoter of the cytochrome P450 family 19 (CYP19) gene, which prevents the assembly of a stable transcription complex and inhibits of CYP19 promoter activity [243]. Chen *et al.* showed that a dominant negative USF1 construct, which lacked the basic DNA-binding domain but retained the dimerization domain, repressed the promoter activity of the aortic preferentially expressed gene-1 (APEG-1). Wild type USF1, but not USF2a, transactivated APEG-1 activity leading to differentiation of vascular smooth muscle cells [244]. A study on the rat gene encoding the plasminogen activator inhibitor 1 (PAI-1) reported that overexpressed USF2a inhibited rat PAI-1 gene expression via direct binding to E-box in hepatocytes [245].

5.3.4 Differential role of USF1 and USF2 in transcriptional activity

The homozygous USF-deficient mice models permitted to investigate the differential transcriptional role of USF1 and USF2. These studies also clarified the essential role of USFs for the embryonic development. Utilizing USF-$1^{-/-}$ and $USF2^{-/-}$ single homozygous as well as $USF1^{-/-}$/$USF2^{-/-}$ double homozygous mice, this work demonstrated that USF-1-null mice are viable, fertile and essentially normal, whereas USF2 knockout mice displayed high mortality

rate and growth defects. Sirito *et al.* reported on the asymmetrical cross-regulation of USFs proteins in fetal fibroblasts isolated from USF1$^{-/-}$ and USF2$^{-/-}$ mice. According to these authors, USF1 null mice exhibited an elevated level of USF2, which might compensate for the USF1 defect. In contrast, USF2 knockout mice had a reduced level of USF1 and displayed decreased fertility [246]. Two studies by Vallet and colleagues on the differential role of USF1 and USF2 in the transcriptional response of liver genes to glucose demonstrated that the USF1/USF2 heterodimer represents the major USF activity in hepatocytes that confers the glucose-induced expression of the gene encoding the glycolytic L-type pyruvate kinase (L-PK). In wildtype rodents, both USFs participate in carrying out a regulated normal glucose response. In USF1$^{-/-}$ mice, however, a normal transcriptional response of the L-PK gene to glucose is sufficiently sustained by the USF2, even though the USF2 homodimer exhibits only 40-50% of residual USF binding activity. Conversely, in USF2$^{-/-}$ mice, the USF1 homodimer was shown be less efficient than the USF1/2 heterodimer for promoting L-PK gene expression in response to glucose. The authors suggested that USF dimers *per se* have different transactivating properties as provided by the distinct N-terminal activation domain of USF1 and USF2 [247]. Interestingly, this study did not observe altered liver expression of USF1 in USF2 null mice or, conversely, altered USF2 gene expression in USF1 null mice [248]. A weak transcriptional activity of USF1 was also described by Desbarats *et al.* [249]. These authors suggested that the distance between the E-box and the transcriptional start site might influence the transactivation efficacy of USF1. In addition, the different transcriptional activity between USF1 and USF2 might stem from their divergent N-terminal transcription activation domains [205], which in turn, might result in distinct interactions of USF1 and USF2 with other regulatory factors [225, 250-252]. Work by Allen and colleagues on the USF1 mediated regulation of PAI-1 in human keratinocytes showed that USF1 transcriptional activity might be modified by a transcriptional co-repressor or a co-activator, which, in turn, depends on the abundance of TGF-β1 [253]. In addition, USF1 transcriptional effects could be not only gene-/and cell- type dependent but also E-box specific.

5.3.5 Antiproliferative effects of USF on cancer progression

USFs and c-MYC are both bHLH/LZ transcription factors and target the same DNA binding site, the CACGTG E-box palindrome. c-MYC plays an important role in various processes of cellular transformation and proliferation whereas USFs often display antiproliferative properties. This antagonism between c-MYC and USFs on cellular transformation was demonstrated by *in vivo* experiments with rat embryo fibroblasts. The DNA binding and transactivation domains of USFs were required for this antagonism [208,

254]. The USF loss of function in many cancer cell lines implied that USFs might suppresses tumor progression. This transcriptional effect of USFs is also cell type context dependent. Although HeLa cervical carcinoma and Sao-2 osteosarcoma cells had similar endogenous USF protein levels und DNA binding activities. USFs in HeLa cells are transcriptionally active leading to growth inhibition, while USFs in Sao-2 lack transcriptional activity and do not mediate a slowdown in the proliferation rate of these cells [209]. The authors developed a model in which USFs' antiproliferative activity was shown to be controlled by interaction with a coactivator via the USF specific domain (USR). In HeLa cells, the USR domain exhibits a dual function. It was sufficient for USF2 to show transcriptional activity at a promoter containing an initiator element. In case of a promoter lacking such initiator element, cofactor binding to the USR triggered a conformational change to expose the activation domain in HeLa cells. In Sao-2 cells, however, this cofactor might be missing and thus USFs remained inactive [209]. Han *et al.* confirmed this cell type-dependent USF transcriptional activation in their study on human topoisomerase IIIα in HeLa and Sao-2 cells [255]. Inactivity of USF2 is not only restricted to Sao-2 cells but also extends to some lines of breast cancer cells. Ismail *et al.* documented that USF1 and 2 exhibited strong transcriptional activities in the non-tumorigenic human breast cancer cells, yet were completely inactive in transformed breast cancer cells. Loss of USF function in breast cancer cells has been implicated during carcinogenesis whereas c-MYC overexpression favors a rapid proliferation [256]. IGF2R (mannose 6-phosphate/insulin-like growth factor 2 receptor), a USF2 specific target, was transactivated by overexpression of USF2 only in non-tumorigenic mammary epithelial cells (MCF-10A) but not in breast cancer cells (MCF7 and MDA-MB231). The authors suggested that the defect in USF2 function in breast cancer cell might contribute to the down-regulation of IGF2R and some cofactors might be also involved in this regulation [257].

Besides this antagonism between USFs and c-MYC, both factors can also act in concert with regard to gene regulation. USF and c-MYC both up-regulate the promoter activity of CXCR4, a coreceptor for T cell-tropic HIV-1 entry [258]. Another example, the gene for cell cycle and cell growth control factor CDK4 has been identified as being co-regulated by c-MYC and USF2. In non-tumorigenic breast epithelial cells, c-MYC and USF2 cooperatively activate the transcriptional activity of CDK4, whereas expression of this gene is independently controlled by both transcription factors in breast cancer cells. The authors suggested that this cooperation or co-stabilization of c-MYC and USF at the CDK4 promoter

existed only in normal cell but not in cancer cells due to loss of USF function in the latter [230].

5.4 Melanoma: UV signaling in a hypoxic microenvironment

The incidence of malignant melanoma worldwide is increasing faster than any other cancer [259]. Although melanoma accounts for only 10% of all skin cancers, it is the most biologically aggressive common skin cancer and leads to 80% of skin cancer related deaths [260]. Particularly prone to develop this cancer is fair-skinned Caucasians who freckle or sunburn easily without tanning. Consequentially, melanoma incidence peaks in Australia, New Zealand, Scandinavia and Northern America [261]. The only effective treatment of melanoma is the wide margin surgical excision of the lesion during the early phase of the disease. Advanced melanoma is able to metastasize and commonly resistant to conventional therapeutic interventions [262]. Triggered by intermittent exposure to the mutagenic qualities of the ultraviolet (UV) fraction within the solar spectrum, melanoma can develop via the malignant transformation of melanocytes that reside at the dermal-epidermal junction as well as in hair follicles (Fig. 6). UV wavelengths range from 200-400 nm and can be further subdivided into UVA (320-400 nm), UVB (280-320 nm) and UVC (200-280 nm) bands. Unlike UVC, UVA and UVB actually reach the Earth's surface and harmfully affect exposed skin by causing an excess of DNA lesions that overwhelm the cells repair capacity. UVB is considered to represent the most carcinogenic waveband and causes two types of DNA lesions: pyrimidine (6-4) pyrimidone photoproducts and cyclobutane pyrimidine dimers. Both types of lesions can result in genetic mutations such as the C→T or CC→TT transitions. The latter transition is the hallmark of UV-induced mutagenesis. Compared with UVB, UVA-induced melanoma is not well characterized. However, UVA is also able to mutate DNA, predominantly via injuries spawned through the generation of ROS [259].

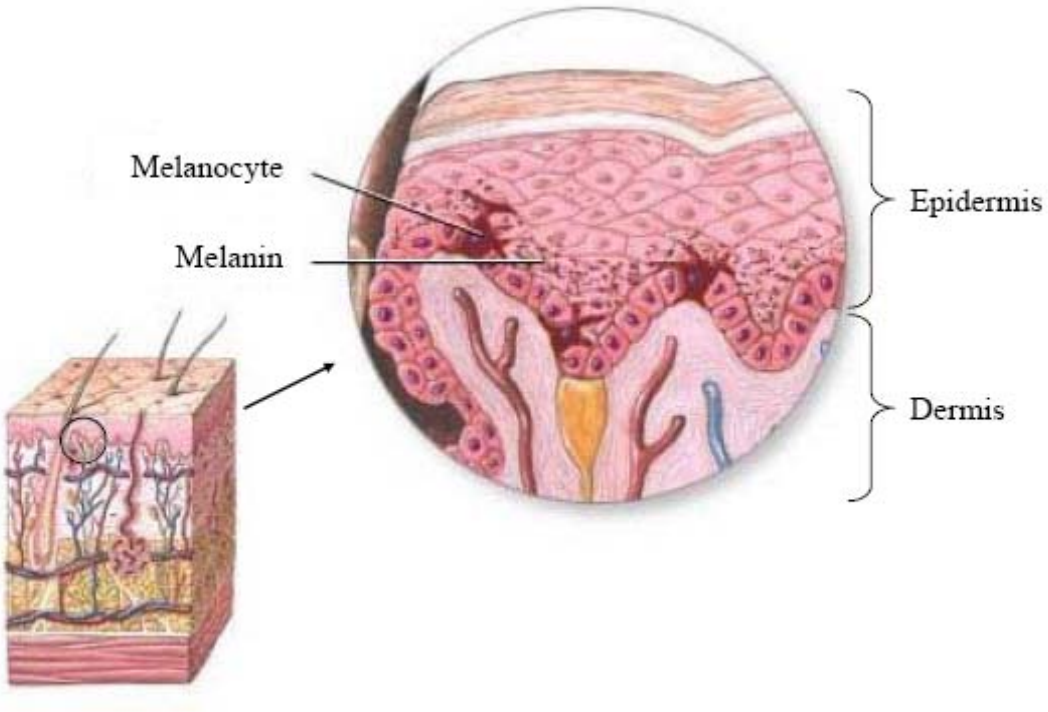

Figure 6 Location of melanocytes in epidermis-dermis junction in the skin. Melanocytes are cells located in the bottom layer (the stratum basale) of the skin's epidermis and produce dark pigment called melanin to protect UV radiation.

5.4.1 Tanning response: MITF mediated basal and USF mediated UV-induced gene control

The tanning response of melanocytes is responsible to protect the skin against sunburning and UV-induced DNA damage. It centers on the synthesis of the brown-black pigment (eu)melanin in specialized organelles termed melanosomes. Mature melanosomes are released from melanocytes via exocytosis, transferred to surrounding keratinocytes and culminate in the common darkening of the skin during the days following the UV exposure. Melanin has a dual photoprotective function in the skin: it absorbs of ultraviolet photons and scavenges of ROS. Genes, encoding melanin-synthesizing enzymes, include tyrosinase (TYR), tyrosinase-related-protein 1 (TRP-1) and dopachrome tautomerase (DCT) [235].

The synthesis of melanin is the result of a complex signaling network involving paracrine factors secreted by cutaneous keratinocytes (e.g. α-melanocyte specific hormone, α-MSH), specific receptors (e.g. melanocortin 1 receptor, MC1R), transcription factors (e.g. i: microphthalmia-associated transcription factor, MITF; ii: upstream stimulatory factors, USFs) and downstream effector genes directly involved in pigment manufacture (TYR, TRP-1 and DCT) [214]. The secreted melanocortin α-MSH, encoded by the pro-opiomelanocortin (POMC) gene and liberated through proteolytic processing of the POMC precursor polypeptide, is recognized by its cognate heterotimeric G-protein receptor MC1R on the surface of melanocytes. This ligand/receptor interaction sets in motion a cAMP signaling

cascade which subsequently activates, via the transducing actions of protein kinase A (PKA) and the cAMP response element binding protein (CREB), the expression of the melanocyte specific form of MITF through activation [263].

MITF belongs to the bHLH/LZ family of transcription factors. MITF transactivates expression of TYR, TRP-1 [263] and DCT genes through binding to M-box (CATGTG) sequences in the respective promoter. Therefore, MITF plays a critical role in the basal pigmentation of human skin. In addition, it also regulates target genes whose products control key aspects of melanocyte differentiation and proliferation, melanosome transport and melanoma progression [264]. Recently, the group of Dummer (University Hospital Zurich) underscored MITF's role in supporting tumor expansion by reporting that expression and activity of MITF is a key feature in proliferative clones of melanoma cells, while this transcription factor was found absent in invasive cohorts of this cancer [265]. Remarkably, cAMP signaling is known to stimulate transcription of the HIF-1α gene and some of its downstream targets (e.g. VEGF) in a melanocyte-specific and MITF-dependent manner. Elevation of HIF-1 abundance is elicited through the binding of MITF to multiple E-boxes nestled within the promoter of the human HIF-1α gene. Thus, the presence of a normoxic cAMP/MITF/HIF-1/VEGF cascade in melanocytes and melanoma cells might critically contribute to aspects of differentiation and progression of these cutaneous neoplasms [266].

In contrast to MITF's control of the basal synthesis of melanin, USFs serve as key stress-responsive transcriptional inducers of genes encoding melanin manufacturing enzymes (e.g. TYR) in response to UV-stimulation (Fig.7). The UV-induced tanning response in melanocytes and melanoma cells is mediated through the p38-stress activated MAP kinase pathway. USF1 is phosphorylated at Thr^{153} by the p38 stress-activated kinase and thus able to directly up-regulate POMC, MC1R, TYR, TRP-1 and DCT genes through binding to the same E-box as MITF. Indeed, all these genes failed to be activated following UV stimulation in a $USF^{-/-}$ melanocyte cell line [267]. However, USF1 function can regulate genes in more than one way. Recently, Corre and co-workers identified a novel post-translational modification of USF1. They reported that various stimuli including DNA damage, oxidative stress and cellular infection, were able to acetylate USF1 on lysine199 in a phospho-T^{153} dependent manner. This two-step post-translational modification of USF1 directs the factor to operate at DNA level in a positive or negative fashion. While low level of stress cumulates in the phosporylation on Thr^{153} of USF1 and consequently triggers a positive gene regulation with regard to cell cycle control or tanning response. Massive stress results in a phospho-dependent acetylation of USF1 in conjunction with a marked down-regulation of targeted genes [268].

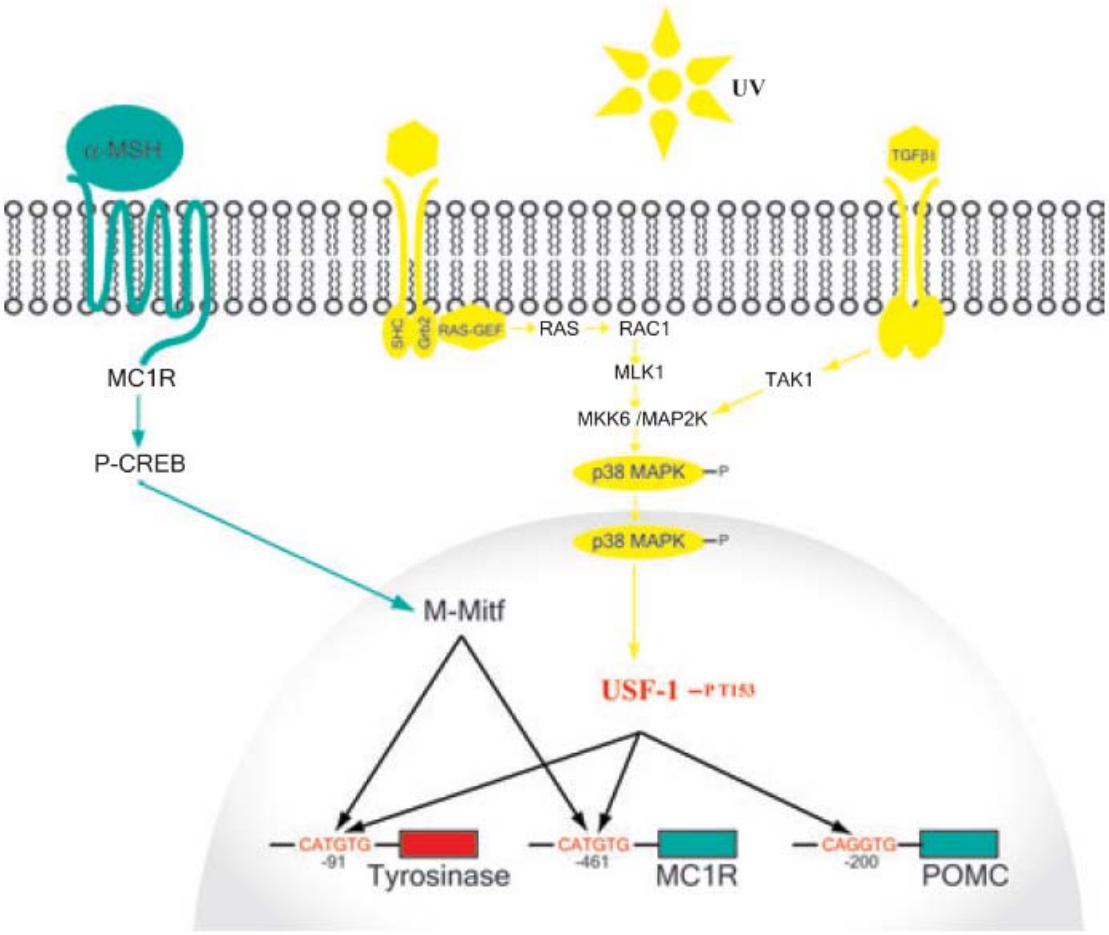

Figure 7 Tanning response via MITF and USF-1 signaling pathways in melanocytes. In response to UV radiation, USF-1 is phosphorylated on Thr-153 via p38 kinase. Phosphorylated USF1 binds to specific E-box within the promoter of TYR, MC1R and POMC leading to gene activation. Besides UV induced melanin synthesis, MITF signaling pathway is responsible for basal pigmentation. Binding of the paracrine melanocortin α-MSH to MC1R on the surface of melanocytes stimulates a cAMP pathway along with the downstream effectors PKA and CREB which together results in the activation of MITF. MITF is key for the basal gene expression of TYR, MC1R and POMC, hence responsible for constitutive level of skin pigmentation [214].

5.4.2 Oxygen and HIF-1α in skin

In the skin of mice and humans oxygen levels range from 1.5 to 5% O_2 [269-271]. Surprisingly, oxygen concentrations even in healthy skin are sufficiently low to stabilize HIF-1α and result in the up-regulated expression of the HIF-1 targeted carbonic anhydrase IX (CAIX) [272] and glucose transporter-1 (Glut-1) marker genes. In clinical and xenografted melanoma, even more limited and spatially or temporarily heterogenous oxygen tensions have been documented [273]. Hypoxia in these malignant masses often resides in narrow bands of cells adjacent to necrotic regions beyond the diffusion capacity of oxygen from blood vessels (typically 100–150 μm). Exemplified by the murine B16 cell line, melanoma cells subjected to low oxygen levels (1-2% O_2/24h) will markedly induce HIF-1α protein and activate HIF-1 signaling [266]. Moreover, when cultured B16 melanoma cells were exposed to sequential rounds of hypoxia and confluence, they progressed from a relatively benign phenotype to a

highly malignant and autonomously (i.e. unaffected by serum withdrawal) growing clonal variant within weeks [274]. Clearly, deprivation of oxygen in melanomas associates with increasingly malignant cell behavior. In this context, the hypoxia/HIF-1α signal is known to be required for an efficient melanocyte transformation, particularly in those cases where carcinogenesis is driven through a hyperactive AKT oncogene [275, 276]. This line of work further elicited the necessity of an active mammalian target of rapamycin (mTOR) kinase for the formation of AKT-driven melanomas, potentially through regulation of protein translation and HIF-1α activity during mild hypoxia. Conversely, intra-tumoral injection of a HIF-1α targeting shRNA-expressing plasmid into B16 intradermal xenografts greatly suppressed the growth of this tumor model and linked HIF-1α activity to mass accumulation and progression of melanomas *in vivo* [277]. Victor *et al.* even noted incidence of migration and invasion of wild type uveal melanoma (Mum2B) under normoxic conditions was higher than in HIF-1α knockdown Mum2B clones. Therefore, the relative low basal (normoxic) HIF-1α content in cells seems to play physiologically important role in contributing to the control of basal expression of its target genes including CXCR4, integrin β8 and antiopoietin-like factor [278].

5.4.3 Hypoxia/UV crosstalk in melanoma

Hypoxia and UV induced signaling pathways can interact at DNA level in synergy or as antagonists. As elaborated above, hypoxic preconditioning can attenuate UV-induced oxidative stress and aid in protecting fibroblasts and keratinocytes against UV induced apoptosis [279, 280].

Exposure of epidermal keratinocytes to physiological doses of UVB (10-50mJ/cm^2, equivalent to 0.2-1 minimal erythema doses) identified more than 100 UVB-induced or suppressed genes including effectors of angiogenesis, cell cycle, DNA repair, apoptosis and many more. For example, a microarray analysis of UVB-regulated genes in normal keratinocytes (NHKC) found that VEGF, one of 57 UVB-induced genes, was up-regulated by UVB (20mJ/cm^2), whereas expression of the angiogenesis inhibitor thrombospondin-1 (TSP-1) was suppressed by UVB irradiation [281, 282]. Another study confirmed this finding in UVB irradiated HaCaT keratinocytes and proposed that UVB might regulate the balance of angiogenesis in keratinocytes by inducing of VEGF expression and repressing of TSP-1 protein level [283]. Recently, UVB exposure was reported to stimulate HIF-1α expression in human keratinocytes. Here, a cytotoxic dose of 200mJ/cm^2 of UVB managed to a control HIF-1α expression with a biphasic profile--first inhibitory then stimulatory through UV mediated ROS generation. The rapid production of cytoplasmic ROS was required for this

dramatic decrease of HIF-1α, while the delayed mitochondrial ROS production up-regulated HIF-1α. The corresponding UVB induced phosphorylation and accumulation of HIF-1α was triggered by p38 MAPK and JNK signaling and mediated through production of mitochondrial ROS [284].

It is worth stressing that skin cells (often keratinocytes) were always subjected to UV radiation under non-physiological high oxygen concentrations (air) in gene profiling investigations. Not surprisingly, oxidative stress and ROS play a major role in the cellular and transcriptomic UV exposure of cells kept in air. Yet, when Matsuda and colleagues subjected normal human embryonic fibroblast-like HE49 cells to UVC radiation under physiologically hypoxic (5% O_2) and artificial normoxic (20% O_2) conditions, they found that hypoxic cells experienced a lesser build-up of ROS, lesser incidence of apoptosis and enhanced cell survival when receiving UV irradiation [279]. Analogously, Xing *et al.* reported that apoptotic rates of UVC irradiated corneal stromal cells were significantly reduced by incubation with hypoxia-preconditioned medium compared to normoxic controls. The authors suggested that hypoxia preconditioning protected stromal fibroblast and keratinocytes from UV induced apoptosis through HIF-1 mediated expression and secretion of protective factors [280]. Besides known UV-mediated induction of HIF-1 in keratinocytes, HIF-2α was recently also found to be up-regulated via an ATF3 (activating transcription factor 3) dependent pathway in human keratinocytes (HaCaT) subjected to UVC (4mJ/cm^2) at 21% oxygen. Subsequently, loss of function of HIF-2α evidenced that HIF-2α, rather than HIF-1α, mainly contributes to the UV-mediated cell death via the triggered activation of caspases 3 and 7 activation [285]. Thus, *physiological* skin-mimicking tanning responses and transcriptomic/proteomic programs have not yet been elaborated for UV-irradiated cutaneous keratinocytes and melanocytes/melanoma cells. More often than not, studies choose to elicit gene and protein responses under highly artificial hyperoxic and genotoxic conditions.

5.5 Human genes co-targeted by HIF-1α and USFs: PAI-1, TERT, L-PK and P4Hα(I)

On the molecular level, several human genes have previously been worked out to be co-regulated by HIF-1 and USF pathways. To date, this list of co-targeted genes includes those encoding the plasminogen activator inhibitor-1 (PAI-1), telomerase reverse transcriptase (TERT), L-type pyruvate kinase (L-PK) and Prolyl-4-hydroxylase α (I) (P4Hα(I)).

The plasminogen activator inhibitor type-1 (PAI-1) is the primary physiological inhibitor of tissue-type and the urokinase-type plasminogen activators (tPA and uPA). Both tPA and uPA are key fibrinolytic serine proteases which convert the proenzyme plasminogen

to the active fibrin-degrading protease plasmin. PAI-1 is multifunctional protein which modulates proteolytic processes and also participates in cancer metastasis [286]. The group of Kietzmann previously reported that the gene for rat PAI-1 (rPAI-1) was flanked by two HRE sites (HRE-1 and HRE-2), located at -182/-166 and -168/-152 from the transcription start site [287]. They demonstrated by gel supershift assays a high-affinity tethering of USF2a to rPAI-1 HRE-1 and a weaker attachment to HRE-2. HIF-1, on the other hand, attached preferably to the HRE-2 site and this complex was responsible for the enhanced rPAI-1 promoter transcriptional activity under mild hypoxia (8% oxygen). USF2a, once docked to the adjacent HRE, was able to down-regulate the HIF-1-mediated induction of rPAI-1 in primary rat hepatocytes co-transfected with USF2a and HIF-1α expression plasmids under 8% oxygen exposure [245]. Additionally, over-expression of USF2a inhibited the expression of rPAI-1 in rat hepatocytes, but not in human hepatoma cells (HepG2) [288].

The study on human PAI-1 (hPAI-1) documented two canonical E-boxes and one HRE site within the promoter of hPAI-1. The HRE site, located at -199/-181 from the transcription start site, was elicited as functional HIF-1 binding site [104]. The CACGTG E-boxes (E4 and E5) were located at -571/-552 and -689/-670 from the transcription start site. E4 and E5 served as direct binding sites for USF2a and were strictly required for the USF mediated elevation of hPAI-1 expression. Although USFs did not directly bind to the HRE, USF/E-box co-occupying complexes were critical for the transactivation of hPAI-1 promoter activity during hypoxia. A cautionary note regarding the significance of these cross-talk scenarios comes from the obvious cell specificity of the USF2a mediated hPAI-1 control [288]. Whereas in human hepatoma cells USF2a induced expression of hPAI-1, the same factor directly contributed in the transcriptional down-regulation of hPAI-1 in primary rat hepatocytes.

Telomerase reverse transcriptase TERT, the catalytic subunit of telomerase, is an essential component for enzymatic activity of telomerase and responsible for maintaining the ends of chromosomes during the division of stem, germ and many cancer cells. The gene encoding human TERT (hTERT) contains two functional HIF-α binding motifs (i: -165/-158; ii: +44/+51 relative to transcription start site). These two HRE sites are essential for the maximal induction of hTERT under hypoxia [107]. Under normoxic conditions, data by Yatabe *et al.* provide evidence for the avid attachment of c-MYC to either HRE motif in both *in vitro* and *in vivo* settings. The authors also documented a facilitated *in vivo* binding of HIF-1 to the TERT promoter when human cervical cancer cells (ME180) were challenged by hypoxia. Consequently, HIF-1 controls telomerase activity through transactivation of hTERT,

which, in turn, promotes the malignant progression of cervical cancer [108]. Besides HIF-1 and c-MYC, USFs are known to also regulate hTERT promoter activity. USFs can also bind to either HRE in the hTERT promoter and are known to suppress expression of hTERT in certain cancer cells (e.g. oral cancer cells). Thus, USFs might act as transcriptional repressor for hTERT in oral cancer cells. Consequently, loss of USF function is associated with an increase in hTERT activity, telomere maintenance and oral carcinogenesis [289]. Goueli and Janknecht documented the *in vitro* and *in vivo* interaction of the USF1/USF2 heterodimer with the upstream E-boxes of hTERT in both hTERT positive and negative cells. However, USF binding stimulated hTERT expression only in immortalized hTERT positive cells and not in non-immortalized hTERT-negative cells. Moreover, this study also revealed a further enhancement of the USF-driven hTERT activity by recruitment of the USF/p300 complex to hTERT promoter. Recruitment of USF/p300 onto hTERT DNA, in turn, was markedly attenuated through inhibition of p38-MAP kinase pathway [227].

The third example of a HIF/USF crosstalk converging onto a co-regulated target is the gene encoding the glycolytic enzyme L-type pyruvate kinase (L-PK). L-PK catalyzes the formation of pyruvate and ATP from phosphoenolypyruvate and ADP. Its gene contains a glucose response element (GlcRE) (-165/-149), which is composed of the two imperfect CACGGG and CCCGTG E-boxes separated by a 5-nucleotides spacer. Occupation of the GlcRE motif is responsible for the induction of L-PK by high glucose. USFs have been identified to dock to this GlcRE *in vitro* and thereby stimulate transcription of L-PK [290, 291]. Additionally, binding of HIF-1 to this GlcRE within the L-PK promoter was verified by EMSA [292]. Although this GlcRE seemed to function as low affinity site for HIF-1, it would still be possible that the HIF protein complex could compete with an effective USF/GlcRE interaction and disturb the USF-driven glucose dependent activation of the L-PK gene in the presence of high glucose and venous pO_2 (8% oxygen) [99, 292].

Lastly, human prolyl-4-hydroxylase α (I) (P4Hα(I)), one subunit of the main collagen hydroxylase that modifies proline and lysine residues in these extracellular matrix filaments, has been characterized as USF1/2 target gene. According to the report by Chen *et al.*, direct docking of USF1/2 to the -135 E-box of this gene positively regulates P4Hα(I) promoter activity both *in vitro* and *in vivo* [293]. Yet, both mRNA and protein levels of rat P4Hα(I) were elevated by hypoxia. The rat P4Hα(I) gene is also flanked by a functional HIF-1 binding HRE at -79/-86 on the antisense strand from the transcription start site [106].

6 General objectives

Poor cellular oxygenation, often occurring in form of heterogenous pO_2 profiles in solid malignancies, aids in promoting tumor growth, virulence and malignant progression, in part, via the hypoxia inducible transcription factor 1α (HIF-1α) signaling pathway. Since HIF-1α is stabilized and activated under hypoxic conditions, the strategies to inactivate HIF-1α function through a genetic or pharmaceutical manipulation of the hydroxylation-dependent pathway in tumor cells are currently under intense investigation. Another means to modulate HIF-1 transcriptional activity in an O_2- and hydroxylation-independent manner is thought to work through competing transcription factors. This consideration has been supported by several publications which had looked at other transcription factors, including c-MYC and upstream stimulatory factor (USF) to antagonize HIF-1-mediated gene regulation in cancer cells [98, 158, 288, 294].

We previously utilized the tripartite globin-2 gene (hb2) promoter (phb2) of the planktonic crustacean *Daphnia magna* as luciferase reporter to analyze the responsible motifs and factors underlying the prominent hypoxic induction of hb2 in heterologous transfections of human cancer cells. Two of the three E-boxes within phb2, placed at -258 and -107, were found to act as functional HIF-1 binding sites (i.e. are HREs) and were critically required for the maximal hypoxic induction of the phb2 luciferase reporter. The third motif, a CACGTG palindromic E-box at -146, interacted with an unknown constitutive transcription factor. Mutating this palindrome and disabling the constitutive factor from binding significantly increased the HIF-1 load on phb2 and amplified the reporter's hypoxic induction from 5 to 15 fold. This finding revealed that the unknown CACGTG factor was able to interfere with the hypoxia-driven induction of the phb2 reporter when transfected into human cancer cells (i.e. human hepatoma cells Hep3B) [295].

CACGTG-palindromes are notably underrepresented in mammalian cells among functional HIF elements [88, 100, 296]. Instead, these E-boxes often serve as high affinity sites for non-HIF complexes of bHLH factors, e.g. normoxic MYC/MAX heterodimers or constitutive ARNT/ARNT homodimers [154, 158, 297, 298]. In addition, CACGTG E-boxes are avidly recognized by STRA13/DEC1 [299], ATF-1 and CREB-1 [300] and USF complexes [210]. Furthermore, functional CACGTG palindromes have been reported to confer hypoxic suppression rather than induction upon target genes [158, 301]. Thus, palindrome complexes are predestined to exert a possible fine-tuning of HIF's transcriptional

read out. Indeed, multiple interactive mechanisms of HIF-1, either with MYC or USFs, have been reported (see sections 5.1.1 and 5.5 for details).

For all these reasons, the aims of my PhD project included the *a) identification of the phb2 palindrome binding entity across several human cancer cells and b) analysis of co-regulatory effects of this factor and HIF-1 on targeted human genes by in vitro and in vivo approaches.*

Regarding the first part of this thesis, the unknown constitutive CACGTG binding factor, which could significantly suppress the HIF-1/HRE-driven transactivation of the globin-2 gene, was identified in an EMSA based supershift survey. For this EMSA survey, specific antibodies against above mentioned CACGTG binding factors (USF1, 2a, 2b; ARNT; MYC; DEC1; ATF-1) were used along with normoxic nuclear extracts from human hepatoma cells (Hep3B), human breast cancer cell (MCF7) and human cervical carcinoma cells (HeLa). As a result, upstream stimulatory factors 1 and 2a (USF1 and 2a) were recognized as the main phb2-palindrome binding factors across all cell lines tested. The EMSA data were re-evaluated through independent pull-down assays of Hep3B, HeLa and MCF7 nuclear proteins using biotinylated phb2 oligonucleotides that were immobilized onto streptavidin coated magnetic beads.

While the *Daphnia* hb2 promoter was a valuable model for the initial analysis of the crosstalk between E-box binding activities, naturally we wanted to characterize the signaling events within the promoter of *human* HRE/E-box candidate genes, i.e. those containing a CACGTG palindrome E-box adjacent to or overlapping with a validated or suggested HRE motif.

To achieve this objective, a human genome-wide computational scan was conducted by Dr. Pavel Hradecky (AltraBio, Lyon, France). He searched a 5'-VNVBRCGTG-3' (V=not T; N= any; B=not A; R=A or G) HRE consensus motif [40] and a 5'-CACGTG-3' palindrome E-box within 1000bp upstream of the transcription start site of a promoter of a given gene. The distance of both motifs should be less than 100bp. 5' location and distance of both motifs were adopted from the *Daphnia* hb2 gene, coordinates (i.e. transcription start sites) of the human genes were taken from UCSC's known genes archive (hg18). Hundreds of HRE/E-box candidate genes were retrieved in the screen. We selected a few models for future studies, provided that the alignment of the homologous human-mouse-rat promoter regions had established the respective motifs to be conserved, and thus of likely functional importance.

Picked promoters with human-mouse-rat conserved cis-elements were cloned as luciferase reporter constructs and included four HRE/E-box candidates (i. lactate

dehydrogenase A, LDHA; ii. Bcl-2/E1B 19 kDa interacting protein 3, BNIP3; iii. Melanocortin 1 receptor, MC1R; iv. 4E-binding protein 1; 4EBP1) along with HIF-1 specific (prolyl hydroxylase domain 2, PHD2) and USF specific control targets (tyrosinase, TYR) to systematically examine the possible convergence of HIF and USF signaling cascades at DNA level. Experimental evaluation of these putative HIF/USF co-targets was carried out in a step-wise manner. Firstly, we examined which of the HRE/E-box reporters of the human candidate genes was responsive to hypoxia. Of the reporters screened, only the LDHA and BNIP3 constructs were robustly stimulated by low pO_2 across all three cell lines tested (Hep3B, HeLa, MCF7). Secondly, we assessed any co-regulation of these reporters as a function of over-expressed HIF-1α and USF1/2a proteins. Thirdly, to evaluate this HIF/USF convergence onto BNIP3 and LDHA motifs by an independent approach, we manipulate human cancer cells with small-interfering RNAs (siRNAs) in transient Hep3B assays or generated short hairpin RNA (shRNA) based stable MCF7 clones to silence the transcription of individual components of the HIF-1 (HIF-1α) and USF pathways (USF1, USF2a). Finally, physiological binding and interaction of HIF-1 and USFs within the promoter of LDHA and BNIP3 was assessed by parallel chromatin immunoprecipitation and EMSA analyses.

As described in the introduction, melanoma cells and melanocytes are considered to be a more physiological model for the gene regulation by HIF-1 and USF cascades. On one hand, to respond to an appropriate UV stimulus, USF signaling is key in inducing the sunblocking pigmentation that is initiated by the p38 MAP kinase-mediated phosphorylation of USF1. On the other hand, the skin of mice and humans display oxygen levels ranging from 1.5 to 5% O_2 [269-271]. Such low levels of cellular oxygenation in normal skin specifically exist at the hypovascular junction of epidermis and dermis, i.e. the layer of human skin that houses melanocytes and primary melanoma cells. The extent of this chronic hypoxia was found sufficient for the stabilization and activation of HIF-1α and several of its targets (GLUT1, CAIX) [272, 276]. Of course, even more limited and heterogenous oxygen tension (5-10 mmHg) in human melanoma xenografts has been documented [273] (see section 5.4.1 for detail).

Therefore, the third part of this thesis focused on the co-regulation of HRE/E-box genes by physiologically stimulated HIF-1α (stimulus: hypoxia) and USF (stimulus: UV irradiation) signaling pathways in human melanoma cells. Initially, we should establish the optimal UV conditions to induce phosphorylation of USF1. For this purpose, we irradiated human melanoma cells to different doses and wave-bands (UVB, UVC) of UV and assessed different post-irradiation time periods before examining the results by USF1 Western blots.

Next, we employed quantitative real time PCR to analyze the impact on various control and experimental genes when human melanoma cells were subjected to a dual stimulus set by 1% oxygen and UVB irradiation.

7 Own research

The following sections summarize the data submitted in the manuscripts enclosed with this work.

7.1 Identifying the unknown transcription factor that exerts HIF/HRE-interference from the -146 CACGTG E-box within the promoter of *Daphnia magna*'s globin-2 gene

As mentioned above, palindrome CACGTG motifs frequently serve as a strong binding sites for several non-HIF bHLH transcription factors including ARNT [154, 298], MYC [152, 153], USFs [210], STRA13/DEC1 [299], ATF-1 and CREB-1 [300]. Semenza and colleagues were the first to describe that a constitutively expressed factor could recognize the same DNA sequence as HIF-1 within the promoter of genes encoding glycolytic enzymes and the enhancer of EPO. A decreased binding of HIF-1 in hypoxia protein extract resulted from a competition with a binding of the constitutive factor [88, 302].

Our previous study on the control of the hypoxia inducible globin-2 (hb2) gene of *Daphnia* revealed that the cooperative binding of HIF-1 to two of the promoter's functional HREs was completely required for the enhanced transcriptional activity of the gene's tripartite promoter (phb2) during low pO_2. In transfections of human hepatoma cells (Hep3B), we noted that the binding of an unknown constitutive factor to the third phb2 motif, a CACGTG palindrome at position -146, significantly weakened the HIF/HRE-mediated hypoxic induction of the reporter. This finding suggested that a constitutive and cancer cell expressed CACGTG-binding factor was able to interfere with the HIF-1/HRE-driven induction of a downstream oxygen-sensitive target [295].

To identify this unknown HIF-interference factor, an EMSA supershift survey was conducted using the -146 CACGTG sequence of the phb2 and different antibodies USF, DEC1, MYC, ARNT and ATF-1. Given the constitutive nature of the -146 constituents, the survey was carried out with normoxic nuclear extracts from human hepatoma cells (Hep3B), human breast cancer cell (MCF7) and human cervical carcinoma cells (HeLa). The screening revealed that USF1 and USF2 functioned as main bHLH factors enabling to bind *in vitro* to the phb2 palindrome at -146. In addition, DEC1 participated as a minor addition to this constitutive complex. Next, we carried out oligonucleotide-based pull-down assays and were able to confirm the avid interaction of USF1, USF2a and USF2b with the oligoucleotide housing the wildtype, but not mutant, CACGTG palindrome of the -146 phb2 motif.

7.2 Co-regulatory effects of HIF-1 and USFs on human HRE/E-box genes

The *Daphnia* globin 2 promoter had served as valuable model for the initial exploration of the cross-talk between HIF-1 and USF signaling pathways. Ultimately, however, we wanted to learn which *human* genes feature a similar HRE/E-box configuration of adjacent or overlapping candidate HRE and CACGTG palindromes in their promoter and thus might be co-responsive to incoming HIF and USF signals. As explained in General Objective (section 5) and our manuscript, a human genome-wide computational scan was conducted by Dr. P. Hradecky. According to his results, several HRE/E-box and control genes were selected and cloned into luciferase reporter plasmid for further analysis. Selection of HRE/E-box and control genes was always guided by our own alignments of promoter regions, which were established the conservation, hence alleged functionality, of the respective motif in a human-mouse-rat matrix of species. The final list of generated luciferase reporter constructs included HIF-1 specific (prolyl hydroxylase domain 2, PHD2) and USF-specific (tyrosinase, TYR) control promoters as well as the 5' regulatory DNA of four HRE/E-box candidate genes (lactate dehydrogenase A, LDHA; Bcl-2/E1B 19 kDa interacting protein3, BNIP3; eukaryotic translation initiation factor 4E binding protein 1, 4EBP1; melanocortin receptor 1, MC1R). Of those, the PHD2 and BNIP3 constructs were kindly provided as generous gifts provided by other labs (see manuscript for acknowledgments).

Luciferase assay for analysis of co-regulation of these four HRE/E-box candidate genes by HIF/USF signaling cascades

To determine the hypoxia responsiveness of the above HRE/E-box candidate genes, Hep3B, HeLa and MCF7 cells were transfected with the luciferase reporter constructs of the corresponding promoter. According to these luciferase assays, of the four HRE/E-box candidates 4EBP1, LDHA, MC1R and BNIP3, only the LDHA and BNIP3 reporter revealed a robust up-regulation by hypoxic conditions (16h, 1% O_2) in all three cell lines. We went on to analyze the impact of over-expression of a) HIF-1α, b) USF1 and 2a and c) HIF-1α + USFs in subsequent luciferase assays. Over-expression of HIF-1α amplified the hypoxic activity of the BNIP3 reporter robustly in Hep3B (i.e. 2.8 fold → 6.6 fold, endogenous hypoxia/normoxia (H/N) ratio of relative luciferase activities → H/N ratio with over-expressed HIF-1α) and moderately in HeLa cells (H/N: 2.7 → 3.2 fold). Importantly, this potentiated hypoxia response of BNIP3 by exogenous HIF-1α was significantly impaired by simultaneous co-transfection with USF1 or USF2a, but not USF2b, in Hep3B and HeLa cells. Endogenous and HIF-1α-mediated up-regulation of hypoxic LDHA reporter activity was

similarly reduced by over-expression of USF1 or USF2a in a dose-dependent manner due to the enhanced normoxic transcription from the LDHA promoter.

Next, we opted to revisit the mutual influence of these pathways on one another by using an RNA interference loss-of-function approach in order to gain independence of the potentially artificial over-expression of considered HIF-1 and USF factors. For this purpose, we generated, and verified, a small hairpin RNA (shRNA)-based stable MCF7 knockdown line for USF2a along with equally treated and selected shRNA control clones. We also received as generous gift a stable HIF-1α shRNA MCF7 knockdown clone from Dr. D. Stiehl. The ~7-fold hypoxic induction by endogenous pathways of the LDHA reporter, was further enhanced in the USF2a knockdown clone (H/N: 9.3-fold), due to the significantly reduced normoxic reporter activation to ~60% of control cells. HIF-1α shRNA-based loss-of-function completely obliterated LDHA induction in low pO_2. In USF2a knockdown cells, over-expressed HIF-1α augmented primarily the normoxic reporter activity, hinting to HIF's take-over of the USF-deficient control of the LDHA promoter. Conversely, when adding exogenous USF1 and 2a, the LDHA reporter responded again with a marked increase of its normoxic and hypoxic activities in HIF-1α knockdown cells. It thus appears that HIF-1 and USFs substitute one another in the LDHA promoter and compensate the loss-of-function of the other activity.

Transfection with BNIP3 luciferase reporter construct in these kd MCF7 variants revealed that a) HIF-1α loss-of-function again completely abrogated the hypoxic expression of the BNIP3 luciferase reporter, thereby confirming the strict requirement of HIF-1α to control the induction of the BNIP3 gene in MCF7 during low oxygen and b) USF-HIF competition for BNIP3 was indicated in USF2a kd MCF7 through a tenuous increase in the hypoxic stimulation of the reporter relative to shRNA control cells. To reveal this competition more clearly we resorted to reporter transfections in conjunction with transient siRNA-based manipulations of HIF-1α, USF1 and USF2a protein levels in Hep3B cells. Here, the HIF/USF competition for BNIP3 was made evident through a significant raise of hypoxic reporter activities in cells treated with USF1 siRNA. There also was an increase in the hypoxic induction of the BNIP3 reporter in siUSF2a treated cells.

Characterization the in vivo and in vitro binding of HIF-1 and USFs to BNIP3 and LDHA promoter DNA

To examine the *in vivo* binding of HIF-1 and USFs to the promoter of BNIP3 and LDHA, chromatin immunoprecipitation (ChIP) assays were performed in HeLa, Hep3B and

MCF7 cells. For BNIP3, ChIP revealed the dominant *in vivo* binding of HIF-1α to the promoter (region assessed: -509/-196 from translation start site) in deoxygenated cells along with the weak and constitutive attachment of USF1 and 2a to this DNA. Remarkably, some HIF-1α had successfully escaped proteolytic degradation since it was detected, as heterodimer, bound to the BNIP3 promoter in normoxic cells. Towards the precise location of bound HIF and USF proteins in the regulatory region of the human BNIP3 gene, EMSA screens with a single site oligonucleotide (-259 to -236) characterized the BNIP3 E-box as a surprisingly poor HIF-1 motif during hypoxia. In contrast, constitutive USF1 and 2a complexes were attracted to this site with high-affinity. Thus, the BNIP3 HRE at -251/-246 is in hypoxic cells co-targeted by HIF-1 and USFs.

LDHA ChIP analysis clearly demonstrated the co-occupation of USF1 and USF2a to the human LDHA promoter (region: -2533/-2376 from translation start site) *in vivo* during periods of normoxia. Therefore, these data strengthen the role of USFs as physiological drivers of aerobic glycolysis in cancer cells (Warburg effect). In contrast, binding of HIF-1 to the upstream LDHA DNA under high oxygen levels was negligible in both cell lines (contrast to BNIP3 promoter). In low O_2, HIF-1 dominates the LDHA promoter in MCF7 cells, while both USFs maintain their association with this DNA. DNA-attachment of HIF-1 does not appear to displace USFs from the upstream recognition sites of LDHA, in support of the notion that maximal LDHA transcription during low pO_2 stems from a parallel and independent transcriptional control by HIF-1 and USF1/2a. Follow-up EMSA's disentangled the specific binding motifs of HIF-1 and USFs within the LDHA promoter. The palindrome in region II of LDHA (-2367 to -2362: 5'-CACGTG-3') and the E-box in region III (-2353 to -2345: 5'-GACGTG-3' on anti-sense strand) functioned in these assays as specific USF2 (reg. II) and HIF-1 (reg. III) binding sites, respectively. Region I of the LDHA 5' flank (-2465 to -2460: 5'-CACGTG-3'), known to act as MYC binding site at position -175/–180 from the transcription start site of the rat LDHA gene [160], represented a weak HIF-1 site and strong USF1 and USF2a site. Presence of these distinct, non-overlapping sites in the LDHA promoter by HIF-1 and USFs might be an important element for the mutually independent influence of either cascade in regulating this HRE/E-box gene (contrast to BNIP3 sites and mode of regulation).

7.3 Study on HIF-1/USFs signaling pathways during hypoxia/UV co-stimulation of human melanoma cells.

Human M000921 melanoma cells: Western blot for phosphorylation of USF1 and real-time PCR for target genes expression TYR and MC1R under UV radiation

The human M000921 melanoma cell line, directly isolated from a patient, was kindly provided by Prof. R. Dummer's lab (University hospital of Zurich). M000921 cells were exposed to three different doses of UVC (254 nm): 2, 4 and 8mJ/cm^2. Cells were harvested at 2h and 6h post- irradiation. 80µg whole cell extract was subjected to Western blot to monitor the UV-induced phosphorylation of USF1 as a reflection of the physiological, tanning-like activation of USF signaling in cultured melanomas. Results indicated that UVC (8mJ/cm^2, 2h) induced the appearance of a band of lesser mobility corresponding to 45kDa phosphorylated form of USF1 (p-USF1). P-USF1 was made visible using the rabbit polyclonal anti-USF1 (C-20; sc-229) from Santa Cruz Biotechnology, INC, because the original anti-USF1M antiserum used in our manuscript failed to detect the low migrated USF1 band. Extending the post-irradiation exposure to 6h yielded a visible phosphorylated form of USF1 in all three doses of UVC. Repeating the experiment with 4mJ/cm^2 UVC at 2h and 6h post-irradiation collection of cells confirmed the induction of p-USF1 in M000921 cells (Fig. 8A). To evaluate the impact of such UV exposure, M000921 cells were irradiated with these three doses (2, 4, 8mJ/cm^2) of UVC and cell viability was assessed by Trypanblue staining at 8, 24 and 48h post-irradiation time points. Growth rates of control and UVC treated M000921 cells at the 48h post-irradiation time point clearly demonstrated the marked slow-down (2mJ/cm^2 UVC) or complete arrest of growth (8mJ/cm^2 UVC), whereas growth rates of non-irradiated controls showed an average 5-6 increase after 48h (data not shown). To minimize the cytotoxic impact of UVC radiation on these cells, we choose low doses of UVC (1, 2 and 4mJ/cm^2) for further gene expression profiling as a function of UVC exposure.

To examine the UVC response of TYR and MC1R gene expression in M000921, cells were exposed to three different doses of UVC, 1, 2 and 4mJ/cm^2. Growth arrest and DNA-damage-inducible, 45 alpha (GADD45a), a DNA damage marker gene, was taken as positive control since elevated GADD45a transcription is a known response of melanoma and melanocytes to UV [303, 304]. Total mRNA was isolated from M000921 cells according to the TRIzol® reagent manual (Invitrogen) after 5h of UVC exposure. Real-time quantitative PCR (qPCR) revealed the dose-dependent up-regulation of GADD45a mRNA levels in M000921 cells subjected to UVC irradiation (fold induction of GADD45a mRNA by UVC: ~2.5 fold at 1mJ/cm^2; 4 fold at 2mJ/cm^2 and 5 fold at 4mJ/cm^2; see Fig. 8B). Surprisingly, TYR and MC1R mRNA transcripts responded with a dose-dependent down-regulation, not induction, in UVC irradiated M000921 cells (TYR / MC1R mRNA levels: reduction to 60% / 40% of non-irradiated cells, respectively, when M000921 cells had been irradiated with 4mJ/cm^2 of UVC; Fig. 8B). Since we did not observe any up-regulation of TYR and MC1R

even at low doses (1 and 2mJ/cm^2) of UVC, our finding is at odds with those of Galibert *et al.* [235]. The stimulated transcription of GADD45a even by a low dose of 1mJ/cm^2 UVC implied ongoing DNA damage throughout all UVC-irradiation protocols of M000921 cells. Moreover, UVC wave bands are hardly of physiological relevance, since this quality of ultraviolet radiation is absorbed by atmospheric ozone and does not reach the Earth's surface. UVB radiation (312 nm), on the other hand, has clearly pathophysiological significance since it is thought to represent the most carcinogenic waveband [259]. Thus, we switched to UVB for further tests in M000921.

A.

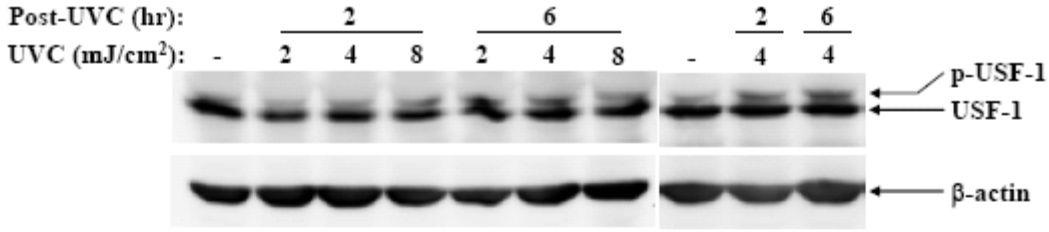

B.

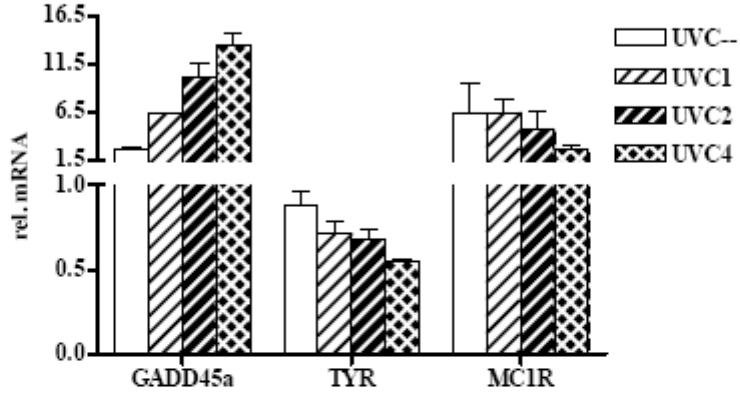

C.

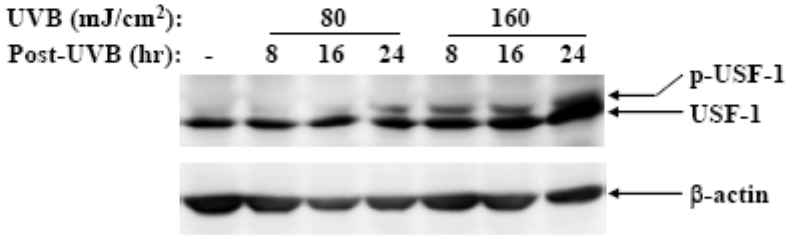

D.

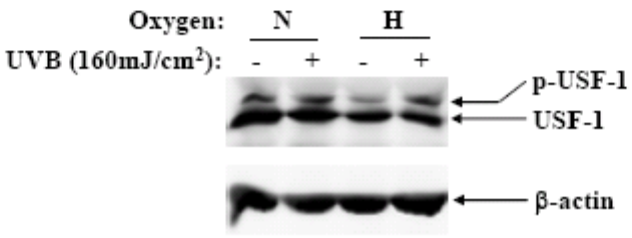

Figure 8 Exposure of M000921 melanoma cells to UV irradiation (A) Western blot analysis for p-USF1 in M000921 cells irradiated with three different doses (2, 4 and 8mJ/cm^2) of UVC (254nm) and exposed to normoxia. Whole cell extracts were isolated at 2h and 6h after irradiation und subjected to Western blot analysis with anti-USF1 (C-20, Santa Cruz). (B) Real-time qPCR was performed using total mRNAs extracted from normoxic M000921 cells at 5h post-exposure to 1, 2 and 4mJ/cm^2 of UVC. Relative mRNA levels of GADD45a, TYR and MC1R genes were normalized by L28 mRNA and documented by mean expression ± SD of two independent experiments. (C) Western blot analysis for p-USF1 in M000921 cells which were harvested at time points 8, 16 and 24h after irradiation with two doses (80 and 160mJ/cm^2) of UVB (312nm) under normoxia. (D) Western blot analysis for p-USF1 in M000921 cells harvested at 8h post-UVB (160mJ/cm^2). For co-stimulation of hypoxia and UV cascades, cells were exposed to 1% oxygen for 16h prior to UVB (160mJ/cm^2) and were grown for another 8h after irradiation under hypoxia.

To start out, normoxic M000921 cells were irradiated with two 80 and 160mJ/cm^2 doses of UVB (312nm) and subsequently harvested at 8, 16 and 24h post-irradiation time points. Immunoblots revealed occurrence of phosphorylated USF1 24h after low dose of UVB (80mJ/cm^2). A higher UVB dose (160mJ/cm^2) could induce p-USF1 even at 8h post-irradiation (Fig. 8C). En route to the hypoxia/UV exposures, we compared the impact on USF signaling under normoxic/UVB and hypoxic/UVB co-stimulation scenarios in M000921 cells. Prior to UVB stimulation, cells were exposed to 1% oxygen for 16h, then irradiated with UVB (160mJ/cm^2) in the hypoxic camber and then grown for another 8h either in air (N, normoxic cells) or under 1% oxygen (H, hypoxic cells). Unexpectedly, we observed a similar extent in the phosphorylation of USF1 in both non-irradiated and irradiated cells under normoxia (Fig. 8D). Further exposures and immunoblots also yielded ambiguous results so that a clear and reproducible induction of USF1 phosphorylation never emerged. Since M000921 cells had also not yet been characterized for the UV-mediated induction of the USF1 cascade, we opted to switch to human melanoma 501mel cells, a well-characterized UV response resource.

501mel cells: USF1 phosphorylation and expression of control and HRE/E-box target genes under single and dual stimulation regimes

In adopting previously published protocols, human melanoma 501mel cells were exposed to 8, 20, 40 and 80mJ/cm^2 doses of UVB radiation and 2 or 5h post-irradiation recovery periods until harvest [267, 268]. To exclude any disturbance on the induction of USF phosphorylation by varying O_2 concentrations, normoxic 501mel cells were UVB-irradiated and kept for recovery under normoxia (contrast to treatment of normoxic M000921 cells, see above). In 501mel cells exposed to air or 1% oxygen, USF1 was optimally phosphorylated by 40mJ/cm^2 UVB and 2 or 5h post-irradiation response time points (Fig. 9A). As with M000921 cells, hypoxia/UV dual stimulation of 501mel cells (Fig. 9A) included a 1% O_2/16h adaptation (HIF-1 activation) period prior to the UVB stimulus. However, subsequent

experiments with 501mel cells, while revealing a clear UVB induced USF1 phosphorylation during normoxic pO_2, resulted in unpredictable USF1 activation profiles in hypoxia. In some exposures, hypoxia (1% O_2/16h) alone yielded USF1 phosphorylation (Fig. 9B left panel).

To better understand the nature of the observed double banding pattern of USF1 upon UV irradiation, we recalled that phosphorylation of USF1 is thought of being exclusively mediated by p38 (MAP) kinase in response to UV light [235]. To verify that the lesser migrating USF1 band corresponds to the phosphorylated form of USF1 (p-USF1), 501mel cells were treated with 10μM or 20μM of the specific p38 inhibitor SB203580 (SB in Fig. 9B) for 1h prior to UVB exposure. Unexpectedly, this UVB induced second band of lesser mobility of USF1 was completely refractory to SB203580 (Fig. 9B right panel), implying either that USF1 phosphorylation in our batch of 501mel cells is carried out by alternative kinases, distinct of p38, or that the upper band does not represent p-USF1 but perhaps a different UV-induced post-translational modification of USF1.

For expression profiling, 501mel cells were subjected to four different conditions: air - UVB, air + UVB, 1% O_2 - UVB and 1% O_2 + UVB. For an appropriate co-stimulation of hypoxia/UVB signaling and to avoid saturating p38 kinase activation by hypoxia alone (see above, Fig. 9B left), the hypoxic exposure prior to UVB (40mJ/cm^2) stimulation was reduced from 16h to 2h. After UVB exposure, cells were kept for additional 5h in normoxic or hypoxic atmosphere followed by total mRNAs extraction. In subsequent qPCRs TYR, MC1R, PHD2, LDHA and BNIP3 mRNA levels expression were elucidated for the aforementioned conditions. As expected, mRNA level of the HIF-1 target PHD2 was 3-4 fold induced by hypoxia. In contrast, transcription of the USF targeted genes, TYR and MC1R, was unaffected by oxygen in 501mel cells. Also BNIP3 mRNA was robustly (4-fold) up-regulated by hypoxia, while the LDHA transcript only showed a marginal (1.5 fold) hypoxic induction. 1% O_2- UVB and 1% O_2+UVB regimes did not alter the original hypoxia response of PHD2, LDHA and BNIP3 transcript (Fig. 9C). To our surprise and disappointment, there was no transcriptional activation of either TYR or MC1R mRNAs to air + UVB or 1% O_2+UVB co-stimulatory exposures in 501mel cells (Fig. 9C).

To assess if this lack of TYR or MC1R induction by UV stems from a technical or cell related problem, we resorted again to UVC treatment despite the unphysiological nature of this signal (see above). Thus, normoxic 501mel cells were irradiated with three different UVC doses (1, 2 and 4mJ/cm^2). To analyze alteration of GADD45a, TYR and MC1R mRNA levels, total RNA was isolated 5h after UVC irradiation and qPCR was performed. Similar to M000921 cells, GADD45a mRNA levels in 501mel cells were dose-dependently up-regulated

by UVC irradiation, while steady state levels of TYR and MC1R transcripts were reduced by UVC exposure (Fig. 9D). The amplitude of this down-regulation was considerable. A dose of 4mJ/cm^2 of UVC decreased TYR and MC1R mRNA levels to 45% and 30% of control levels

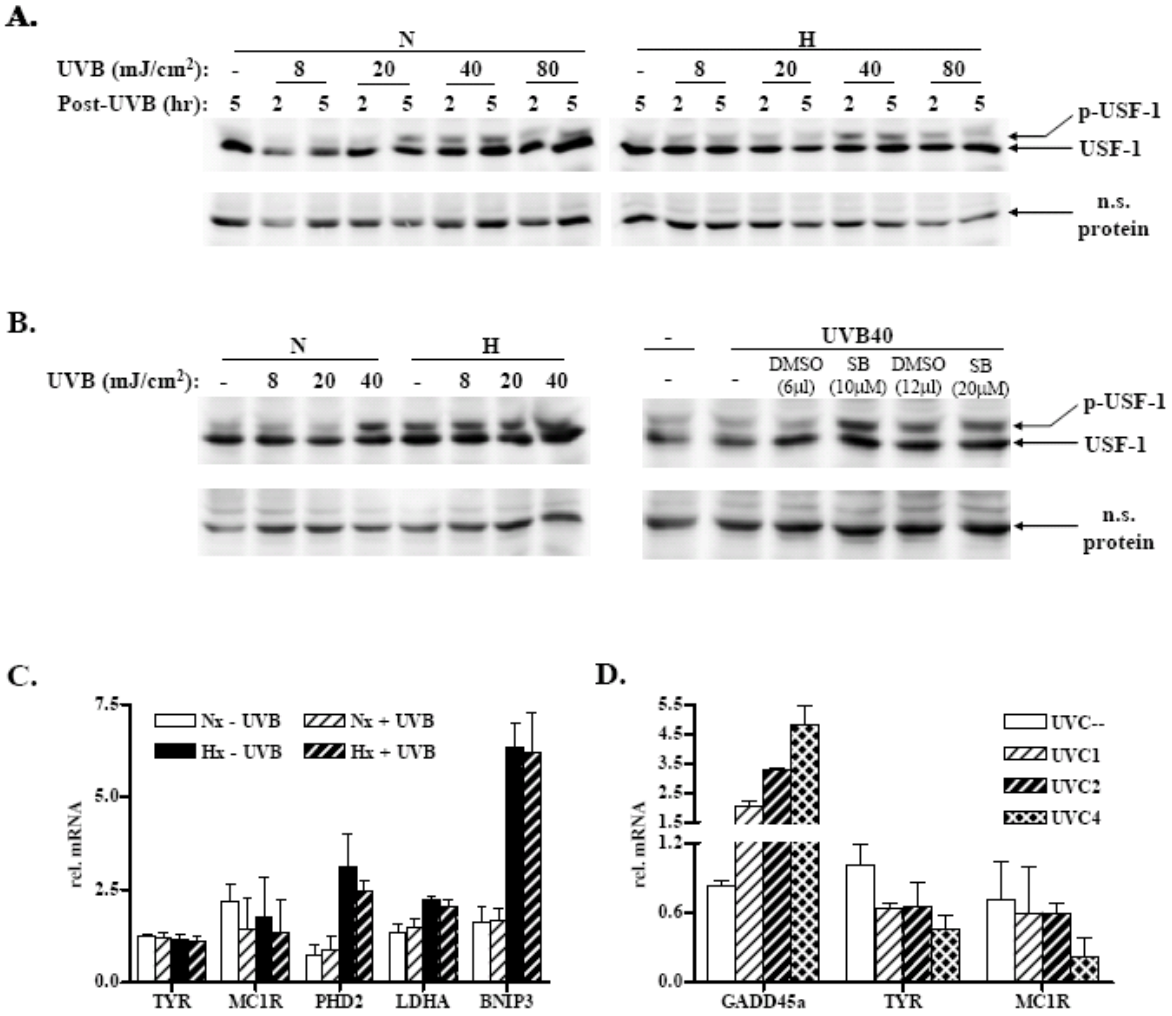

Figure 9 Exposure of human melanoma 501mel cells to UV irradiation. (A) Western blot analysis using anti-USF1 antibody (C-20, Santa Cruz) and whole cell extracts of 501mel cells subjected to four different doses (8, 20, 40 and 80mJ/cm^2) of UVB (312nm). Protein was harvested at indicated post-UVB stimulation time points. Cells were exposed to air (N) (left panel) and 1% oxygen (H) (right panel), respectively. For combined stimulation of hypoxia and UVB, cells were exposed to 1% oxygen for 2h prior to UVB and were grown for another 2 and 5h after irradiation under hypoxia. (B) Western blot analysis for p-USF1 in normoxic and hypoxic 501mel cells exposed to three different doses of UVB as indicated with protein harvests at 5h post-UVB (left panel). Normoxic 501mel cells were pre-treated with the p38 family kinase inhibitor SB203580 (at 10µM and 20µM final concentration, 1h prior to UVB exposure) (right panel). (C) Real-time qPCR was performed for TYR, MC1R, PHD2, LDHA and BNIP3 gene expression in 501mel cells exposed to UVB (40mJ/cm^2; 5h post-UV harvest) and hypoxia (2h → +UVB → 5h post-UV harvest). Relative mRNA expression level of these five genes was normalized by L28 and recorded as mean expression ± SD of two independent experiments. (D) Real-time qPCR for GADD45a, TYR and MC1R transcripts was performed using total mRNAs extracted from normoxic 501mel cells at 5h after exposure to 1, 2 and 4mJ/cm^2 of UVC. Relative mRNA levels were normalized by L28 and recorded as mean expression ± SD of two independent experiments.

(no UVC exposure) in 501mel cells, respectively (Fig. 9D). This lack of UV response together with the resistance of the UV-induced modification of USF1 to the p38 inhibitor SB203580 (Fig. 9B, right) point either to defects in the UV-induced USF signaling pathway or to UV-

triggered post-translational alterations of USF1 (= upper band in Western blots) that are distinct from a phosphorylation. In this context, various stresses have recently been reported to lead to an acetylation of USF1, which, in turn, no longer activates but suppresses the transcription of targeted genes [268]. For future work it will be necessary to find out if exposure of 501mel and M000921 cells to UVB and UVC under our cell culture conditions analogously resulted in USF1 acetylation rather than phosphorylation.

8 Conclusions and Outlook

8.1 Conclusions

Low oxygen partial pressure (hypoxia) is a main characteristic of human solid tumors. Control and workings of the hypoxic-inducible factor 1 (HIF-1) are relatively well understood. In hypoxic cells, the alpha subunits HIF-1α and -2α are rendered stable, translocate into the nucleus and dimerize with HIF-1β aka ARNT to generate the HRE-binding HIF-1 and HIF-2 heterodimeric complexes that are responsible for promoting tumor growth in various cancer settings. The discovery of PHD and FIH-1 class dioxygenases as O_2 sensors of the HIF-1/-2 signaling pathway opens the opportunity to pharmacologically manipulate both abundance and transcriptional activity of the HIF cascade. The supply of high-affinity PHD/FIH-1 substrates or inhibitors and generation of gain-of-function mutant PHD/FIH-1 variants can antagonize excessive HIF function in malignant growths. Yet, all the PHD/FIH-based interceptions of HIF signaling require oxygen. To effectively target a derailed HIF pathway in severely hypoxic or even anoxic cells alternative and hydroxylase-independent means are needed. HIF-competing transcription factors might be such a novel approach to modulate or interfere with the hypoxic adaptations of neoplastic cells that are governed by HIF-1 and HIF-2.

We previously reported on the specific binding of a constitutive, human hepatoma cell (Hep3B)-expressed transcription factor to the CACGTG E-box palindrome at position -146 adjacent to two functional HREs in the promoter of a hypoxia inducible globin2 gene (hb2) of *Daphnia magna* (i.e. phb2). Interaction of this complex with the -146 phb2 palindrome counteracted with the HIF-driven induction of a phb2 luciferase reporter [295].

As mentioned in the 6th and 7th sections, E-box palindromes of the CACGTG type are frequently bound by homo- or heterodimeric complexes of several bHLH transcription factors including ARNT, MYC, USF, STRA13/DEC1, ATF-1 and CREB-1 [152-154, 210, 298-300]. A recent review reported two modes of HIF-mediated hypoxic suppression of MYC transactivation of gene expression: one mode is that HIF displaces MYC from the MYC-activated promoter thereby leading to hypoxic repression of cell cycle and DNA repair genes; the other mode is the HIF-driven activation of the expression of MAX interactor 1 (MXI1), which is an inhibitor of MYC [294]. In addition, other bHLH/PAS family transcription factors, e.g. Single Minded 1 and 2 (SIM 1 and 2), can functionally interfere with HIF-1 transactivation by sequestering ARNT [305, 306].

To study the precise mechanisms by which the palindrome complex in phb2 interferes with the transcriptional activity of HIF-1, the aims of this thesis were twofold: *1) to identify this phb2 CACGTG-binding transcription factor and describe its occurrence across several cancer cell lines and 2) to investigate the factors interplay with HIF-1α in the control of co-targeted genes.*

To identify which of the above mentioned bHLH transcription factors are able to bind to the -146 CACGTG E-box in phb2, electrophoretic mobility shift assays (EMSA) and oligonucleotide pull-down assays were performed with nuclear extracts from Hep3B, HeLa and MCF7 cell lines. Both methods consistently and reproducibly (n=2-3 supershifts; n=2-4 pull-downs per cell line) identified USF1 and USF2a/2b as the main *in vitro* complex of the -146 CACGTG-palindrome of phb2 in the nuclear extracts of all three cancer cell lines. Furthermore, the oligonucleotide-based pull-down surveys demonstrated the avid tethering of USF proteins to the symmetric phb2 E-box whereas the asymmetric TACGTG HRE motifs of the *Daphnia* promoter were found to strongly attract HIF-1. This observation agreed not only with several papers describing CACGTG-palindromes as comparatively poor HIF-1/-2 binding motifs [87, 100, 296] but also with the EMSA results of the various phb2 cis-elements reported in the earlier publication [295]. Co-immunoprecipitations failed to show any direct interaction between HIF-1 subunits and USF2a. Krones *et al.* provided similar evidence that there was no physical direct interaction between HIF-1 and USF in their study on the cross-talk of HIF and USF on L-type pyruvate kinase (L-PK) [292]. In conclusion, the -146 CACGTG palindrome of *Daphnia's* hb-2 promoter functions unequivocally as strong docking site for USF1 and 2a in human cancer cells and the USF complex exerts its indirect interference onto the HIF/HRE-mediated transactivation of the downstream reporter.

The *Daphnia* hb2 gene promoter was considered as technical tool to initiate the investigation of the interplay HIF-1/HRE and USF/CACGTG complexes. Ultimately, we wanted to learn which *human* genes, flanked by an adjacent or overlapping HRE/palindrome (PAL) motif signature in their promoter, might be co-targeted by HIF and USF signals. As explained General Objective (section 6) and in our manuscript, we finally obtained a range of luciferase reporter constructs including only HIF-specific (PHD2) and USF-specific gene (TYR) promoters as well as 4 HRE/E-box candidate genes: 4EBP1, LDHA, MC1R and BNIP3 for further investigation in Hep3B, MCF7 and HeLa cells.

When assessing hypoxia (1% O_2, 16hr) responsiveness of these HRE/E-box reporters, only LDHA and BNIP3 construct showed markedly elevated luciferase transcription during

low oxygen across all three cell lines. This hypoxic induction of LDHA and BNIP3 expression was consistent with two previous publications [90, 100].

Next, the interplay between HIF-1α and USF1/2a in the LDHA promoter was evaluated by overexpressing (Hep3B, HeLa) or silencing (MCF7) HIF and USF components in the indicated cancer cells. Co-overexpression of HIF-1α and USF1 led to a mutual increase in the LDHA promoter activity in Hep3B and HeLa cells, but surprisingly not in MCF7. We surmised that in MCF7 an extremely efficient production and/or promoter attachment of exogenous HIF-1α completely saturated the LDHA sites even under normoxia (18-fold normoxic enhancement of LDHA promoter activity by exogenous HIF-1α), thus rendering this DNA no longer accessible for accessory USFs. Short-hairpin RNA-based stable knockdown of HIF-1α and USF2a in MCF7 revealed HIF-1 and USFs could compensate the silencing of the other activity and further confirmed the mutually supporting effect of both signaling pathways on LDHA promoter.

The following EMSA and chromatin immunoprecipitation (ChIP) analyses allowed to reveal the *in vivo* convergence of HIF and USF pathways onto the LDHA promoter as well as to determine the distinct binding sites of these factors within this DNA. According to our ChIP results, USF1 and 2a bind to LDHA promoter in oxygen-independent manner whereas HIF-1α resides in the promoter exclusively during hypoxic periods. Docking of HIF-1 to the LDHA promoter left the USF attachment to this DNA undisturbed. Utilizing the EMSA technique, we observed that HIF-1α and USF1/2a could mutually occupy the CACGTG site at position -2465, named region I. However, USF1/2 exhibited a much stronger binding affinity to this motif than HIF-1α. The other CACGTG element at position -2367, called region II, was exclusively bound by USF1/2a whereas the GACGTG (on the antisense strand) at position -2353 (region III) turned out to act as specific HIF-1 binding site. Two previous studies on rat and mouse LDHA evidenced the occupancy of c-MYC and HIF-1 to the same region of the genes' promoter. Shim *et al.* reported that the constitutive transactivation of rat LDHA gene expression required the direct occupancy of c-MYC at two E-boxes, corresponding to regions I and II of human LDHA mentioned above [160]. On the other hand, Semenza's lab validated in 1996 a strong binding HIF-1α binding site in mouse LDHA, which corresponded to region III in human LDHA [87]. Both papers reported that c-MYC and HIF-1α could transactivate LDHA expression.

In contrast to LDHA, the mutual control of the BNIP3 luciferase construct occurred via a competitive effect between HIF-1α and USF1/2a. It was particularly noticeable when Hep3B or HeLa cells were co-transfected with HIF-1α together with a low amount (15ng) of

USF1/2a plasmids. Loss-of-function (LoF) approaches to knockdown either HIF-1α or USF signaling pathway in Hep3B cells reproduced this competitive effect in the sense that siUSF1 treatment achieved a significantly potentiated hypoxic BNIP3 activity while siUSF2a manipulation yielded a raise in the hypoxic/normoxic ratio of the reporters' transcription. Thus, the HIF-1α-mediated hypoxic induction of BNIP3 can be antagonized by active USF signaling.

Subsequent EMSA and ChIP data for BNIP3 demonstrated the binding of HIF-1 under *in vitro* and *in vivo* conditions to the HRE site at position -246 of the promoter in line with an earlier report by Kothari *et al.* [90]. Although this HRE site reads as CACGTG E-box palindrome, to date, there is no literature available with regard to a competition of HIF-1 with other transcription factors for the same BNIP3 site. Our ChIP and EMSA data provided convincing evidence that USF 1 and 2a also, yet constitutively, interacted with the -246 BNIP3 HRE site *in vivo* and *in vitro*. In contrast, interaction of a HIF-1/HRE complex formed predominantly but not exclusively under hypoxic pO_2. Some HIF-1α had obviously escaped proteolytic degradation and functioned as transcriptionally competent factor since it remained tethered, as HIF-1 heterodimer, to the BNIP3 promoter even in normoxic cells. Moreover, the hypoxic dominance of HIF-1 interaction with the BNIP3 HRE did not displace attached USF proteins, suggesting that the latter might actually attach to accessory motifs in close proximity to the HRE rather than the HRE itself. Interaction of USF1 and 2a with these accessory motifs allows for a basal transcription activity of BNIP3 under normoxic condition and perhaps for a fine-tuned hypoxic activation of the BNIP3 gene via HIF-1. Activated USF signaling lends itself to interfere with the HIF-driven control of BNIP3 in deoxygenated cancer cells.

During the silencing of USF2a in MCF7 (shRNA-based stable knockdown) and USF1 or USF2a in Hep3B cells (siRNA-based transient knockdowns), we unexpectedly yet reproducibly observed that USF1 protein level was also visibly reduced in USF2a knockdown MCF7 and Hep3B cells. A similar asymmetrical cross-regulation of USF1 by USF2a was seen in mouse embryonic fibroblasts (MEF) of $USF1^{-/-}$ or $USF2a^{-/-}$ mice [246]. However, this finding was challenged by a report of Vallet *et al.* on USF1 and 2a protein levels from the liver of $USF1^{-/-}$ or $USF2a^{-/-}$ knockout mice. They did not observe any alteration of USF1 protein level in the liver of $USF2^{-/-}$ mice [248]. In our study, used siRNA and shRNA recognized the partially conserved region at nucleotides 786-806 of USF2a (i.e. the shRNA used for generating the USF2a kd MCF7 clone contained an octamer (nucleotides 787-794: CCAGACTG) which is conserved in USF1 and USF2a transcripts). Thus, either the reduction of USF1 mRNA in cells transfected by the siUSF2a siRNA/shRNA resulted from the

insufficient USF2a specificity of the sequence or USF2a is required to directly or indirectly activate USF1 transcription in certain cancer cells.

Returning to the HIF/USF cross-talk at DNA level, we also aimed to utilize a more physiological strategy to study the differential impact of both cascades on the control of human HRE/E-box genes. This strategy was to be independent of any overexpression or RNAi-based knockdown scenarios to avoid common drawbacks associated with these artificial and exaggerated expression manipulations. Here we utilized human melanoma cells to investigate the coactivation of HIF-1 and USF signaling through simultaneous exposure of the cells to hypoxia and UV irradiation. As described in section 5.4.2, human melanocytes and primary melanoma growths reside in a persistently hypoxic microenvironment of the epidermis-dermis junction whose cells, even without malignant transformation, exhibit the physiological activation of HIF-1 and its downstream gene targets [275, 276, 278, 307]. It is within this context that the USF cascade activates the UV-triggered tanning response program in melanocytes/melanoma cells [235, 267, 268]. Thus, our pilot project on the convergence of hypoxia/HIF and UV/USF signaling events at DNA level in melanoma cells aimed to address this crosstalk under physiological conditions.

To titrate UV conditions (wavebands, energy dose) that would yield an optimal activation of USF1 and downstream melanogenesis constituents, we used as readout the UV-mediated activation of the stress kinase p38 pathway which is the responsible signal for the transcriptional activation of USF1 via phosphorylation in melanoma cells [214, 235]. Beyond p38/USF signaling responsible for the UV-induced tanning response, a functional cyclic AMP (cAMP) pathway is also essential to mediate a proper melanin pigmentation in melanocytes [308]. The paracrine signal to activate the cAMP cascade in melanocytes is the α-MSH peptide hormone. α-MSH is one of several cleavage products of a large precursor peptide called pro-opiomelanocortin (POMC) that is synthesized in cutaneous keratinocytes. For a constitutive pigmentation, secreted α-MSH binds to the simultaneously induced quantities of MC1R on the surface of melanocytes [308-310]. This ligand/receptor interaction sets off the stimulated production of the cAMP second messenger which leads to the nuclear translocation of the microphthalmia-associated transcription factor (MITF) and the MITF-mediated basal transcription of TYR and MC1R to keep a steady state of tanning response in melanocytes [308].

All melanoma cells utilized for this thesis were cultured with a 10% CO_2 atmosphere and in the presence of 10% non-heated FBS. For our initial experiments we worked with the human M000921 melanoma cells, directly isolated from a patient at the Dermatology

Department, University Hospital Zurich (group of Prof. R. Dummer). M000921 cells are proliferative, non-pigmented human melanoma cells, express both mRNA and protein components of key players of the basal (i.e. MITF) or UV induced branch (USFs) of melanin synthesis [214].

To test if this USF1 activation is translated onto the changed expression of USF target genes (tyrosinase, TYR; melanocortin 1 receptor, MC1R), we checked by real-time quantitative PCR (qPCR) the expression profile of TYR and MC1R mRNAs as a function of UVC irradiation. We included with growth arrest and DNA-damage-inducible, 45 alpha (GADD45a), a known UV-inducible marker of DNA double-strand breakage [303, 304] to parallel assess the severity of any mutagenic UV impact on the cells. Optimally, the UV conditions should trigger an activation of the tanning response genes TYR, MC1R while not stimulating an elevated expression of GADD45a, since we wanted to keep DNA damage in the cells to a minimum. However, the qPCR data demonstrated a dose-dependent increase in GADD45a mRNA level when M000921 cells were subjected to 1, 2 and 4mJ/cm^2 doses of UVC, whereas these quantities of UVC irradiation resulted in decreasing TYR and MC1R transcript levels.

Various publications provided clear evidence that TYR or MC1R mRNA levels were up-regulated by UVC [235, 311] or UVB stimulation [267, 312, 313]. Yet, Hara *et al.* observed by reverse-transcription PCR that a marked UVB-triggered induction of TYR mRNA levels occurred only in several melanoma cell lines and not in others. This cell specific UVB-mediated increase in TYR transcripts was not correlated with melanoma's ability of pigmentation [314]. Ota *et al.*, on the other hand, documented a nearly 2-fold increase in TYR mRNA expression after repeated exposure to 5mJ/cm^2 of UVB for 7 consecutive days for three pigmented murine melanocytes, melan-a2, melan-b and melan-s. The non-pigmented murine melanocyte line, melan-c, exhibited no TYR response to UVB [315]. Further complexity is added in regard to the data by Scott and colleagues who reported on a two-step regulation of MC1R mRNA in melanocytes exposed to low (7mJ/cm^2) or moderate (14mJ/cm^2) doses of UVB: a down-regulation of MC1R mRNA level at 6hr and an up-regulation at 24hr post-irradiation. The authors proposed that UVB directly induced DNA damage as well as stimulated the production of α-MSH. Induced α-MSH, in turn, acted as paracrine factor and mediated the effects of UVB on survival of melanocytes [316]. Thus, the overall emerging picture for UV-triggered activation of tanning response genes is surprisingly heterogeneous. The recent discovery by Corre *et al.* of a novel 47-kDa USF1 specific band in immunoblot analyses in response to prolonged periods of cellular stress, might provide some

explanation for these variable outcomes [268]. The authors found that exposure to the above stressors (DNA damage, oxidative stress, cellular infection) caused USF1 to be acetylated at Lys199 in a manner depending on the prior phosphorylation of Thr153. Remarkably, this phospho-acetylated USF1 lost transcriptional activity leading to the marked down-regulated expression of several of the genes implicated in pigmentation (TYR, POMC and MC1R) and cell cycle progression (CCNB1, CDC2 and TERT) [268].

Therefore, we hypothesized that UVC irradiated cells may have been stressed too much by the completely non-physiological UVC wave-band, which resulted in the reduction of TYR and MC1R mRNA levels. In contrast to UVC, UVB wavelengths (290–320 nm) are able to traverse the atmosphere and to reach the Earth's surface. UVB qualities of the ultraviolet spectrum are the most effective waveband in eliciting sunburns or melanogenesis. At the same time, UVB is also considered the main causative agent of many of the mutagenic and transforming effects attributed to UV exposure [259, 281, 317]. For these reasons, we next exposed M000921 cells to UVB (312nm). Unfortunately, we did not succeed in achieving a reproducible UV-induced USF1 phosphorylation in M000921 cells. A USF1 band of lesser mobility was either seen even in non-irradiated cells or remained undetectable in UVB treated cells. Even though the group of Prof. Dummer had established basal expression of MITF, TYR and DCT in M000921 cells, no validation had been carried out until these experiments here in regard to cells' ability to activate USF signaling upon UV irradiation. Thus, for further experiments, we switched to the human melanoma cell line 501mel, a well established tool for analyses of UV-triggered gene responses including the robust (3-7 fold) induction of POMC and MC1R mRNA levels by UVB irradiation (80mJ/cm^2) [267].

Four different doses of UVB and two post-irradiation time points were investigated in normoxic and hypoxic 501mel cells. For combined stimulation of hypoxia and UVB signaling, cells were exposed to 1% oxygen for 16h prior to UVB and were grown for another 2 or 5h after irradiation under hypoxia. Exposure of 501mel cells to 40mJ/cm^2 of UVB yielded the induction of a USF1 band with lesser mobility at both time points (2 and 5h post-irradiation) and both oxygen concentrations (21% and 1% oxygen 16h). However, this appearance of the alleged p-USF1 species in response to UVB (UVB: 40mJ/cm^2, 5h post-UVB) displayed a considerable variability under normoxia in following immunoblots. Furthermore, hypoxia (1% oxygen, 16h) alone seemed to be able to generate p-USF1. There is some literature indicating hypoxia as stimulus for the p38 kinase pathway in human prostate cancer cells (LNCaP) [318] or mouse neuroblastoma cells (Neuro2a) [319]. Thus, p38-driven USF1 phosphorylation triggered by oxygen deprivation is not entirely surprising for some cell

backgrounds. Even when we subjected 501mel cells to a shortened hypoxic exposure of 7h without any UVB irradiation, we could still observe this more slowly migrating USF1 species (data not shown). To further analyze this confounding effect, we applied with compound SB203580, a highly specific inhibitor of p38 kinase activity. Treatment of 501mel melanoma cells with 10μM SB203580 is known to abrogate the UV-induced phosporylation of USF1 [235]. To our surprise, 10 or 20 μM final concentrations of SB203580 had no affect on the formation of the p-USF1 band, suggesting that the observed "p-USF1" still may not correspond with the phosphorylated species of USF1.

Furthermore, qPCR analyses of TYR, MC1R, PHD2, LDHA and BNIP3 expression revealed a profound hypoxic induction of PHD2 and BNIP3 genes and a marginal one for LDHA in 501mel cells. Yet, UVB irradiation failed to cause any up-regulation of TYR and MC1R mRNAs regardless of the oxygen concentration.

At this point we had to assess if our batch of 501mel cells was actually capable of any UV response, since UVC-mediated up-regulation of TYR mRNA in 501mel cells was reported by Galibert *et al.* [235]. Despite the non-physiological nature of this stimulus, we subjected our melanoma cells also to UVC irradiation (UVC: 1, 2 and 4mJ/cm^2; response: 5h post-UVC) and recorded GADD45a, TYR and MC1R mRNA steady state levels. We obtained an overall UVC expression profile very similar to that of M000921 cells. As can be seen in Fig. 9D, exposure to the above detailed UVC conditions resulted in an up-regulation of GADD45a mRNA and a down-regulation of both TYR and MC1R transcripts in 501mel cells. Either cell line is apparently incapable to elicit positive responses of tanning genes when facing UVB or UVC challenges. This could stem from a cell-related or a UV-related problem. Since it is known that in the absence of the cAMP inducing α-MSH signal, a single irradiation of melanocytes with 28mJ/cm^2 of UVB leads to a decrease, rather than increase, of TYR activity as well as protein levels [320], defects in either the p38 or cAMP cascade in our melanoma lines could underlie the failure to induce tanning components (TYR, MC1R) in response to UVB/UVC signals.

Therefore, addressing the following key questions will be of vital importance to still make this line of work a successful endeavor:

a) Is the observed down-regulation of TYR and MC1R mRNAs in UVB/UVC-exposed M000921 and 501mel cell lines associated with the acetylated form of USF1, which switches the factor from trans-activator to trans-inactivator [268]?

b) Are our batches of M000921 and 501mel cell lines defective in either the p38/USF-mediated or the α–MHC/guanylate cyclase/cAMP-mediated pathways that are known to work

side by side for an appropriate tanning response in melanoyctes/melanoma cells (details below)? If so, which cell lines are better tools in regard to these signaling mechanisms and UV-triggered gene responses?

Answers to both questions can be obtained by any of the following approaches:

i) The appearance of the true p-USF1 species is associated with the auto-phosphorylation of p38 itself, yielding p-p38, in response to UV radiation [235]. Thus, one needs to test intact p38 signaling in UV irradiated melanoma cells by measuring the p-p38/total p38 ratio as indicator of the functionality of this cascade in melanoma cells. Specific antibodies for phosphorylated and total p38 are commercially available [321]. As additional readout for a functional p38 cascade, treatment of cells with p38 kinase inhibitor SB203580 should reverse the appearance of a lesser-mobility USF1 band.

ii) Our suspicion that the observed USF1 species of lesser mobility in SDS-PAGE gels did not correspond to the phosphorylated form of the transcription factor stems mainly from the complete resistance of the signal to the specific p38 kinase inhibitor SB203580. Thus, attempts should be made to isolate the upper USF1 band from preparative gels and conduct mass spectrometric determinations of its peptide masses in order to reveal the nature of its post-translational modification. In parallel, one should treat cells with specific deacetylase inhibitor trichostatin A [268] to see if this drug causes an increase in the upper USF1 band signal. If so, this would lend strong credibility to the notion that the UV-induced species is the acetylated repressing, and not the phosphorylated inducing form of USF1.

iii) Other melanoma lines need to be screened for an UV-conferred up-regulation of TYR and MC1R mRNA levels, and if affirmative, also for the appearance of a p-USF1 species (reversal by SB203580 treatment). Those cell lines which both criteria characterized the existence of an intact UV-induced tanning response cascade will be subjected to HRE/E-box reporter (LDHA, BNIP3) transfections in conjunction with hypoxia-only, UV-only and hypoxia/UV dual exposure regiments.

iv) To test the USF-specific impact on HIF-driven LDHA or BNIP expression can be done by co-transfecting cells, prior to hypoxia/UV dual exposures, with the dominant-negative A-USF variant which contains USF heterodimerization domain but lacks of USF-specific region [209], and determining if the modified reporter response converts back to its normal hypoxic activity.

v) In addition, even those melanoma cells that remain unresponsive to UV signals as judged by the criteria in (iii), may not be completely non-informative, since the suspected defects in p38 signaling can be circumvented through transfections with a constitutively

active USF1 mutant (T153E) which has been generated in Galibert's lab in 2001 [235]. That way, the transcriptional impact of a phosphorylation-independent USF1 construct on HRE/E-box promoters can still be assessed in hypoxic, HIF-1 positive melanoma cells (to be validated). Similarly, suspected defects in the cAMP pathway (e.g. α-MHC application yields no TYR/MC1R mRNA response and no MITF nuclear translocation) can also be addressed since cAMP signaling is mimicked through 10μM of forskolin [321]. This surrogate treatment should be used to recover TYR or MC1R responsiveness in cells with suspected defects in the cAMP cascade.

8.2 Outlook

Our current data on human cancer cells revealed the agonistic and antagonistic interactions of HIF-1 and USFs on the promoters of the human LDHA and BNIP3 genes. The relevance of this finding lies within the potential to gain mechanistic insights into the crosstalk of hypoxia- and UV-signaling components and apply this research to the biology of human melanoma cells. Melanocytes and primary melanoma cells reside in a chronically hypoxic cutaneous microenvironment and carry out the UV-induced tanning response during which the natural sun-blocking pigment melanin is synthesized to protect the skin from any mutagenic insult by intermittent or persistent ultraviolet radiation.

Based on the data obtained in this pilot study with human melanoma cells, a follow-up project is required to further optimize the conditions leading to a robust, reproducible and USF-dependent induction of tanning response effector genes by UV irradiation (i.e. pursue experimental answers to issues raised in points i-v, above). At the same time, conditions should be selected for a minimal DNA breakage. Once these irradiation conditions have been worked out, subsequent focus should lie on investigating the crosstalk between hypoxia/HIF-1 and UV/USF cascades in HRE/E-box-reporter transfected melanoma cells that will be subjected to hypoxia-only, UV-only and hypoxia/UV-dual stimulation regimes. Thus, the main tasks of the follow-up work will be:

1) to establish the optimal UV irradiation conditions using the following readouts: a) TYR, MC1R mRNA induction and formation of p-USF1 species; b) Trypan blue viability assay for assessment of UV-mediated cytotoxicity; c) GADD45a mRNA and p53 protein induction for assessment of UV-mediated DNA damage.

2) to carry out a genome-wide comparison of hypoxia-only, UV-only and hypoxia+UV exposed melanoma cells to reveal hypoxia-regulated genes which are also

susceptible to UV signals. How widespread are HIF/USF cooperative or antagonistic inter-relationships and which genes are affected and which way?

So far, UVB or UVA -induced alterations in gene expression profiles have been elaborated by cDNA microarray and real-time qPCR human keratinocytes or melanocytes [281, 282, 303, 322]. Consequently, there is hardly any available data about UV-regulated transcriptome profiles, including the responses of tanning effector genes, for human melanoma cells. Worse, the transcriptomic/proteomic studies existing to date for the elucidation of UV-responsive genes recorded these profiles under non-physiologically hyperoxic, hence genotoxic, conditions. Thus, systematic and physiologically meaningful screens of the UV-mediated expression profiles in deoxygenated, HIF-1 positive and tanning competent cell systems, are urgently needed. Hypoxia/UV co-responsive genes found by the approach in (2) will be validated by real-time qPCR and ChIP approaches using both wild type and stable knockdown HIF-1α or USF1 clones of the transcriptome-screened melanoma cell line.

Part B Hypoxia-mediated myoglobin expression in human breast cancer

9 Background

Myoglobin (Mb) and hemoglobin (Hb) are two well known members of the family of globin proteins. Globins are heme-binding proteins which can reversibly bind oxygen and other diatomic gases via the iron atom in the centre of the porphyrin chromophore. The heterotetrameric Hb (human HbA1 = $\alpha_2\beta_2$) transports oxygen in the blood, whereas monomeric Mb temporarily stores and transports oxygen within vertebrate heart and skeletal muscle cells [323]. Mb is a cytoplasmic hemoprotein, exclusively expressed in cardiac myocytes and oxidative skeletal muscle fibers. Besides Mb and Hb, two other family members, neuroglobin (Ngb) and cytoglobin (Cgb), have recently been discovered. Ngb is mainly expressed in the cytoplasm of neuronal (brain and retina) cells, whereas Cgb is primarily expressed in fibroblasts and fibroblast-related cell types in a broad variety of organs including liver, heart, muscle, gut, kidney, lung and pancreas. Both globins bind oxygen reversibly and may be involved in cellular oxygen homeostasis [324-326].

9.1 Structure and function of myoglobin

The three-dimensional structure of sperm whale myoglobin was first delineated by Kendrew and his colleague over 50 years ago [327, 328]. Since then, a number of works continually refined the tertiary structure of Mb. Collectively, these studies established that Mb is a single polypeptide chain consisting of eight α-helices. These α helices wrap around a central pocket containing a prosthetic protoheme group which is bracketed by two histidine residues (His^{64} and His^{93}). The iron interacts with six ligands, four of which are provided by the nitrogen atoms of the four pyroles of the porphyrin ring system. The imidazole side chain of His^{93} provides the fifth ligand for stabilization of the heme group. The sixth ligand position, which is unoccupied in deoxymyoglobin, acts as the binding site for O_2, and for other gaseous ligands such as carbon monoxide (CO) or nitric oxide (NO) [329, 330].

Similar to hemoglobin, binding of O_2 to Mb does not oxidize the central iron ion. Rather, binding of O_2, known as oxygenation, can switch deoxyMb (Mb) to oxyMb (MbO_2) without change in the valency of the ferrous iron atom (i.e. $Mb^{Fe2+} + O_2 \rightarrow Mb^{Fe2+}O_2$). Oxidation of the iron from a ferrous (Fe^{2+}) to a ferric ion (Fe^{3+}) found in the so-called Met

form of the protein can occur during oxidative insults (e.g. ischemia-reperfusion) and renders Mb or Hb incapable to bind any more O_2. To prevent a pathological build up of Met-Mb or Met-Hb, cytochrome b5/b5 reductase systems (i.e. Met-Hb reductase) have evolved to reduce ferric into ferrous iron within the heme of the protein. Thus, a ferrous iron (Fe^{2+}) is critical for the reversible binding of the O_2 or CO ligand.

In diving mammals (e.g. sperm whale, seals), concentrations of Mb of 4-5 mM expressed in the cardiac and skeletal muscles aid as temporary O_2 store during the breath-hold period of the dive [329, 331]. This wealth of the protein helps to postpone or alleviate tissue hypoxia when no ambient O_2 can be acquired. Striated muscle in humans, on the other hand, contains on average 200 μM of Mb. Here the alleged main function of Mb has shifted more towards the facilitation of oxygen diffusion from the periphery of the cell to the mitochondria. However, unlike tetrameric Hb with its sigmoid-shaped oxygen equilibrium curve that illustrates the cooperativity of binding the ligand by all four subunits, monomeric Mb has a single O_2-binding site and thus exhibits a hyperbolic O_2 equilibrium curve characteristic of normal Michaelis-Menten enzyme kinetics (Fig. 10) [330]. The oxygen-binding curves of Mb and Hb also indicate the completely different oxygen binding affinities of both hemoproteins. While human HbA1 has a P_{50} (i.e. oxygen partial pressure at 50% saturation) of approximately 27mmHg, in contrast, human Mb displays a much stronger binding of O_2 (P_{50} of 3mmHg) [332]. During normal exercise, 40-70% of Mb will remain saturated with dioxygen ($Mb+O_2 \leftrightarrow MbO_2$) [331].

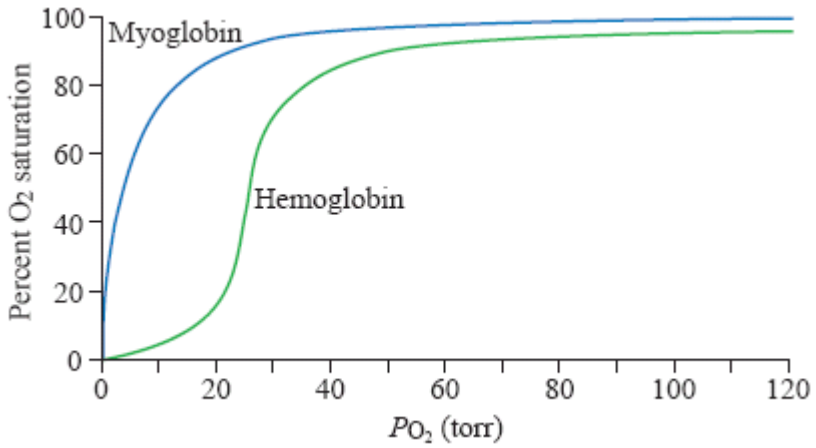

Figure 10 Oxygen-binding curves of myoglobin (Mb) and hemoglobin (Hb). Mb and Hb function as oxygen transporter. Myoglobin displays a hyperbolic-shaped oxygen-binding curve, in contrast, hemoglobin displays a sigmoidal-shaped oxygen-binding curve [330].

The oxygen-binding curve implies further that Mb-bound oxygen starts to significantly dissociate from the protein only when intracellular $pO_2 < 10$mmHg, i.e. during severe hypoxic

conditions. Animals, which live in low oxygen environments, adapted various means to better survive hypoxia, including increased capillary densities, Mb concentration and volume densities of mitochondria. That way, oxygen can still adequately be delivered to the mitochondria and aerobic metabolism be maintained, while the organism encounters markedly reduced levels in ambient oxygen.

As stated above, Mb has been proposed to function in the facilitated oxygen diffusion in human cardiomyocytes by J. and B. Wittenberg [323]. However, this function still is rather controversially discussed. Based on measurements and calculation of oxygen transport by Mb in skeletal muscle, various studies suggested that contribution of myoglobin to intracellular oxygen transport in intact red muscle was of minor importance [333, 334]. An additional role of Mb is the proteins' regulation of NO bioavailability within the cardiomyocyte. MbO_2 can rapidly and effectively scavenge NO through the following diffusion-limited reaction: $MbO_2 + NO \rightarrow$ Met-Mb + NO_3^- (oxymyoglobin +NO → ferric iron met-myoglobin + nitrate) [335]. Furthermore, cardiomyocytes expressed Mb functions as a scavenger not only of NO but also of ROS and thus participates in protecting the heart from these highly reactive radicals [336].

To understand the *in vivo* role of Mb in striated muscle, $Mb^{-/-}$ mice were generated by two laboratories via the deletion of exon 2 of the single copy Mb gene. Exon 2 encodes the heme-binding domain including both coordinating histidines, and thus is essential for a functional protein. Experiments with these knockout survivors showed that Mb-deficient mice can grow normally, are fertile and exhibit normal exercise capacity as well as a normal ventilatory response to low oxygen levels [337]. However, these $Mb^{-/-}$ mice developed several important compensatory adaptations in the heart to support and uphold an O_2 delivery during exercise despite the lack of this O_2 carrier. These compensations included increased capillary densities and blood O_2 carrying capacity as well as elevated hematocrit values [338]. Subsequent studies of skeletal muscles in $Mb^{-/-}$ animals also showed these compensation mechanisms. Additionally, the work by Grange *et al.* demonstrated a fiber type transition (from slow myofibers (type I) to fast myofibers (type II) in soleus), augmented expression of HIF-1α and -2α, of stress proteins such as heat shock protein 27, of the angiogenic vascular endothelial growth factor and of enhanced nitric oxide metabolism in response to Mb deficiency in muscle and cardiomyocytes [339, 340]. These findings were critical in enhancing our understanding of the workings of Mb as oxygen transporter and regulator of NO and ROS homeostasis in striated muscle.

9.2 Hypoxia mediated myoglobin expression

For a long time we have known the impacts of exercise and hypoxia on Mb expression in oxidative muscle fibers (reviewed in:[341]). For example, Vogt *et al.* reported that endurance training promoted development of tissue hypoxia in human skeletal muscle and, subsequently, elevated Mb mRNA steady state concentrations in conjunction with increasing level of HIF-1α transcripts [46]. The study by Fraser and colleagues on Mb in the hypoxia-tolerant carp, however, expanded occurrence and hypoxia-responsiveness of Mb even to non-muscle tissues. One of two carp myoglobin transcripts, Myg-1, was expressed not only in muscle but also in liver, kidney, heart and gills of the fish. Moreover, Myg-1 mRNA and protein was strongly induced by hypoxia in these tissues. In contrast, expression of Myg-2 was restricted to brain and independent on oxygen [342]. Additionally, a study on a long-term (for 3 weeks) response to severe hypoxia in zebrafish revealed a robust myoglobin induction in the gills [343].

Outside of striated muscle, human Mb was recently shown to be expressed in epithelial tumors which had faced intermittent periods of hypoxia and oxidative stresses during cancer progression. In contrast to normal breast epithelial cells (MCF-10A), *de novo* mRNA and protein Mb expression was shown for breast cancer cells (e.g. MCF7). Furthermore, this Mb protein expression in MCF7 cells was confirmed to be induced in response to 48h/1% O_2 exposures. Immunohistochemistry confirmed this induction of Mb in other human carcinomas as well. Moreover, Mb expression was also induced by several other stimuli, such as oxidative stress and mitogenic signals (epidermal growth factor) [344]. Galluzzo *et al.* reported that Mb was able to attenuate the hypoxia-mediated cancer progression by enhancing the oxygenation of the resulting xenografts when Mb was overexpressed in A549 human lung carcinoma cells and MDA-MB435 human breast cancer cells by transferring an Mb expressing lentiviral construct. In this system, Mb expression yielded a marked reduction of tumor angiogenesis and significantly inhibited tumor growth as well as metastatic spreading [345].

Despite the evidence above for an O_2-responsive transcriptional control of the Mb gene, sequence comparison by Wystub *et al.* failed to detect conserved HREs when comparing the upstream flanks of human, mouse and rat Mb genes. Rather, the authors noticed conserved mRNA stabilization signals within the 3' untranslated regions (utr) of the Mb gene [346]. A recent study on hypoxia mediated Mb expression in cultured mouse C2C12 myoblasts and whole animals documented that hypoxia alone could not stimulate the induction of the Mb gene. Analysis of 10-kb of upstream DNA of mouse, human and rat Mb

genes failed to show any conserved HRE site for HIF-1 complex. This study reported that the hypoxic induction of Mb operates independently of HIF-1. Rather, levels of low oxygen would trigger a calcium signaling event, which in turn activates the calcineurin/NFAT pathway that underlies the hypoxia-mediated Mb expression [347].

10 General objectives

Recently, Flonta *et al.* reported that Mb was strongly detectable in different epithelial human breast tumors and cell lines, but not in cells of normal breast tissue. The authors also showed for MCF7 breast carcinoma cells that hypoxia is able to induce Mb protein levels [344]. As part of a larger collaborative effort we aimed to further extend our understanding of the expression, regulation and function of Mb and of the proteins' prognostic impact in human breast cancer. Our immunohistochemical survey involved analysis of Mb in human breast cancer specimens (n=917) and revealed endogenous expression in 71% of invasive breast carcinomas, preferentially of luminal-type. Mb positivity correlated with expression of the estrogen receptor alpha (ERα) and a favorable patient prognosis. A positive correlation of the hemoprotein with hypoxia-inducible factor 2α (HIF-2α) and carbonic anhydrase IX (CAIX) suggested oxygen to regulate Mb in breast carcinomas. Indeed, Mb mRNA and protein levels were robustly induced by prolonged hypoxia in different breast cancer cell lines, thus confirming this set of data of the Flonta's study.

The aim of my part of this project was therefore to clarify whether the hypoxia-induced Mb expression in cultivated MDA-MB-468 and MCF7 human breast carcinoma cell lines is HIF-dependent.

Main research objectives included:

1) to determine the kinetics of the hypoxia-mediated induction of Mb protein at 1% oxygen
2) to investigate the requirement of HIF for this induction of Mb by using transient knockdown approaches with siRNAs directed against HIF-1α, HIF-2α or both;
3) to generate stable short hairpin RNA (shRNA)-based Mb knockdown MDA-MB-468 clones for further characterization of potential respiratory and tumorigenic properties of Mb in human breast cancer cells.

11 Own research

The following section summarizes my own contribution included in the manuscript "myoglobin in breast cancer" enclosed in this dissertation.

11.1 Hypoxia-induced myoglobin protein levels in MDA-MB-468 and MCF7 breast cancer cell lines

Our collaborators could provide solid evidence for the mRNA level activation of Mb gene transcription by prolonged hypoxia (1% O_2) in human MDA-MB-468 and MCF7 breast cancer cell lines. Mb protein level response to hypoxia was analyzed for the same cells subjected to 72h normoxia or 4, 8, 24, 48 and 72h hypoxia (1% O_2). In SDS PAGE analyses, breast cancer cell expressed Mb protein showed identical mobility relative to muscle expressed Mb (biopsied material). In agreement with RNA expression data, both cell lines induced Mb protein between 3.4 and 5.1-fold following a hypoxia exposure of 48h or longer. In addition, the HIF response was transient in hypoxic MCF7 cells. Here, induction of the predominant species, HIF-1α, peaked at 4h hypoxia, followed by a steady decline of the protein content thereafter. In contrast, hypoxic MDA-MB-468 cells expressed preferably HIF-2α whose induction persisted for up to 72h of 1% O_2.

11.2 Involvement of HIF-1α and -2α in Mb induction in MDA-MB-468 subjected to prolonged deprivation of oxygen

To study the role of HIF in the hypoxic induction of Mb, we utilized siRNA oligonucleotides specifically directed against nucleotides 1380-1400 of HIF-1α mRNA (Entrez accession number: AF304431.1) and nucleotides 1260-1280 of HIF-2α mRNA (Entrez accession number: NM_001430.3), respectively. To gain the optimal knockdown efficacy in MDA-MB-468 cells, two different final concentrations of siRNA oligonucleotides (100nM and 200nM for single siRNA; 50/50nM and 100/100nM for combined siRNAs) and two hypoxic exposures (24h + 48h/1% O_2, starting at 18h post-siRNA transfection) were tested. Subsequently, changes in HIF-1α and -2α protein level were detected by Western blot. Maximal knockdown efficacy of HIF-1α or 2α was achieved at 48h hypoxia exposure with final concentrations of 200nM for single siRNAs and 100nM for each siRNA for the combined targeting of HIF-1α and -2α. As negative control, MDA-MB-468 cells were

transfected with a non-targeting siRNA pool of scrambled sequences (siControl) at a final concentration of 200nM.

Since induction of Mb protein levels was robustly detected from 48h hypoxia onwards, the siRNA assay focused on control and HIF-1α (= siHIF-1α), -2α (= siHIF-2α) and combined knockdown effects (= siHIF-1α/2α) after 52h to 96h of exposure to 1% O_2. A maximal ~7-fold induction of Mb protein was reached at 72h hypoxia during the siControl transfections. This 72h-peak induction was reduced to ~4-fold upon single HIF-1α or -2α siRNA treatment. Moreover, the combination of both siRNAs, with ~30% residual content of either HIF factor remaining, significantly attenuated the Mb induction to ~1.7 fold at 72h hypoxia. Therefore, this data implied both HIF-1 and HIF-2 in participating in the peak stimulation of Mb during prolonged periods of low oxygen.

11.3 Stable Mb knockdown MDA-MB-468 clones

To demonstrate a functional relevance of Mb in breast cancer cells, stable knockdown Mb MDA-MB-468 clones were generated using short hairpin RNAs (shRNA) that target the mRNA of human myoglobin at nucleotides 284-304 (constr. 83), 483-503 (constr. 84), 340-360 (constr. 85) and 415-435 (constr. 86) (positions in accordance to GenBank™ accession number NM_203377). Inserted into the mammalian expression vector pLKO.1-puro, these four shRNA constructs, were purchased as bacterial glycerol stock from Sigma-Aldrich (Basel, Switzerland). Stable shRNA Mb knockdown MDA-MB-468 cells were established by overnight calcium phosphate transfection followed by selection and maintenance in 0.75μg/ml puromycin containing medium. Mb protein levels in knockdown and control cells were analyzed by Western blot as described above**.** Myoglobin level in clones 83#4, 83#8, 83#9, 84#31 and 86#13 was strongly suppressed, whereas Mb level in clones 84#2, 84#5, 84#20, 85#14 and 85#18 remained unaltered. Densitometry of β-actin normalized Mb band intensities from 3 independent analysis showed that the Mb protein level was most strongly reduced in 3 individual clones 83#4, 83#8 and 84#31 with residual contents at 20%, 20% and 30%, respectively. Clones 84#5, 84#20 and 85#14, which had been subjected to the same transfection/selection procedure but where Mb remained unaltered, were taken as negative controls. Due to unexplainable technical problems, clones 83#8 and 84#31 lost knockdown effect in later passages. Ultimately, clone 83#4 was taken as stable knockdown Mb for further functional tests.

13 Conclusion and outlook

Since Ray Lankester's [348] first identification, Mb is commonly thought to solely occur at milli- to micromolar concentrations in cardiac myocytes and type I and IIa skeletal muscle fibers of mammals. In myocytes, the monomeric hemoprotein is widely accepted to function as temporary "store" for oxygen and able to buffer short phases of exercise-induced increases in O_2 flux during which it supplies the gas to mitochondria [330]. Another, more controversially discussed role is Mbs' facilitation of oxygen diffusion within muscle cells [333, 334]. Mb knockout mice which were generated by two laboratories in the late 90's [337, 338] exhibited normal exercise capacity and no signs of compromised cardiac energetics due to multiple systemic compensations [338]. However, follow-up studies stressed the importance of functional myoglobin in maintaining nitric oxide (NO) homeostasis in muscle through either scavenging [336] or producing the NO molecule [349]. That way, Mb might participate in tuning vasodilatory responsiveness and protecting the cytochrome c oxidase in the respiratory chain from inhibition by elevated NO concentrations [341, 350].

Work on the common carp and zebrafish recently revealed an unexpected multiplicity of Mb genes and protein expression in non-muscle tissues, such as liver, brain and gills (see [341] for review). Furthermore, in these fish species expression of certain Mb isoforms was strongly up-regulated by reduced tissue oxygenation in the liver and gills of these fish [342, 343, 351]. In humans, the single-copy Mb gene synthesizes the protein at concentrations of ~200-300 μM in striated muscle, whose expression is highly responsive to chronic muscular activity or hypoxia [330, 352]. In human skeletal muscle, Mb in mitochondria rich oxidative myofibers shows elevated synthesis in response to exposure to high altitudes [352] or intense endurance training under reduced oxygen pressures [46, 330, 352]. Striated muscle of mice shows *in vivo* induction of the Mb gene by chronic hypoxia. The master regulator of cellular O_2 homeostasis HIF-1 has been implicated in the mouse for this transcriptional activation [353]. The possibility that HIF-1 might generally be involved in the induction of Mb is supported by two observations. First, stimulation of the HIF-1 pathway in muscle is triggered by exercise with or without hypoxia and mechanical stress (stretching) [46, 354, 355]. Second, the HIF-1/Mb system is colocalized in oxidative skeletal myofibers (type I and IIA fibers) [330, 356]. Therefore, the link between hypoxia/HIF signaling and Mb production can reasonably be extended onto neoplastic tissues. The logical next step is to provide experimental proof for this supposition.

Our own collaborative breast cancer study (see manuscript for detail) initially looked at the *in vivo* and *in vitro* abundance of Mb products. Mb mRNA expression was upregulated in nine of ten matched (same patient) normal/tumor tissue samples with a median tumor-to-normal up-regulation of 352 fold. With regard to breast cell lines, Mb mRNA was not detectable in benign MCF12A epithelial cells, while ten breast cancer cell lines (incl. MDA-MB231, MCF7) expressed detectable but low amounts of Mb mRNA. Three breast cancer cell lines, including the MDA-MB-468 line, contained abundant quantities of the Mb transcript. When using tissue microarrays and a validated monoclonal Mb antibody, our survey detected Mb protein in normal breast tissue (n=56 cases), intratumoral ductal carcinoma in situ (DCIS; n=155) and invasive breast cancer (n=917). In normal breast tissue, staining was observed in secretory luminal epithelial cells, but not in myoepithelial cells. In invasive carcinoma, the number of Mb positive or negative cases was markedly higher than in normal tissue. Increased expression of Mb in breast carcinomas occurred independently of rhabdomyoid tumor differentiation. With increasing transformation and aggressiveness (normal tissue → DCIS → invasive carcinoma) the proportion of Mb negative and strongly positive tissues both gained in frequency.

In invasive breast carcinomas Mb expression was associated with better histological tumor differentiation and with estrogen (ERα) and progesterone receptor (PgR) positivity. High Mb expression was also significantly associated with longer overall patient survival (five-year survival rate of Mb-pos. cases 83% *vs.* 75% in Mb-negative cases). Positive correlations of presence of Mb were found to the hypoxia-inducible factor 2α (HIF-2α) (correlation coefficient, cc=0.257, p=0.001), carbonic anhydrase IX (CaIX; cc=0.361, p=0.001), cytoglobin (Cygb; cc=0.361, p=0.001) and E-cadherin (E-Cad; cc=0.207, p=0.001). In contrast, no significant correlation was found with HIF-1α, glucose transporter 1 (GLUT1), the proliferation indicating Ki-67 marker and microvessel density.

To study the responsiveness of the Mb gene, the effect of hypoxia (1% O_2; 4, 8, 24, 48, 72h) was analyzed by quantitative real-time PCR (qPCR) in four different cell lines: the benign breast cell line MCF12A, the ERα-negative breast cancer cell lines MDA-MB-231 (low basal Mb expression) and MDA-MB-468 (high basal Mb expression), and the ERα positive cell line MCF7 (medium basal Mb expression). Whereas transcription of the Mb gene was unaltered by hypoxia in the benign MCF12A cells, normalized steady state levels of Mb mRNA increased 3-4 fold in hypoxic MDA-MB-468, MDA-MB-231 and MCF7 cells. In all cases, a robust activation of the Mb gene required at least 24h or 48h of hypoxia to take effect.

Activation of the Mb gene by prolonged hypoxic exposure MCF7 cells was also noted in the study of Flonta *et al.* [344].

Thus, the aim of my contribution to the "Mb in breast cancer"-project was to analyze the control of hypoxia over Mb synthesis at the protein level and to examine whether this hypoxic induction of Mb requires the activity of HIF-1 or HIF-2. To tackle this task, I worked with two human breast carcinoma cell lines: MDA-MB-468 and MCF7. I also generated stable shRNA-based Mb knockdown clones of MDA-MB-468 cells.

I found the Mb protein, in agreement with the RNA expression profiling, 3-5 fold up-regulated during prolonged hypoxia in both MDA-MB-468 and MCF7 breast carcinoma cells, although MDA-MB-468 cells displayed a much higher basal level of Mb protein than MCF7 cells. Other colleagues in the team were able to quantitate that the amount of Mb protein in 10^6 normoxic MDA-MB-468 cells as ~65 ng or 4 pmol by using a commercial chemiluminescence based Mb-assay.

Towards the control of this induction, distinct HIF-gene preferences and stabilization kinetics became apparent in these two breast cancer cells. The HIF response was transient in hypoxic MCF7 cells where the predominant species, HIF-1α, peaked at 4h hypoxia, followed by a steady decline of the protein content thereafter. In contrast, hypoxic MDA-MB-468 cells expressed preferably HIF-2α whose induction persisted for up to 72h of 1% O_2. Similar patterns of transient HIF-1α versus persistent HIF-2α induction profiles during maintained hypoxia were previously reported for human lung endothelial cells or human hepatoma cells (Hep3B) [357]. These kinetic distinctions between the HIF-α subunits are difficult to reconcile with a common PHD and/or FIH control mechanism.

To our surprise, the most effective suppression of the 7-fold induction of Mb protein levels occurred in MDA-MB-468 cells subjected to 72 h hypoxia, when cells were simultaneously transfected with siRNAs directed against HIF-1α and -2α. This double silencing of both HIF subunits significantly attenuated the Mb induction from 7 to ~1.7 fold. The residual gene activation or protein stabilization must use HIF-independent mechanisms. In contrast to that, silencing of either HIF-1α or -2α alone did not significantly attenuate the hypoxia-triggered elevation of Mb in MDA-MB-468 cells. It thus becomes clear that both HIF-1 and HIF-2 actively participate in the peak stimulation of Mb at 72h of hypoxic exposure. Before and after this time point, the impact of any siRNA-HIF treatment resulted in hypoxic response time-courses of Mb that were indistinguishable (52-56h hypoxia), or insignificantly reduced (96h hypoxia), compared to siControl experiments. Transactivation of the Mb gene in breast cancer expressed apparently proceeds in HIF-dependent and -

independent signaling waves. During these experiments we also noted, as did other studies on MCF7 cells before us [358], that single siRNA treatments against one HIF-α resulted in a reciprocal surplus accumulation of the other factor during periods of low pO_2 (e.g. HIF-2α knockdown potentiates HIF-1α accumulation in hypoxia to 1.6-fold higher stead state levels as siControl transfections).

Posttranscriptional controls might participate in the hypoxic stimulation of some Mbs, because several hypoxia inducible mRNA stabilization signals have been discovered in the 3' untranslated regions (UTR) of human and rodent sequences [346]. The standard promoter of the Mb gene that is driving the expression in striated muscle cells has been characterized in 1984 by Weller *et al.* for the human and in 1986 by Blanchetot *et al.* for the mouse Mb gene [359, 360]. This TATA box promoter contains no candidate HRE [346]. Consequently, expression of the standard Mb transcript (Mb-s) was found in our team effort to be not affected by O_2.

However, we also noted the hypoxia-activated transcription of a non-canonical Mb mRNA (alternative transcript: Mb-a), transcribed from a promoter that is located proximal to the 5' UTR exon -1. EST evidence and our own comparison of the copy numbers of the alternative versus standard Mb mRNAs expressed in MDA-MB-468 cells suggested that Mb-a can tentatively be regarded as a cancer-specific transcript due to its ~300 fold higher expression level relative to Mb-s. Discovery of the O_2-responsiveness of Mb-a, in conjunction with the found HIF-1/-2-driven transactivation of the Mb gene during hypoxia (above), prompted the search for candidate HREs as potential regulatory sites for the alternative transcript. Scanning the complete genomic region of human and mouse *Mb* genes for HRE motifs yielded a candidate HRE, which consists of two inverted HIF-1 binding sites at an interval of 6 bp, embedded in a conserved stretch of 53 bp. The 53bp stretch of the Mb-HRE has 93% sequence similarity to an upstream promoter region from the human heat shock protein HSPB1 gene that encodes the Hsp27 protein. Interestingly, promoter assays had already suggested that this observed HRE of HSPB1 is indeed functional in mediating HIF-1 responses [361]. Based on these findings, breast cancer cells induce the Mb gene in response to longer periods of low oxygen via an alternative and perhaps tumor specific promoter whose enhanced activity depends, in part, on the binding of HIF-1/-2 to the HRE located 2.7 kb upstream from the ATG codon. We thus are beginning to obtain a mechanistic rationale for the significant positive correlation of Mb protein with HIF-2α and CAIX in breast carcinomas (see manuscript for detail). Logical follow-up studies of this discovery and to better understand the mechanism of the hypoxic induction of Mb transcripts and proteins in human

breast cancer cells, would be to a) evaluate occurrence of Mb-a in breast tumors and the transcripts association with regional tumor hypoxia; b) repeat Mb-a/Mb-s copy number assessment for matched tumor/healthy breast tissue sample; c) engineer a fluorophore-labeled Mb-a antisense RNA to detect and inhibit Mb expression *in situ* and d) examine whether the Mb-HRE functions as direct HIF-1/2 binding site *in vivo* and *in vitro*.

14 References

1. Gray, L.H., et al., *The concentration of oxygen dissolved in tissues at the time of irradiation as a factor in radiotherapy.* Br J Radiol, 1953. **26**(312): p. 638-48.
2. Thomlinson, R.H. and L.H. Gray, *The histological structure of some human lung cancers and the possible implications for radiotherapy.* Br J Cancer, 1955. **9**(4): p. 539-49.
3. Brown, J.M., *The hypoxic cell: a target for selective cancer therapy--eighteenth Bruce F. Cain Memorial Award lecture.* Cancer Res, 1999. **59**(23): p. 5863-70.
4. Brown, J.M. and W.R. Wilson, *Exploiting tumour hypoxia in cancer treatment.* Nat Rev Cancer, 2004. **4**(6): p. 437-47.
5. Vaupel, P. and L. Harrison, *Tumor hypoxia: causative factors, compensatory mechanisms, and cellular response.* Oncologist, 2004. **9 Suppl 5**: p. 4-9.
6. Vaupel, P., et al., *Current status of knowledge and critical issues in tumor oxygenation. Results from 25 years research in tumor pathophysiology.* Adv Exp Med Biol, 1998. **454**: p. 591-602.
7. Brown, J.M. and A.J. Giaccia, *The unique physiology of solid tumors: opportunities (and problems) for cancer therapy.* Cancer Res, 1998. **58**(7): p. 1408-16.
8. Murphy, B.J., *Regulation of malignant progression by the hypoxia-sensitive transcription factors HIF-1alpha and MTF-1.* Comp Biochem Physiol B Biochem Mol Biol, 2004. **139**(3): p. 495-507.
9. Graeber, T.G., et al., *Hypoxia-mediated selection of cells with diminished apoptotic potential in solid tumours.* Nature, 1996. **379**(6560): p. 88-91.
10. Reynolds, T.Y., S. Rockwell, and P.M. Glazer, *Genetic instability induced by the tumor microenvironment.* Cancer Res, 1996. **56**(24): p. 5754-7.
11. Semenza, G., *Signal transduction to hypoxia-inducible factor 1.* Biochem Pharmacol, 2002. **64**(5-6): p. 993-8.
12. Carmeliet, P. and R.K. Jain, *Angiogenesis in cancer and other diseases.* Nature, 2000. **407**(6801): p. 249-57.
13. Hanahan, D. and J. Folkman, *Patterns and emerging mechanisms of the angiogenic switch during tumorigenesis.* Cell, 1996. **86**(3): p. 353-64.
14. Brizel, D.M., et al., *Tumor oxygenation predicts for the likelihood of distant metastases in human soft tissue sarcoma.* Cancer Res, 1996. **56**(5): p. 941-3.
15. Hockel, M., et al., *Association between tumor hypoxia and malignant progression in advanced cancer of the uterine cervix.* Cancer Res, 1996. **56**(19): p. 4509-15.
16. Yeung, S.J., J. Pan, and M.H. Lee, *Roles of p53, MYC and HIF-1 in regulating glycolysis - the seventh hallmark of cancer.* Cell Mol Life Sci, 2008. **65**(24): p. 3981-99.
17. Dubois, L., et al., *Inhibition of 4E-BP1 sensitizes U87 glioblastoma xenograft tumors to irradiation by decreasing hypoxia tolerance.* Int J Radiat Oncol Biol Phys, 2009. **73**(4): p. 1219-27.
18. Guppy, M., S. Brunner, and M. Buchanan, *Metabolic depression: a response of cancer cells to hypoxia?* Comp Biochem Physiol B Biochem Mol Biol, 2005. **140**(2): p. 233-9.
19. Hoogewijs D., T.N.B., Webster K.A., Powell-Coffman J.A., Tokishita S., Yamagata H., Hankeln T., Burmester T., Rytkonen K.T., Nikinmaa M., Abele D., Heise K., Lucassen M., Fandrey J., Maxwell P.H., Pahlman S., Gorr T.A., *From critters to cancers: bridging comparative and clinical research on oxygen sensing, HIF signaling, and adaptations towards hypoxia.* Int. Comp. Biol., 2007. **47**(4): p. 552-577.
20. Wouters, B.G., et al., *Control of the hypoxic response through regulation of mRNA translation.* Semin Cell Dev Biol, 2005. **16**(4-5): p. 487-501.
21. Cummins, E.P. and C.T. Taylor, *Hypoxia-responsive transcription factors.* Pflugers Arch, 2005. **450**(6): p. 363-71.
22. Taylor, C.T. and E.P. Cummins, *The role of NF-kappaB in hypoxia-induced gene expression.* Ann N Y Acad Sci, 2009. **1177**: p. 178-84.
23. Lu, D.Y., et al., *Hypoxia-induced matrix metalloproteinase-13 expression in astrocytes enhances permeability of brain endothelial cells.* J Cell Physiol, 2009. **220**(1): p. 163-73.
24. Oikawa, M., et al., *Hypoxia induces transcription factor ETS-1 via the activity of hypoxia-inducible factor-1.* Biochem Biophys Res Commun, 2001. **289**(1): p. 39-43.
25. Lee, M., et al., *Sp1-dependent regulation of the RTP801 promoter and its application to hypoxia-inducible VEGF plasmid for ischemic disease.* Pharm Res, 2004. **21**(5): p. 736-41.
26. Sanchez-Elsner, T., et al., *A cross-talk between hypoxia and TGF-beta orchestrates erythropoietin gene regulation through SP1 and Smads.* J Mol Biol, 2004. **336**(1): p. 9-24.
27. Estes, S.D., D.L. Stoler, and G.R. Anderson, *Normal fibroblasts induce the C/EBP beta and ATF-4 bZIP transcription factors in response to anoxia.* Exp Cell Res, 1995. **220**(1): p. 47-54.

28. Teng, X., et al., *C/EBP-beta mediates iNOS induction by hypoxia in rat pulmonary microvascular smooth muscle cells.* Circ Res, 2002. **90**(2): p. 125-7.
29. Lo, L.W., et al., *Endothelial exposure to hypoxia induces Egr-1 expression involving PKCalpha-mediated Ras/Raf-1/ERK1/2 pathway.* J Cell Physiol, 2001. **188**(3): p. 304-12.
30. Semenza, G.L., *Oxygen-regulated transcription factors and their role in pulmonary disease.* Respir Res, 2000. **1**(3): p. 159-62.
31. Yan, S.F., et al., *Hypoxia-associated induction of early growth response-1 gene expression.* J Biol Chem, 1999. **274**(21): p. 15030-40.
32. Aebersold, D.M., et al., *Expression of hypoxia-inducible factor-1alpha: a novel predictive and prognostic parameter in the radiotherapy of oropharyngeal cancer.* Cancer Res, 2001. **61**(7): p. 2911-6.
33. Schindl, M., et al., *Overexpression of hypoxia-inducible factor 1alpha is associated with an unfavorable prognosis in lymph node-positive breast cancer.* Clin Cancer Res, 2002. **8**(6): p. 1831-7.
34. Shibaji, T., et al., *Prognostic significance of HIF-1 alpha overexpression in human pancreatic cancer.* Anticancer Res, 2003. **23**(6C): p. 4721-7.
35. Goldberg, M.A., S.P. Dunning, and H.F. Bunn, *Regulation of the erythropoietin gene: evidence that the oxygen sensor is a heme protein.* Science, 1988. **242**(4884): p. 1412-5.
36. Semenza, G.L., et al., *Hypoxia-inducible nuclear factors bind to an enhancer element located 3' to the human erythropoietin gene.* Proc Natl Acad Sci U S A, 1991. **88**(13): p. 5680-4.
37. Wang, G.L., et al., *Hypoxia-inducible factor 1 is a basic-helix-loop-helix-PAS heterodimer regulated by cellular O2 tension.* Proc Natl Acad Sci U S A, 1995. **92**(12): p. 5510-4.
38. Wang, G.L. and G.L. Semenza, *Purification and characterization of hypoxia-inducible factor 1.* J Biol Chem, 1995. **270**(3): p. 1230-7.
39. Manalo, D.J., et al., *Transcriptional regulation of vascular endothelial cell responses to hypoxia by HIF-1.* Blood, 2005. **105**(2): p. 659-69.
40. Wenger, R.H., D.P. Stiehl, and G. Camenisch, *Integration of oxygen signaling at the consensus HRE.* Sci STKE, 2005. **2005**(306): p. re12.
41. Centanin, L., T.A. Gorr, and P. Wappner, *Tracheal remodelling in response to hypoxia.* J Insect Physiol, 2009.
42. Gorr, T.A., M. Gassmann, and P. Wappner, *Sensing and responding to hypoxia via HIF in model invertebrates.* J Insect Physiol, 2006. **52**(4): p. 349-64.
43. Fandrey, J., T.A. Gorr, and M. Gassmann, *Regulating cellular oxygen sensing by hydroxylation.* Cardiovasc Res, 2006. **71**(4): p. 642-51.
44. Hopfl, G., O. Ogunshola, and M. Gassmann, *HIFs and tumors--causes and consequences.* Am J Physiol Regul Integr Comp Physiol, 2004. **286**(4): p. R608-23.
45. Wenger, R.H., et al., *Nucleotide sequence, chromosomal assignment and mRNA expression of mouse hypoxia-inducible factor-1 alpha.* Biochem Biophys Res Commun, 1996. **223**(1): p. 54-9.
46. Vogt, M., et al., *Molecular adaptations in human skeletal muscle to endurance training under simulated hypoxic conditions.* J Appl Physiol, 2001. **91**(1): p. 173-82.
47. Wiener, C.M., G. Booth, and G.L. Semenza, *In vivo expression of mRNAs encoding hypoxia-inducible factor 1.* Biochem Biophys Res Commun, 1996. **225**(2): p. 485-8.
48. Huang, L.E., et al., *Activation of hypoxia-inducible transcription factor depends primarily upon redox-sensitive stabilization of its alpha subunit.* J Biol Chem, 1996. **271**(50): p. 32253-9.
49. Jewell, U.R., et al., *Induction of HIF-1alpha in response to hypoxia is instantaneous.* Faseb J, 2001. **15**(7): p. 1312-4.
50. Bruick, R.K. and S.L. McKnight, *A conserved family of prolyl-4-hydroxylases that modify HIF.* Science, 2001. **294**(5545): p. 1337-40.
51. Epstein, A.C., et al., *C. elegans EGL-9 and mammalian homologs define a family of dioxygenases that regulate HIF by prolyl hydroxylation.* Cell, 2001. **107**(1): p. 43-54.
52. Ivan, M., et al., *HIFalpha targeted for VHL-mediated destruction by proline hydroxylation: implications for O2 sensing.* Science, 2001. **292**(5516): p. 464-8.
53. Jaakkola, P., et al., *Targeting of HIF-alpha to the von Hippel-Lindau ubiquitylation complex by O2-regulated prolyl hydroxylation.* Science, 2001. **292**(5516): p. 468-72.
54. Huang, L.E., et al., *Regulation of hypoxia-inducible factor 1alpha is mediated by an O2-dependent degradation domain via the ubiquitin-proteasome pathway.* Proc Natl Acad Sci U S A, 1998. **95**(14): p. 7987-92.
55. King, A., M.A. Selak, and E. Gottlieb, *Succinate dehydrogenase and fumarate hydratase: linking mitochondrial dysfunction and cancer.* Oncogene, 2006. **25**(34): p. 4675-82.
56. MacKenzie, E.D., et al., *Cell-permeating alpha-ketoglutarate derivatives alleviate pseudohypoxia in succinate dehydrogenase-deficient cells.* Mol Cell Biol, 2007. **27**(9): p. 3282-9.
57. Stebbins, C.E., W.G. Kaelin, Jr., and N.P. Pavletich, *Structure of the VHL-ElonginC-ElonginB complex: implications for VHL tumor suppressor function.* Science, 1999. **284**(5413): p. 455-61.

58. Kamura, T., et al., *Activation of HIF1alpha ubiquitination by a reconstituted von Hippel-Lindau (VHL) tumor suppressor complex.* Proc Natl Acad Sci U S A, 2000. **97**(19): p. 10430-5.
59. Krek, W., *VHL takes HIF's breath away.* Nat Cell Biol, 2000. **2**(7): p. E121-3.
60. Maxwell, P.H., et al., *The tumour suppressor protein VHL targets hypoxia-inducible factors for oxygen-dependent proteolysis.* Nature, 1999. **399**(6733): p. 271-5.
61. Kallio, P.J., et al., *Regulation of the hypoxia-inducible transcription factor 1alpha by the ubiquitin-proteasome pathway.* J Biol Chem, 1999. **274**(10): p. 6519-25.
62. Sutter, C.H., E. Laughner, and G.L. Semenza, *Hypoxia-inducible factor 1alpha protein expression is controlled by oxygen-regulated ubiquitination that is disrupted by deletions and missense mutations.* Proc Natl Acad Sci U S A, 2000. **97**(9): p. 4748-53.
63. Jeong, J.W., et al., *Regulation and destabilization of HIF-1alpha by ARD1-mediated acetylation.* Cell, 2002. **111**(5): p. 709-20.
64. Lando, D., et al., *FIH-1 is an asparaginyl hydroxylase enzyme that regulates the transcriptional activity of hypoxia-inducible factor.* Genes Dev, 2002. **16**(12): p. 1466-71.
65. Lando, D., et al., *Asparagine hydroxylation of the HIF transactivation domain a hypoxic switch.* Science, 2002. **295**(5556): p. 858-61.
66. Acker, T. and H. Acker, *Cellular oxygen sensing need in CNS function: physiological and pathological implications.* J Exp Biol, 2004. **207**(Pt 18): p. 3171-88.
67. Hirsila, M., et al., *Characterization of the human prolyl 4-hydroxylases that modify the hypoxia-inducible factor.* J Biol Chem, 2003. **278**(33): p. 30772-80.
68. Marxsen, J.H., et al., *Hypoxia-inducible factor-1 (HIF-1) promotes its degradation by induction of HIF-alpha-prolyl-4-hydroxylases.* Biochem J, 2004. **381**(Pt 3): p. 761-7.
69. D'Angelo, G., et al., *Hypoxia up-regulates prolyl hydroxylase activity: a feedback mechanism that limits HIF-1 responses during reoxygenation.* J Biol Chem, 2003. **278**(40): p. 38183-7.
70. Stiehl, D.P., et al., *Increased prolyl 4-hydroxylase domain proteins compensate for decreased oxygen levels. Evidence for an autoregulatory oxygen-sensing system.* J Biol Chem, 2006. **281**(33): p. 23482-91.
71. Khanna, S., et al., *Oxygen-sensitive reset of hypoxia-inducible factor transactivation response: prolyl hydroxylases tune the biological normoxic set point.* Free Radic Biol Med, 2006. **40**(12): p. 2147-54.
72. Carrero, P., et al., *Redox-regulated recruitment of the transcriptional coactivators CREB-binding protein and SRC-1 to hypoxia-inducible factor 1alpha.* Mol Cell Biol, 2000. **20**(1): p. 402-15.
73. Ebert, B.L. and H.F. Bunn, *Regulation of transcription by hypoxia requires a multiprotein complex that includes hypoxia-inducible factor 1, an adjacent transcription factor, and p300/CREB binding protein.* Mol Cell Biol, 1998. **18**(7): p. 4089-96.
74. Ema, M., et al., *Molecular mechanisms of transcription activation by HLF and HIF1alpha in response to hypoxia: their stabilization and redox signal-induced interaction with CBP/p300.* Embo J, 1999. **18**(7): p. 1905-14.
75. Kallio, P.J., et al., *Signal transduction in hypoxic cells: inducible nuclear translocation and recruitment of the CBP/p300 coactivator by the hypoxia-inducible factor-1alpha.* Embo J, 1998. **17**(22): p. 6573-86.
76. Wenger, R.H., *Cellular adaptation to hypoxia: O2-sensing protein hydroxylases, hypoxia-inducible transcription factors, and O2-regulated gene expression.* Faseb J, 2002. **16**(10): p. 1151-62.
77. Hur, E., et al., *Mitogen-activated protein kinase kinase inhibitor PD98059 blocks the trans-activation but not the stabilization or DNA binding ability of hypoxia-inducible factor-1alpha.* Mol Pharmacol, 2001. **59**(5): p. 1216-24.
78. Richard, D.E., et al., *p42/p44 mitogen-activated protein kinases phosphorylate hypoxia-inducible factor 1alpha (HIF-1alpha) and enhance the transcriptional activity of HIF-1.* J Biol Chem, 1999. **274**(46): p. 32631-7.
79. Fukuda, R., et al., *Insulin-like growth factor 1 induces hypoxia-inducible factor 1-mediated vascular endothelial growth factor expression, which is dependent on MAP kinase and phosphatidylinositol 3-kinase signaling in colon cancer cells.* J Biol Chem, 2002. **277**(41): p. 38205-11.
80. Arsham, A.M., et al., *Phosphatidylinositol 3-kinase/Akt signaling is neither required for hypoxic stabilization of HIF-1 alpha nor sufficient for HIF-1-dependent target gene transcription.* J Biol Chem, 2002. **277**(17): p. 15162-70.
81. Semenza, G.L., *Targeting HIF-1 for cancer therapy.* Nat Rev Cancer, 2003. **3**(10): p. 721-32.
82. Feldser, D., et al., *Reciprocal positive regulation of hypoxia-inducible factor 1alpha and insulin-like growth factor 2.* Cancer Res, 1999. **59**(16): p. 3915-8.
83. Gorlach, A., et al., *Thrombin activates the hypoxia-inducible factor-1 signaling pathway in vascular smooth muscle cells: Role of the p22(phox)-containing NADPH oxidase.* Circ Res, 2001. **89**(1): p. 47-54.
84. Hellwig-Burgel, T., et al., *Interleukin-1beta and tumor necrosis factor-alpha stimulate DNA binding of hypoxia-inducible factor-1.* Blood, 1999. **94**(5): p. 1561-7.
85. Moon, E.J., et al., *Hepatitis B virus X protein induces angiogenesis by stabilizing hypoxia-inducible factor-1alpha.* Faseb J, 2004. **18**(2): p. 382-4.

86. Wakisaka, N., et al., *Epstein-Barr virus latent membrane protein 1 induces synthesis of hypoxia-inducible factor 1 alpha.* Mol Cell Biol, 2004. **24**(12): p. 5223-34.
87. Semenza, G.L., et al., *Hypoxia response elements in the aldolase A, enolase 1, and lactate dehydrogenase A gene promoters contain essential binding sites for hypoxia-inducible factor 1.* J Biol Chem, 1996. **271**(51): p. 32529-37.
88. Semenza, G.L., et al., *Transcriptional regulation of genes encoding glycolytic enzymes by hypoxia-inducible factor 1.* J Biol Chem, 1994. **269**(38): p. 23757-63.
89. Grabmaier, K., et al., *Strict regulation of CAIX(G250/MN) by HIF-1alpha in clear cell renal cell carcinoma.* Oncogene, 2004. **23**(33): p. 5624-31.
90. Kothari, S., et al., *BNIP3 plays a role in hypoxic cell death in human epithelial cells that is inhibited by growth factors EGF and IGF.* Oncogene, 2003. **22**(30): p. 4734-44.
91. Miyazaki, K., et al., *Identification of functional hypoxia response elements in the promoter region of the DEC1 and DEC2 genes.* J Biol Chem, 2002. **277**(49): p. 47014-21.
92. Coulet, F., et al., *Identification of hypoxia-response element in the human endothelial nitric-oxide synthase gene promoter.* J Biol Chem, 2003. **278**(47): p. 46230-40.
93. Firth, J.D., et al., *Oxygen-regulated control elements in the phosphoglycerate kinase 1 and lactate dehydrogenase A genes: similarities with the erythropoietin 3' enhancer.* Proc Natl Acad Sci U S A, 1994. **91**(14): p. 6496-500.
94. Wang, G.L. and G.L. Semenza, *Characterization of hypoxia-inducible factor 1 and regulation of DNA binding activity by hypoxia.* J Biol Chem, 1993. **268**(29): p. 21513-8.
95. Ebert, B.L., J.D. Firth, and P.J. Ratcliffe, *Hypoxia and mitochondrial inhibitors regulate expression of glucose transporter-1 via distinct Cis-acting sequences.* J Biol Chem, 1995. **270**(49): p. 29083-9.
96. Okino, S.T., C.H. Chichester, and J.P. Whitlock, Jr., *Hypoxia-inducible mammalian gene expression analyzed in vivo at a TATA-driven promoter and at an initiator-driven promoter.* J Biol Chem, 1998. **273**(37): p. 23837-43.
97. Lu, S., et al., *Identification of an additional hypoxia responsive element in the glyceraldehyde-3-phosphate dehydrogenase gene promoter.* Biochim Biophys Acta, 2002. **1574**(2): p. 152-6.
98. Kim, J.W., et al., *Hypoxia-inducible factor 1 and dysregulated c-Myc cooperatively induce vascular endothelial growth factor and metabolic switches hexokinase 2 and pyruvate dehydrogenase kinase 1.* Mol Cell Biol, 2007. **27**(21): p. 7381-93.
99. Kietzmann, T., A. Krones-Herzig, and K. Jungermann, *Signaling cross-talk between hypoxia and glucose via hypoxia-inducible factor 1 and glucose response elements.* Biochem Pharmacol, 2002. **64**(5-6): p. 903-11.
100. Firth, J.D., B.L. Ebert, and P.J. Ratcliffe, *Hypoxic regulation of lactate dehydrogenase A. Interaction between hypoxia-inducible factor 1 and cAMP response elements.* J Biol Chem, 1995. **270**(36): p. 21021-7.
101. Sowter, H.M., et al., *HIF-1-dependent regulation of hypoxic induction of the cell death factors BNIP3 and NIX in human tumors.* Cancer Res, 2001. **61**(18): p. 6669-73.
102. Palmer, L.A., et al., *Hypoxia induces type II NOS gene expression in pulmonary artery endothelial cells via HIF-1.* Am J Physiol, 1998. **274**(2 Pt 1): p. L212-9.
103. Minchenko, A., et al., *Hypoxia-inducible factor-1-mediated expression of the 6-phosphofructo-2-kinase/fructose-2,6-bisphosphatase-3 (PFKFB3) gene. Its possible role in the Warburg effect.* J Biol Chem, 2002. **277**(8): p. 6183-7.
104. Fink, T., et al., *Identification of a tightly regulated hypoxia-response element in the promoter of human plasminogen activator inhibitor-1.* Blood, 2002. **99**(6): p. 2077-83.
105. Metzen, E., et al., *Regulation of the prolyl hydroxylase domain protein 2 (phd2/egln-1) gene: identification of a functional hypoxia-responsive element.* Biochem J, 2005. **387**(Pt 3): p. 711-7.
106. Takahashi, Y., et al., *Hypoxic induction of prolyl 4-hydroxylase alpha (I) in cultured cells.* J Biol Chem, 2000. **275**(19): p. 14139-46.
107. Nishi, H., et al., *Hypoxia-inducible factor 1 mediates upregulation of telomerase (hTERT).* Mol Cell Biol, 2004. **24**(13): p. 6076-83.
108. Yatabe, N., et al., *HIF-1-mediated activation of telomerase in cervical cancer cells.* Oncogene, 2004. **23**(20): p. 3708-15.
109. Krishnamachary, B., et al., *Regulation of colon carcinoma cell invasion by hypoxia-inducible factor 1.* Cancer Res, 2003. **63**(5): p. 1138-43.
110. Rolfs, A., et al., *Oxygen-regulated transferrin expression is mediated by hypoxia-inducible factor-1.* J Biol Chem, 1997. **272**(32): p. 20055-62.
111. Lok, C.N. and P. Ponka, *Identification of a hypoxia response element in the transferrin receptor gene.* J Biol Chem, 1999. **274**(34): p. 24147-52.
112. Tacchini, L., et al., *Transferrin receptor induction by hypoxia. HIF-1-mediated transcriptional activation and cell-specific post-transcriptional regulation.* J Biol Chem, 1999. **274**(34): p. 24142-6.

113. Forsythe, J.A., et al., *Activation of vascular endothelial growth factor gene transcription by hypoxia-inducible factor 1.* Mol Cell Biol, 1996. **16**(9): p. 4604-13.
114. Liu, Y., et al., *Hypoxia regulates vascular endothelial growth factor gene expression in endothelial cells. Identification of a 5' enhancer.* Circ Res, 1995. **77**(3): p. 638-43.
115. Gerber, H.P., et al., *Differential transcriptional regulation of the two vascular endothelial growth factor receptor genes. Flt-1, but not Flk-1/KDR, is up-regulated by hypoxia.* J Biol Chem, 1997. **272**(38): p. 23659-67.
116. Rankin, E.B., et al., *Hypoxia-inducible factor-2 (HIF-2) regulates hepatic erythropoietin in vivo.* J Clin Invest, 2007. **117**(4): p. 1068-77.
117. Yeo, E.J., et al., *Contribution of HIF-1alpha or HIF-2alpha to erythropoietin expression: in vivo evidence based on chromatin immunoprecipitation.* Ann Hematol, 2008. **87**(1): p. 11-7.
118. Levy, A.P., et al., *Transcriptional regulation of the rat vascular endothelial growth factor gene by hypoxia.* J Biol Chem, 1995. **270**(22): p. 13333-40.
119. Shweiki, D., et al., *Vascular endothelial growth factor induced by hypoxia may mediate hypoxia-initiated angiogenesis.* Nature, 1992. **359**(6398): p. 843-5.
120. Stein, I., et al., *Stabilization of vascular endothelial growth factor mRNA by hypoxia and hypoglycemia and coregulation with other ischemia-induced genes.* Mol Cell Biol, 1995. **15**(10): p. 5363-8.
121. Lewis, C.E., et al., *Cytokine regulation of angiogenesis in breast cancer: the role of tumor-associated macrophages.* J Leukoc Biol, 1995. **57**(5): p. 747-51.
122. Strieter, R.M., et al., *Role of C-X-C chemokines as regulators of angiogenesis in lung cancer.* J Leukoc Biol, 1995. **57**(5): p. 752-62.
123. Gillies, R.J., et al., *Causes and effects of heterogeneous perfusion in tumors.* Neoplasia, 1999. **1**(3): p. 197-207.
124. Vaupel, P. and M. Hockel, *Blood supply, oxygenation status and metabolic micromilieu of breast cancers: characterization and therapeutic relevance.* Int J Oncol, 2000. **17**(5): p. 869-79.
125. Eberhard, A., et al., *Heterogeneity of angiogenesis and blood vessel maturation in human tumors: implications for antiangiogenic tumor therapies.* Cancer Res, 2000. **60**(5): p. 1388-93.
126. Pasteur, L., *Experiences et vues nouvelles sur la nature des fermentations.* Comp Rend Acad Sci, 1861. **52**: p. 1260-1264.
127. Iyer, N.V., et al., *Cellular and developmental control of O2 homeostasis by hypoxia-inducible factor 1 alpha.* Genes Dev, 1998. **12**(2): p. 149-62.
128. Seagroves, T.N., et al., *Transcription factor HIF-1 is a necessary mediator of the pasteur effect in mammalian cells.* Mol Cell Biol, 2001. **21**(10): p. 3436-44.
129. Stubbs, M., C.L. Bashford, and J.R. Griffiths, *Understanding the tumor metabolic phenotype in the genomic era.* Curr Mol Med, 2003. **3**(1): p. 49-59.
130. Webster, K.A., *Regulation of glycolytic enzyme RNA transcriptional rates by oxygen availability in skeletal muscle cells.* Mol Cell Biochem, 1987. **77**(1): p. 19-28.
131. Webster, K.A., *Evolution of the coordinate regulation of glycolytic enzyme genes by hypoxia.* J Exp Biol, 2003. **206**(Pt 17): p. 2911-22.
132. Boutilier, R.G., *Mechanisms of cell survival in hypoxia and hypothermia.* J Exp Biol, 2001. **204**(Pt 18): p. 3171-81.
133. Buck, L.T. and P.W. Hochachka, *Anoxic suppression of Na(+)-K(+)-ATPase and constant membrane potential in hepatocytes: support for channel arrest.* Am J Physiol, 1993. **265**(5 Pt 2): p. R1020-5.
134. Hochachka, P.W., et al., *Unifying theory of hypoxia tolerance: molecular/metabolic defense and rescue mechanisms for surviving oxygen lack.* Proc Natl Acad Sci U S A, 1996. **93**(18): p. 9493-8.
135. Krumschnabel, G., et al., *Oxygen-dependent energetics of anoxia-tolerant and anoxia-intolerant hepatocytes.* J Exp Biol, 2000. **203**(Pt 5): p. 951-9.
136. Kim, J.W. and C.V. Dang, *Multifaceted roles of glycolytic enzymes.* Trends Biochem Sci, 2005. **30**(3): p. 142-50.
137. An, W.G., et al., *Stabilization of wild-type p53 by hypoxia-inducible factor 1alpha.* Nature, 1998. **392**(6674): p. 405-8.
138. Dang, C.V. and G.L. Semenza, *Oncogenic alterations of metabolism.* Trends Biochem Sci, 1999. **24**(2): p. 68-72.
139. Gatenby, R.A. and R.J. Gillies, *Why do cancers have high aerobic glycolysis?* Nat Rev Cancer, 2004. **4**(11): p. 891-9.
140. Semenza, G.L., et al., *'The metabolism of tumours': 70 years later.* Novartis Found Symp, 2001. **240**: p. 251-60; discussion 260-4.
141. Warburg, O., *Ist die aerobe Glykolyse spezifisch für die Tumoren?* Biochem. Z., 1929. **204**: p. 482-483.
142. Warburg, O., *On the origin of cancer cells.* Science, 1956. **123**(3191): p. 309-14.
143. Nielsen, F.U., et al., *Effect of changing tumor oxygenation on glycolytic metabolism in a murine C3H mammary carcinoma assessed by in vivo nuclear magnetic resonance spectroscopy.* Cancer Res, 2001. **61**(13): p. 5318-25.

144. Guppy, M., et al., *Contribution by different fuels and metabolic pathways to the total ATP turnover of proliferating MCF-7 breast cancer cells.* Biochem J, 2002. **364**(Pt 1): p. 309-15.
145. Zu, X.L. and M. Guppy, *Cancer metabolism: facts, fantasy, and fiction.* Biochem Biophys Res Commun, 2004. **313**(3): p. 459-65.
146. Franchi, A., P. Silvestre, and J. Pouyssegur, *A genetic approach to the role of energy metabolism in the growth of tumor cells: tumorigenicity of fibroblast mutants deficient either in glycolysis or in respiration.* Int J Cancer, 1981. **27**(6): p. 819-27.
147. Brand, K.A. and U. Hermfisse, *Aerobic glycolysis by proliferating cells: a protective strategy against reactive oxygen species.* Faseb J, 1997. **11**(5): p. 388-95.
148. Kim, J.W., et al., *HIF-1-mediated expression of pyruvate dehydrogenase kinase: a metabolic switch required for cellular adaptation to hypoxia.* Cell Metab, 2006. **3**(3): p. 177-85.
149. Papandreou, I., et al., *HIF-1 mediates adaptation to hypoxia by actively downregulating mitochondrial oxygen consumption.* Cell Metab, 2006. **3**(3): p. 187-97.
150. Simon, M.C., *Coming up for air: HIF-1 and mitochondrial oxygen consumption.* Cell Metab, 2006. **3**(3): p. 150-1.
151. Koukourakis, M.I., et al., *Pyruvate dehydrogenase and pyruvate dehydrogenase kinase expression in non small cell lung cancer and tumor-associated stroma.* Neoplasia, 2005. **7**(1): p. 1-6.
152. Grandori, C., et al., *The Myc/Max/Mad network and the transcriptional control of cell behavior.* Annu Rev Cell Dev Biol, 2000. **16**: p. 653-99.
153. Grandori, C., et al., *Myc-Max heterodimers activate a DEAD box gene and interact with multiple E box-related sites in vivo.* Embo J, 1996. **15**(16): p. 4344-57.
154. Swanson, H.I. and J.H. Yang, *Specificity of DNA binding of the c-Myc/Max and ARNT/ARNT dimers at the CACGTG recognition site.* Nucleic Acids Res, 1999. **27**(15): p. 3205-12.
155. Gordan, J.D., et al., *HIF-2alpha promotes hypoxic cell proliferation by enhancing c-myc transcriptional activity.* Cancer Cell, 2007. **11**(4): p. 335-47.
156. Koshiji, M., et al., *HIF-1alpha induces cell cycle arrest by functionally counteracting Myc.* Embo J, 2004. **23**(9): p. 1949-56.
157. Koshiji, M., et al., *HIF-1alpha induces genetic instability by transcriptionally downregulating MutSalpha expression.* Mol Cell, 2005. **17**(6): p. 793-803.
158. Mazure, N.M., et al., *Repression of alpha-fetoprotein gene expression under hypoxic conditions in human hepatoma cells: characterization of a negative hypoxia response element that mediates opposite effects of hypoxia inducible factor-1 and c-Myc.* Cancer Res, 2002. **62**(4): p. 1158-65.
159. Fantin, V.R., J. St-Pierre, and P. Leder, *Attenuation of LDH-A expression uncovers a link between glycolysis, mitochondrial physiology, and tumor maintenance.* Cancer Cell, 2006. **9**(6): p. 425-34.
160. Shim, H., et al., *c-Myc transactivation of LDH-A: implications for tumor metabolism and growth.* Proc Natl Acad Sci U S A, 1997. **94**(13): p. 6658-63.
161. Dang, C.V., et al., *Oncogenes in tumor metabolism, tumorigenesis, and apoptosis.* J Bioenerg Biomembr, 1997. **29**(4): p. 345-54.
162. Marsden, V.S. and A. Strasser, *Control of apoptosis in the immune system: Bcl-2, BH3-only proteins and more.* Annu Rev Immunol, 2003. **21**: p. 71-105.
163. Hengartner, M.O. and H.R. Horvitz, *The ins and outs of programmed cell death during C. elegans development.* Philos Trans R Soc Lond B Biol Sci, 1994. **345**(1313): p. 243-6.
164. Mellor, H.R. and A.L. Harris, *The role of the hypoxia-inducible BH3-only proteins BNIP3 and BNIP3L in cancer.* Cancer Metastasis Rev, 2007. **26**(3-4): p. 553-66.
165. Strasser, A., L. O'Connor, and V.M. Dixit, *Apoptosis signaling.* Annu Rev Biochem, 2000. **69**: p. 217-45.
166. Li, P., et al., *Cytochrome c and dATP-dependent formation of Apaf-1/caspase-9 complex initiates an apoptotic protease cascade.* Cell, 1997. **91**(4): p. 479-89.
167. Nicholson, D.W. and N.A. Thornberry, *Caspases: killer proteases.* Trends Biochem Sci, 1997. **22**(8): p. 299-306.
168. Chen, G., et al., *The E1B 19K/Bcl-2-binding protein Nip3 is a dimeric mitochondrial protein that activates apoptosis.* J Exp Med, 1997. **186**(12): p. 1975-83.
169. Ray, R., et al., *BNIP3 heterodimerizes with Bcl-2/Bcl-X(L) and induces cell death independent of a Bcl-2 homology 3 (BH3) domain at both mitochondrial and nonmitochondrial sites.* J Biol Chem, 2000. **275**(2): p. 1439-48.
170. Webster, K.A., R.M. Graham, and N.H. Bishopric, *BNip3 and signal-specific programmed death in the heart.* J Mol Cell Cardiol, 2005. **38**(1): p. 35-45.
171. Vande Velde, C., et al., *BNIP3 and genetic control of necrosis-like cell death through the mitochondrial permeability transition pore.* Mol Cell Biol, 2000. **20**(15): p. 5454-68.
172. Bellot, G., et al., *Hypoxia-induced autophagy is mediated through hypoxia-inducible factor induction of BNIP3 and BNIP3L via their BH3 domains.* Mol Cell Biol, 2009. **29**(10): p. 2570-81.

173. Tracy, K. and K.F. Macleod, *Regulation of mitochondrial integrity, autophagy and cell survival by BNIP3.* Autophagy, 2007. **3**(6): p. 616-9.
174. Papandreou, I., et al., *Hypoxia signals autophagy in tumor cells via AMPK activity, independent of HIF-1, BNIP3, and BNIP3L.* Cell Death Differ, 2008. **15**(10): p. 1572-81.
175. Tracy, K., et al., *BNIP3 is an RB/E2F target gene required for hypoxia-induced autophagy.* Mol Cell Biol, 2007. **27**(17): p. 6229-42.
176. Maiuri, M.C., et al., *Functional and physical interaction between Bcl-X(L) and a BH3-like domain in Beclin-1.* Embo J, 2007. **26**(10): p. 2527-39.
177. Zhang, H., et al., *Mitochondrial autophagy is an HIF-1-dependent adaptive metabolic response to hypoxia.* J Biol Chem, 2008. **283**(16): p. 10892-903.
178. Mazure, N.M. and J. Pouyssegur, *Atypical BH3-domains of BNIP3 and BNIP3L lead to autophagy in hypoxia.* Autophagy, 2009. **5**(6): p. 868-9.
179. Chinnadurai, G., S. Vijayalingam, and S.B. Gibson, *BNIP3 subfamily BH3-only proteins: mitochondrial stress sensors in normal and pathological functions.* Oncogene, 2008. **27 Suppl 1**: p. S114-27.
180. Ebbesen, P., et al., *Taking advantage of tumor cell adaptations to hypoxia for developing new tumor markers and treatment strategies.* J Enzyme Inhib Med Chem, 2009. **24 Suppl 1**: p. 1-39.
181. Kubasiak, L.A., et al., *Hypoxia and acidosis activate cardiac myocyte death through the Bcl-2 family protein BNIP3.* Proc Natl Acad Sci U S A, 2002. **99**(20): p. 12825-30.
182. Kim, J.Y. and J.H. Park, *ROS-dependent caspase-9 activation in hypoxic cell death.* FEBS Lett, 2003. **549**(1-3): p. 94-8.
183. Bruick, R.K., *Expression of the gene encoding the proapoptotic Nip3 protein is induced by hypoxia.* Proc Natl Acad Sci U S A, 2000. **97**(16): p. 9082-7.
184. Sowter, H.M., et al., *Expression of the cell death genes BNip3 and NIX in ductal carcinoma in situ of the breast; correlation of BNip3 levels with necrosis and grade.* J Pathol, 2003. **201**(4): p. 573-80.
185. Manka, D., Z. Spicer, and D.E. Millhorn, *Bcl-2/adenovirus E1B 19 kDa interacting protein-3 knockdown enables growth of breast cancer metastases in the lung, liver, and bone.* Cancer Res, 2005. **65**(24): p. 11689-93.
186. Wouters, B.G., et al., *Targeting hypoxia tolerance in cancer.* Drug Resist Updat, 2004. **7**(1): p. 25-40.
187. Zhou, J., et al., *Tumor hypoxia and cancer progression.* Cancer Lett, 2006. **237**(1): p. 10-21.
188. Fei, P., et al., *Bnip3L is induced by p53 under hypoxia, and its knockdown promotes tumor growth.* Cancer Cell, 2004. **6**(6): p. 597-609.
189. Dong, Z., et al., *Up-regulation of apoptosis inhibitory protein IAP-2 by hypoxia. Hif-1-independent mechanisms.* J Biol Chem, 2001. **276**(22): p. 18702-9.
190. Dong, Z., et al., *Apoptosis-resistance of hypoxic cells: multiple factors involved and a role for IAP-2.* Am J Pathol, 2003. **163**(2): p. 663-71.
191. Abe, T., et al., *Upregulation of BNIP3 by 5-aza-2'-deoxycytidine sensitizes pancreatic cancer cells to hypoxia-mediated cell death.* J Gastroenterol, 2005. **40**(5): p. 504-10.
192. Akada, M., et al., *Intrinsic chemoresistance to gemcitabine is associated with decreased expression of BNIP3 in pancreatic cancer.* Clin Cancer Res, 2005. **11**(8): p. 3094-101.
193. Erkan, M., et al., *Loss of BNIP3 expression is a late event in pancreatic cancer contributing to chemoresistance and worsened prognosis.* Oncogene, 2005. **24**(27): p. 4421-32.
194. Okami, J., D.M. Simeone, and C.D. Logsdon, *Silencing of the hypoxia-inducible cell death protein BNIP3 in pancreatic cancer.* Cancer Res, 2004. **64**(15): p. 5338-46.
195. Bacon, A.L., et al., *Selective silencing of the hypoxia-inducible factor 1 target gene BNIP3 by histone deacetylation and methylation in colorectal cancer.* Oncogene, 2007. **26**(1): p. 132-41.
196. Murai, M., et al., *Aberrant DNA methylation associated with silencing BNIP3 gene expression in haematopoietic tumours.* Br J Cancer, 2005. **92**(6): p. 1165-72.
197. Murai, M., et al., *Aberrant methylation and silencing of the BNIP3 gene in colorectal and gastric cancer.* Clin Cancer Res, 2005. **11**(3): p. 1021-7.
198. Carmeliet, P., et al., *Role of HIF-1alpha in hypoxia-mediated apoptosis, cell proliferation and tumour angiogenesis.* Nature, 1998. **394**(6692): p. 485-90.
199. Akakura, N., et al., *Constitutive expression of hypoxia-inducible factor-1alpha renders pancreatic cancer cells resistant to apoptosis induced by hypoxia and nutrient deprivation.* Cancer Res, 2001. **61**(17): p. 6548-54.
200. Shimizu, S., et al., *Prevention of hypoxia-induced cell death by Bcl-2 and Bcl-xL.* Nature, 1995. **374**(6525): p. 811-3.
201. Chen, D., et al., *Direct interactions between HIF-1 alpha and Mdm2 modulate p53 function.* J Biol Chem, 2003. **278**(16): p. 13595-8.
202. Hansson, L.O., et al., *Two sequence motifs from HIF-1alpha bind to the DNA-binding site of p53.* Proc Natl Acad Sci U S A, 2002. **99**(16): p. 10305-9.
203. Wenger, R.H., et al., *Up-regulation of hypoxia-inducible factor-1alpha is not sufficient for hypoxic/anoxic p53 induction.* Cancer Res, 1998. **58**(24): p. 5678-80.

204. Ebbesen, P., et al., *Linking measured intercellular oxygen concentration to human cell functions.* Acta Oncol, 2004. **43**(6): p. 598-600.
205. Sirito, M., et al., *Ubiquitous expression of the 43- and 44-kDa forms of transcription factor USF in mammalian cells.* Nucleic Acids Res, 1994. **22**(3): p. 427-33.
206. Sirito, M., et al., *Members of the USF family of helix-loop-helix proteins bind DNA as homo- as well as heterodimers.* Gene Expr, 1992. **2**(3): p. 231-40.
207. Kirschbaum, B.J., P. Pognonec, and R.G. Roeder, *Definition of the transcriptional activation domain of recombinant 43-kilodalton USF.* Mol Cell Biol, 1992. **12**(11): p. 5094-101.
208. Luo, X. and M. Sawadogo, *Antiproliferative properties of the USF family of helix-loop-helix transcription factors.* Proc Natl Acad Sci U S A, 1996. **93**(3): p. 1308-13.
209. Qyang, Y., et al., *Cell-type-dependent activity of the ubiquitous transcription factor USF in cellular proliferation and transcriptional activation.* Mol Cell Biol, 1999. **19**(2): p. 1508-17.
210. Viollet, B., et al., *Immunochemical characterization and transacting properties of upstream stimulatory factor isoforms.* J Biol Chem, 1996. **271**(3): p. 1405-15.
211. Saito, T., et al., *Cloning and characterization of a novel splicing isoform of USF1.* Int J Mol Med, 2003. **12**(2): p. 161-7.
212. Howcroft, T.K., et al., *Upstream stimulatory factor regulates major histocompatibility complex class I gene expression: the U2DeltaE4 splice variant abrogates E-box activity.* Mol Cell Biol, 1999. **19**(7): p. 4788-97.
213. Lefrancois-Martinez, A.M., et al., *Upstream stimulatory factor proteins are major components of the glucose response complex of the L-type pyruvate kinase gene promoter.* J Biol Chem, 1995. **270**(6): p. 2640-3.
214. Corre, S. and M.D. Galibert, *Upstream stimulating factors: highly versatile stress-responsive transcription factors.* Pigment Cell Res, 2005. **18**(5): p. 337-48.
215. Ferre-D'Amare, A.R., et al., *Structure and function of the b/HLH/Z domain of USF.* Embo J, 1994. **13**(1): p. 180-9.
216. Jaiswal, A.S. and S. Narayan, *Upstream stimulating factor-1 (USF1) and USF2 bind to and activate the promoter of the adenomatous polyposis coli (APC) tumor suppressor gene.* J Cell Biochem, 2001. **81**(2): p. 262-77.
217. Sato, M., et al., *Transcriptional control of the rat heme oxygenase gene by a nuclear protein that interacts with adenovirus 2 major late promoter.* J Biol Chem, 1989. **264**(17): p. 10251-60.
218. Sawadogo, M. and R.G. Roeder, *Interaction of a gene-specific transcription factor with the adenovirus major late promoter upstream of the TATA box region.* Cell, 1985. **43**(1): p. 165-75.
219. Du, H., A.L. Roy, and R.G. Roeder, *Human transcription factor USF stimulates transcription through the initiator elements of the HIV-1 and the Ad-ML promoters.* Embo J, 1993. **12**(2): p. 501-11.
220. Roy, A.L., et al., *Cooperative interaction of an initiator-binding transcription initiation factor and the helix-loop-helix activator USF.* Nature, 1991. **354**(6350): p. 245-8.
221. Andrews, G.K., et al., *The transcription factors MTF-1 and USF1 cooperate to regulate mouse metallothionein-I expression in response to the essential metal zinc in visceral endoderm cells during early development.* Embo J, 2001. **20**(5): p. 1114-22.
222. Firlej, V., et al., *Pea3 transcription factor cooperates with USF-1 in regulation of the murine bax transcription without binding to an Ets-binding site.* J Biol Chem, 2005. **280**(2): p. 887-98.
223. Ge, Y., et al., *Physical and functional interactions between USF and Sp1 proteins regulate human deoxycytidine kinase promoter activity.* J Biol Chem, 2003. **278**(50): p. 49901-10.
224. Chiang, C.M. and R.G. Roeder, *Cloning of an intrinsic human TFIID subunit that interacts with multiple transcriptional activators.* Science, 1995. **267**(5197): p. 531-6.
225. Roy, A.L., et al., *Cloning of an inr- and E-box-binding protein, TFII-I, that interacts physically and functionally with USF1.* Embo J, 1997. **16**(23): p. 7091-104.
226. Breen, G.A. and E.M. Jordan, *Transcriptional activation of the F(1)F(0) ATP synthase alpha-subunit initiator element by USF2 is mediated by p300.* Biochim Biophys Acta, 1999. **1428**(2-3): p. 169-76.
227. Goueli, B.S. and R. Janknecht, *Regulation of telomerase reverse transcriptase gene activity by upstream stimulatory factor.* Oncogene, 2003. **22**(39): p. 8042-7.
228. Galibert, M.D., et al., *Recognition of the E-C4 element from the C4 complement gene promoter by the upstream stimulatory factor-1 transcription factor.* J Immunol, 1997. **159**(12): p. 6176-83.
229. North, S., et al., *Regulation of cdc2 gene expression by the upstream stimulatory factors (USFs).* Oncogene, 1999. **18**(11): p. 1945-55.
230. Pawar, S.A., et al., *Evidence for a cancer-specific switch at the CDK4 promoter with loss of control by both USF and c-Myc.* Oncogene, 2004. **23**(36): p. 6125-35.
231. Kingsley-Kallesen, M.L., D. Kelly, and A. Rizzino, *Transcriptional regulation of the transforming growth factor-beta2 promoter by cAMP-responsive element-binding protein (CREB) and activating transcription factor-1 (ATF-1) is modulated by protein kinases and the coactivators p300 and CREB-binding protein.* J Biol Chem, 1999. **274**(48): p. 34020-8.

232. Iynedjian, P.B., *Identification of upstream stimulatory factor as transcriptional activator of the liver promoter of the glucokinase gene.* Biochem J, 1998. **333 (Pt 3)**: p. 705-12.
233. Roth, U., K. Jungermann, and T. Kietzmann, *Modulation of glucokinase expression by hypoxia-inducible factor 1 and upstream stimulatory factor 2 in primary rat hepatocytes.* Biol Chem, 2004. **385**(3-4): p. 239-47.
234. Wang, D. and H.S. Sul, *Upstream stimulatory factor binding to the E-box at -65 is required for insulin regulation of the fatty acid synthase promoter.* J Biol Chem, 1997. **272**(42): p. 26367-74.
235. Galibert, M.D., S. Carreira, and C.R. Goding, *The Usf-1 transcription factor is a novel target for the stress-responsive p38 kinase and mediates UV-induced Tyrosinase expression.* Embo J, 2001. **20**(17): p. 5022-31.
236. Imagawa, S., et al., *Hepatocyte growth factor regulates E box-dependent plasminogen activator inhibitor type 1 gene expression in HepG2 liver cells.* Arterioscler Thromb Vasc Biol, 2006. **26**(10): p. 2407-13.
237. Xiao, Q., A. Kenessey, and K. Ojamaa, *Role of USF1 phosphorylation on cardiac alpha-myosin heavy chain promoter activity.* Am J Physiol Heart Circ Physiol, 2002. **283**(1): p. H213-9.
238. Cheung, E., et al., *DNA-binding activity of the transcription factor upstream stimulatory factor 1 (USF-1) is regulated by cyclin-dependent phosphorylation.* Biochem J, 1999. **344 Pt 1**: p. 145-52.
239. Carthew, R.W., L.A. Chodosh, and P.A. Sharp, *An RNA polymerase II transcription factor binds to an upstream element in the adenovirus major late promoter.* Cell, 1985. **43**(2 Pt 1): p. 439-48.
240. Moncollin, V., et al., *Purification of a factor specific for the upstream element of the adenovirus-2 major late promoter.* Embo J, 1986. **5**(10): p. 2577-84.
241. Carter, R.S., P. Ordentlich, and T. Kadesch, *Selective utilization of basic helix-loop-helix-leucine zipper proteins at the immunoglobulin heavy-chain enhancer.* Mol Cell Biol, 1997. **17**(1): p. 18-23.
242. Takahashi, Y., et al., *Inhibition of the transcription of CYP1A1 gene by the upstream stimulatory factor 1 in rabbits. Competitive binding of USF1 with AhR.Arnt complex.* J Biol Chem, 1997. **272**(48): p. 30025-31.
243. Jiang, B. and C.R. Mendelson, *USF1 and USF2 mediate inhibition of human trophoblast differentiation and CYP19 gene expression by Mash-2 and hypoxia.* Mol Cell Biol, 2003. **23**(17): p. 6117-28.
244. Chen, Y.H., et al., *Upstream stimulatory factors regulate aortic preferentially expressed gene-1 expression in vascular smooth muscle cells.* J Biol Chem, 2001. **276**(50): p. 47658-63.
245. Samoylenko, A., et al., *The upstream stimulatory factor-2a inhibits plasminogen activator inhibitor-1 gene expression by binding to a promoter element adjacent to the hypoxia-inducible factor-1 binding site.* Blood, 2001. **97**(9): p. 2657-66.
246. Sirito, M., et al., *Overlapping roles and asymmetrical cross-regulation of the USF proteins in mice.* Proc Natl Acad Sci U S A, 1998. **95**(7): p. 3758-63.
247. Vallet, V.S., et al., *Glucose-dependent liver gene expression in upstream stimulatory factor 2 -/- mice.* J Biol Chem, 1997. **272**(35): p. 21944-9.
248. Vallet, V.S., et al., *Differential roles of upstream stimulatory factors 1 and 2 in the transcriptional response of liver genes to glucose.* J Biol Chem, 1998. **273**(32): p. 20175-9.
249. Desbarats, L., S. Gaubatz, and M. Eilers, *Discrimination between different E-box-binding proteins at an endogenous target gene of c-myc.* Genes Dev, 1996. **10**(4): p. 447-60.
250. Blanar, M.A. and W.J. Rutter, *Interaction cloning: identification of a helix-loop-helix zipper protein that interacts with c-Fos.* Science, 1992. **256**(5059): p. 1014-8.
251. Kurschner, C. and J.I. Morgan, *USF2/FIP associates with the b-Zip transcription factor, c-Maf, via its bHLH domain and inhibits c-Maf DNA binding activity.* Biochem Biophys Res Commun, 1997. **231**(2): p. 333-9.
252. Pognonec, P., et al., *Cross-family interaction between the bHLHZip USF and bZip Fra1 proteins results in down-regulation of AP1 activity.* Oncogene, 1997. **14**(17): p. 2091-8.
253. Allen, R.R., L. Qi, and P.J. Higgins, *Upstream stimulatory factor regulates E box-dependent PAI-1 transcription in human epidermal keratinocytes.* J Cell Physiol, 2005. **203**(1): p. 156-65.
254. Choe, C., N. Chen, and M. Sawadogo, *Decreased tumorigenicity of c-Myc-transformed fibroblasts expressing active USF2.* Exp Cell Res, 2005. **302**(1): p. 1-10.
255. Han, S.Y., et al., *Cell type-dependent regulation of human DNA topoisomerase III alpha gene expression by upstream stimulatory factor 2.* FEBS Lett, 2001. **505**(1): p. 57-62.
256. Ismail, P.M., T. Lu, and M. Sawadogo, *Loss of USF transcriptional activity in breast cancer cell lines.* Oncogene, 1999. **18**(40): p. 5582-91.
257. Szentirmay, M.N., et al., *The IGF2 receptor is a USF2-specific target in nontumorigenic mammary epithelial cells but not in breast cancer cells.* J Biol Chem, 2003. **278**(39): p. 37231-40.
258. Moriuchi, M., et al., *USF/c-Myc enhances, while Yin-Yang 1 suppresses, the promoter activity of CXCR4, a coreceptor for HIV-1 entry.* J Immunol, 1999. **162**(10): p. 5986-92.
259. Jhappan, C., F.P. Noonan, and G. Merlino, *Ultraviolet radiation and cutaneous malignant melanoma.* Oncogene, 2003. **22**(20): p. 3099-112.

260. Houghton, A.N. and D. Polsky, *Focus on melanoma.* Cancer Cell, 2002. **2**(4): p. 275-8.
261. Berwick, M. and C. Wiggins, *The current epidemiology of cutaneous malignant melanoma.* Front Biosci, 2006. **11**: p. 1244-54.
262. Satyamoorthy, K., T. Bogenrieder, and M. Herlyn, *No longer a molecular black box--new clues to apoptosis and drug resistance in melanoma.* Trends Mol Med, 2001. **7**(5): p. 191-4.
263. Bertolotto, C., et al., *Microphthalmia gene product as a signal transducer in cAMP-induced differentiation of melanocytes.* J Cell Biol, 1998. **142**(3): p. 827-35.
264. Steingrimsson, E., N.G. Copeland, and N.A. Jenkins, *Melanocytes and the microphthalmia transcription factor network.* Annu Rev Genet, 2004. **38**: p. 365-411.
265. Hoek, K.S., et al., *In vivo switching of human melanoma cells between proliferative and invasive states.* Cancer Res, 2008. **68**(3): p. 650-6.
266. Busca, R., et al., *Hypoxia-inducible factor 1{alpha} is a new target of microphthalmia-associated transcription factor (MITF) in melanoma cells.* J Cell Biol, 2005. **170**(1): p. 49-59.
267. Corre, S., et al., *UV-induced expression of key component of the tanning process, the POMC and MC1R genes, is dependent on the p-38-activated upstream stimulating factor-1 (USF-1).* J Biol Chem, 2004. **279**(49): p. 51226-33.
268. Corre, S., et al., *Target gene specificity of USF-1 is directed via p38-mediated phosphorylation-dependent acetylation.* J Biol Chem, 2009. **284**(28): p. 18851-62.
269. Evans, N.T. and P.F. Naylor, *The oxygen tension gradient across human epidermis.* Respir Physiol, 1967. **3**(1): p. 38-42.
270. Lartigau, E., et al., *Intratumoral oxygen tension in metastatic melanoma.* Melanoma Res, 1997. **7**(5): p. 400-6.
271. Stewart, F.A., J. Denekamp, and V.S. Randhawa, *Skin sensitization by misonidazole: a demonstration of uniform mild hypoxia.* Br J Cancer, 1982. **45**(6): p. 869-77.
272. Potter, C.P. and A.L. Harris, *Diagnostic, prognostic and therapeutic implications of carbonic anhydrases in cancer.* Br J Cancer, 2003. **89**(1): p. 2-7.
273. Brurberg, K.G., B.A. Graff, and E.K. Rofstad, *Temporal heterogeneity in oxygen tension in human melanoma xenografts.* Br J Cancer, 2003. **89**(2): p. 350-6.
274. Stackpole, C.W., L. Groszek, and S.S. Kalbag, *Benign-to-malignant B16 melanoma progression induced in two stages in vitro by exposure to hypoxia.* J Natl Cancer Inst, 1994. **86**(5): p. 361-7.
275. Bedogni, B. and M.B. Powell, *Skin hypoxia: a promoting environmental factor in melanomagenesis.* Cell Cycle, 2006. **5**(12): p. 1258-61.
276. Bedogni, B., et al., *The hypoxic microenvironment of the skin contributes to Akt-mediated melanocyte transformation.* Cancer Cell, 2005. **8**(6): p. 443-54.
277. Takahashi, Y., M. Nishikawa, and Y. Takakura, *Suppression of tumor growth by intratumoral injection of short hairpin RNA-expressing plasmid DNA targeting beta-catenin or hypoxia-inducible factor 1alpha.* J Control Release, 2006. **116**(1): p. 90-5.
278. Victor, N., et al., *Involvement of HIF-1 in invasion of Mum2B uveal melanoma cells.* Clin Exp Metastasis, 2006. **23**(1): p. 87-96.
279. Matsuda, N., et al., *Differential activation of ERK 1/2 and JNK in normal human fibroblast-like cells in response to UVC radiation under different oxygen tensions.* Photochem Photobiol, 2000. **72**(3): p. 334-9.
280. Xing, D., et al., *Hypoxia preconditioning protects corneal stromal cells against induced apoptosis.* Exp Eye Res, 2006. **82**(5): p. 780-7.
281. Enk, C.D., et al., *The UVB-induced gene expression profile of human epidermis in vivo is different from that of cultured keratinocytes.* Oncogene, 2006. **25**(18): p. 2601-14.
282. Howell, B.G., et al., *Microarray analysis of UVB-regulated genes in keratinocytes: downregulation of angiogenesis inhibitor thrombospondin-1.* J Dermatol Sci, 2004. **34**(3): p. 185-94.
283. Yano, K., et al., *Ultraviolet B irradiation of human skin induces an angiogenic switch that is mediated by upregulation of vascular endothelial growth factor and by downregulation of thrombospondin-1.* Br J Dermatol, 2005. **152**(1): p. 115-21.
284. Rezvani, H.R., et al., *Hypoxia-inducible factor-1alpha, a key factor in the keratinocyte response to UVB exposure.* J Biol Chem, 2007. **282**(22): p. 16413-22.
285. Turchi, L., et al., *Hif-2alpha mediates UV-induced apoptosis through a novel ATF3-dependent death pathway.* Cell Death Differ, 2008. **15**(9): p. 1472-80.
286. Duffy, M.J., P.M. McGowan, and W.M. Gallagher, *Cancer invasion and metastasis: changing views.* J Pathol, 2008. **214**(3): p. 283-93.
287. Kietzmann, T., U. Roth, and K. Jungermann, *Induction of the plasminogen activator inhibitor-1 gene expression by mild hypoxia via a hypoxia response element binding the hypoxia-inducible factor-1 in rat hepatocytes.* Blood, 1999. **94**(12): p. 4177-85.

288. Dimova, E.Y. and T. Kietzmann, *Cell type-dependent regulation of the hypoxia-responsive plasminogen activator inhibitor-1 gene by upstream stimulatory factor-2.* J Biol Chem, 2006. **281**(5): p. 2999-3005.
289. Chang, J.T., et al., *Upstream stimulatory factor (USF) as a transcriptional suppressor of human telomerase reverse transcriptase (hTERT) in oral cancer cells.* Mol Carcinog, 2005. **44**(3): p. 183-92.
290. Diaz Guerra, M.J., et al., *Functional characterization of the L-type pyruvate kinase gene glucose response complex.* Mol Cell Biol, 1993. **13**(12): p. 7725-33.
291. Vaulont, S., et al., *Proteins binding to the liver-specific pyruvate kinase gene promoter. A unique combination of known factors.* J Mol Biol, 1989. **209**(2): p. 205-19.
292. Krones, A., K. Jungermann, and T. Kietzmann, *Cross-talk between the signals hypoxia and glucose at the glucose response element of the L-type pyruvate kinase gene.* Endocrinology, 2001. **142**(6): p. 2707-18.
293. Chen, L., et al., *Human prolyl-4-hydroxylase alpha(I) transcription is mediated by upstream stimulatory factors.* J Biol Chem, 2006. **281**(16): p. 10849-55.
294. Lendahl, U., et al., *Generating specificity and diversity in the transcriptional response to hypoxia.* Nat Rev Genet, 2009.
295. Gorr, T.A., et al., *Hypoxia-induced synthesis of hemoglobin in the crustacean Daphnia magna is hypoxia-inducible factor-dependent.* J Biol Chem, 2004. **279**(34): p. 36038-47.
296. Wenger, R.H. and M. Gassmann, *Oxygen(es) and the hypoxia-inducible factor-1.* Biol Chem, 1997. **378**(7): p. 609-16.
297. Sogawa, K., et al., *Enhanced expression of catalytic subunit isoform PP1 gamma 1 of protein phosphatase type 1 associated with malignancy of osteogenic tumor.* Cancer Lett, 1995. **89**(1): p. 1-6.
298. Swanson, H.I., W.K. Chan, and C.A. Bradfield, *DNA binding specificities and pairing rules of the Ah receptor, ARNT, and SIM proteins.* J Biol Chem, 1995. **270**(44): p. 26292-302.
299. Turley, H., et al., *The hypoxia-regulated transcription factor DEC1 (Stra13, SHARP-2) and its expression in human tissues and tumours.* J Pathol, 2004. **203**(3): p. 808-13.
300. Kvietikova, I., et al., *The transcription factors ATF-1 and CREB-1 bind constitutively to the hypoxia-inducible factor-1 (HIF-1) DNA recognition site.* Nucleic Acids Res, 1995. **23**(22): p. 4542-50.
301. Narravula, S. and S.P. Colgan, *Hypoxia-inducible factor 1-mediated inhibition of peroxisome proliferator-activated receptor alpha expression during hypoxia.* J Immunol, 2001. **166**(12): p. 7543-8.
302. Semenza, G.L. and G.L. Wang, *A nuclear factor induced by hypoxia via de novo protein synthesis binds to the human erythropoietin gene enhancer at a site required for transcriptional activation.* Mol Cell Biol, 1992. **12**(12): p. 5447-54.
303. Jean, S., et al., *The expression of genes induced in melanocytes by exposure to 365-nm UVA: study by cDNA arrays and real-time quantitative RT-PCR.* Biochim Biophys Acta, 2001. **1522**(2): p. 89-96.
304. Pedeux, R., et al., *Specific induction of gadd45 in human melanocytes and melanoma cells after UVB irradiation.* Int J Cancer, 2002. **98**(6): p. 811-6.
305. Moffett, P., M. Reece, and J. Pelletier, *The murine Sim-2 gene product inhibits transcription by active repression and functional interference.* Mol Cell Biol, 1997. **17**(9): p. 4933-47.
306. Woods, S.L. and M.L. Whitelaw, *Differential activities of murine single minded 1 (SIM1) and SIM2 on a hypoxic response element. Cross-talk between basic helix-loop-helix/per-Arnt-Sim homology transcription factors.* J Biol Chem, 2002. **277**(12): p. 10236-43.
307. Stockwin, L.H., et al., *Proteomic analysis of plasma membrane from hypoxia-adapted malignant melanoma.* J Proteome Res, 2006. **5**(11): p. 2996-3007.
308. Busca, R. and R. Ballotti, *Cyclic AMP a key messenger in the regulation of skin pigmentation.* Pigment Cell Res, 2000. **13**(2): p. 60-9.
309. Chakraborty, A.K., et al., *Production and release of proopiomelanocortin (POMC) derived peptides by human melanocytes and keratinocytes in culture: regulation by ultraviolet B.* Biochim Biophys Acta, 1996. **1313**(2): p. 130-8.
310. Schauer, E., et al., *Proopiomelanocortin-derived peptides are synthesized and released by human keratinocytes.* J Clin Invest, 1994. **93**(5): p. 2258-62.
311. Gilchrest, B.A., et al., *Mechanisms of ultraviolet light-induced pigmentation.* Photochem Photobiol, 1996. **63**(1): p. 1-10.
312. Aberdam, E., C. Romero, and J.P. Ortonne, *Repeated UVB irradiations do not have the same potential to promote stimulation of melanogenesis in cultured normal human melanocytes.* J Cell Sci, 1993. **106 (Pt 4)**: p. 1015-22.
313. Imokawa, G., M. Miyagishi, and Y. Yada, *Endothelin-1 as a new melanogen: coordinated expression of its gene and the tyrosinase gene in UVB-exposed human epidermis.* J Invest Dermatol, 1995. **105**(1): p. 32-7.
314. Hara, H., et al., *Role of gene expression and protein synthesis of tyrosinase, TRP-1, lamp-1, and CD63 in UVB-induced melanogenesis in human melanomas.* J Invest Dermatol, 1994. **102**(4): p. 495-500.

315. Ota, A., J.S. Park, and K. Jimbow, *Functional regulation of tyrosinase and LAMP gene family of melanogenesis and cell death in immortal murine melanocytes after repeated exposure to ultraviolet B.* Br J Dermatol, 1998. **139**(2): p. 207-15.
316. Scott, M.C., I. Suzuki, and Z.A. Abdel-Malek, *Regulation of the human melanocortin 1 receptor expression in epidermal melanocytes by paracrine and endocrine factors and by ultraviolet radiation.* Pigment Cell Res, 2002. **15**(6): p. 433-9.
317. Sesto, A., et al., *Analysis of the ultraviolet B response in primary human keratinocytes using oligonucleotide microarrays.* Proc Natl Acad Sci U S A, 2002. **99**(5): p. 2965-70.
318. Khandrika, L., et al., *Hypoxia-associated p38 mitogen-activated protein kinase-mediated androgen receptor activation and increased HIF-1alpha levels contribute to emergence of an aggressive phenotype in prostate cancer.* Oncogene, 2009. **28**(9): p. 1248-60.
319. Aoto, M., et al., *Essential role of p38 MAPK in caspase-independent, iPLA(2)-dependent cell death under hypoxia/low glucose conditions.* FEBS Lett, 2009. **583**(10): p. 1611-8.
320. Im, S., et al., *Activation of the cyclic AMP pathway by alpha-melanotropin mediates the response of human melanocytes to ultraviolet B radiation.* Cancer Res, 1998. **58**(1): p. 47-54.
321. Newton, R.A., et al., *Human melanocytes expressing MC1R variant alleles show impaired activation of multiple signaling pathways.* Peptides, 2007. **28**(12): p. 2387-96.
322. Murakami, T., et al., *Expression profiling of cancer-related genes in human keratinocytes following non-lethal ultraviolet B irradiation.* J Dermatol Sci, 2001. **27**(2): p. 121-9.
323. Wittenberg, J.B. and B.A. Wittenberg, *Myoglobin function reassessed.* J Exp Biol, 2003. **206**(Pt 12): p. 2011-20.
324. Burmester, T., et al., *Cytoglobin: a novel globin type ubiquitously expressed in vertebrate tissues.* Mol Biol Evol, 2002. **19**(4): p. 416-21.
325. Burmester, T. and T. Hankeln, *Neuroglobin: a respiratory protein of the nervous system.* News Physiol Sci, 2004. **19**: p. 110-3.
326. Hankeln, T., et al., *Neuroglobin and cytoglobin in search of their role in the vertebrate globin family.* J Inorg Biochem, 2005. **99**(1): p. 110-9.
327. Kendrew, J.C., *Myoglobin and the structure of proteins.* Science, 1963. **139**: p. 1259-66.
328. Kendrew, J.C., et al., *A three-dimensional model of the myoglobin molecule obtained by x-ray analysis.* Nature, 1958. **181**(4610): p. 662-6.
329. Garry, D.J., S.B. Kanatous, and P.P. Mammen, *Emerging roles for myoglobin in the heart.* Trends Cardiovasc Med, 2003. **13**(3): p. 111-6.
330. Ordway, G.A. and D.J. Garry, *Myoglobin: an essential hemoprotein in striated muscle.* J Exp Biol, 2004. **207**(Pt 20): p. 3441-6.
331. Hochachka, P.W., *The metabolic implications of intracellular circulation.* Proc Natl Acad Sci U S A, 1999. **96**(22): p. 12233-9.
332. Davis, R.W. and S.B. Kanatous, *Convective oxygen transport and tissue oxygen consumption in Weddell seals during aerobic dives.* J Exp Biol, 1999. **202**(Pt 9): p. 1091-113.
333. Jurgens, K.D., T. Peters, and G. Gros, *Diffusivity of myoglobin in intact skeletal muscle cells.* Proc Natl Acad Sci U S A, 1994. **91**(9): p. 3829-33.
334. Wittenberg, J.B., *Myoglobin-facilitated oxygen diffusion: role of myoglobin in oxygen entry into muscle.* Physiol Rev, 1970. **50**(4): p. 559-636.
335. Eich, R.F., et al., *Mechanism of NO-induced oxidation of myoglobin and hemoglobin.* Biochemistry, 1996. **35**(22): p. 6976-83.
336. Flogel, U., et al., *Myoglobin: A scavenger of bioactive NO.* Proc Natl Acad Sci U S A, 2001. **98**(2): p. 735-40.
337. Garry, D.J., et al., *Mice without myoglobin.* Nature, 1998. **395**(6705): p. 905-8.
338. Godecke, A., et al., *Disruption of myoglobin in mice induces multiple compensatory mechanisms.* Proc Natl Acad Sci U S A, 1999. **96**(18): p. 10495-500.
339. Grange, R.W., et al., *Functional and molecular adaptations in skeletal muscle of myoglobin-mutant mice.* Am J Physiol Cell Physiol, 2001. **281**(5): p. C1487-94.
340. Meeson, A.P., et al., *Adaptive mechanisms that preserve cardiac function in mice without myoglobin.* Circ Res, 2001. **88**(7): p. 713-20.
341. Riggs, A.F. and T.A. Gorr, *A globin in every cell?* Proc Natl Acad Sci U S A, 2006. **103**(8): p. 2469-70.
342. Fraser, J., et al., *Hypoxia-inducible myoglobin expression in nonmuscle tissues.* Proc Natl Acad Sci U S A, 2006. **103**(8): p. 2977-81.
343. van der Meer, D.L., et al., *Gene expression profiling of the long-term adaptive response to hypoxia in the gills of adult zebrafish.* Am J Physiol Regul Integr Comp Physiol, 2005. **289**(5): p. R1512-9.
344. Flonta, S.E., et al., *Expression and functional regulation of myoglobin in epithelial cancers.* Am J Pathol, 2009. **175**(1): p. 201-6.
345. Galluzzo, M., et al., *Prevention of hypoxia by myoglobin expression in human tumor cells promotes differentiation and inhibits metastasis.* J Clin Invest, 2009. **119**(4): p. 865-75.

346. Wystub, S., et al., *Interspecies comparison of neuroglobin, cytoglobin and myoglobin: sequence evolution and candidate regulatory elements.* Cytogenet Genome Res, 2004. **105**(1): p. 65-78.
347. Kanatous, S.B., et al., *Hypoxia reprograms calcium signaling and regulates myoglobin expression.* Am J Physiol Cell Physiol, 2009. **296**(3): p. C393-402.
348. Lankester, E.R., *Ueber das Vorkommen von Haemoglobin in den Muskeln der Mollusken und die Verbreitung desselben in den lebendigen Organismen.* Pflugers Arch. Gesamte. Physiol., 1871. **4**: p. 315-320.
349. Hendgen-Cotta, U.B., et al., *Nitrite reductase activity of myoglobin regulates respiration and cellular viability in myocardial ischemia-reperfusion injury.* Proc Natl Acad Sci U S A, 2008. **105**(29): p. 10256-61.
350. Brunori, M., *Nitric oxide moves myoglobin centre stage.* Trends Biochem Sci, 2001. **26**(4): p. 209-10.
351. Cossins, A.R., et al., *Diverse cell-specific expression of myoglobin isoforms in brain, kidney, gill and liver of the hypoxia-tolerant carp and zebrafish.* J Exp Biol, 2009. **212**(Pt 5): p. 627-38.
352. Reynafarje, B., *Myoglobin content and enzymatic activity of muscle and altitude adaptation.* J Appl Physiol, 1962. **17**: p. 301-5.
353. Fordel, E., et al., *Hypoxia/ischemia and the regulation of neuroglobin and cytoglobin expression.* IUBMB Life, 2004. **56**(11-12): p. 681-7.
354. Ameln, H., et al., *Physiological activation of hypoxia inducible factor-1 in human skeletal muscle.* Faseb J, 2005. **19**(8): p. 1009-11.
355. Chang, H., et al., *Regulation of hypoxia-inducible factor-1alpha by cyclical mechanical stretch in rat vascular smooth muscle cells.* Clin Sci (Lond), 2003. **105**(4): p. 447-56.
356. Mason, S.D., et al., *Loss of skeletal muscle HIF-1alpha results in altered exercise endurance.* PLoS Biol, 2004. **2**(10): p. e288.
357. Graven, K.K., et al., *HIF-2alpha regulates glyceraldehyde-3-phosphate dehydrogenase expression in endothelial cells.* Biochim Biophys Acta, 2003. **1626**(1-3): p. 10-8.
358. Carroll, V.A. and M. Ashcroft, *Role of hypoxia-inducible factor (HIF)-1alpha versus HIF-2alpha in the regulation of HIF target genes in response to hypoxia, insulin-like growth factor-I, or loss of von Hippel-Lindau function: implications for targeting the HIF pathway.* Cancer Res, 2006. **66**(12): p. 6264-70.
359. Blanchetot, A., M. Price, and A.J. Jeffreys, *The mouse myoglobin gene. Characterisation and sequence comparison with other mammalian myoglobin genes.* Eur J Biochem, 1986. **159**(3): p. 469-74.
360. Weller, P., et al., *Organization of the human myoglobin gene.* Embo J, 1984. **3**(2): p. 439-46.
361. Whitlock, N.A., et al., *Hsp27 upregulation by HIF-1 signaling offers protection against retinal ischemia in rats.* Invest Ophthalmol Vis Sci, 2005. **46**(3): p. 1092-8.

15 Manuscripts

Manuscript 1: Interaction of HIF and USF signaling pathways at human genes flanked by hypoxia-response elements and E-box palindromes

Junmin Hu[1], Daniel P. Stiehl[2], Claudia Setzer[1], Pavel Hradecky[3], Max Gassmann[1], Thomas A. Gorr[1]

[1] Institute of Veterinary Physiology, University of Zurich, Switzerland;

[2] Institute of Physiology, University of Zurich, Switzerland;

[3] AltraBio, Lyon, France

Short title: HIF-USF interaction

Total word count:

Total character count (excluding spaces): 38247

Word count for Material and Method section (words): 1717

Word count for Introduction, Results and Discussion sections (words): 5637

*** corresponding author:** Thomas A. Gorr, PhD

Institute of Veterinary Physiology, Zurich Center of Integrative Human Physiology, University of Zurich, Winterthurerstrasse 260, 8057 Zurich, Switzerland

tgorr@access.uzh.ch ☎ +41 (0)44 635 8807 +41 (0)44 635 8932

Abstract

A constitutive CACGTG binding activity in human cancer cells was previously found to interfere with the HIF-driven hypoxic activation of a *Daphnia* globin gene promoter construct (phb2) from adjacent HIF-1 binding hypoxia response elements (HREs). Using gel supershift and pull-down assays we now identify upstream stimulatory factor (USF) 1 and 2 as the primary phb2 CACGTG-binding entity in human hepatoma (Hep3B), cervical carcinoma (HeLa) and breast carcinoma (MCF7) cell lines. A genome-wide computational scan for HRE and CACGTG motifs co-occurring adjacently in upstream sequences retrieved multiple O_2-sensitive *human* genes. Luciferase (LUC) reporter of the human HRE/CACGTG bibox promoter constructs LDHA/LUC (lactate dehydrogenase A/LUC) and BNIP3/LUC (Bcl-2/E1B 19 kDa interacting protein 3/LUC) showed robustly elevated luciferase activities in transfected Hep3B, HeLa and MCF7 cells during hypoxia. Chromatin immunoprecipitation confirmed the *in vivo* convergence of HIF-1α, USF1 and USF2a onto LDHA and BNIP3 promoters. Hep3B and HeLa cell co-transfections of LDHA or BNIP3 reporter with HIF-1α and USF1/2a expression plasmids or specific siRNAs directed against each transcription factor revealed clear evidence for cooperative (LDHA) or competitive (BNIP3) crosstalk modes between HIF and USF pathways. Thus, USF signaling might operate to fine-tune or restrain cell type-specifically HIF-mediated gene expression in hypoxic nuclei.

Introduction

The key regulators of cells' responses to inadequate oxygenation (hypoxia) are the hypoxia inducible transcription factor 1 and 2 (HIF-1 and -2) (44, 60). Relaying minutes-to-hours of hypoxia onto the level of DNA via HIF is a highly conserved signalling event across the animal kingdom (1, 17). During low oxygen partial pressures (pO_2), the mammalian HIF-1 complex controls the activity of numerous genes as heterodimer composed of HIF-1α and HIF-1β subunits (12, 59). Whereas HIF-1β, also known as ARNT (aryl hydrocarbon receptor nuclear translocator), is constitutively present, the activity of the HIF-α subunits is regulated as a function of pO_2. Homologs of prolyl hydroxylase domain 1-3 (PHD1-3) dioxygenases in both *C. elegans* and mammalian cells were identified to act as oxygen sensors of HIF (10, 26, 27). In the presence of oxygen and 2-oxoglutarate, the Fe (II)-dependent hydroxylation of two proline residues in HIF-1α and -2α is catalyzed by PHDs. Subsequently, this hydroxylated HIF-α is recognized by the von Hippel-Lindau tumor suppressor protein (VHL) and rapidly degraded via the ubiquitin-proteasome pathway (26, 32). A second, O_2-requiring post-translational modification of HIF-1α/-2α occurs at an asparagine residue within the C-terminal trans-activation domain. Hydroxylation of this particular Asn is catalyzed by asparaginyl hydroxylase called factor inhibiting HIF (FIH) to prohibit HIF-α/co-activator interaction and to block trans-activation of genes under high oxygen (35, 36). During hypoxia, both PHD and FIH reactions are inhibited, leading to α/β-subunit dimerization in the nucleus and binding to hypoxia response element (HRE) within target genes. HIF-1/-2 execute their transcriptional activity by recruiting co-activators such as p300/CBP (9, 28). Being members of canonical CANNTG E-box motifs, HREs consist of a mandatory consensus 5'-VNVBRCGTG-3' (62) (V=not T; N= any; B=not A; R=A or G). To date, several hundred potential (38) and more than 70 validated hypoxia-responsive gene targets of HIF-1 have been identified. Through this transcriptional outflow, HIF-1 is able to reprogram cellular metabolism, growth, apoptosis, and O_2 supply in response to declining pO_2 (62).

Our previous work utilized the globin-2 gene (hb2) promoter (phb2) of the planktonic crustacean *Daphnia magna*, housing two functional HREs at position -258 and -107 and one CACGTG E-box palindrome (PAL) at -146, as luciferase reporter to analyze the responsible motifs and factors underlying the prominent hypoxic induction of hb2 in heterologous transfections of human cancer cells. An unknown constitutive CACGTG factor in human cancer cells was found to be able to interfere with the HIF-1-driven induction of the phb2 luciferase reporter (16). Here, we report on the identification of the primary phb2 CACGTG factor across several cancer cell lines as a complex of O_2-independently acting upstream stimulatory factors 1 and 2 (USF1, USF2).

To launch a comprehensive analysis of the capacity of USF signaling to generally fine-tune or interfere with HIF's transcriptional outflow, we implemented a genome-wide computational scan to

identify candidate human genes that have adjacent or overlapping HRE and PAL motifs in their upstream sequence. Our results suggest the occurrence both of competitive (BNIP3 promoter) and cooperative (LDHA promoter) crosstalk modes when HIF-1/USF signalling pathways were over-expressed or silenced. This study, therefore, points to the potential of the oxygen-independent USF pathway to influence, and even inhibit, HIF-mediated gene expression in human cancer cells.

Materials and methods

Cell culture: Human hepatoma cells (Hep3B), human cervical cells (HeLa) and human breast cancer cells (MCF7) were maintained in high glucose (4.5g/l) Dulbecco's modified Eagle's medium (DMEM) as described earlier (4). Cells were cultured at 37°C in incubators ventilated with room air in a water-saturated, 5% CO_2 containing atmosphere, which corresponds at sea level to a partial oxygen pressure of 141.6 mmHg or 18.6% O_2 ("normoxia"). Hypoxic cells were subjected to 1% O_2/5% CO_2/balance N_2 for 16h in a HERA Cell240 incubator (Heraeus).

Antibodies: Mouse monoclonal anti-ATF-1 antibody (25C10G: sc-270) was purchased from Santa Cruz Biotech, INC. Rabbit polyclonal anti-USF1M, anti-USF2F, anti-USF2G, anti-USF2Z and anti-USF2aO antibodies were kindly provided by Prof. B. Viollet (58). Generous additional antibody gifts included: a) rabbit anti human DEC1 (CW27) (56); b) rabbit anti human MYC (55); c) rabbit anti mouse ARNT (anti-mARNT R-1 lgG) (24); d) rabbit anti human ARNT (anti-hARNT C34) (51); e) rabbit anti human USF full length antibody (USF FL) (29).

Computational sequence scan: Repeat-masked human genome sequence in FASTA format (hg18, build 36.1 finished human genome assembly by International Human Genome Project of March 2006) was downloaded from the UCSC Genome Bioinformatics Site (http://hgdownload.cse.ucsc.edu/goldenPath/hg18/bigZips/, database accessed on October 2, 2006). Sequence coordinates of the annotated features on the genome assembly (transcriptional and coding sequence start and end) were obtained from the same source (http://genome.ucsc.edu/cgi-bin/hgTables, database accessed on October 3, 2006). The computational scan was implemented as a PERL script and performed for individual chromosomes, using as input the genomic sequence and the list of feature coordinates. We searched within 1000 nucleotides upstream of the annotated 5`end of the transcript for the co-occurrence of a consensus HRE motif (62) and a CACGTG palindrome (PAL), and permitted, as seen in phb2, a maximal motif-motif distance of 100 nucleotides. Identifiers of these putative bibox (HRE+PAL) genes fulfilling the search criteria, together with the motif coordinates and their relative position with respect to the gene, were written into an output file.

Luciferase reporter: Genomic DNA, isolated from HeLa cells using TRIzol Reagent ™ (Invitrogen, Basel, Switzerland), was used as template for the amplification of the promoter region surrounding the HRE, E-box palindrome (PAL) or bibox (= HRE + PAL) motifs via nested PCR (for primers, see Supplement Table ST 1). The 3'-end of any given amplicon always extended into the first exon of the respective gene. In detail, we amplified and cloned the following promoter regions (start/end always in regard to translation start ATG codon): a) human 4EBP1 gene, -518/+403; b) human MC1R gene, -880/+9; c) human LDHA gene, -2617/+530; d) human TYR gene, -400/+108. The PCR products were

TOPO-cloned into the pCRII-TOPO vector (Invitrogen). Following a KpnI/XhoI digestion for 4EBP1/pCRII and TYR/pCRII, a XhoI/HindIII digestion for MC1R/pCRII, and a HindIII/HindIII digestion for the LDHA/pCRII construct in accordance to a preceding re-amplification of the construct with a reverse primer carrying an extra HindIII site (see Table ST 1), the liberated insert was ligated into pGL3-basic luciferase vector (Promega AG, Dübendorf, Switzerland) to generate the luciferase reporter constructs. The BNIP3/pGL3-basic luciferase reporter vector was kindly provided by Prof. J. Okami (42). PHD2 luciferase reporter plasmid (P2P (-607/+3) wt) is a truncated version of the previously published human PHD2 promoter (40). HIF-1α expression plasmid (i.e. pcDNA3.1-hHIF-1-PK tag) was a generous gift from Prof. P. Maxwell's lab. All USF expression plasmids (pCR3-USF1, pCR3-USF2a and pCR3-USF2b) were kindly given to us by Prof. B. Viollet (41).

*Electrophoretic Mobility Shift Assay (EMSA)***:** Nuclear protein extracts of Hep3B, HeLa and MCF7 cells were isolated as previously reported (16). Protein concentrations of the extracts were measured by the BioRad method (Bio-Rad Laboratories, Reinach BL, Switzerland). Analysis of in vitro protein-DNA interaction by EMSA was done as described earlier (16). All oligonucleotide sequences used as probes are shown in Supplement Table ST 2. For gel supershifts, 1.5 µl rabbit anti-USF1M, rabbit anti-USF2G or 1.0 µl mouse anti-HIF-1α (mgc3) were added into the reaction, respectively, followed by a 30 min pre-incubation at room temperature. Negative supershift controls included 1.5 µl pre-immune serum from the same rabbit to be immunized against USF1M or USF2G, as well as 1.0 µl rabbit anti-human IgG (code: 309-005-003 Jackson Immuno Research).

Pull-down assay: Wildtype and mutated phb2 -146 palindrome or -107 HRE oligonucleotides (see Supplement Table ST 2), biotinylated at the 5' end and PAGE purified, were annealed into double stranded DNA and immobilized on streptavidin-coated magnetic beads (Dynal Biotech, Oslo, Norway). The pull down assay was adopted from a previous protocol (18).

Western blot: Proteins were resolved in 10% SDS acrylamide gels and transferred onto a nitrocellulose membrane (Whatman GmbH, Dassel, Germany). The membrane was incubated with primary antibodies diluted in 5% milk TBS-T: (a) anti-HIF1α (mgc3) (1:500) or (b) anti-USF-1M or anti-USF-2G (1:750) at 4°C overnight. The signal was detected with horseradish peroxidase-conjugated goat anti-mouse or anti-rabbit diluted 1:5000 and luminol substrate (100mM Tris-HCl pH8.5, 9% H_2O_2, 1.25mM Luminol (in DMSO), 0.225mM p-coumaric acid (in DMSO)).

Co-immunoprecipitation: 150 µg nuclear protein was diluted with a Tris buffer (50 mM Tris-HCl, pH7.4, 150 mM NaCl, 5 mM EDTA, 0.5% NP-40, 1 mM sodium vanadate and 0.5 mM PMSF) and 20 µl mouse anti-HIF-1α or 0.75 µg anti-mARNT or 2.5 µl USF antiserum were added. The nuclear extract/antibody mix was rotated at 4°C over night. The next day, 40 µl of sepharose G beads were

added into the mix and incubated at 4°C for another 2.5h. The nuclear extract/antibody/sepharose beads mix was collected by centrifugation (3300xg, 1min), the pellet boiled at 95°C in 1×SDS sample buffer for 10min and the supernatant analyzed by Western blot.

Transient reporter transfection: Half-confluent Hep3B, HeLa and MCF7 cells seated in ∅6cm plates were transfected overnight using the calcium phosphate method with different luciferase reporter constructs and β–galactosidase plasmid to normalize luciferase activity to varying transfection efficiencies. To carry out co-transfections, 15-500ng HIF-1α plasmid and/or 15-100ng USF1, USF2a or USF2b plasmid were added. In each transfection, pUC18 plasmid was used as filler DNA for a total of 2-3μg DNA. On the following day, each batch of transfected cells was split into two for parallel 16h normoxia (N) and hypoxia (H) exposure. After 16h N/H exposure cells were lysed and luciferase activity was measured using a commercially available Luciferase Assay System (Promega AG) and a SIRIUS Luminometer (Berthold Technologies, GmbH &Co. KG, Bad, Wildbad, Germany). Luciferase activity was normalized by β-galactosidase activity (β-galactosidase enzyme assay kit; Promega AG) and relative luciferase activity expressed in percent (% RLA) of the total activity of all normoxic and hypoxic reactions of a given assay.

Reporter transfections and siRNA transient knock down of HIF-1α, USF1 or USF2a: The specific siRNA HIF-1α and siRNA USF1 oligonucleotides were selected based on previous publications (3, 11, 25). siRNA USF2a oligonucleotides targeted nucleotides 786-806 of human USF2a mRNA. All siRNA sequences (see Supplement Table ST 3) were synthesized by Dharmacon Research Inc. Si*CONTROL* non-targeting siRNA pool #2 was used as scrambled siRNA control (Dharmacon). Half-confluent Hep3B cells were transfected with a total of 200nM of siRNAs using Oligofectamine™ reagent (Invitrogen). In the combined USF1+USF2a siRNA transfection targeting both USFs, 100nM of each siRNA were added to the cells. To perform siRNA manipulation together with a BNIP3 promoter luciferase reporter assay, Hep3B cells were transfected 30h post-siRNA transfection with 150ng BNIP3/LUC reporter construct and 40ng β-galactosidase plasmid in a total amount of 500ng DNA per well using Invitrogen's Calcium Phosphate Kit followed by parallel 16h normoxia and hypoxia exposure and luciferase assay as above**.**

Stable HIF-1α and USF-2a knockdown MCF7 clones: To generate stable HIF-1α and USF2a knockdown MCF7 cells, we used MISSION shRNA bacterial glycerol stocks of the shRNA lentiviral plasmid (pLKO.1-puro) kit (Sigma-Aldrich, Basel, Switzerland). The HIF-1α and USF2a kits are both composed of five individual shRNAs each, that target HIF-1α (accession number NM_001530) and USF2a (accession number NM_003367), respectively at different mRNA sections. 1×10^6 MCF7 cells were transfected either with 3μg of each of the 5 shRNA HIF-1α plasmids using polyethyleneimine as described earlier (52), or with 6μg of each of the 5 shRNA USF2a plasmids using the calcium

phosphate method. 48h post-transfection, single clones were selected in medium containing 1.0 μg/ml puromycin followed by Western blot analysis.

Chromatin Immunoprecipitation (ChIP) assay: ChIP assays were performed in human Hep3B, HeLa and MCF7 cells subsequent to a 4h exposure to normoxic (air) or hypoxic (1% O_2) atmospheres as described in (23). In brief, genomic DNA was crosslinked with bound proteins using 1% formaldehyde in 1× phosphate-buffered saline (PBS) for 10min at room temperature and sonicated in a Bioruptor™ UCD-200 (Diagenode sa, Liège, Belgium) or a Sonifier cell disruptor B15 (Branson) into fragments with an average length of 500-1000bp. For immunoprecipitation of the DNA/protein mix, 4.5 μl rabbit polyclonal anti-HIF-1α IgG (ab2185, Abcam, Cambridge, UK), 10 μl rabbit polyclonal anti-USF1M or anti-USF2G was added into the chromatin solution. 10 μl pre-immune rabbit antiserum and 2.5 μl rabbit anti-human IgG were used as negative controls. The purified DNA was amplified by PCR using the ChIP primer pairs shown in Supplement Table ST 4.

Statistics: Using the STATA 10.0 software package (Stata™ 10.0; StataCorp, College Station, USA) we compared the mean relative luciferase activity (RLA) data shown in the individual panels in Figures 3 and 6 for each reporter assay and within the *same* oxygen category (either normoxic or hypoxic results). Significance of RLA differences between samples was calculated in two ways, i.e. for a) control transfections without overexpressed HIF/USF *versus* experimental co-transfections with overexpressed HIF/USF (i.e. endo/exo tests, *used symbols: asterisk, circle*), and b) control co-transfections with overexpressed HIF-1α *versus* co-transfections with overexpressed combinations of HIF-1α and USF proteins (i.e. hif/combi tests, *used symbols: plus, diamond*). Each population of normoxic or hypoxic reporter assay results was assessed for normality and for equal variances between compared samples. Next, statistical significance (i.e. p value < 0.05) was calculated in accordance with these tests by i) one-way Anova modelling and post-hoc Sidak corrections when assumptions of normality and variance equality were maintained (e.g. Fig. 3B, C; *when p-value < 0.05, used symbols: circle, diamond*), and ii) non-parametric Kruskal-Wallis tests plus Wilcoxon rank-sums for pairwise RLA comparisons when assumptions were violated (e.g. Fig. 3A, D; *for p-value < 0.05, used symbols: asterisk, plus*). Respective symbols are shown in gray within the RLA bar for a given endo/exo or hif/combi test.

Results

CACGTG palindromic E-boxes often serve as binding sites for several basic helix-loop-helix (bHLH) transcription factors, including ARNT (53, 54), MYC (21, 22), USFs (58), STRA13/DEC1 (56), ATF-1 and CREB-1 (34). To identify the factor(s) responsible for the HIF-interfering constitutive activity at the -146 CACGTG element within the promoter of the hb2 gene (phb2) of *Daphnia magna* (16), along with the factor(s) occurrence across different cancer cells, we conducted an EMSA survey using normoxic nuclear extracts from human hepatoma (Hep3B), cervical carcinoma (HeLa) and breast carcinoma cells (MCF7). Since HeLa and MCF7 EMSA screens yielded compatible results, Figure 1A presents Hep3B data only (*Fig. 1A*). The protein components within the constitutive complex (cc) of the -146 phb2 activity were identified using specific antibodies directed against USFs, DEC1, MYC, ARNT and ATF-1. Of these five factors screened by supershifts (ss), only USF1 and USF-2 were recognized as main in vitro binding factors of the -146 phb2 palindrome (Fig. 1A, lanes 3, 5, 7, 9, 11) while all other factors either failed (MYC, ATF-1) to bind to this motif or interacted (DEC1) with it only as minor contribution (Fig. 1A, lane 15; ~5-10% of total pool). Increasing volume of anti-USF1M (left) and anti-USF2G (right) antiserum in the binding reaction nuclear extracts from normoxic (N) and hypoxic (H) Hep3B reduced the intensity of the CACGTG complex in a dose-dependent manner (Suppl. Fig. S1A). This dose-dependent reduction additionally underscores the specific participation of USFs in the CACGTG complex, because addition of the same maximal volume of pre-immune serum (PI-1M and PI-2G) left the complex's intensity unaffected. Moreover, binding of USF proteins to the -146 phb2 E-box is clearly oxygen-independent (Suppl. Fig. S1A). Based on Viollet et al.'s work on the characteristic of USFs to homo- or heterodimerize to a different extent according to cell type (58), we were furthermore able to delineate the slightly different mobility of bands within the CACGTG-bound constitutive complex (cc) as USF1/2 heterodimers (i.e. USF1/2a, USF1/2b, fast complex, "1/2"), 1/1 homodimers (medium complex, 1/1) or 2/2 homodimers (slow complex, 2/2) (Suppl. Fig. S1A).

We re-evaluated our EMSA results through independent pull-down assays of Hep3B, HeLa and MCF7 nuclear proteins using biotinylated phb2 oligonucleotides, bound to streptavidin coated magnetic beads. In a representative assay with HeLa normoxic (N) and hypoxic (H) nuclear extracts (Fig. 1B+C), wildtype biotinylated oligonucleotides (w-bio), containing the -146 CACGTG phb2 E-box, were able to pull down 43 kDa USF1 (Fig. 1B), 44 kDa USF2a and 38 kDa USF2b proteins regardless of pO_2 (Fig. 1C). The specificity of this USF binding reaction was confirmed due to the markedly reduced (50× comp.) or abolished (m-bio) binding of any USF to the phb2 E-box either upon addition of 50 fold molar excess of competing wildtype oligonucleotides (50× comp.) into the reaction or when using beads coated with -146 mutant (m-bio) E-box motifs (5'-CAATGT-3'). Similar results were obtained with extracts from Hep3B and MCF7 cells (not shown). Based on these mutually corroborating and reproducible data in Fig. 1, we concluded that USF1 and USF2 complexes are the

main phb2 CACGTG binding factors in three different cancer cells (Hep3B, HeLa, MCF7). Subsequent co-immunoprecipitation experiments demonstrated the interactive precipitation of HIF-1α by ARNT proteins and vice versa, but failed to reveal any physical contact between USF2a and either subunit of HIF-1 (HIF-1α, ARNT) (see Suppl. Fig. S2). Thus, the USF-HIF interference in phb2 is indirect and DNA context dependent (19).

While the *Daphnia* hb2 promoter was a valuable model for the initial analysis of the crosstalk between E-box binding activities, naturally we wanted to characterize the signaling events within the promoter of *human* bibox candidate genes, i.e. those containing a CACGTG palindrome E-box adjacent to a validated or suggested HRE motif. To achieve this objective, a computational scan of human genome sequence was conducted, in which we checked within 1000 nucleotides upstream of the transcription start site for the presence of a 5'-VNVBRCGTG-3' HRE consensus motif (62) and a 5'-CACGTG-3' palindrome E-box with a motif-motif distance of ≤100bp. 5' location and distance of both motifs were adopted from the *Daphnia* hb2 gene, coordinates (i.e. transcription start sites) of the human genes were taken from UCSC's known genes archive (hg18). According to these criteria, some 383 genes fitted the bibox definition and included with VEGF-C (vascular endothelial growth factor C), LDHA (lactate dehydrogenase A), PGM2 (phosphoglucomutase 2), BNIP3L (Bcl-2/E1B 19 kDa interacting protein 3-like) and BAX (Bcl-2–associated X protein) several known hypoxia induced expressions (*Excel file: "Human bibox candidate genes" with total of 383 entries of annotated human HRE/CACGTG candidate genes is available as Supplement*). From this list, different bibox candidate genes were selected for future studies, provided that the alignment of the homologous human-mouse-rat (hmr) promoter regions had established the respective motifs to be conserved, and, thus, of likely functional importance (Suppl. Fig. S3). Comparing the hmr alignments of the promoters of BNIP3L with those of its close relative, the known HIF-1 target BNIP3 (Bcl-2/E1B 19 kDa interacting protein 3), yielded a remarkably conserved HRE region for the latter gene, prompting us to study the transcriptional control of BNIP3 rather than of BNIP3L itself (Suppl. Fig. S3).

The respective promoter regions were amplified from genomic DNA, cloned, sequence confirmed and inserted into basic pGL3 luciferase reporter plasmids. That way, we either received as generous gifts (i.e. BNIP3 and PHD2), or generated ourselves (all others), a set of luciferase promoter reporters that ranged from HIF-1 specific (prolyl hydroxylase domain 2, PHD2) (52) to USF specific targets (tyrosinase, TYR) (15) and included four bibox candidates (4EBP1, LDHA, MC1R, BNIP3) to examine the possible interaction of HIF and USF signalling cascades at DNA level (see *Table 1* for relevant cis-elements and adjacent or intermittent DNA). Initially, we set out to examine the hypoxia responsiveness of these bibox candidate promoters. Respective reporter transfections of Hep3B, MCF7 and HeLa cells included negative control reactions with empty pGL3 basic luciferase vector (Fig. 2, "bVec") which, indeed, lacked a hypoxia response in any of these cells. In contrast, the HIF-1-

driven PHD2 luciferase construct was induced approximately 3-fold in Hep3B, 8-fold in MCF7 and 4-fold in HeLa in response to a 16h exposure at 1% O_2 (*Fig. 2*). Luciferase assays with the four bibox candidates 4EBP1, LDHA, MC1R and BNIP3 revealed only for LDHA (~2 fold) and BNIP3 (4-7 fold) a robust up-regulation by hypoxic conditions in Hep3B, MCF7 and HeLa cells. The 4EBP1 and MC1R constructs, in contrast, lacked any O_2 sensitivity in any of the cell lines (Fig. 2).

Next, we investigated the possible co-regulation of BNIP3 and LDHA by HIF and USF cascades in response to the co-transfection of these bibox reporters with HIF-1α and USF1, 2a or 2b expression plasmids. Efficacy of these co-transfections was stereotypically compared to endogenous reporter expression (*Fig. 3*; leftmost H/N double-bar in each particular reporter transfection; no numbers underneath). In pilot studies (not shown), we had carefully titrated for each cell line the amount of HIF-1α plasmid needed for an optimal *hypoxic induction* of either reporter (i.e. minimal normoxic gene activation by over-expressed HIF-1α, achieved with 15ng plasmid for BNIP3 and 100ng plasmid for LDHA construct), and of any USF plasmid needed for an optimal *specific activation* of either reporter construct (i.e. minimal non-specific binding of over-expressed USFs to pGL3 backbone; achieved with 15ng of any USF plasmid) (see Fig. 3). Transfected TYR reporter yielded, regardless of O_2 tension, a 4-7-fold increased activity upon co-transfection of USF1, and an up to 20-fold elevated activity upon over-expression of USF2a. Over-expression of HIF-1α did not impact TYR expression (Fig. 3A). On the other hand, a 2.7 fold induced PHD2 reporter activity, which entirely depended on the presence of a functional wildtype HRE in the PHD2 promoter as seen in Table 1 (i.e., transfection data with HRE-mutant PHD2 constructs, not shown), was increased up to 3.8 fold upon HIF-1α over-expression. The impact of over-expressed USFs on the PHD2 reporter was either negligible (USF1) or within the range of the non-specific stimulation that the over-expressed factor exerted on the vector backbone (USF2a). Therefore, both control reporters responded specifically to the over-expression of their respective transcriptional driver(s) (Fig. 3A).

As mentioned above, the promoter activity of LDHA was induced by endogenous hypoxia signals almost 2-fold in Hep3B (Fig. 3B). Co-transfection of cells with 20, 40 or 100ng of USF-1 plasmid elevated the activity of LDHA luciferase dose-dependently as a function of the USF1 level. Over-expressed USF2a and 2b were even more able to activate the LDHA promoter. Yet, any over-expressed USF augmented LDHA luciferase activity predominantly under normoxia, thereby reducing the original hypoxic induction to an almost constitutive expression pattern in Hep3B (Fig. 3B) and MCF7 cells (not shown). Similarly, over-expressed HIF-1α (100ng plasmid) stimulated the LDHA promoter under normoxic and hypoxic pO_2. However, when Hep3B cells were simultaneously co-transfected with HIF-1α and USF1 (2x100ng plasmid; Fig. 3B), LDHA expression levels superseded those of any over-expression scheme of the individual transcription factors. Convergence of co-active HIF-1 and USF signals on the LDHA promoter are mutually supportive in driving the gene.

The BNIP3 reporter was nearly 3-fold induced by endogenous (HIF-1) hypoxic signalling pathways in Hep3B (Fig. 3C) and HeLa cells (Fig. 3D). Co-transfection with USF1 and 2a, or with USF2b, enhanced BNIP3 promoter activity in both cell lines particularly under normoxia and consequently weakened the hypoxic induction of the reporter to 1.5-2.4 fold. Over-expression of HIF-1α amplified the hypoxic activity of the BNIP3 reporter robustly in Hep3B (6.6 fold; Fig. 3C) and moderately in HeLa cells (3.2 fold, Fig. 3D). Importantly, this potentiated hypoxia response of BNIP3 by exogenous HIF-1α was significantly impaired by simultaneous co-transfection with USF1 or USF2a, but not USF2b, in Hep3B and HeLa cells (Figs. 3C+D: see ↓ arrows). Increasing the added amount of USF1/2a plasmids further (15→100ng plasmid), eventually converted the hypoxic trans-activation of the reporter into an increasingly constitutive response, especially in Hep3B cells (Fig. 3C). These data suggest that HIF-1α and USF1 or USF2a compete dose-dependently with each other for the control of the BNIP3 promoter.

For further inspection of a physiological interaction of HIF-1 and USFs with the promoter of BNIP3 and LDHA, we performed chromatin immunoprecipitation (ChIP) assays in Hep3B, HeLa, and MCF7 cells. No DNA was amplified in the IP lane when either a non-specific lgG or a pre-USF immunization serum was used. Regarding the promoter of LDHA (*Fig. 4A*; left panel: Hep3B; right panel: MCF7), the ChIP data indicated a hypoxia-specific interaction of the amplified 159bp region with HIF-1α that contrasted with a comparatively weak, constitutive interaction with USFs. The notion that USFs target (MCF7) or even dominate (Hep3B) the LDHA promoter in oxygenated cells is in accord with our co-transfection assays. In the BNIP3 ChIP assay (Fig. 4B), specific precipitates suggested that the BNIP3 E-box in Hep3B (left) and MCF7 cells (right panel) can switch in its occupancy from a HIF-1 site during hypoxia to a cis-element for a mixed collection of factors, including USFs and, surprisingly, HIF-1 complexes during normoxic pO_2. The fact that USF1/2 complexes remained attached to the BNIP3 314bp promoter fragment, even when HIF-1 overtook the occupancy of the -251/-246 E-box (Tab. 1) in deoxygenated cells, suggests the presence of non-canonical USF cis elements in or adjacent to this HRE. In this regard, note the occurrence of two conserved CACGCN motifs, each being separated from the BNIP3 HRE by a triple-nucleotide spacer sequence (Suppl. Fig. S3).

To elucidate the precise location of HIF-1 and USF1/2 sites in the LDHA and BNIP3 promoter, we opted to carry out additional EMSA screens with Hep3B, HeLa and MCF7 normoxic and hypoxic nuclear extracts. Representative results are shown for LDHA (MCF7 nuclear extracts, *Fig. 5A*) and BNIP3 (Hep3B nuclear extracts, Fig. 5B) in Figure 5. The wildtype CACGTG-motif in region I of the LDHA promoter (Fig. 5A: reg.I wt) was avidly bound by constitutive proteins (cc) which could be supershifted (ss) by anti-USF2G (lanes 9-10), and to a lesser extent, anti-USF1M antibodies (lanes 6-

7). The region I wt oligonucleotide also formed a tenuous hypoxia-regulated complex which could be supershifted by the specific anti-HIF-1α IgG mgc3 (Fig. 5A, lane 4). Another radiolabeled oligonucleotide, spanning the wildtype region II and III (reg.II/III ww) was tightly bound both by HIF-1α and USF1/2 (Fig. 5A, lower panel; detection of HIF-1α ss: lane 4; USF1 ss: lanes 6+7; USF2 ss: 9+10). When using a reg.II/III double site oligonucleotide carrying a mutation in region II and an unaltered wildtype sequence in region III (reg.II/III mw), only the hypoxia inducible complex, supershifted by anti-HIF-1α (mgc3) IgG, was detected in conjunction with a complete loss of the constitutive binding activity by USFs (Fig. 5A: reg. II/III mw). The reverse sequence alteration in region III but not II (reg. II/III wm) left the oligonucleotide attachment by the constitutive USF complex undisturbed, but erased any interaction with HIF-1. It thus appears that region I of the LDHA promoter is, in vitro, mutually occupied by HIF-1 and USF complexes. However, the affinity of HIF-1 to this region seems to be much reduced compared to USFs. On the other hand, region II acts as exclusive, high-affinity site for USFs, whereas region III functions to attach HIF-1 to the LDHA promoter in deoxygenated nuclei. Corresponding BNIP3 EMSAs confirmed the mutual binding of HIF-1 and USF1/2 to the -259/-236 DNA that contains the HRE at -251/-246 (Supplement Table ST 2) (Fig. 5B). Specific supershifts were able to positively identify HIF-1α (ss: lane 4) as constituent of a hypoxic activity (lane 2), and USF1 (ss: lanes 6+7) and USF2 (ss: lanes 9+10) as participants of a constitutive complex (cc; lanes 1+2) of the BNIP3 promoter (Fig. 5B).

The important observation of a competitive effect between over-expressed HIF-1 and USF constituents on the BNIP3 promoter activity in Hep3B cells (see Fig. 3C), warranted a re-examination of BNIP3 reporter transfections, this time into cells where either signalling cascade had been silenced through the prior use of specific siRNAs. While the steady state abundance of HIF-1α, USF1 and USF2a proteins remained unaffected in cells transfected with scrambled siRNA (siContr., compare signals to non-transfected (non-TF) cells), exposing Hep3B cells to siRNAs specifically directed against HIF-1α (siHIF-1α), USF1 (siUSF1), USF2a (siUSF2a) or the combination of both USFs (siUSF1/2a) resulted in a drastically diminished expression of the respective factor. Additionally, cells subjected to a USF1 knockdown (siUSF1), left the USF2a expression unaltered. In contrast, absence of USF2a (siUSF2a) was accompanied by a strong reduction of USF1 protein level (*Fig. 6A*, USF1 signal in siUSF2a). The knockdown effect of any siRNA was stable up to 72h post-siRNA transfection.

Transfection of scrambled siRNA (siContr.) had no effect on the 4-fold hypoxic induction of the BNIP3 reporter. In stark contrast, subjecting Hep3B cells to HIF-1α siRNA completely abrogated this induction to baseline (Fig. 6B). When examining whether USF1 or/and USF2a silencing could influence the hypoxic response of BNIP3, we found that absence of USF1 resulted in a significantly increased BNIP3 promoter activity under hypoxia in comparison to siContr measurements. Although

suppression of USF2a raised fold hypoxic induction from 4.4 (siContr) to 5.7 (siUSF2a), data variance prohibited this difference to reach the level of significance (Fig. 6B).

In addition to transient knockdowns, we also evaluated the convergence of HIF-1 and USF1/2 pathways at the level of DNA using stable shRNA-based HIF-1α and USF2a knockdown clones in MCF7 cells. Beyond the expected specificity of the respective knockdown effect, the stable knockdown clones also confirmed: a) the marked reduction of USF1 protein levels upon the USF2a knockdown (Supplement Fig. S4A); b) the absolute USF2a requirement to exert a constitutively stimulated expression of the TYR reporter (Fig. S4B); c) the absolute HIF-1α requirement to exert a hypoxia-inducible expression of the PHD2 and LDHA reporter (Fig. S4C+D); d) the USF2a involvement in transactivating the LDHA promoter during periods of high oxygen (Fig. S4D); and e) the capacity HIF-1 and USFs to mutually substitute one another in the trans-activation of LDHA should the other activity be impaired or eliminated by a genetic or molecular loss-of-function event (Fig. S4D).

Discussion

One way to fine-tune, or inhibit, HIF's transcriptional outflow independently of hydroxylase activities could be through competing transcription factors. We reported (16) on a constitutive hepatoma cell (Hep3B) transcription activity that specifically bound to the E-box like CACGTG palindrome at position -146 in the hypoxia responsive globin 2 promoter (phb2) of *Daphnia magna*. Binding of this Hep3B factor was found to counteract the HIF-driven induction of the phb2 reporter from HREs at adjacent -258 and -107 positions. Whatever the binding entity to CACGTG motifs among candidate transcription factors is, these palindrome occupying complexes can evidently engage in positive or negative crosstalk with nearby HIF/HRE complexes (30, 37, 39). A more physiological understanding of hypoxic signalling requires to analyze transcriptional control mechanisms not just as a function of the stability/activity of HIF-1 *per se*, but as a function of the interplay that governs the hierarchy by which HIF-1 and related complexes gain access to DNA and regulate expression. In this context, the main objectives of the current study aimed to 1) identify the phb2 CACGTG-binding entity in human cancer cells and 2) investigate the factors interplay with HIF-1α in the control of co-targeted genes.

To determine which of the non-HIF bHLH complexes listed in the Results section is capable of binding the phb2 CACGTG palindrome in vitro, we employed EMSA supershifts and oligonucleotide pull-down assays (Fig. 1). Both methods consistently and reproducibly identified USF1 and USF2a/2b as the main phb2 CACGTG-complex in nuclear extracts from Hep3B and HeLa (Fig. 1) or MCF7 cell lines. Our pull-down assays also documented the opposite binding preferences of HIF-1 and USFs to phb2 cis-elements (Suppl. Fig. S1B+C). While HIF-1 exerted a measurably higher affinity to the asymmetric -107 phb2 HRE than to the symmetrical -146 phb2 palindrome (Suppl. Fig. S1B, 50x comp. lanes), USF factors displayed avid in vitro adherence to the -146 phb2 palindrome and an easily competed, lower affinity to the -107 phb2 HRE (Suppl. Fig. S1C, 50x comp. lanes). Thus, the single base substitution within the hexameric core of both these phb2 E-boxes (i.e. -107 HRE: 5'-TACGTG-3'; -146 palindrome: 5'-CACGTG-3'), and presumably additional changes in neighboring nucleotides, are important contributors to confer the vastly differing affinities of HIF and USF transcription factors to these motifs. This observation fits well with the general perception that CACGTG-palindromes tend to attract non-HIF bHLH factors (39, 51, 53, 54), and, consequentially, are notably underrepresented as *functional* HIF elements (14, 46, 61). Our co-immunoprecipitations further confirmed the lack of any physical protein-protein interaction between HIF-1 subunits and USFs (Supplement Fig. S2). Thus, USF1/2a/2b were considered the main and constitutive protein factors which indirectly interfere with the HIF/HRE-driven induction of hb2 globin gene (16) by binding to the phb2 CACGTG palindrome in HeLa, Hep3B and MCF7 cancer cells.

Upstream stimulatory factors (USFs) belong to the basic-helix-loop-helix-leucine zipper (bHLH/ZIP) family of transcription factors and exist, in human cells, as three different, ubiquitously expressed isoforms, USF1, USF2a and 2b, with molecular masses of 43, 44 and 38kDa respectively (49, 50, 58). Physiologically, USFs have been implicated in conferring the UV-induced tanning response in melanocytes and are key players in immune response, cell cycle and glucid-lipid metabolism gene regulation networks (5). In line with a possible fine-tuning of HIF's transcriptional read out by competing palindrome complexes, three human genes have been examined to date for their co-regulation by HIF and USF pathways: the genes encoding plasminogen activator inhibitor-1 (PAI-1) (8, 13, 43), the catalytic subunit of the telomerase, the telomerase reverse transcriptase (TERT) (2, 20, 63) and the glycolytic enzyme L-type pyruvate kinase (L-PK) which catalyzes the formation of pyruvate and ATP from phosphoenolypyruvate and ADP (33).

The *Daphnia* hb2 gene promoter had served as initial tool to narrow down the investigation of such E-box interference to the responsible players. Ultimately, we wanted to learn which *human* genes feature a similar bibox configuration of adjacent candidate HRE and CACGTG palindromes (PAL) in their promoter and thus might be co-responsive to incoming HIF and USF signals. As explained in the result section, we selected four human candidate genes which contained closely adjacent or over-lapping CACGTG PAL and HRE motifs within their promoter for further investigation in Hep3B, HeLa and MCF7 cells. Figure 2 revealed that only the LDHA (~2 fold) and BNIP3 (3.5-7 fold) reporter yielded a robust up-regulation by hypoxic conditions across all three cell lines. These results are consistent with previous studies which had already demonstrated for human LDHA and BNIP3 to be hypoxia-inducible HIF-1 target genes in HeLa and MCF7, respectively (14, 31).

When assessing the control of the LDHA reporter in Hep3B cells, our data showed the preferential stimulation of this promoter under high rather than low oxygen levels by over-expressed USFs. Co-transfecting increasing amounts of USF1 into Hep3B cells revealed a dose-dependent up-regulation followed by a saturated expression of LDHA, in particular under normoxia (Fig. 3B). A previous study had already described rat LDHA as a MYC targeted gene and further noticed the weak up-regulation of the gene by USFs under normoxia (47). Over-expression of HIF-1α similarly accentuated the LDHA reporter activity above endogenous levels. The fact that over-expressed HIF-1α is known to saturate the proteolytic machinery of the cell might explain why the normoxic trans-activation of the LDHA reporter increased equally efficient under the regime of surplus HIF-1α (H/N ratios 1.9→1.8). The combinatorial overproduction of exogenous HIF-1α and USF1 factors (Fig. 3B, 100ng each plasmid) in Hep3B cells yielded LDHA expression levels that superseded those of any over-expression scheme of the individual factors. Hence, this data suggests that coproduction of exogenous HIF-1α/USF1 results in a cooperative transcriptional activation of the LDHA reporter.

To follow up whether HIF-1 and USF1 or USF2a indeed engage in the coordinated control of the LDHA target, we conducted chromatin immunoprecipitation analyses. As a result, this ChIP data clearly documented the in vivo co-occupancy of endogenous HIF-1α, USF1 and USF2a to the LDHA promoter (region: -2533/-2375 from translation start site; 159bp amplicon) in hypoxic Hep3B (Fig. 4A, left panel) and MCF7 cells (Fig. 4A, right panel). USF1 and USF2a clearly stayed attached to the LDHA promoter during periods of normoxia in either cell. In additional gel shift assays we aimed to disentangle the occupancy of the three potential LDHA binding sites (region I-III, Tab. 1). Two of those three sites, namely the palindrome at reg. II (-2367 to -2362 from translation start site: 5'-CACGTG-3') and the asymmetric E-box at reg. III (-2353 to -2345; 5'-GACGTG-3' on anti-sense strand) are highly conserved in mouse, rat and human (Supplement Fig. S3) and have been reported to act as HIF-1 binding sites in mouse LDHA promoter (14, 45). Subsequently, Shim et al. showed that both E-box sites at region I and II within rat LDHA promoter serve to tether MYC to the gene (47). In our hands, the region II palindrome and region III asymmetric E-box functioned in vitro as USF1/2 (reg. II) and HIF-1 (reg. III) binding site, respectively (Fig. 5A lower panel). Region I of the 5' flank of the LDHA gene (-2465 to -2460; 5'-CACGTG-3'), represents a weak HIF-1 site and strong USF1, USF2a sites as well (Fig. 5A upper panel).

The role of USFs' in transactivating LDHA in oxygenated cells implies the factors as physiological drivers of aerobic glycolysis in cancer cells (Warburg effect). A MYC- or USF-mediated trans-activation of LDHA might, perhaps, shift the reversible interconversion between lactate and pyruvate in favor of the latter product. The cell would gain from the continued fuelling of mitochondria with NADH stemming from this reaction. In contrast, binding of HIF-1 to the upstream LDHA DNA under high oxygen levels was negligible in both Hep3B and MCF7 cells. In low O_2, HIF-1 dominates the LDHA promoter in MCF7 cells, while both USFs maintain their association with this DNA. DNA-attachment of HIF-1, therefore, does not appear to displace USFs from the upstream recognition sites of LDHA, in support of the notion that maximal LDHA transcription during low pO_2 results from the parallel and cooperative transcriptional control by HIF-1 and USF1/2a (Fig. 3B+4A). The presence of distinct, non-overlapping sites in the LDHA promoter thus might be a key feature for the mutually cooperative regulation of this gene by HIF-1 and USF pathways.

Co-transfection of Hep3B and HeLa cells with HIF-1, USF1 and 2a revealed that USF1 or 2a activity can dose-dependently interfere with the HIF-1-mediated BNIP3 induction during low oxygen (see ↓ arrows, Fig. 3C+D). Conversely, transient knockdown of USF1 function in Hep3B cells resulted in a significantly augmented BNIP3 promoter activity during hypoxia (Hx-siCon vs. Hx-siUSF1 kd; $p < 0.05$) (Fig. 6B). We also noted an increase, albeit not statistically significant, in the hypoxic induction of the BNIP3 reporter when Hep3B cells were treated with anti-USF2a siRNA (Fig. 6B: H/N = 4.4 fold, siContr → 5.7 fold, siUSF2a). The HRE at the position -251/-246 in the promoter of human BNIP3 gene was first identified by Kothari et al. to function as a direct binding site for HIF-1, which,

in turn, was found necessary for the transcriptional activation of the gene under hypoxia (31). Our ChIP data for Hep3B (Fig. 4B, left panel) and MCF7 cells (Fig. 4B right panel) reveal the dominant in vivo binding of HIF-1α to the BNIP3 promoter (region assessed: -509/-196 from translation start site) in deoxygenated cells along with the weak and constitutive tethering of USF1 and 2a to this DNA.

Remarkably, and in contrast to the LDHA regulation, we noticed some HIF-1α had successfully escaped proteolytic degradation since we detected it bound, as heterodimer, to the BNIP3 promoter in normoxic cells (Fig. 4B; Hep3B and MCF7 cells). Contrary to common perception, HIF-1α is not necessarily depleted entirely from oxygenated cancer cells - some might actually survive bound to DNA. The relevance, however, of functional HIF-1 in oxygenated cancer cells, that had not received the common trigger for enhanced alpha subunit translation by virtue of increasing cytokine/growth factor concentrations (see (7) for review), remains unclear. Moreover, HIF-1 also does not control the activity of its targets in form of a simple one-site/one-factor ON/OFF switch. Rather, transcriptional activity of co-regulated genes like BNIP3 results from a highly dynamic binding equilibrium, where, for example, expression and activity of USF factors determines to what extent HIF-1 actually *can* bind and control the considered promoter. Control of BNIP3 expression switches from a HIF-dictated (hypoxia) to a HIF/USF competed mode (normoxia). These findings demonstrate the capacity of activated USF factors to modulate or disturb HIF-1 signalling on several key tumor-promoting genes in different cell backgrounds.

Our EMSA screen with a single site oligonucleotide (-259 to -236; Suppl. Table ST 2) characterized the BNIP3 E-box as a surprisingly poor HIF-1 motif during hypoxia (Fig. 5B, lanes 2-4). In contrast, constitutive USF1 and 2a complexes (cc) were attracted to this site with high-affinity (Fig. 5B, lanes 5-7 and 8-10). Thus, the BNIP3 HRE at -251/-246 is in hypoxic cells co-targeted by HIF-1 and USFs, yet predominant in vivo binding occurs via HIF/HRE complexes (Fig. 4B). We hypothesize that USFs are able to either directly displace bound HIF-1α from the BNIP3 E-box at the position -251/-246 or prohibit effective binding of the hypoxia inducible factor to this site from the immediately adjacent and conserved CACGCN motifs (Supplement Fig. S3). In any event, the fact that USF1/2 complexes remained attached to the BNIP3 promoter fragment even in deoxygenated cells suggests that both basal (normoxic) and inducing (hypoxic) activities of HIF-1 are under surveillance of palindrome factors.

Given that HIF and USF signalling pathways evidently converge in vivo onto the promoter of the LDHA and BNIP3 genes in MCF7 cells (Fig. 4), we chose a second loss-of-function (LoF) approach by generating two stable MCF7 shRNA knockdown (kd) lines for HIF-1α and USF2a (Supplement. Fig. S4A). To our surprise, USF1 levels were visibly diminished in the chosen shRNA-based stable MCF7 USF2a knockdown clone (Supplement Fig. 4A, lower panel), as was seen in siUSF2a-treated

Hep3B cells (Fig. 6A). Similar cross-talk between USF gene products has been observed by some (48), but not others (57), to occur in mouse embryonic fibroblast (MEF) cell lines of USF1$^{-/-}$ or USF2a $^{-/-}$ mice, where USF1$^{-/-}$ MEFs showed an enhanced USF2 expression, while those of USF2 knockout mice exhibited a significant reduction of USF1 protein level (48). Such carry-over knockdown of USF1 in USF2a kd cells may reflect the necessity of USF2a for the optimal production of USF1 (USF2a → USF1), while the reverse transcriptional and/or translational autoregulation (USF1 → USF2a) does not seem to operate in the cancer cells used here. Reporter transfections of these shNA MCF7 clones left little doubt on the specific USF2a requirement to constitutively drive the TYR reporter (Fig. S4B), and of HIF-1α to exert the hypoxia-inducible expression of the PHD2 and LDHA constructs (Fig. S4C+D). Endogenous USF2a was indeed engaged in transactivating the LDHA promoter during periods of high oxygen (Fig. S4D: H/N 7.0 fold, wt cells → 9.3 fold in USF2a kd cells) while over-expressed HIF-1α and USFs were found to mutually compensate for the LoF of the other activity in support of the cooperative trans-activation of LDHA by either pathway (Fig. S4D; see ↑ arrows).

Collectively, the shown over-expression and siRNA/shRNA based manipulations of HIF-1α vs. USF1 and USF2a transcription factors are in line with mutually cooperative and antagonistic interactions in regard of the transcriptional control of LDHA and BNIP3 target genes, respectively. Our evidence for this crosstalk includes both in vitro and in vivo data and was sampled across a diverse panel of cancer cell lines (i.e. Hep3B, HeLa, MCF7). Two different models are considered to account for these observations in our study (*Fig. 7*). An LDHA-type pathway convergence represents a mutually supportive regulation of USFs by HIF-1, and vice versa, when bound to closely adjacent yet distinct motifs. This cooperation becomes particularly noticeable when using over-expressed factors, i.e. when both pathways are activated in parallel (Fig. 7A). Conversely, the BNIP3-type model conveys our observations that an oxygen-independent activation of USF signalling is able to counteract HIF-1-driven transactivation by displacing bound or blocking incoming HIF-1 from occupying the BNIP3 HRE/palindrome composite motif (Fig. 7B). The HIF/USF competition for the BNIP3 promoter thus emphasizes the extent of fine-tuning and dynamics that is possible when different pathways converge upon the same gene. Generally speaking, it appears that a gene's capacity to attract HIF-1/-2 is a multi-level coordinated response, where accessory factors are also engaging to precisely tailor or disrupt HIF's transcriptional outflow independently of hydroxylase activities and in accordance to the specific needs of the cell. Future work should assess the genome-wide implications of the tuning or inhibitory impact by activated USF transcription factors on the HIF-1 mediated gene activation in human cancer cells.

Acknowledgements

We are grateful to Prof. Benoit Viollet (Institut Cochin INSERM, Universite Paris Descartes Dpt Endocrinology, Metabolism and Cancer, Paris France) for his generous gifts of USF antibodies and expression plasmids, for reading the manuscript and for his unwavering willingness to act as expert sounding board throughout the project. We also thank the following colleagues for their kind contributions of various materials as mentioned in the paper: Prof. Adrian L. Harris (John Radcliffe Hospital, Oxford, UK); Dr. Makoto Tsuneoka (Kurume University, Fukuoka, Japan); Prof. Richard S. Pollenz (University of South Florida, Tampa); Prof. Kazuhiro Sogawa (Tonoku University, Sendai, Japan); Prof. Robert G. Roeder (the Rockefeller University, New York, USA); Prof. P. Maxwell (University College London, London, UK) and Prof. J. Okami (University of Michigan). We thank Ms. Kristin Wollenick (Institute of Physiology, University of Zurich) for generating the short version of PHD2 luciferase reporter plasmid and Mr. Kristian Reveles Jensen for his motivated help in the project while being a BUSS-2008 summer student at the University of Zurich. Further thanks go to Prof. L. Poellinger, Dr. K. Gradin and X. Zheng who all provided a great opportunity for one of us (JH) to learn the chromatin immunoprecipitation (ChIP) technique at Karolinska Institute, Stockholm, Sweden. This work was made possible by funding from the EU's 6th framework programme (Euroxy consortium; partners: MG, TAG) and a grant from the Swiss National Science Foundation (MG).

References

1. **Centanin, L., T. A. Gorr, and P. Wappner.** 2009. Tracheal remodelling in response to hypoxia. J Insect Physiol., in press; doi:10.1016/j.jinsphys.2009.05.008.
2. **Chang, J. T., H. T. Yang, T. C. Wang, and A. J. Cheng.** 2005. Upstream stimulatory factor (USF) as a transcriptional suppressor of human telomerase reverse transcriptase (hTERT) in oral cancer cells. Mol Carcinog **44:**183-92.
3. **Chen, L., Y. H. Shen, X. Wang, J. Wang, Y. Gan, N. Chen, J. Wang, S. A. LeMaire, J. S. Coselli, and X. L. Wang.** 2006. Human prolyl-4-hydroxylase alpha(I) transcription is mediated by upstream stimulatory factors. J Biol Chem **281:**10849-55.
4. **Chilov, D., T. Hofer, C. Bauer, R. H. Wenger, and M. Gassmann.** 2001. Hypoxia affects expression of circadian genes PER1 and CLOCK in mouse brain. Faseb J **15:**2613-22.
5. **Corre, S., and M. D. Galibert.** 2005. Upstream stimulating factors: highly versatile stress-responsive transcription factors. Pigment Cell Res **18:**337-48.
6. **Corre, S., A. Primot, E. Sviderskaya, D. C. Bennett, S. Vaulont, C. R. Goding, and M. D. Galibert.** 2004. UV-induced expression of key component of the tanning process, the POMC and MC1R genes, is dependent on the p-38-activated upstream stimulating factor-1 (USF-1). J Biol Chem **279:**51226-33.
7. **Dery, M. A., M. D. Michaud, and D. E. Richard.** 2005. Hypoxia-inducible factor 1: regulation by hypoxic and non-hypoxic activators. Int J Biochem Cell Biol **37:**535-40.
8. **Dimova, E. Y., and T. Kietzmann.** 2006. Cell type-dependent regulation of the hypoxia-responsive plasminogen activator inhibitor-1 gene by upstream stimulatory factor-2. J Biol Chem **281:**2999-3005.
9. **Ema, M., K. Hirota, J. Mimura, H. Abe, J. Yodoi, K. Sogawa, L. Poellinger, and Y. Fujii-Kuriyama.** 1999. Molecular mechanisms of transcription activation by HLF and HIF1alpha in response to hypoxia: their stabilization and redox signal-induced interaction with CBP/p300. Embo J **18:**1905-14.
10. **Epstein, A. C., J. M. Gleadle, L. A. McNeill, K. S. Hewitson, J. O'Rourke, D. R. Mole, M. Mukherji, E. Metzen, M. I. Wilson, A. Dhanda, Y. M. Tian, N. Masson, D. L. Hamilton, P. Jaakkola, R. Barstead, J. Hodgkin, P. H. Maxwell, C. W. Pugh, C. J. Schofield, and P. J. Ratcliffe.** 2001. C. elegans EGL-9 and mammalian homologs define a family of dioxygenases that regulate HIF by prolyl hydroxylation. Cell **107:**43-54.
11. **Esteban, M. A., M. G. Tran, S. K. Harten, P. Hill, M. C. Castellanos, A. Chandra, R. Raval, S. O'Brien T, and P. H. Maxwell.** 2006. Regulation of E-cadherin expression by VHL and hypoxia-inducible factor. Cancer Res **66:**3567-75.
12. **Fandrey, J., T. A. Gorr, and M. Gassmann.** 2006. Regulating cellular oxygen sensing by hydroxylation. Cardiovasc Res **71:**642-51.
13. **Fink, T., A. Kazlauskas, L. Poellinger, P. Ebbesen, and V. Zachar.** 2002. Identification of a tightly regulated hypoxia-response element in the promoter of human plasminogen activator inhibitor-1. Blood **99:**2077-83.
14. **Firth, J. D., B. L. Ebert, and P. J. Ratcliffe.** 1995. Hypoxic regulation of lactate dehydrogenase A. Interaction between hypoxia-inducible factor 1 and cAMP response elements. J Biol Chem **270:**21021-7.
15. **Galibert, M. D., S. Carreira, and C. R. Goding.** 2001. The Usf-1 transcription factor is a novel target for the stress-responsive p38 kinase and mediates UV-induced Tyrosinase expression. Embo J **20:**5022-31.
16. **Gorr, T. A., J. D. Cahn, H. Yamagata, and H. F. Bunn.** 2004. Hypoxia-induced synthesis of hemoglobin in the crustacean Daphnia magna is hypoxia-inducible factor-dependent. J Biol Chem **279:**36038-47.
17. **Gorr, T. A., M. Gassmann, and P. Wappner.** 2006. Sensing and responding to hypoxia via HIF in model invertebrates. J Insect Physiol **52:**349-64.
18. **Gorr, T. A., C. V. Rider, H. Y. Wang, A. W. Olmstead, and G. A. LeBlanc.** 2006. A candidate juvenoid hormone receptor cis-element in the Daphnia magna hb2 hemoglobin gene promoter. Mol Cell Endocrinol **247:**91-102.
19. **Gorr, T. A., T. Tomita, P. Wappner, and H. F. Bunn.** 2004. Regulation of Drosophila hypoxia-inducible factor (HIF) activity in SL2 cells: identification of a hypoxia-induced variant isoform of the HIFalpha homolog gene similar. J Biol Chem **279:**36048-58.
20. **Goueli, B. S., and R. Janknecht.** 2003. Regulation of telomerase reverse transcriptase gene activity by upstream stimulatory factor. Oncogene **22:**8042-7.
21. **Grandori, C., S. M. Cowley, L. P. James, and R. N. Eisenman.** 2000. The Myc/Max/Mad network and the transcriptional control of cell behavior. Annu Rev Cell Dev Biol **16:**653-99.
22. **Grandori, C., J. Mac, F. Siebelt, D. E. Ayer, and R. N. Eisenman.** 1996. Myc-Max heterodimers activate a DEAD box gene and interact with multiple E box-related sites in vivo. Embo J **15:**4344-57.

23. **Gustafsson, M. V., X. Zheng, T. Pereira, K. Gradin, S. Jin, J. Lundkvist, J. L. Ruas, L. Poellinger, U. Lendahl, and M. Bondesson.** 2005. Hypoxia requires notch signaling to maintain the undifferentiated cell state. Dev Cell **9:**617-28.
24. **Holmes, J. L., and R. S. Pollenz.** 1997. Determination of aryl hydrocarbon receptor nuclear translocator protein concentration and subcellular localization in hepatic and nonhepatic cell culture lines: development of quantitative Western blotting protocols for calculation of aryl hydrocarbon receptor and aryl hydrocarbon receptor nuclear translocator protein in total cell lysates. Mol Pharmacol **52:**202-11.
25. **Holmquist-Mengelbier, L., E. Fredlund, T. Lofstedt, R. Noguera, S. Navarro, H. Nilsson, A. Pietras, J. Vallon-Christersson, A. Borg, K. Gradin, L. Poellinger, and S. Pahlman.** 2006. Recruitment of HIF-1alpha and HIF-2alpha to common target genes is differentially regulated in neuroblastoma: HIF-2alpha promotes an aggressive phenotype. Cancer Cell **10:**413-23.
26. **Ivan, M., K. Kondo, H. Yang, W. Kim, J. Valiando, M. Ohh, A. Salic, J. M. Asara, W. S. Lane, and W. G. Kaelin, Jr.** 2001. HIFalpha targeted for VHL-mediated destruction by proline hydroxylation: implications for O2 sensing. Science **292:**464-8.
27. **Jaakkola, P., D. R. Mole, Y. M. Tian, M. I. Wilson, J. Gielbert, S. J. Gaskell, A. Kriegsheim, H. F. Hebestreit, M. Mukherji, C. J. Schofield, P. H. Maxwell, C. W. Pugh, and P. J. Ratcliffe.** 2001. Targeting of HIF-alpha to the von Hippel-Lindau ubiquitylation complex by O2-regulated prolyl hydroxylation. Science **292:**468-72.
28. **Kallio, P. J., K. Okamoto, S. O'Brien, P. Carrero, Y. Makino, H. Tanaka, and L. Poellinger.** 1998. Signal transduction in hypoxic cells: inducible nuclear translocation and recruitment of the CBP/p300 coactivator by the hypoxia-inducible factor-1alpha. Embo J **17:**6573-86.
29. **Kaulen, H., P. Pognonec, P. D. Gregor, and R. G. Roeder.** 1991. The Xenopus B1 factor is closely related to the mammalian activator USF and is implicated in the developmental regulation of TFIIIA gene expression. Mol Cell Biol **11:**412-24.
30. **Kim, J. W., P. Gao, Y. C. Liu, G. L. Semenza, and C. V. Dang.** 2007. Hypoxia-inducible factor 1 and dysregulated c-Myc cooperatively induce vascular endothelial growth factor and metabolic switches hexokinase 2 and pyruvate dehydrogenase kinase 1. Mol Cell Biol **27:**7381-93.
31. **Kothari, S., J. Cizeau, E. McMillan-Ward, S. J. Israels, M. Bailes, K. Ens, L. A. Kirshenbaum, and S. B. Gibson.** 2003. BNIP3 plays a role in hypoxic cell death in human epithelial cells that is inhibited by growth factors EGF and IGF. Oncogene **22:**4734-44.
32. **Krek, W.** 2000. VHL takes HIF's breath away. Nat Cell Biol **2:**E121-3.
33. **Krones, A., K. Jungermann, and T. Kietzmann.** 2001. Cross-talk between the signals hypoxia and glucose at the glucose response element of the L-type pyruvate kinase gene. Endocrinology **142:**2707-18.
34. **Kvietikova, I., R. H. Wenger, H. H. Marti, and M. Gassmann.** 1995. The transcription factors ATF-1 and CREB-1 bind constitutively to the hypoxia-inducible factor-1 (HIF-1) DNA recognition site. Nucleic Acids Res **23:**4542-50.
35. **Lando, D., D. J. Peet, J. J. Gorman, D. A. Whelan, M. L. Whitelaw, and R. K. Bruick.** 2002. FIH-1 is an asparaginyl hydroxylase enzyme that regulates the transcriptional activity of hypoxia-inducible factor. Genes Dev **16:**1466-71.
36. **Lando, D., D. J. Peet, D. A. Whelan, J. J. Gorman, and M. L. Whitelaw.** 2002. Asparagine hydroxylation of the HIF transactivation domain a hypoxic switch. Science **295:**858-61.
37. **Lendahl, U., K. L. Lee, H. Yang, and L. Poellinger.** 2009. Generating specificity and diversity in the transcriptional response to hypoxia. Nat Rev Genet **10:**821-832.
38. **Manalo, D. J., A. Rowan, T. Lavoie, L. Natarajan, B. D. Kelly, S. Q. Ye, J. G. Garcia, and G. L. Semenza.** 2005. Transcriptional regulation of vascular endothelial cell responses to hypoxia by HIF-1. Blood **105:**659-69.
39. **Mazure, N. M., C. Chauvet, B. Bois-Joyeux, M. A. Bernard, H. Nacer-Cherif, and J. L. Danan.** 2002. Repression of alpha-fetoprotein gene expression under hypoxic conditions in human hepatoma cells: characterization of a negative hypoxia response element that mediates opposite effects of hypoxia inducible factor-1 and c-Myc. Cancer Res **62:**1158-65.
40. **Metzen, E., D. P. Stiehl, K. Doege, J. H. Marxsen, T. Hellwig-Burgel, and W. Jelkmann.** 2005. Regulation of the prolyl hydroxylase domain protein 2 (phd2/egln-1) gene: identification of a functional hypoxia-responsive element. Biochem J **387:**711-7.
41. **North, S., X. Espanel, F. Bantignies, B. Viollet, V. Vallet, P. Jalinot, G. Brun, and G. Gillet.** 1999. Regulation of cdc2 gene expression by the upstream stimulatory factors (USFs). Oncogene **18:**1945-55.
42. **Okami, J., D. M. Simeone, and C. D. Logsdon.** 2004. Silencing of the hypoxia-inducible cell death protein BNIP3 in pancreatic cancer. Cancer Res **64:**5338-46.
43. **Samoylenko, A., U. Roth, K. Jungermann, and T. Kietzmann.** 2001. The upstream stimulatory factor-2a inhibits plasminogen activator inhibitor-1 gene expression by binding to a promoter element adjacent to the hypoxia-inducible factor-1 binding site. Blood **97:**2657-66.

44. **Semenza, G. L.** 2009. Regulation of oxygen homeostasis by hypoxia-inducible factor 1. Physiology (Bethesda) **24:**97-106.
45. **Semenza, G. L., B. H. Jiang, S. W. Leung, R. Passantino, J. P. Concordet, P. Maire, and A. Giallongo.** 1996. Hypoxia response elements in the aldolase A, enolase 1, and lactate dehydrogenase A gene promoters contain essential binding sites for hypoxia-inducible factor 1. J Biol Chem **271:**32529-37.
46. **Semenza, G. L., P. H. Roth, H. M. Fang, and G. L. Wang.** 1994. Transcriptional regulation of genes encoding glycolytic enzymes by hypoxia-inducible factor 1. J Biol Chem **269:**23757-63.
47. **Shim, H., C. Dolde, B. C. Lewis, C. S. Wu, G. Dang, R. A. Jungmann, R. Dalla-Favera, and C. V. Dang.** 1997. c-Myc transactivation of LDH-A: implications for tumor metabolism and growth. Proc Natl Acad Sci U S A **94:**6658-63.
48. **Sirito, M., Q. Lin, J. M. Deng, R. R. Behringer, and M. Sawadogo.** 1998. Overlapping roles and asymmetrical cross-regulation of the USF proteins in mice. Proc Natl Acad Sci U S A **95:**3758-63.
49. **Sirito, M., Q. Lin, T. Maity, and M. Sawadogo.** 1994. Ubiquitous expression of the 43- and 44-kDa forms of transcription factor USF in mammalian cells. Nucleic Acids Res **22:**427-33.
50. **Sirito, M., S. Walker, Q. Lin, M. T. Kozlowski, W. H. Klein, and M. Sawadogo.** 1992. Members of the USF family of helix-loop-helix proteins bind DNA as homo- as well as heterodimers. Gene Expr **2:**231-40.
51. **Sogawa, K., R. Nakano, A. Kobayashi, Y. Kikuchi, N. Ohe, N. Matsushita, and Y. Fujii-Kuriyama.** 1995. Possible function of Ah receptor nuclear translocator (Arnt) homodimer in transcriptional regulation. Proc Natl Acad Sci U S A **92:**1936-40.
52. **Stiehl, D. P., R. Wirthner, J. Koditz, P. Spielmann, G. Camenisch, and R. H. Wenger.** 2006. Increased prolyl 4-hydroxylase domain proteins compensate for decreased oxygen levels. Evidence for an autoregulatory oxygen-sensing system. J Biol Chem **281:**23482-91.
53. **Swanson, H. I., W. K. Chan, and C. A. Bradfield.** 1995. DNA binding specificities and pairing rules of the Ah receptor, ARNT, and SIM proteins. J Biol Chem **270:**26292-302.
54. **Swanson, H. I., and J. H. Yang.** 1999. Specificity of DNA binding of the c-Myc/Max and ARNT/ARNT dimers at the CACGTG recognition site. Nucleic Acids Res **27:**3205-12.
55. **Tsuneoka, M., F. Nakano, H. Ohgusu, and E. Mekada.** 1997. c-myc activates RCC1 gene expression through E-box elements. Oncogene **14:**2301-11.
56. **Turley, H., C. C. Wykoff, S. Troup, P. H. Watson, K. C. Gatter, and A. L. Harris.** 2004. The hypoxia-regulated transcription factor DEC1 (Stra13, SHARP-2) and its expression in human tissues and tumours. J Pathol **203:**808-13.
57. **Vallet, V. S., M. Casado, A. A. Henrion, D. Bucchini, M. Raymondjean, A. Kahn, and S. Vaulont.** 1998. Differential roles of upstream stimulatory factors 1 and 2 in the transcriptional response of liver genes to glucose. J Biol Chem **273:**20175-9.
58. **Viollet, B., A. M. Lefrancois-Martinez, A. Henrion, A. Kahn, M. Raymondjean, and A. Martinez.** 1996. Immunochemical characterization and transacting properties of upstream stimulatory factor isoforms. J Biol Chem **271:**1405-15.
59. **Wang, G. L., B. H. Jiang, E. A. Rue, and G. L. Semenza.** 1995. Hypoxia-inducible factor 1 is a basic-helix-loop-helix-PAS heterodimer regulated by cellular O2 tension. Proc Natl Acad Sci U S A **92:**5510-4.
60. **Webb, J. D., M. L. Coleman, and C. W. Pugh.** 2009. Hypoxia, hypoxia-inducible factors (HIF), HIF hydroxylases and oxygen sensing. Cell Mol Life Sci. **66:**3539-54.
61. **Wenger, R. H., and M. Gassmann.** 1997. Oxygen(es) and the hypoxia-inducible factor-1. Biol Chem **378:**609-16.
62. **Wenger, R. H., D. P. Stiehl, and G. Camenisch.** 2005. Integration of oxygen signaling at the consensus HRE. Sci STKE **2005:**re12.
63. **Yatabe, N., S. Kyo, Y. Maida, H. Nishi, M. Nakamura, T. Kanaya, M. Tanaka, K. Isaka, S. Ogawa, and M. Inoue.** 2004. HIF-1-mediated activation of telomerase in cervical cancer cells. Oncogene **23:**3708-15.

Legend

Fig. 1 EMSA supershifts and pull–down analysis to identify CACGTG complex in phb2. (A) EMSA supershift screen to identify factor(s) which bind to the -146 CACGTG motif in phb2. The following antibodies were added into the binding reactions with Hep3B normoxic nuclear extracts. Lane 1: no antibody; lane 2: non-specific IgG; lane 3: anti-USF1 full length IgG; lane 4: pre-immune serum from same rabbit used to generate anti-USF1M antibody (=PI-1M); lane 5: anti-USF1M IgG; lane 6: PI-2F; lane 7: anti-USF2F IgG; lane 8: PI-2G; lane 9: anti-USF2G IgG; lane 10: PI-2Z; lane 11: anti-USF2Z IgG; lane 12: PI-2aO; lane 13: anti-USF2aO IgG; lanes 14, 16, 18, 20 and 22: non-specific IgG; lane 15: anti-DEC1 IgG; lane 17: anti-MYC IgG; lane 19: anti-hARNT IgG; lane 21: anti-mARNT IgG; lane 23: anti-ATF1. cc: constitutive CACGTG complex; ss: supershifted CACGTG complex. (B+C) Pull-down analysis with beads coated with -146 phb2 E-box-carrying oligonucleotides (5'-CACGTG-3') and HeLa normoxic and hypoxic nuclear extracts. Binding specificity was assessed either through beads coated with -146 mutant (m-bio) E-box motifs (5'-CAATGT-3') or with binding reactions containing 50-fold molar excess of free wild type oligonucleotide as competitor (50×comp.). Immunoblot of bound factors with (B) anti-USF1M and (C) left panel: anti-USF2G antibody; right panel: anti-USF2aO antibody. Staining of non-specific (ns) proteins indicated as loading control. N: air; H: 1% O_2 16h.

Table 1. E-box palindromes and HRE sites in promoters of human genes. HIF-1 and USF co-regulated candidate genes: 4EBP1, LDHA, MC1R and BNIP3; control genes: TYR and PHD2. Translation start site ATG as +1 (in brackets). 5' flanking region upstream of ATG is given for human TYR, PHD2, 4EBP1, LDHA, MC1R and BNIP3 genes. HRE and E-box palindromes are capitalized. Conserved hmr HREs: bold + underlined; variable HREs: bold only. Conserved hmr palindromes: E-boxes: italicized + underlined; variable E-box: in italics only. For conservation: see alignments in Suppl. Fig. S3.

Fig. 2 Endogenous response of human PHD2, 4EBP1, LDHA, MC1R and BNIP3 luciferase reporter. Hep3B (A), MCF7 (B) and HeLa (C) cells were transfected with 2.0μg of 4EBP1, LDHA and MC1R or 1.5μg of PHD2 or BNIP3 luciferase reporter plasmid in a total of 3μg plasmid. After 16h hypoxic (1% O_2) exposure (H, black bars) or normoxic (air) exposure (N, white bars), relative luciferase activity was determined and normalized with β–galactosidase activity (%RLA, as mean ± SD). Plasmid-free transfections (null) and transfections with the empty pGL3 basic vector (bVec) were used as negative controls. N: air; H: 1% O_2 16h. Mean H/N-fold inductions of each reporter are indicated above the respective pair of columns.

Fig. 3 Regulation of BNIP3 and LDHA luciferase activity by over-expressed HIF-1α and USFs. (A) Hep3B transfections of USF and HIF-1 control reporter using either 1.5μg TYR plasmid or 0.5μg

PHD2 plasmid. (B) Hep3B transfections with 0.3µg LDHA reporter plasmid. (C) Hep3B or (D) HeLa transfections with 0.3µg BNIP3 reporter plasmid. For reporter regulation by over-expressed HIF-1α and USFs, ng amounts of HIF-1α and USF expression plasmids used are indicated underneath the respective co-transfection. Relative luciferase activity is given as in Fig. 2 (mean ± SD %RLA; n = 3 independent experiments). N: air; H: 1% O_2 16h. Mean H/N-fold inductions of each reporter are indicated above respective pair of columns. Statistics done in regard to same O_2 category (i.e. N or H): a) endo/exo test = endogenous controls (reporter alone; no overexpressed HIF/USF) *versus* reporter co-transfection (reporter with exogenous HIF/USF); b) hif/combi test: reporter + exogenous HIF1α *versus* reporter + exogenous (HIF1α + USF1/2a); symbols for $p < 0.05$ for i) non-parametric Wilcoxon rank-sum tests (endo/exo = ✱; hif/combi = ✚); ii) Anova/Sidak tests (endo/exo = ●; hif/combi = ◆) (see Material & Methods for details).

Fig. 4 Chromatin immunoprecipitation determination of in vivo HIF-1 and USF binding to LDHA and BNIP3 promoters. ChIP assay was performed in Hep3B (left panels) and MCF7 (right panels) cells using indicated antibodies or pre-immune serum and non-specific antibody IgG as negative controls. Purified DNA was subjected to PCR using LDHA primer (panel A: 159bp amplicon) or BNIP3 primer (panel B: 314bp amplicon). N: air; H: 1% O_2 4h. PI-2G pre-immune serum for anti-USF2G; neg. PCR with H_2O.

Fig. 5 EMSA supershifts with LDHA and BNIP3 E-box oligonucleotides. Gel supershift using LDHA HRE and E-box palindrome oligonucleotides together with MCF7 nuclear extracts (panel A) and BNIP3 HRE oligonucleotides together with Hep3B nuclear extracts (panel B). All oligonucleotides used in this EMSA are listed in Suppl. Table ST 2. For HIF-1α or USFs gel supershifts, 1µl of the indicated specific antibody was used in comparison with pre-immune serum (PI-1M or PI-2G) or non-specific lgG as negative control. N, H, cc, ss: as above.

Fig. 6 Transient siRNA knockdown of HIF-1α, USF1 and USF2a and the regulation of BNIP3 promoter activity in Hep3B cells. (A) Western blot analysis to display knockdown efficiency for HIF-1α, USF1 and USF2a. Cells were harvested at two post-siRNA transfection time points: 48h and 72h, corresponding to 6h and 30h hypoxia exposure (1% O_2), respectively. As negative controls, transfections with scrambled siRNA (siContr.) and non-transfected cells (non-TF) were used. (B) BNIP3 Luciferase assay (0.15µg plasmid) in Hep3B cells treated with siRNAs. %RLA value, normalized to β–galactosidase activity, is mean ± SD of 4 independent experiments. N: air; H: 1% O_2 16h. Mean H/N-fold inductions of each reporter are indicated above respective pair of columns. Statistics were done in regard to same O_2 category (i.e. N or H) as detailed in Material & Methods. Pairwise comparison of BNIP3 relative luciferase activity (RLA) values treated with siContr RNA versus any BNIP3-RLA of the HIF-1α, USF1, USF2a or USF1/2a siRNA treatments (=siTF, siRNA

against named transcription factor) was carried out using a non-parametric Wilcoxon rank-sum tests. Significant siContr/siTF RLA differences ($p < 0.05$) are indicated by black (normoxic data) or white asterisks (hypoxic data) before gray background.

Fig. 7 Models for convergences of HIF and USF signals onto HRE and E-box palindrome containing bibox promoter. A LDHA-type (A) and BNIP3-type (B) model of the HIF/USF crosstalk as indicated. See text for discussion.

Table 1

Gene	Sequence 5′-3′	Ref.
*h*TYR	-183 -178 -91 -86 gaaaagtcagt*CATGTG*cttttca---gccaaga*CATGTG*ataat---aggaaga(atg)	(6)
*h*PHD2	-413 -408 gccgtggtg**TACGTG**cagagcgcgcagagcgagt---gccgccgccgcc(atg)	(40)
*h*4EBP1	-179 -174 -120 -115 ggggatcc*CACGTG*gaagc--caaatcccagg**GGCGTG**gggcgg--gagacc(atg)	
*h*LDHA	-2465 -2460 -2367 -2362 -2353 -2348 cagcg*CACGTG*gagcg--actca*CACGTG*ggttcccg**CACGTC**cgccggc--aat(atg)	(45); (47)
*h*MC1R	-742 -737 -461 -456 acgttga*CAGCTG*agttgctg--ccccgg*CATGTG*gccgccct--ggacaggact(atg)	(6)

Figure 1

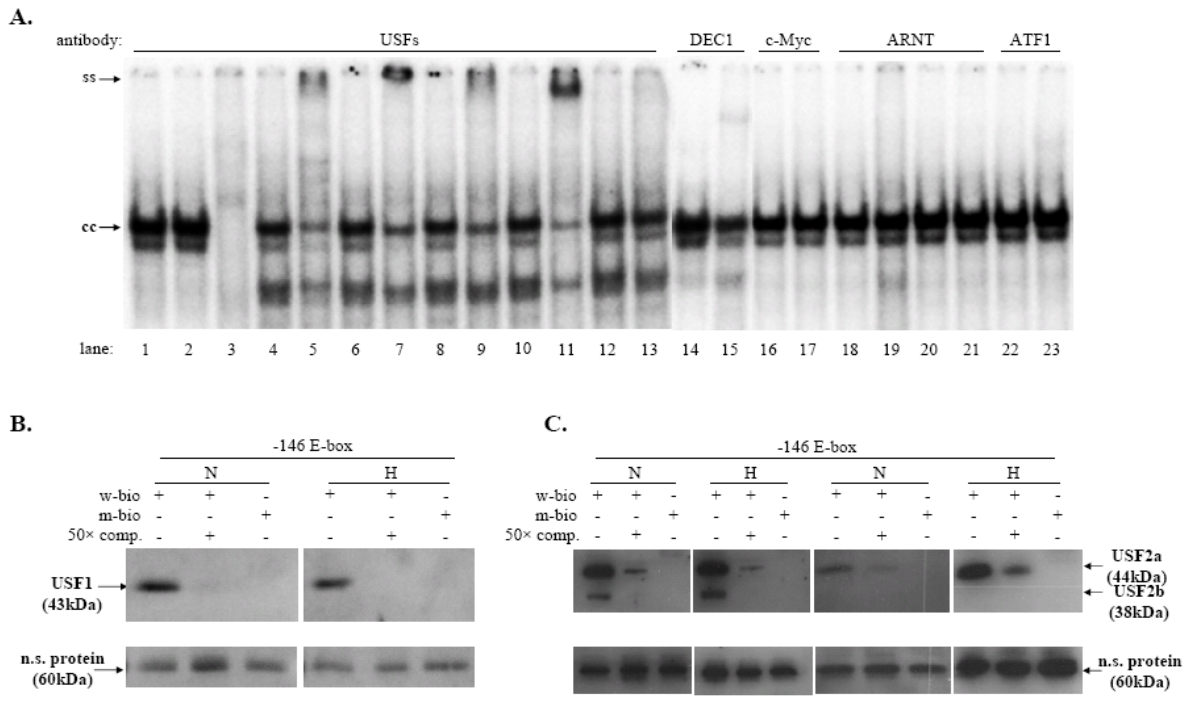

Figure 2

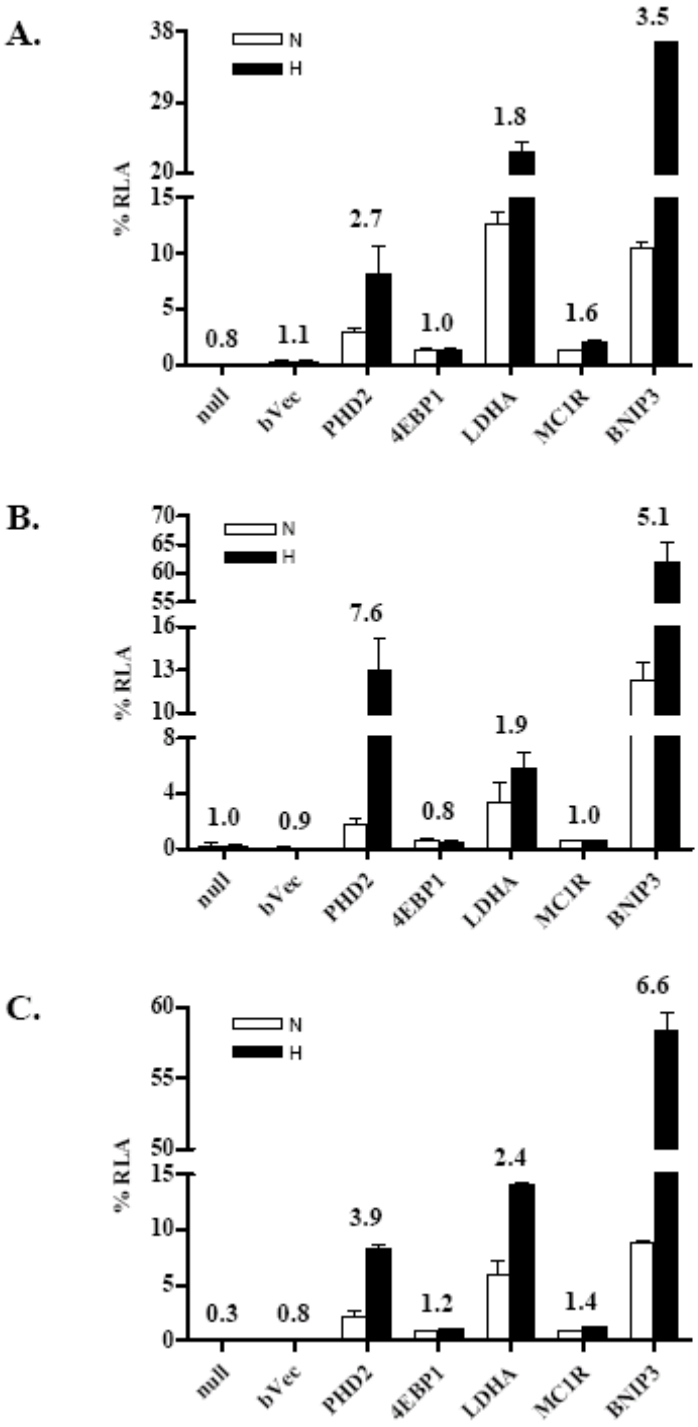
A.
B.
C.
N
H
% RLA
0.8
1.1
2.7
1.0
1.8
1.6
3.5
1.0
0.9
7.6
0.8
1.9
1.0
5.1
0.3
0.8
3.9
1.2
2.4
1.4
6.6
null
bVec
PHD2
4EBP1
LDHA
MC1R
BNIP3

Figure 3

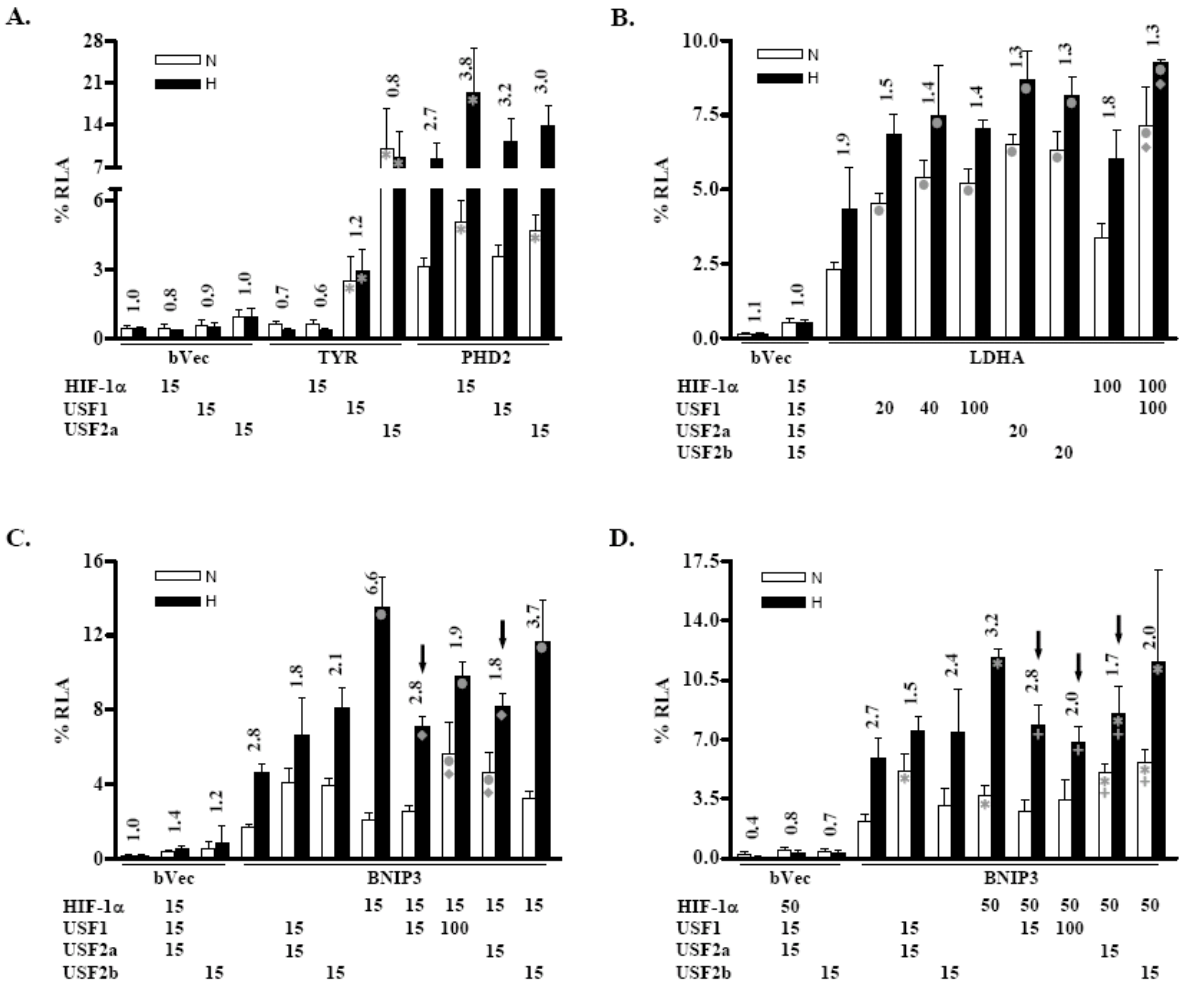

Figure 4

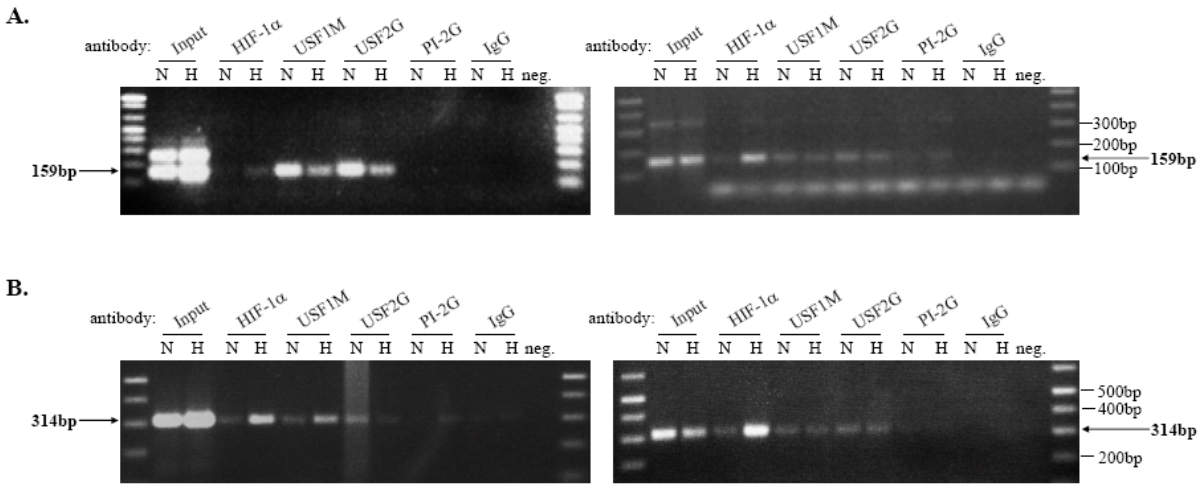

Figure 5

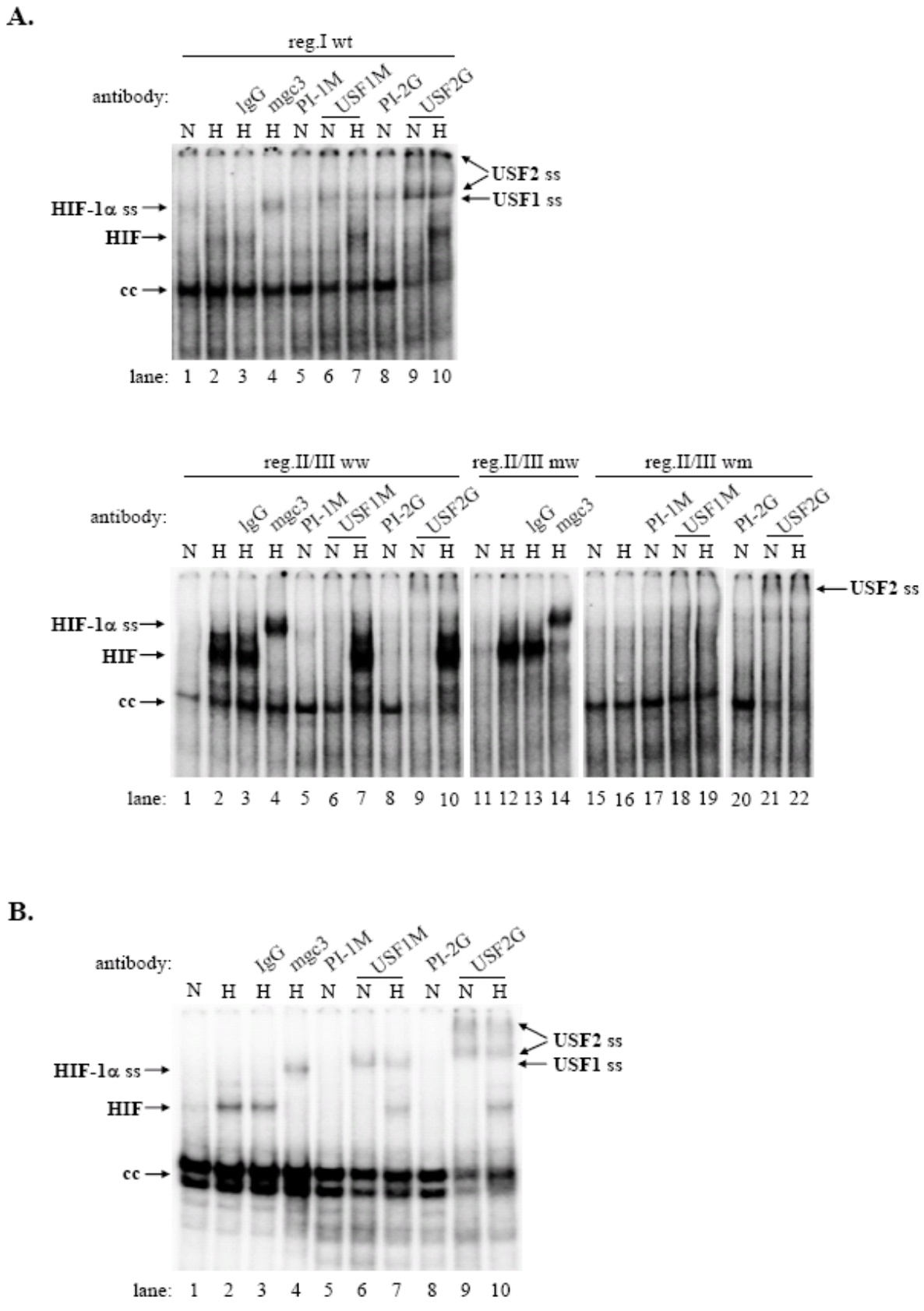
A.
reg.I wt
antibody:
IgG
mgc3
PI-1M
USF1M
PI-2G
USF2G
N H H H N N H N N H
USF2 ss
USF1 ss
HIF-1α ss
HIF
cc
lane: 1 2 3 4 5 6 7 8 9 10
reg.II/III ww
reg.II/III mw
reg.II/III wm
antibody:
IgG
mgc3
PI-1M
USF1M
PI-2G
USF2G
N H H H N N H N N H N H H H N H N N H N N H
USF2 ss
HIF-1α ss
HIF
cc
lane: 1 2 3 4 5 6 7 8 9 10 11 12 13 14 15 16 17 18 19 20 21 22
B.
antibody:
IgG
mgc3
PI-1M
USF1M
PI-2G
USF2G
N H H H N N H N N H
USF2 ss
USF1 ss
HIF-1α ss
HIF
cc
lane: 1 2 3 4 5 6 7 8 9 10

Figure 6

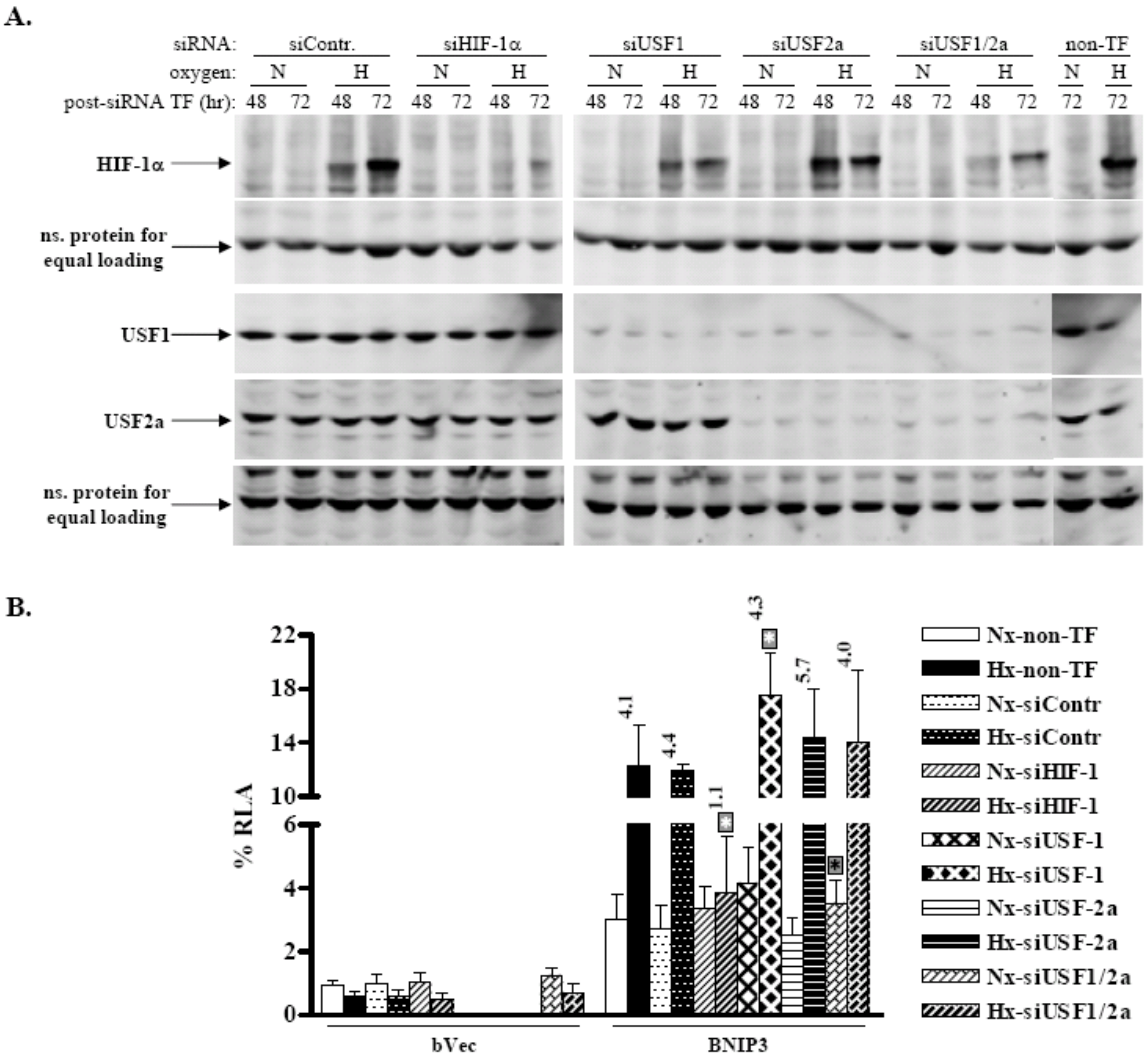
A.
siRNA:
siContr.
siHIF-1α
siUSF1
siUSF2a
siUSF1/2a
non-TF
oxygen:
N
H
post-siRNA TF (hr):
48
72
HIF-1α
ns. protein for equal loading
USF1
USF2a
ns. protein for equal loading
B.
% RLA
22
18
14
10
6
4
2
0
4.1
4.4
1.1
4.3
5.7
4.0
bVec
BNIP3
Nx-non-TF
Hx-non-TF
Nx-siContr
Hx-siContr
Nx-siHIF-1
Hx-siHIF-1
Nx-siUSF-1
Hx-siUSF-1
Nx-siUSF-2a
Hx-siUSF-2a
Nx-siUSF1/2a
Hx-siUSF1/2a

Figure 7

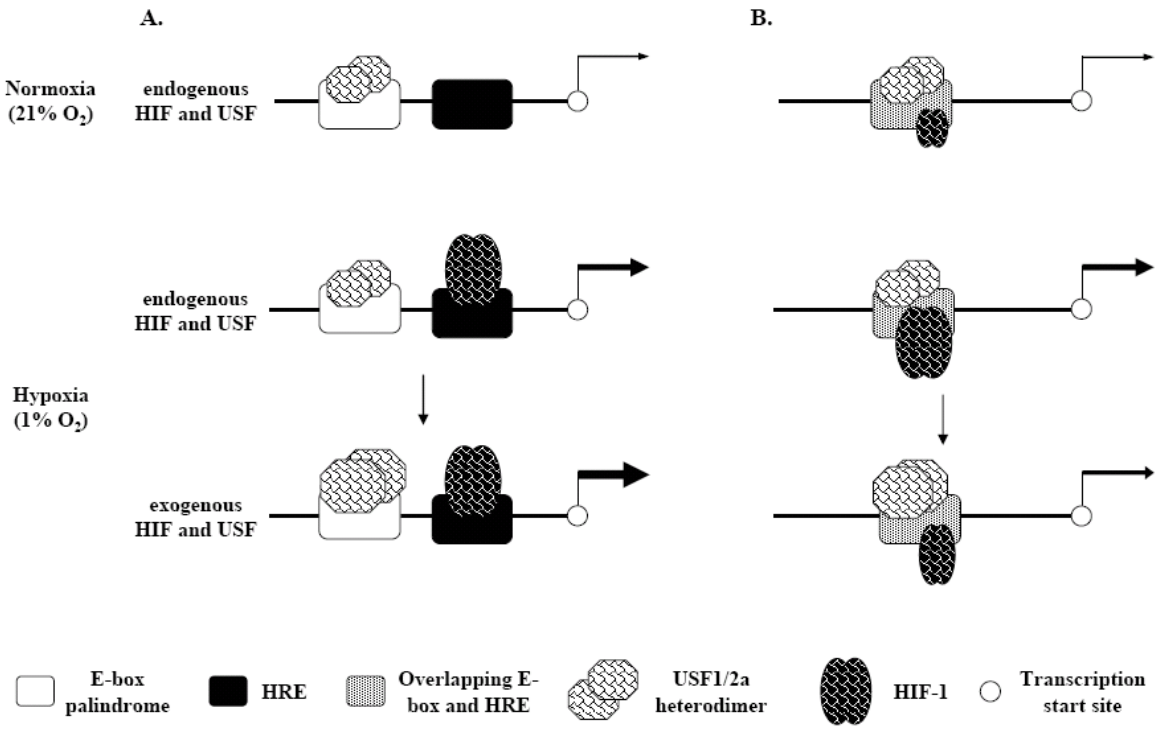
A.
B.
Normoxia (21% O2)
endogenous HIF and USF
endogenous HIF and USF
Hypoxia (1% O2)
exogenous HIF and USF
E-box palindrome
HRE
Overlapping E-box and HRE
USF1/2a heterodimer
HIF-1
Transcription start site

Supplement:

Supplement Fig. S1: USFs bind preferentially to the -146 palindrome and HIF-1 to the -107 HRE of *Daphnia's* hb2 promoter

Additional evidence for the interaction of USFs with the -146 phb2 CACGTG palindrome was obtained by adding increasing volumes of anti-USF1M (left) and anti-USF2G (right) antiserum into the binding reaction with nuclear extracts from normoxic (N) and hypoxic (H) Hep3B cells. The intensity of the constitutive CACGTG complex (cc) was observed to be reduced in a dose-dependent manner. In contrast, addition of the maximal volume of pre-immune serum (PI-1M and PI-2G) left the complex's intensity unaffected. As can be seen, binding of USF complexes to the -146 phb2 E-box is oxygen-independent (Fig. S1A). An earlier work had established the following isoform-specificity of each of the anti-USF antisera used: anti-USF1M serum recognizes USF1 (domain M), anti-USF2G recognizes USF2a or 2b (domain G) and anti-USF2aO recognizes USF2a (domain O) (7). Equipped with this knowledge, we were able in additional supershift experiments (not shown) to delineate the slightly different mobility of bands within the CACGTG-bound constitutive complex (Fig. S1A; cc) as summarized here: USF1/2 heterodimers (i.e. USF1/2a, USF1/2b, fast complex, "1/2"), 1/1 homodimers (medium complex, "1/1") or 2/2 homodimers (slow complex, "2/2") (Fig. S1A; see also (7))

Our initial report on the regulation of *Daphnia* globin gene 2 (hb2) had shown that the asymmetric TACGTG elements at positions -258 and -107 of the promoter were absolutely necessary for the hypoxic induction of the hb2 gene (2). To test whether these two sites indeed comprise avid HIF binding sequences (i.e. are HREs), we applied the pull-down assay with beads coated either with wildtype -107 HRE or -146 E-box oligonucleotides for a relative comparison of HIF's in vitro binding affinity. As can be seen in Fig. S1B, the amount of pulled HIF-1α protein left attached to the beads in the competed reactions (50× comp.) clearly demonstrates HIF's hypoxia-induced, high-affinity interaction with the -107 HRE and low-affinity interaction with the -146 palindromic E-box. In contrast, USFs display opposite in vitro binding behavior, with a tight interaction of USF2a and 2b to the -146 E-box and a weak, easily competed one to the -107 HRE (note 50x comp. lanes in Fig. S1C). The pull-down assay thus demonstrates the opposite binding preferences of USF1/2 (primarily to CACGTG motif) versus HIF-1 complexes (primarily to TACGTG HRE) within the phb2 DNA in confirmation of our previous observations (2).

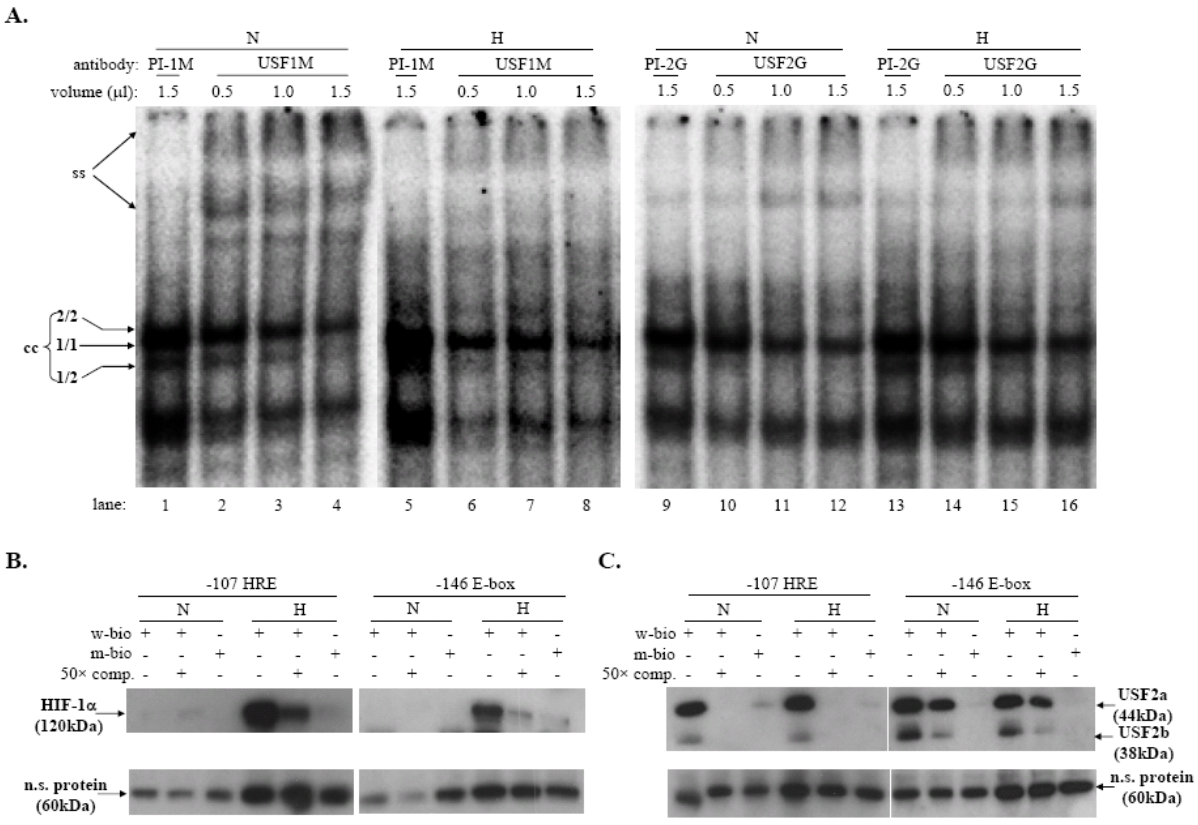

Suppl. Fig. S1: Dose-dependent USF supershift analysis (A) and pull-down assay (B, C) with -107 HRE and -146 E-box of phb2 promoter (A) Dose dependent gel supershift with normoxic and hypoxic nuclear extracts from Hep3B cells by applying increasing volume of anti-USF1M or USF2G IgGs into the binding reaction as indicated. Representative PIs were used as negative controls. cc: constitutive CACGTG complex; ss: supershifted CACGTG complex**.** (B and C) Pull-down analysis either with -107 HRE wild type oligonucleotides (-107 HRE: 5'-TACGTG-3') or with -146 E-box wild type biotinylated oligonucleotides (-146 E-box: 5'-CACGTG-3') using HeLa normoxic and hypoxic nuclear protein. (B) HIF-1α detection with anti-HIF-1α antibody (mgc3); (C) USF2a/2b detection with anti-USF2G antibody. Staining of non-specific (ns) proteins indicated as loading control. N: air; H: 1% O_2 16h.

Supplement Fig. S2: Co-immunoprecipitation between HIF-1 subunits and USF factors

To assess whether the observed (2) USF-HIF interference in phb2 results from a direct or indirect contact between these transcription complexes, we conducted bidirectional co-immunoprecipitation (Co-IP) experiments. Positive Co-IP controls clearly confirmed precipitation (IP lanes), hence physical contact, between HIF-1α with immobilized ARNT (Fig. S2A), or conversely, ARNT with immobilized HIF-1α upon the subunits accumulation in hypoxic (H) extracts (Fig. S2B). As expected, the minuscule amount of HIF-1α present in normoxic (N) extracts is reflected by a small quantity of pulled ARNT protein (Fig. S2B left). However, neither immobilization scheme for the HIF-1α or HIF-1β (ARNT) subunit resulted in any detectable precipitation of USF2a (Fig. S2A and B right). Lack of co-immunoprecipitation suggests the absence of any physical interaction between HIF-1α or ARNT with USFs. Rather, the USF-HIF interference seems to be DNA context dependent.

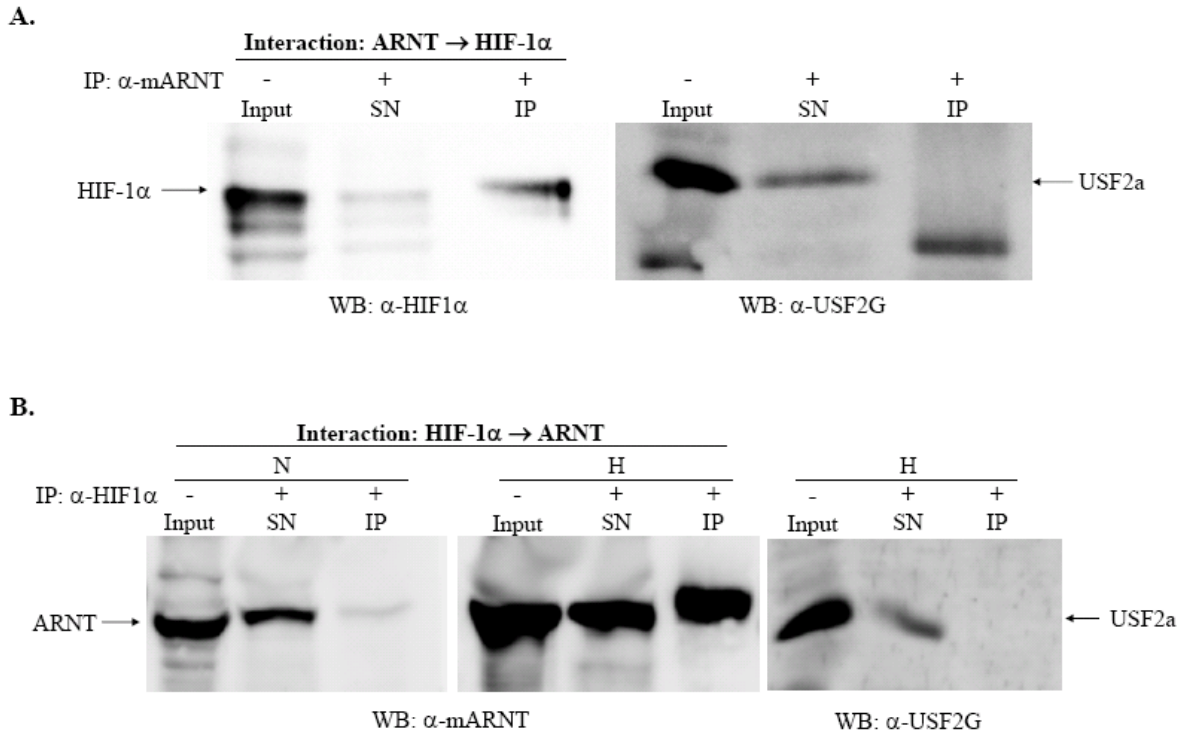

Suppl. Fig. S2 Co-immunoprecipitation with HeLa normoxic and hypoxic nuclear extracts (A) HIF-1α (left) or USF2a (right) Western blot of extracts immunoprecipitated (IP) by anti mouse ARNT IgG compared to non-precipitated supernatants (SN). (B) ARNT (left) or USF2a (right) Western blot of extracts imunoprecipitated (IP) by anti HIF-1α IgG compared to non-precipitated supernatants (SN). Input: only nuclear extract (25μg); SN: supernatant from IP; IP: immunoprecipitation fraction, N: air; H: 1% O_2 16h.

Supplement Fig. S3: Human genes selected for HIF or USF control and HIF+USF co-targeted reporter constructs

Sequence analysis (see text, Table 1) and promoter alignment revealed human-mouse-rat (hmr) conservation of HREs and/or E-box palindromes in the promoters of the following control (a+b) and bibox candidate genes (c-f) Alignment examples are presented here only for TYR, PHD2, LDHA and BNIP3 promoter regions (Fig. S3):

a) human tyrosinase (TYR): USF specific target gene with two hmr conserved CATGTG E-boxes (-183/-178 and -91/-86). E-box (-183/-178) validated as direct binding site for USF1 (1).

b) human prolyl hydroxylase domain 2 (PHD2): HIF-1 specific target gene with hm conserved HRE (-413/-408) as functional HIF-1 binding site (4).

c) human 4E-binding protein 1 (4EBP1): contains hmr conserved E-box palindrome (-179/-174) and non-conserved HRE candidate (-123/-115).

d) human lactate dehydrogenase A (LDHA): contains distinct, hmr conserved CACGTG palindrome (region II -2367/-2362) and CACGTC site (region III -2353/-2348; reads as reverse-complement: GACGTG) as well as another CACGTG E-box (region I -2465/-2460) with hm conservation. Region I and II: validated MYC binding sites (6). Region II and III: validated in vitro HIF-1 binding sites (5).

e) human melanocorticotropin 1 receptor (MC1R): contains two E-boxes, one of which with hm conservation (-461/-456) whose role in controlling MC1R expression in response to UVB (80mJ/cm^2) is known thanks to the work of Corre et al. (1) .

f) human BCL2/E1B 19 kDa interacting protein 3 (BNIP3): contains hmr conserved HRE (-251/-246), a validated functional HIF-1 site (3), which is identical to E-box palindrome.

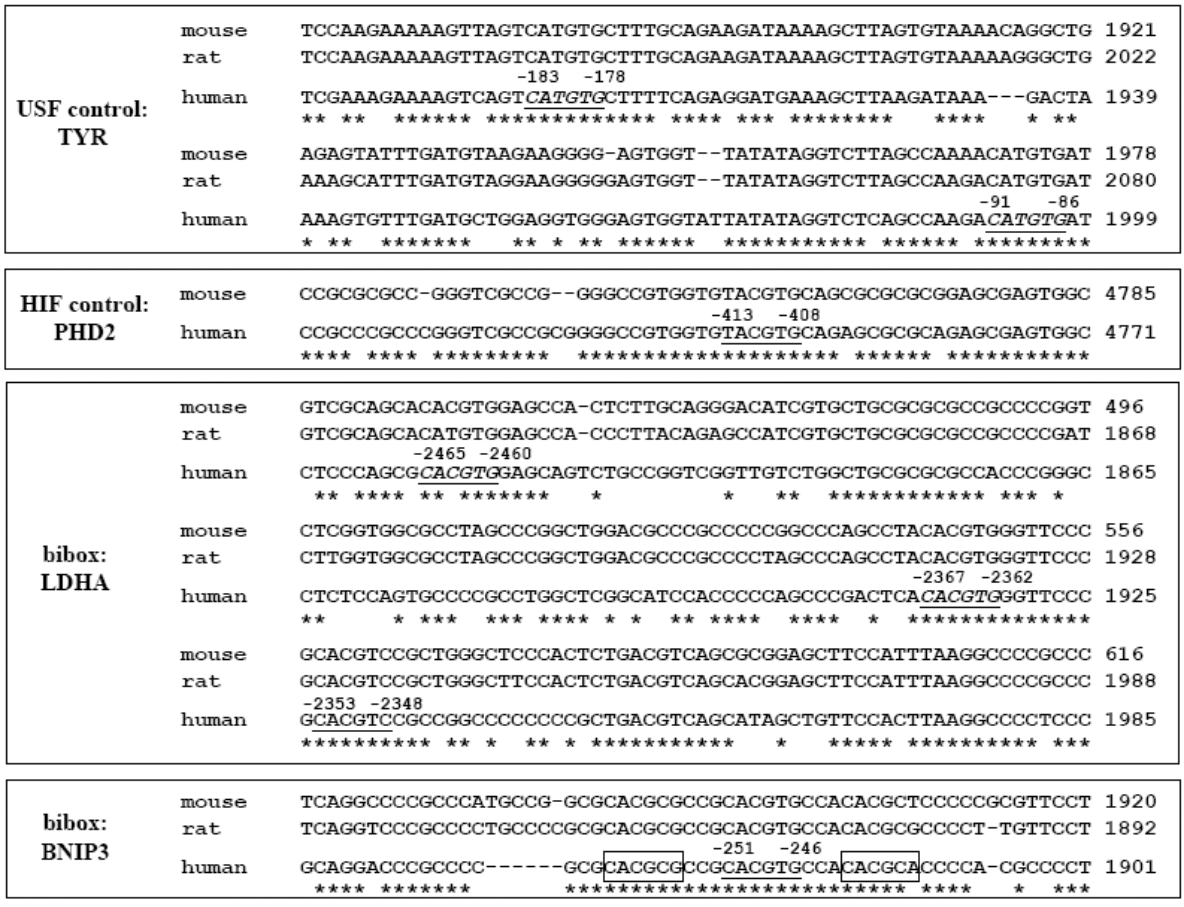

Suppl. Fig. S3 Mouse-rat-human alignments of relevant HRE, E-box palindrome or bibox containing promoter regions for genes TYR, PHD2, LDHA and BNIP3. TYR with two hmr conserved CATGTG E-boxes (italics + underlined). PHD2 with known functional HRE (underlined). LDHA with known functional HRE (underlined) and E-box palindromes (italics + underlined). BNIP3 with known functional HRE (underlined) and conserved CACGCN regions, three nucleotides apart on either side of the HRE (boxed).

Supplement Fig. S4: Stable HIF-1α and USF2a shRNA knockdown clones of MCF7 cells

We also evaluated DNA-level convergence of HIF-1 and USF1/2 pathways using stable shRNA-based HIF-1α and USF2a knockdown clones in MCF7 cells (see Materials & Methods for details). Western analyses of two independent clones demonstrated the strong suppression of HIF-1α (i.e. HIF-1α kd) and USF2a (i.e. USF2a kd) protein levels, respectively, and showed, as expected, that either knockdown did not impact the other pathway in question. The chosen control clone also underwent shRNA transfection and selection yet did not show signs of a down-regulated USF2a expression (Fig. S4A). As with the transient siRNA-based USF2a silencing in Hep3B cells (Fig. 6A), we noted again that USF-1 levels were visibly reduced in the USF-2a knockdown clone (Fig. S4A; see text for discussion).

All three MCF7 clones were transfected with TYR (USF target), PHD2 (HIF-1 target) and LDHA (bibox promoter) reporter constructs to elicit the relative normoxic (N) versus hypoxic (H) luciferase activity in response to intact *versus* dysfunctional HIF-1 or USF2a signalling pathways (a. control: white/black bars; b. HIF-1α kd: white/black dotted bars; c. USF2a kd: white/black hatched bars; Fig. S4B-D). Due to the extremely weak expression of the human TYR gene construct in MCF7 cells (comparable to expression of empty vector; bVec), we did not succeed in measuring a reliable expression impairment in USF2a kd clone relative to control cells (Fig. S4B). Only upon co-transfecting cells with USF1 and USF2a expression plasmids did we manage to detect a differential luciferase activity of the TYR construct with a ~4-fold higher activity in normoxic and hypoxic control and HIF-1α kd than USF2a kd cells, in line with a strict requirement of USFs to activate TYR transcription (Fig. S4B). In contrast, the hypoxic induction of the PHD2 reporter, amounting to a nearly 7-fold H/N differential expression in the control and kd USF2a kd clone, was completely lost in the HIF-1α kd clone. Over-expression of HIF-1α restored some of this induction (Fig. S4C).

The ~7-fold hypoxic induction by endogenous pathways of the LDHA reporter, was further enhanced in the USF2a kd clone (9.3-fold; due to significantly reduced normoxic reporter activation to ~60% of control cells), and completely obliterated in the HIF-1α kd clone (Fig. S4D). Over-expressed HIF-1α elevated both the normoxic and hypoxic activities of the reporter in control and HIF-1 kd MCF7. In contrast, in USF2a kd cells, over-expressed HIF-1α augmented primarily the normoxic reporter activity, hinting to HIF's take-over of the USF-deficient control of the LDHA promoter (Fig. S4D; see ↑ arrow). When adding exogenous USF1 and 2a, the LDHA reporter responded again with a marked increase of it's a) normoxic activity (control + USF2a kd cells) and b) normoxic and hypoxic activities (HIF-1α kd cells; Fig. S4D; see ↑ ↑ arrow). It thus appears that HIF-1 and USFs substitute one another in the LDHA promoter and compensate the loss-of-function of the other activity.

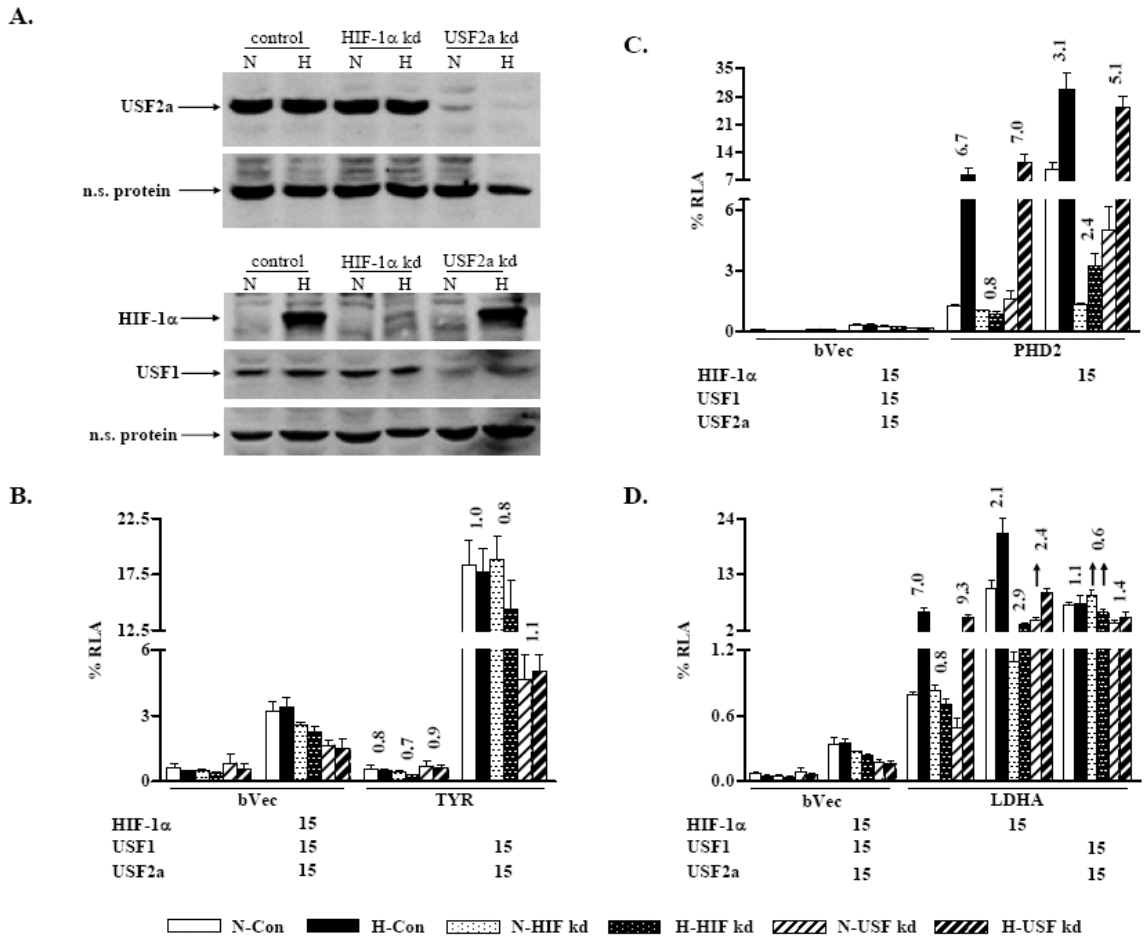

Suppl. Fig. S4 Regulation of LDHA promoter activity in stable HIF-1α and USF2a knockdown clones of MCF7 cells (A) Protein expression in normoxic (N) and hypoxic (H) MCF7 knockdown clones as indicated. Stable silencing of HIF-1α or USF2a expression was achieved using shRNA expressing plasmids (see "Materials and Methods" for details). (B) Luciferase assay of USF control TYR reporter (transfected with 1.5μg TYR reporter). (C) Luciferase assay of HIF-1 control PHD2 reporter (transfected with 0.5μg PHD2 reporter). (D) Luciferase assay of experimental LDHA bibox reporter (transfected with 0.5μg LDHA reporter). % RLA value represents mean ± SD of relative luciferase activity, normalized to activity of co-transfected β-galactosidase (3 independent experiments). N: air; H: 1% O_2 16h.

Supplement Table ST 1: PCR primers for generation of luciferase constructs (HindIII site: underlined)

Primer name	Sequence
4EBP1_F1	5′-GTTGGTTCACTCCTCCTC-3′
4EBP1_R1	5′-CCAACAGATAATACCCATCC-3′
4EBP1_F2	5′-AGCATAACTACTCAATCCCC-3′
4EBP1_R2	5′-CGTGTTTGTTAGGTGTCAG-3′
MC1R_F1	5′-CTGAAAACACCAACCTCTCC-3′
MC1R_R1	5′-CCACACAATATCACCACCTC-3′
MC1R_F2	5′-CTTTCACGCTCTGCCC-3′
MC1R_R2	5′-CACAGCCATAGTCCTGTCC-3′
LDHA_F1	5′-GAGTGGGAGCTGGTAGG-3′
LDHA_R1	5′-GCTATCCAAGGCACAGG-3′
LDHA_F2	5′-CAGGGATGAAGAAGAAACAG-3′
LDHA_R2	5′-TGAGATTTGAGTGGGAGAAC-3′
Tyros_F1	5′-TTGTAGCCTCTTTATGGTCTC-3′
Tyros_R1	5′-TTATTTCCCAAACATTCCTG-3′
Tyros_F2	5′-CTCTATTCCTGACACTACCTCTC-3′
Tyros_R2	5′-CCAATTAGTCTGGGATAAGG-3′
pCRII--F1	5′-CACACAGGAAACAGCTATGAC-3′
LDHA/pCRII-R1	5′-GATAAGCTTTAGAGGATGGGGTCAAGG-3′

Supplement Table ST 2: Oligonucleotide sequences used for EMSA and pull-down experiments. Binding motifs, HREs or E-box palindromes, are underlined and given in bold:

Sequence name	sequence
Daphnia phb2 w-146HRE/+	5′-GAACCATA**CACGTG**CCTCGAGCAG-3′
Daphnia phb2 w-146HRE/-	5′-CTGCTCGAGGCACGTGTATGGTTC-3′
Daphnia phb2 m-146HRE/+	5′-GAACCATA**CAATGT**CCTCGAGCAG-3
Daphnia phb2 m-146HRE/-	5′-CTGCTCGAGGACATTGTATGGTTC-3′
Daphnia phb2 w-107HRE/+	5′-ACACGGCC**TACGTG**ATGATAGCGC-3′
Daphnia phb2 w-107HRE/-	5′-GCGCTATCATCACGTAGGCCGTGT-3′
Daphnia phb2 m-107HRE/+	5′-ACACGGCC**TAATGT**ATGATAGCGC-3′
Daphnia phb2 m-107HRE/-	5′-GCGCTATCATACATTAGGCCGTGT-3′
hBNIP3 HRE wt /+	5′-ACGCGCCG**CACGTG**CCACACGCAC-3′
hBNIP3 HRE wt /-	5′-GTGCGTGTGGCACGTGCGGCGCGT-3′
hBNIP3 HRE mut /+	5′-ACGCGCCG**CAATGT**CCACACGCAC-3′
hBNIP3 HRE mut /-	5′-GTGCGTGTGGACATTGCGGCGCGT-3′
hLDHA reg.I wt/+	5′-TCCCAGCG**CACGTG**GAGCAGTCTG-3′
hLDHA reg.I wt/-	5′-CAGACTGCTCCACGTGCGCTGGGA-3′
hLDHA reg.I mut/+	5′-TCCCAGCG**CAATGT**GAGCAGTCTG-3′
hLDHA reg.I mut/-	5′-CAGACTGCTCACATTGCGCTGGGA-3′
hLDHA reg.II/III ww/+	5′-CGACTCA**CACGTG**GGTTCCCG**CACGTC**CGCCGGC-3′
hLDHA reg.II/III ww/-	5′-GCCGGCGGACGTGCGGGAACCCACGTGTGAGTCG-3′
hLDHA reg.II/III mw/+	5′-CGACTCA**CAATGT**GGTTCCCG**CACGTC**CGCCGGC-3′
hLDHA reg.II/III mw/-	5′-GCCGGCGGACGTGCGGGAACCACATTGTGAGTCG-3′
hLDHA reg.II/III wm/+	5′-CGACTCA**CACGTG**GGTTCCCG**ACATTC**CGCCGGC-3′
hLDHA reg.II/III wm/-	5′-GCCGGCGGAATGTCGGGAACCCACGTGTGAGTCG-3′
hLDHA reg.II/III mm/+	5′-CGACTCA**CAATGT**GGTTCCCG**ACATTC**CGCCGGC-3′
hLDHA reg.II/III mm/-	5′-GCCGGCGGAATGTCGGGAACCACATTGTGAGTCG-3′

Supplement Table ST 3: Double-stranded siRNA oligonucleotide sequences used for transient knockdown HIF-1α, USF1 and USF2a in Hep3B cells

Gene	Genbank accession No.	Targeted region	sense	antisense
HIF-1	AF304431.1	1380-1400	5′-CUGAUGACCAGCAACUUGAdTdT-3′	5′-UCAAGUUGCUGGUCAUCAGdTdT-3′
USF1	NM_007122	79-97	5′-GACCCAACCAGUGUGGCUAdTdT-3′	5′-UAGCCACACUGGUUGGGUCdTdT-3′
USF2a	NM_003367	786-806	5′-UCCAGACUGUAACGCAGACAAdTdT-3′	5′-UUGUCUGCGUUAACAGUCUGGAdTdT-3′

Supplement Table ST 4: PCR primers for LDHA and BNIP3 ChIP assay

Sequence name	Sequence
LDHA forward	5′-ACTCAGGCTCATGGCTC-3′
LDHA reverse	5′-GGCTGGGGGTGGATG-3′
BNIP3 HRE forward	5′-TAGCCAGTGCCCAGAGAGTCC-3′
BNIP3 HRE reverse	5′-ATTGGCCGCGACTTGGG-3′

References

1. **Corre, S., A. Primot, E. Sviderskaya, D. C. Bennett, S. Vaulont, C. R. Goding, and M. D. Galibert.** 2004. UV-induced expression of key component of the tanning process, the POMC and MC1R genes, is dependent on the p-38-activated upstream stimulating factor-1 (USF-1). J Biol Chem **279:**51226-33.
2. **Gorr, T. A., J. D. Cahn, H. Yamagata, and H. F. Bunn.** 2004. Hypoxia-induced synthesis of hemoglobin in the crustacean Daphnia magna is hypoxia-inducible factor-dependent. J Biol Chem **279:**36038-47.
3. **Kothari, S., J. Cizeau, E. McMillan-Ward, S. J. Israels, M. Bailes, K. Ens, L. A. Kirshenbaum, and S. B. Gibson.** 2003. BNIP3 plays a role in hypoxic cell death in human epithelial cells that is inhibited by growth factors EGF and IGF. Oncogene **22:**4734-44.
4. **Metzen, E., D. P. Stiehl, K. Doege, J. H. Marxsen, T. Hellwig-Burgel, and W. Jelkmann.** 2005. Regulation of the prolyl hydroxylase domain protein 2 (phd2/egln-1) gene: identification of a functional hypoxia-responsive element. Biochem J **387:**711-7.
5. **Semenza, G. L., B. H. Jiang, S. W. Leung, R. Passantino, J. P. Concordet, P. Maire, and A. Giallongo.** 1996. Hypoxia response elements in the aldolase A, enolase 1, and lactate dehydrogenase A gene promoters contain essential binding sites for hypoxia-inducible factor 1. J Biol Chem **271:**32529-37.
6. **Shim, H., C. Dolde, B. C. Lewis, C. S. Wu, G. Dang, R. A. Jungmann, R. Dalla-Favera, and C. V. Dang.** 1997. c-Myc transactivation of LDH-A: implications for tumor metabolism and growth. Proc Natl Acad Sci U S A **94:**6658-63.
7. **Viollet, B., A. M. Lefrancois-Martinez, A. Henrion, A. Kahn, M. Raymondjean, and A. Martinez.** 1996. Immunochemical characterization and transacting properties of upstream stimulatory factor isoforms. J Biol Chem **271:**1405-15.

Manuscript 2: Endogenous myoglobin in human breast cancer: Novel insights into regulation, function and clinical relevance

Glen Kristiansen[1], Junmin Hu[2], Daniel P. Stiehl[3], Michael Rose[4], Cordelia Geisler[4], Josefine Gerhardt[1], Florian R. Fritzsche[1], Claudia Lüke[5], Axel-M. Ladhoff[5], Ruth Knüchel[4], Manfred Dietel[5], Holger Moch[1], Zsuzsanna Varga[1], Jean-P. Theurillat[1], James Raleigh[6], Mahesh A. Varia[6], Patrick Subarsky[7], Francesca M. Scandurra[7], Erich Gnaiger[7], Thomas Hankeln[8], Eva Gleixner[8], Max Gassmann[2], Thomas A. Gorr[2]*, Edgar Dahl*[4]

[1] Institute of Surgical Pathology, University Hospital Zurich, Zurich, Switzerland

[2] Institute of Veterinary Physiology, University of Zurich, Zurich, Switzerland

[3] Institute of Physiology, University of Zurich, Zurich, Switzerland

[4] Institute of Pathology, University Hospital of the RWTH, Aachen, Germany

[5] Institute of Pathology, Charité - Universitätsmedizin Berlin, Berlin, Germany

[6] UNC School of Medicine, Chapel Hill, NC, USA

[7] Dept. General and Transplant Surgery, Medical University of Innsbruck, Innsbruck, Austria

[8] Institute of Molecular Genetics, Johannes Gutenberg University Mainz, Mainz, Germany

* Co-senior authors

Short title: Myoglobin Expression in Human Breast Cancer

Word count (including M&M, references and legends): 9970

Character count (including spaces): 66569

Abstract word count: 177

Corresponding author:

Prof. Dr. Glen Kristiansen, M.D.

Institute of Surgical Pathology

UniversitätsSpital Zürich

Schmelzbergstr. 12, 8091 Zürich, Switzerland

Email: glen.kristiansen@usz.ch

Tel +41 44 2553457; Fax +41 44 2554416

Abstract

Immunohistochemical analysis of myoglobin (Mb) in human breast cancer specimens (n=917) revealed endogenous expression in 71% of invasive breast carcinomas preferentially of luminal-type and correlated with hormone receptor status and favourable patient prognosis. A positive correlation with hypoxia-inducible factor 2α (HIF-2α) and carbonic anhydrase IX suggested oxygen to regulate Mb in breast carcinomas. Indeed, Mb mRNA and protein levels were robustly induced by prolonged hypoxia in breast cancer cell lines, in part via HIF-1/-2 dependent transactivation. Interestingly, hypoxically induced Mb mRNA originated from a novel, alternative transcription start site 6 kb upstream of the genuine ATG codon. Functionally, Mb knockdown in MDA-MB468 breast cancer cells resulted in an increased oxygen uptake during mild hypoxia, yet did not impair O_2 diffusion in these cells even under respiration-limiting conditions. Alternative functions of Mb distinct from oxygen sensing and transport, e.g. fatty acid binding, have to be considered to interpret Mb's positive effect on the proliferation and migration of cultured oxygenated breast cancer cells. These unprecedented findings may have fundamental implications for our understanding of non-muscle Mb in solid tumors.

1. Introduction

Human myoglobin (Mb) is considered one of the best characterized proteins with more than 11,200 PubMed-listed publications since Kendrew *et al.* have presented the first three dimensional model of this molecule in 1958 (1). It is commonly described as a cytoplasmic hemoprotein that is solely occurring at milli-to micromolar concentrations in cardiac myocytes and type I and IIa skeletal muscle fibers of mammals. In myocytes, Mb is widely accepted to function as temporary "store" for oxygen, able to buffer short phases of exercise-induced increases in O_2 flux during which it supplies the gas to mitochondria (2). Another, more controversially discussed role is Mbs´ facilitation of oxygen diffusion within muscle cells (3, 4). Although Mb knockout mice exhibited normal exercise capacity and no signs of compromised cardiac energetics due to multiple systemic compensations (5, 6), follow-up studies stressed the importance of functional Mb in maintaining nitric oxide (NO) homeostasis in muscle through either scavenging (7) or producing the NO molecule (8). That way, Mb might participate in tuning vasodilatory responsiveness and protecting the respiratory chain from NO inhibition (9). Further possible functions of Mb in muscle include synthesis of peroxides (10), scavenging of reactive O_2 species (11) and binding of fatty acids (12).

In humans, Mb is synthesized at concentrations of ~200-300 □M in striated muscle and, albeit at much lower levels, in a variety of human tumors including medullomyoblastoma (13), thymolipoma (14), acute leukaemia (15) and desmoplastic small round cell tumors (16). Following an accidental observation of positive Mb staining in several human carcinomas in 2001, we have since then systematically examined Mb expression, regulation, function and prognostic impact in human breast cancer. Now, we are presenting the first comprehensive analysis of Mb expression in a large and representative cohort of human breast cancer (n=917), including a portrayal of the associations between clinico-pathological parameters and the range of Mb synthesis seen in mammary carcinomas. We also observed that, in cultured breast cancer cells, the *de novo* expression of the Mb gene is induced by hypoxia, which, in part, required transactivation by functional hypoxia-inducible factor (HIF) 1 and 2. The functional association of Mb and HIF was further confirmed by tissue expression data. To elicit possible roles of endogenous Mb, we applied both stable and transient RNA interference knockdown approaches to breast cancer cells and recorded altered functional properties of the cells with regard to respiratory, proliferative and migratory activities. We finally shed some light on unusual functions of Mb in the oxygenated cancer by looking at the impact of steroids on the steady state level of the protein and on Mb´s involvement in fatty acid metabolism.

2. Results

Human breast cancer tissue exerts a complex pattern of Mb expression

Following the initial observation of Mb immunoreactivity in conventional immuno-histochemistry analyses, Mb transcript levels were determined in breast biopsies and breast cell lines. Whereas low levels of Mb mRNA were detectable in four of ten cases of healthy breast tissue (Fig. 1A), Mb expression was upregulated in nine of ten matched normal / tumor tissue samples with a median tumor-to-normal up-regulation of 352 fold. With regard to breast cell lines, Mb mRNA was not detectable in benign MCF12A epithelial cells as well as in MDA-MB436, Hs578T, Cal51 tumor cells (Fig. 1B). Ten breast cancer cell lines (MDA-MB231 to MCF7, see Fig. 1B) expressed detectable but low amounts of Mb mRNA while three breast cancer cell lines contained abundant quantities of the Mb transcript, i.e. EFM19, MDA-MB415 and MDA-MB468 cells.

Using a validated monoclonal Mb antibody (Supplement Fig. S1), we next analysed Mb expression on tissue microarrays containing normal tissue (n=56), intratumoral ductal carcinoma in situ (DCIS; n=155) and invasive breast cancer (n=917, clinico-pathological parameters are given in Table 1). In normal breast tissue, staining was observed in secretory luminal epithelial cells, but not in myoepithelial cells (Fig. 2A). Altogether, in normal breast seven percent of cases were negative for Mb, 50% were weakly positive, 39% stained moderately positive and four percent of tissues stained strongly. DCIS showed more abundant Mb staining (Fig. 2B/C) which was pronounced in vital tumor cells near the central comedo necrosis (Fig. 2C). 12% of DCIS cases were negative, 38% weakly positive, 39% moderately positive and 10% were strongly positive. In invasive carcinoma, the number of Mb negative cases was markedly higher than in normal tissue: 29% were negative (Fig. 2D), 31% were weakly positive, 30% were moderately positive (Fig. 2E) and 10% were strongly positive (Fig. 2F). A spotted, mosaic like expression pattern was frequently seen in DCIS and invasive carcinoma (Fig. 2E). Thus, with increasing transformation and aggressiveness (normal tissue → DCIS → invasive carcinoma) the proportion of Mb negative and strongly positive tissues both gain in frequency.

Since myoglobin has been described as a marker of rhabdomyoid differentiation, we analyzed two breast tumors with strong Mb immunoreactivity by transmission electron microscopy (Fig. S2). However, no striated muscle elements could be observed in these cases, suggesting that increased expression of Mb occurs independently of rhabdomyoid tumor differentiation.

Tumor-derived myoglobin expression is linked to estrogen receptor status and favourable prognosis and may present a marker for luminal type breast cancer

In invasive breast carcinomas Mb expression was associated with better histological tumor differentiation according to BRE-grading (correlation coefficient (cc) =-0.116, p=0.001). Mb did not correlate with pT stage, nodal status or tumor type. Mb expression was positively correlated with estrogen (ERα) and progesterone receptor (PgR) positivity (cc=0.206, p=0.001 and cc=0.180, p=0.001) and negatively with the myoepithelial/basal phenotype marker CK5/6 (cc=-0.120, p=0.001). No

correlation with HER2 expression was found. Notably, positive correlations were found to the hypoxia-inducible factor 2α (HIF-2α) (cc=0.257, p=0.001), carbonic anhydrase IX (CaIX; cc=0.361, p=0.001), cytoglobin (Cygb; cc=0.361, p=0.001) and E-cadherin (E-Cad; cc=0.207, p=0.001). No significant correlation was found with HIF-1α, Glucose transporter 1 (GLUT1), Ki-67 and microvessel density. Figure S3 displays a typical example of an Mb positive invasive breast cancer case in conjunction with markers of hypoxia. In a repeated correlation analysis stratified for ERα status, the significant correlations between Mb and PgR, Cygb, CK19, HIF-2α and CaIX could be confirmed for ERα-positive tumors, but failed significance in ERα-negative cases. Analogous to invasive carcinomas, Mb positivity in DCIS was equally correlated with HIF-2α (cc=0.245, p=0.02) and CaIX (cc=0.240, p=0.026), but not with HIF-1α or GLUT1. The positive correlation of Mb with markers of tissue hypoxia (CaIX and -2α) implied a possible control of Mb expression by oxygen.

Towards the prognostic value of Mb and tissue hypoxia markers, univariate Cox analysis revealed histological tumor grade, pT stage, nodal status and hormone receptor (ER/PR) status as significant predictors of overall survival in our patient cohort (Tab. 3). High Mb expression was also significantly associated with longer overall patient survival (five-year survival rate of Mb-pos. cases 83% *vs.* 75% in Mb-negative cases, Fig. 3) but lost significance in bivariate Cox and multivariate analysis. This might point to the positive correlation of Mb with ERα as the underlying determinant for a beneficial prognosis. We additionally classified Mb levels in correlation with a publically available expression dataset (17) (GEO Profiles, http://www.ncbi.nlm.nih.gov/sites/entrez, GDS1329). Here, Mb levels are significantly higher (p=0.005, Kruskal-Wallis test) in the group of luminal tumors compared to basal or apocrine types. These findings along with the positive correlation of Mb with ERα, a better tumor differentiation and improved prognosis and with the negative correlation with the basal phenotype marker CK5/6 all point to Mb as a marker of luminal tumor differentiation.

Myoglobin mRNA and protein is induced in breast cancer cells by HIF1/2 mediated hypoxic stimuli and may be induced by hypoxia in vivo

To study the responsiveness of the Mb gene, the effect of hypoxia (1% O_2; 4, 8, 24, 48, 72h) was analyzed by quantitative real-time PCR (qPCR) in four different cell lines: the benign breast cell line MCF12A, the ERα-negative breast cancer cell lines MDA-MB-231 (low basal Mb expression, see Fig. 1B) and MDA-MB-468 (high basal Mb expression), and the ERα positive cell line MCF7 (medium basal Mb expression). Whereas transcription of the Mb gene was unaltered by hypoxia in the benign MCF12A cells (data not shown), normalized steady state levels of Mb mRNA increased 3-4 fold in hypoxic MDA-MB-468, MDA-MB-231 and MCF7 cells (for MCF7 cells, Fig. 4A). In all cases, a robust activation of the Mb gene required at least 24h or 48h of hypoxia to take effect. Proper hypoxic responsiveness of MCF7 cells was confirmed through assessment of transcription of the highly hypoxia-inducible CaIX transcript (Fig. 4A).

Using a commercial chemiluminescence based Mb-assay we determined the amount of Mb protein present in 10^6 MDA-MB-468 cells to correspond to ~65 ng or 4 pmol. Mb protein level response to hypoxia was analysed for MDA-MB-468 and MCF7 cells subjected to 72h normoxia or 4, 8, 24, 48 and 72h hypoxia (1% O_2). Representative Western blots for MDA-MB-486 (left) or MCF7 (right) are shown at the top of Fig. 4B. The densitometric summary from three independent experiments is depicted as normalized mean intensity (±SD) of the Mb band, relative to its normoxic intensity (=1), in the respective graphs underneath. In agreement with RNA expression levels, both cell lines induced Mb protein between 3.4 and 5.1-fold following a hypoxia exposure of 48h or longer. In addition, the HIF response was transient in hypoxic MCF7 cells. Here, induction of the predominant species, HIF-1α, peaked at 4h hypoxia, followed by a steady decline of the protein content thereafter. In contrast, hypoxic MDA-MB-468 cells expressed preferably HIF-2α whose induction persisted for up to 72h of 1% O_2 (Fig. 4B).

To study the role of HIF in the hypoxic induction of Mb, we utilized siRNA oligonucleotides specifically directed against nucleotides 1380-1400 of HIF-1α mRNA (Entrez accession number: AF304431.1) and nucleotides 1260-1280 of HIF-2α mRNA (Entrez accession number: NM_001430.3), respectively. Since induction of Mb protein levels was robustly detected from 48h hypoxia onwards (Fig. 4B), the siRNA assay focused on control and HIF-1α (= siHIF-1α), -2α (= siHIF-2α) and combined knockdown effects (= siHIF-1α/2α) after 52h to 96h of exposure to 1% O_2 (Fig. 4C). Induction of myoglobin steadily increased during the siControl transfections until a maximum of ~7-fold was reached at 72h hypoxia (Fig. 4C, bottom graph; siControl time course). This 72h-peak induction was reduced to ~4-fold upon HIF-1α or -2α single siRNA treatment. Moreover, the combination of both siRNAs, with ~20% residual content of either HIF factor remaining, significantly attenuated the Mb induction to ~1.7 fold at 72h hypoxia. Our data imply both HIF-1 and HIF-2 in participating in the peak stimulation of Mb to low oxygen.

To clarify if Mb expression also correlates with hypoxic tissue areas *in vivo*, we reanalysed the 155 *ductal carcinoma in situ* (DCIS) cases. DCIS represents an interesting *in vivo* model for hypoxia research since this tumor has no intraductal vasculature. Thus, oxygen can only be supplied by diffusion from the outer basal membrane. This leads to the formation of a radial O_2 diffusion gradient (normoxic rim; hypoxic to anoxic centre) along with a central necrotic area (Fig. 5). Expression of the hypoxia-driven GLUT1 protein closely followed this gradient in our cohort of DCIS and showed a typical zonal distribution in 65% of cases (Fig. 5A). However, with regard to Mb only in 27% of Mb-positive DCIS cases a hypoxia-like gradient with stronger staining in the peri-necrotic region was found (Fig. 5A). The majority of cases (73%) showed a diffuse Mb immunoreactivity (Fig. 5B). This indicates that hypoxia may up-regulate Mb *in vivo*, although in the majority of cases low oxygen alone is insufficient for Mb induction. A similar conclusion was reached when we assessed the possible co-localization between Mb and hypoxic tumor areas as indicated by the hypoxia marker pimonidazole (Fig. S4).

Hypoxic Mb transcript in MDA-MB-468 cells are derived from an alternative Mb gene promoter

Inspection of the human Mb gene locus in comparison to expressed sequence tag (EST) libraries and our own RT-PCR expression data (not shown) indicated the presence of alternatively spliced Mb transcripts in addition to the published mRNA (18). These transcript variants contain different non-coding 5'- untranslated regions (5´-UTR), hence are transcribed from different Mb promoters (Fig. 6A). Comparison of EST numbers revealed that mRNA NM_005368 is the dominant 'standard' transcript (Mb-s) in skeletal and heart muscle tissue. Transcript NM_203377, starting with an upstream exon (designated "-1" by us), was annotated to be derived from seven EST reads, which originated from adenocarcinoma, gastric cancer and adrenal cortex carcinoma cell lines (designated Mb-a for "alternative"). Mb-a mRNA thus represented a candidate for analyzing its expression in breast cancer cells. Calculation of mRNA expression levels of Mb-s compared to Mb-a in the normoxic MDA-MB468 breast cancer cell line revealed a clear preference in expressing the alternative transcript Mb-a, which was roughly 300 fold more abundantly expressed than Mb-s (Fig. 6B). Furthermore, when determining the steady-state levels of Mb-s and Mb-a in MDA-MB-468 cells subjected to either 1 % O_2 for 72 h or normoxia, we found an unaltered Mb-s expression, while the tentatively tumor-associated transcript variant Mb-a exhibited a statistically significant 2.2 fold expression increase in hypoxic compared to normoxic cells. This observation prompted us to inspect the genomic regions of human and mouse Mb/*Mb* genes for the presence of HIF binding hypoxia response elements (HREs). HREs are usually characterized by a conserved consensus binding motif 5´-RCGTG-3´ (19). Using the rVISTA tool we indeed detected one interspecifically conserved putative HRE at approximately 2.7 kb upstream of exon 1 (Fig. 6A), which consists of two inverted HIF-1 binding sites at an interval of 6 bp contained within a conserved stretch of 53 bp. Further sequence comparisons showed that this candidate HRE from the Mb gene has 93% sequence similarity to an upstream promotor region from the human heat shock protein HSPB1 gene (Fig. 6C).

High-resolution respirometry on Mb control and knockdown MDA-MB-468 cells

To test if Mb facilitates the diffusion of oxygen between the cell membrane and mitochondrial compartment of breast cancer cells, we generated short-hairpin RNA (shRNA)-derived stable Mb knockdown clones of MDA-MB-468 cells using four different shRNA constructs (#83-86) to target distinct Mb mRNA nucleotides. Applying Fick's law of diffusion, we aimed to see if the shRNA-mediated loss-of-function (LoF) of Mb protein would yield a steeper oxygen diffusion gradient reflected by a higher $p_{50}(O_2)$ of cell respiration at identical oxygen flow (=per-cell consumption rate, in units of pmol $O_2 \cdot s^{-1} \cdot 10^{-6}$ cells).

O_2 consumption kinetics were investigated by high-resolution respirometry using two control (con) clones (boxed: 84#5 and 85#14) and two knockdown (kd) clones (boxed: 83#4, 84#31) (Fig. 7A). Mb protein from MDA-MB468 cells versus Mb from positive control skeletal muscle biopsies (Fig.

7A, pos.) migrated in SDS PAGE gels with equal mobility. Oxygraph-2k respirometers recorded the O_2 flow per second and million cells (Fig. 7B, red trace) as a function of oxygen concentration (Fig. 7B, blue trace) for the aforementioned clones of MDA-MB-468 cells during four different cellular activity states: i) routine respiration without glucose [= *R*(-G)]; ii) routine respiration with glucose (25 mM) added [= *R*(G)]; iii) maximal respiration through uncoupling of oxidative phosphorylation by FCCP [= *ETS*, capacity of the electron transport system]; iv) residual O_2 consumption, *ROX*, subsequent to poisoning of mitochondria with myxothiazol (see Fig. 7B, annotation). Culture medium was prepared for respirometry by adding 280 IU/ml of catalase to generate, following the injection of 40 □M H_2O_2 during the measurement, a controlled amount of O_2. Thus, extra transitions between oxy-regulated and oxy-conform respiration were added for improved accuracy in the determination of p_{50} data (below). Moreover, addition of glucose reduced rates of routine respiration as a reflection of the Crabtree effect (Fig. 7B), thus allowing to measure oxygen consumption at higher [*R*(-G)] versus lower [*R*(G)] fluxes.

Figures 7C and D display O_2 consumption rates and cellular $p_{50}(O_2)$, respectively, for each individual clone to portray the variability inherent in these data. When comparing routine respiratory activities with and without glucose, we found that glucose addition on average reduced oxygen consumption rates by 9-27%. Surprisingly, all mitochondrial (*R*(-G), *R*(G), *ETS*) and residual (*ROX*) O_2 fluxes were significantly increased in Mb kd cells compared to con cells (con vs. kd pooled data) (Fig. 7C). In contrast, mean ± SD cellular $p50(O_2)$ values under *R*(-G) and *R*(G) conditions were statistically indistinguishable (ns: non-significant) in con versus kd comparisons for either glucose-deficient or -proficient respiration (Fig. 7D). Also, differences in p_{50} values from high versus low oxygen fluxes were non-significant (Fig. 7D). This surprising result was confirmed when plotting the flux control ratio R_{max}/ETS as an exquisitely sensitive marker for cytochrome c oxidase (Cox) turnover under routine states of activity, *R*, and kinetic oxygen saturation of respiration. Again, no direct relationship between p_{50} and oxygen flow at *R*(-G) versus *R*(G) was found (not shown).

Mb knockdown cells exhibit reduced proliferative and migratory capacities

The impact of the Mb LoF on cellular proliferation during a 0-48-96h time course of wildtype (wt), Mb-control (con) and Mb-knockdown (kd) MDA cells was examined under normoxic (Fig. 8A) and hypoxic (1% O_2, Fig. 8B) atmospheres by employing MTT (continuous lines) and Trypan Blue (dotted lines) assays. Whereas the MTT (short for: Dimethylthiazolyldiphenyltetrazolium Bromide) assay infers growth rates from the activity of mitochondrial dehydrogenases that catalyze a tetrazolium → formazan reduction as colorimetric readout, exclusion of Trypan Blue (TB) by intact cellular membranes allows directly, and independently of mitochondrial confounders, to count the numbers of viable cells. The data in Fig. 8A/B are presented in reference to the 0h time point. 96h proliferation ratios (wt/kd, con/kd) are given relative to the growth of kd cells set to 1 (inverted numbers). As illustrated by those ratios, Mb LoF in kd cells slows proliferation and activity of mitochondrial

enzymes more profoundly under hypoxic than normoxic conditions. Mb, it seems, aids in maintaining both proliferative and oxidative capacities of breast cancer cells during prolonged hypoxia.

However, Mb LoF was also linked with a diminished migratory potential in completely aerobic MDA-MB-468 cells. Scratch wound assays determine the dynamics of cell migration precisely by analyzing the time frame of wound closure (Fig. 8C). Already 24 h after wounding, a remarkable retardation of *in vitro* motility was observed in one clone of Mb kd cells (83#4) while the behavior of a second kd clone (83#8) corresponded more closely with the two Mb-expressing con clones. This retardation of *in vitro* motility in the 83#4 Mb kd cells became even more obvious 48 h and 72 h after wounding. Thus Mb-con MDA-MB-468 cells tend to close the wound much faster, showing that loss of Mb expression in this breast cancer cell line is associated with decreased *in vitro* motility of tumor cells under normoxia. Due to the variable outcome with these shRNA-based kd cells, we opted to repeat these experiments based on the transient siRNA-driven knockdown of Mb RNA in MDA-MB-468 cells. Here again, we found a good agreement with the more severe shRNA phenotype, i.e., the knock-down of Mb function to 10% of normal Mb protein levels resulted in a significant retardation of the wound healing reaction of breast cancer cells under normoxic conditions (Fig. 8D).

Non-respiratory functions of Mb in human breast cancer?

The amount of Mb detected in human breast cancer tissue and MDA-MB-468 cells was similar in Western blot analysis (data not shown) and equalled 65 ng per 10^6 tumor cells as described above. Since this minute amount of Mb cannot play a significant role in the maintenance of cellular oxygenation, and since we ruled out a significant impact of Mb on O_2 diffusion gradients in MDA468 cells (Fig. 7 D), Mb functions alternative to respiration support appear more likely. The association of Mb with characteristics of the luminal tumor subtype, namely ERα positivity led us to investigate this point further.

Publically available DNA array expression data (Geoprofiles, GDS2324) (20) had already indicated a tight co-regulation of Mb and ERα mRNAs in the breast cancer cell line MCF7 by showing that estrogen starvation was able to induce, while estrogen application suppressed, Mb transcript in either a time or dose dependent manner (Fig. S5). We repeated this experiment *in vitro* and could confirm the *in silico* data in that application of estrogen to MCF7 breast cancer cells repressed Mb expression potentially in a dose dependent manner (Fig. 9). This prompted us to further analyse the spatial association of both proteins. In normal lobular breast parenchyma, approximately 90% of the strongly Mb positive cells interspersed in secretory epithelia demonstrated a co-localisation of cytoplasmic Mb and nuclear ERα staining (Fig. 10A). In invasive breast carcinomas, this co-expression still was apparent in well differentiated carcinomas (Fig. 10B).

Recently, Mb was described again as a fatty acid (FA) binding protein and suggested to have a role in the transport of FAs in oxygenated cells (12, 21, 22). This prompted us to investigate the possible co-localization of Mb and fatty acid synthase (FASN) in both healthy and cancerous breast

tissue. FASN catalyses the synthesis of unbranched fatty acids and is upregulated in the broad majority of malignant tumors (23). In a direct comparison with Mb in a subset (n=293) of our breast cancer cohort, a highly significant correlation of both proteins was found (CC=0.297, p=0.001). Moreover, in normal breast tissues, a striking spatial concordance in the expression of Mb and FASN was seen (Figure 11A), which was partially retained in (Figure 11B). To check for a possible functional association of Mb expression and intracellular fatty acid levels, we used the FASN inhibitor C75. This inhibitor has been characterized as FASN specific, leading to an almost immediate and irreversible enzyme inhibition (24). In MDA-MB-468 cells, we observed a strong time dependent down-regulation of Mb on transcript and protein level upon FASN inhibition in comparison to control cells (Figure 12), suggesting that Mb expression is indeed regulated by intracellular FA levels and that non-muscle Mb in tumor cells might be involved in controlling fatty acid metabolism.

3. Discussion

This report is the first systematic examination of myoglobin (Mb) expression in a large cohort of breast cancer specimens. It integrates clinical, molecular and functional results to describe novel and unexpected facets of this hemoprotein. We first noticed a supposedly aberrant Mb immunoreactivity in a small series of breast carcinomas. To address whether Mb is being actively produced by tumor cells or, rather, taken up from e.g. adjacent musculature as suggested (25), we analyzed its expression both *in vitro* and *in vivo*. On transcript level, we found Mb strongly upregulated in breast tumors in comparison with adjacent normal ductal tissue. Mb mRNA was also detectable in breast cancer cell lines, in a small subset even at surprisingly high levels. This pointed to an active expression of endogenous Mb in ordinary invasive ductal breast cancer, which were neither muscle-invasive nor did they, as assessed by light microscopy, possess any rhabdomyogenous differentiation. Transmission electron microscopy did also not reveal any striated muscle elements in two strongly Mb positive breast cancer cases. We therefore conclude that Mb is *de novo* expressed in breast cancer cells although rare cases of so-called metaplastic carcinomas of the breast might exist where Mb-positivity stems from the rabdomyogenous differentiation of the cells (26, 27).

On the basis of these encouraging preliminary findings, a large recently described (28) cohort of primary breast cancer including 917 invasive carcinomas and 155 cases of Ductal Carcinoma in situ (DCIS) was analysed for Mb expression. In total, 40% of invasive carcinomas showed moderate to strong Mb expression. However, Mb was also consistently seen in mature secretory epithelia of the healthy breast showing a basal expression in most cells with a particularly clear expression in estrogen receptor positive cells (Fig. 2A). Contrary to earlier reports that found normal epithelia invariably Mb negative (29), luminal cells in healthy breast clearly have the ability to express Mb at detectable levels. That recent small scale pilot study identified endogenous Mb in human epithelial tumors including breast cancer and elucidated several signals, among them hypoxia, that were able to stimulate Mb expression in cultivated MCF7 breast cancer cells (29). However, the study lacked any prognostic, mechanistic and detailed functional data.

Regarding its occurrence in tumors, Mb is preferentially detected in better differentiated, hormone receptor (ER/PR) positive tumors and is associated with a significantly better prognosis. All these features are characteristics of the so called luminal subtype of breast cancer according to Perou *et al.* (30) which shares many molecular similarities with normal secretory epithelia including a strong expression of cytokeratins typical of mature secretory epithelia (CK8/18), hormone receptor (ER/PR) positivity and negativity for HER2 and the basal cell cytokeratins CK5/6. Further support for considering Mb a diagnostic marker of the luminal breast cancer subtype comes from the *in silico* analysis of Farmer *et al.*, in which Mb transcript levels were highest in tumors classified as the luminal subtype (17). Our own immunofluorescent double stainings detected co-localisation of cytoplasmic Mb and nuclear ERα in secretory cells of normal breast tissue. The same intracellular co-localization was found in strongly Mb and ERα-positive invasive ductal carcinomas. Beyond this spatial co-

existence, Mb and ERα transcripts are also co-ordinately and dose-dependently down-regulated when MCF7 cells are subjected to a E2 treatment protocol as we show *in silico* and *in vitro*. This hitherto undescribed co-regulation of Mb with ERα by estrogen is likely to explain the co-expression of the ER with Mb and, hence, the better prognosis of Mb positive tumors.

Mb has different known or alleged functions in muscle tissue including short-term O_2 storage and buffering, facilitating O_2 diffusion, scavenging of NO and ROS and also the reverse (peroxidase activity, NO production) and might be involved in fatty acid metabolism (2, 3, 7, 8, 10-12, 31). The significant correlation of Mb occurrence with established hypoxia markers (HIF-2α, CaIX) in breast carcinomas plus the fact that we observed a hypoxia-associated up-regulation of Mb in 27% of DCIS all aimed our focus on the role of oxygen on Mb expression and function in breast cancers and cancer cell lines. More than 50 years after Thomlinson's and Gray's pioneering discovery to link radiosensitivity with oxygen tension in tumor tissue (32, 33), the existence of regional hypoxia in *most* solid tumors (for review: (34-37) including breast cancer is of high clinical relevance (38). Also, the immunohistochemical detection of the exogenous hypoxia marker pimonidazole led Arcasoy *et al.* to conclude in a series of 26 breast cancer cases that 62% of tumors of the breast are pimonidazole-positive and thus hypoxic (39).

In accordance with the data of Flonta et al. (29), we demonstrate the *de novo* expression and hypoxic responsiveness of human Mb mRNA and protein in human breast cancer cell lines. We found a 3-4 fold up-regulation of Mb mRNA in response to prolonged (>24-48h) exposure to 1% O_2. It is of importance to note, that this hypoxia dependent up-regulation was restricted to tumor cell lines and could not be evoked in the non-transformed epithelial cell line MCF12A. A corresponding 3-5 fold elevation of Mb protein levels during prolonged hypoxia was noted for both MDA-MB-468 and MCF7 breast carcinoma cells.

Towards the control of this induction, we noted distinct HIF-gene preferences and stabilization kinetics in breast cancer cells. Whereas HIF-2α was the predominant factor and persistently elevated in hypoxic MDA-MB-468 cells, a transient induction of HIF-1α was the leading HIF response in hypoxic MCF7 cells. To our surprise, siRNA transfections in MDA-MB-468 cells directed against HIF-1α, -2α or both factors revealed that the ~7-fold peak induction of Mb protein during prolonged (72h) hypoxia (1% O_2) requires the involvement of both HIF species. Thus, both HIF-1 and HIF-2 contribute to the hypoxia transactivation of the Mb gene in breast cancer cells *in vitro*.

The standard promoter of the Mb gene that is driving the expression in striated muscle cells has been characterized in 1984 by Weller *et al.* for the human and in 1986 by Blanchetot *et al.* for the mouse Mb gene (18, 40). This TATA box promoter contains no candidate HRE (41). Consequently, expression of the standard Mb transcript (NM_005368; Mb-s) is not affected by O_2. However, we also observed the hypoxia-activated transcription of a non-canonical Mb mRNA (NM_203377; Mb-a), transcribed from a promoter that is located proximal to the 5' UTR exon -1. EST evidence and our own comparison of the copy numbers of the alternative versus standard Mb mRNAs expressed in

MDA-MB-468 cells (Fig. 6B) suggested that Mb-a, tentatively, can be regarded as a cancer-specific transcript. Discovery of the O_2-responsiveness of Mb-a, in conjunction with the found HIF-1/-2-driven transactivation of the Mb gene during hypoxia (Fig. 6A-C), led us to search for candidate HREs as potential regulatory sites for the alternative transcript. Scanning the complete genomic region of human and mouse *Mb* genes for HRE motifs we discovered a candidate HRE of the Mb gene, which consists of two inverted HIF-1 binding sites at an interval of 6 bp, embedded in a conserved stretch of 53 bp (Fig. 6C). This Mb-HRE has 93% sequence similarity to an upstream promoter region from the human heat shock protein HSPB1 gene that encodes the Hsp27 protein. Interestingly, promoter assays had already suggested that this observed HRE of HSPB1 is indeed functional in mediating HIF-1 responses (42).

Based on these findings, breast cancer cells induce the Mb gene in response to longer periods of low oxygen via an alternative, and perhaps, tumor specific promoter whose enhanced activity depends, in part, on the binding of HIF-1/-2 to the HRE located 2.7 kb upstream from the ATG. We thus are beginning to obtain a mechanistic rationale for the significant positive correlation of Mb with HIF-2α and CAIX in breast carcinomas. However, our *in vivo* data also provide evidence, that Mb can be expressed by breast epithelia irrespective of hypoxia (i.e. normal secretory ductal cells: Fig. 2A; DCIS with diffuse staining: Fig. 5B) and that even severe hypoxia does not necessarily induce Mb expression, as the comparison of Mb and pimonidazole stainings illustrates for breast carcinoma. In the majority of DCIS cases, the expression of Mb did not follow the hypoxia gradient, which clarifies that hypoxia is not acting as sole stimulus to induce Mb *in vivo*. Furthermore, the *in vivo* data linked Mb with HIF-2α rather than HIF-1α, perhaps as a consequence of the mutually exclusive status between active HIF-1α and ERα/PgR signalling in breast cancer cells (43, 44). The positive correlation between Mb and ERα or PgR positivity might preclude a significant linkage of Mb with HIF-1α, or HIF-1α dependent effector genes (e.g. GLUT1), in the investigated carcinoma and DCIS entities.

Towards possible functions of this hemoprotein in tumor cells, we generated shRNA Mb knockdown clones of MDA-MB-468, the breast cancer cell line with the most abundant transcript levels. These knock down cells were comparatively analysed concerning their *in vitro* respiratory and tumorigenic properties. To assess whether Mb confers O_2-buffering or facilitates O_2 diffusion we used high-resolution respirometry to measure O_2 consumption kinetics in Mb expressing (con) and knockdown (kd) MDA-MB-468 cells. We would expect a lower respiration $p_{50}(O_2)$, i.e. a higher Cox turnover, in controls relative to knock down cells provided that cell number and oxygen flux, as well as cell size are comparable between both cell types. We either controlled for these parameters during measurements (cell number, O_2 flux) or found them to be largely overlapping between both genotypes (cell size; not shown). Since cellular $p_{50}(O_2)$ measures lie below 0.1 kPa, there exists only a small scope for oxygen gradients, considering that the $p_{50}(O_2)$ of isolated mitochondria is 0.04 to 0.06 kPa in the active state (Scandurra and Gnaiger, 2009). Within these physical constraints the present study was

unable to provide any evidence for O_2 gradients that are differentially impacted by the presence or absence of Mb protein. In fact, the $p_{50}(O_2)$ of MDA-MB-468 cells was found to lie in a similar range (0.08 kPa), irrespective of expression or knockdown of intracellular Mb (Fig. 7D). While these results do not suggest a functional role of Mb for oxygen transport in small, suspended cells *in vitro*, they do not exclude the possibility of large oxygen gradients developing in the solid tumor and a potential contribution of Mb to facilitated oxygen diffusion under *in vivo* conditions. Regarding the control of mitochondrial function, in MDA-MB-468 cells, routine respiration in the absence of glucose activated only ~55% of the mitochondrial capacity for electron transport, and this was reduced to ~40% in the presence of glucose, which is comparable to various primary cultured cells, such as HUVEC and fibroblasts (45, 46). Mitochondrial oxygen kinetics and coupling control in the malignant MDA-MB-468 cells, therefore, is not indicative of a mitochondrial deficiency frequently considered as a specific feature (Warburg effect) of cancer cells.

In addition to these high resolution respiromety data obtained under O_2-limiting hypoxia, we surprisingly noticed that under mild hypoxia MDA kd cells, relative to control cells, revealed an intensified O_2 uptake rate across all four physiological activity states considered (Fig. 7C; R(-G), R(G), ETS, ROX). As hemoprotein Mb can effectively interact with the gaseous nitric oxide (NO). Mb knockout mouse models (5, 6) have been instrumental to elicit Mb`s critical role in maintaining NO homeostasis in muscle tissue. Whether Mb expressed in neoplasms exerts similar controls remains to be seen. At this point we can only speculate that the activated respiration triggered by the LoF of Mb in MDA kd cells (Fig. 7C) might result from the proteins' capacity to bind, and scavenge, with NO a key stimulus of the mitochondrial biogenesis (see (47) for review).

To our knowledge, only two studies have so far analysed the functions of myoglobin *in vivo* by employing an artificial Mb expression system. Nitta *et al.* induced Mb expression in hepatocytes by an adenoviral gene transfer in rodents, which were henceforth significantly more resistant to hypoxia (48). Galluzzo *et al.* were the first to introduce Mb into tumor cell lines. They engineered A549 human lung carcinoma cells to ectopically express mouse Mb (49). Experimental tumors expressing Mb displayed reduced or no hypoxia, minimal HIF-1α levels, lesser vessel density along with a more differentiated cancer cell phenotype and largely suppressed local and distal metastatic spreading. The authors correlate these beneficial outcomes of Mb over-expression primarily with the reduction of tumor hypoxia (49). Although it is tempting to compare their model *in vivo* finding with our *in vivo* observations from patients, given that higher Mb levels correlate to less aggressive tumor behavior, both situations are quite different. We estimated the amount of endogenous Mb in normoxic MDA-MB-468 breast cancer cells to equate to ~65 ng or 4 pmol of Mb protein present in 10^6 cells. This quantity is certainly far below the μM levels reached by the lentiviral gene transfer (49). While such excessive amounts of ectopic Mb in tumor cells will have a significant impact on tumor respiration and tumor growth, the endogenous picomole quantities of Mb we detected are unlikely to confer meaningful O_2 storage/buffering capacity to the cell. In addition, our respirometry data failed to

provide evidence in support of a functional role of Mb to transport oxygen in small, suspended breast cancer cells *in vitro*. Thus, for these cells, functions of Mb that are not directly linked to the binding and transport of O_2 have to be considered to comprehend the physiological relevance of this protein in breast cancer.

One possible function of Mb that might be tremendously relevant for tumors is fatty acid metabolism. In a multitude of tumors, growth is accompanied with increased fatty acid synthesis and consequently enzymes catalysing these steps are up-regulated and can be used diagnostically and therapeutically (for recent reviews see (23, 50)). The co-localisation of Mb with fatty acid synthase (FASN) we discovered might give a hint towards the fatty acid binding function of tumor Mb. Fatty acid binding properties of Mb have been reported and predicted early (21, 51) and have recently gained further attention (52). According to Flögel and colleagues, lack of Mb in the heart of knockout mice leads to a biochemical shift in cardiac substrate utilization from fatty acid to glucose oxidation which, not only corresponds to an adaptive reduction in O_2 consumption for the equimolar production of ATP, but more so implicates the protein in providing fatty acid substrates for the mitochondriał -oxidation breakdown in vivo (53). Our indirect demonstration, that Mb is likely to be regulated by intracellular fatty acid levels as shown by the inhibition of fatty acid synthase (FASN) now indicates a role for Mb in fatty acid metabolism of cancer cells and clearly warrants further study.

In summary, Mb is endogenously expressed in normal breast tissue and abundantly in a subset of breast cancer cases. The strong functional association of Mb expression with presence of the estrogen receptor (ERα) explains the generally better prognosis of Mb positive tumors, compared to Mb negative tumors. In breast cancer cells, Mb abundance is regulated by hypoxia, estrogen signalling and possibly fatty acid levels. The functional data generated under normoxia implicate unconventional functions of myoglobin, not directly related to the transport of oxygen. Mb`s prospective role in the lipid metabolism of ER-positive tumors provides a reasonable working hypothesis able to link a loss-of-function of this hemoprotein with the observed impairment of the proliferative and migratory capacities of oxygenated cells. Beyond these functional aspects, the regulation in normal and tumor tissue might also be fundamentally different, as the novel description of a tumor specific Mb transcript suggests. Taken together, these findings further broaden our view on the role of non-muscle Mb that may have fundamental implications for our conception of the biology of solid tumors. Finally, we acknowledge that this study has in consequence generated even more pressing questions concerning the functional role of non-muscle Mb for further analysis.

4. Acknowledgements

The excellent technical assistance of Britta Beyer, Annette Bohnert, Martina Bimmler, Martina Storz, Silvia Behnke, Sonja von Serenyi and Daniela Wichmann is thankfully acknowledged. We thank Dr. Peter Uciechowski (Institute of Immunology, RWTH Aachen) for giving access and instruction for the hypoxia workstation. Parts of this work were funded (J.H.) by the Swiss National Science Foundation and by a grant of the Faculty of Medicine (E.D.), RWTH Aachen (START network on tumor marker and their function).

5. Material and methods

5.1 Clinical materials/Patients

The matched tumor/normal samples of invasive ductal breast carcinomas and corresponding normal breast epithelium (n=10) analyzed in this study, have recently been described (54). For immunohistochemistry, our study included tissue micro arrays of normal tissue, intratumoral *ductal carcinoma in situ* and invasive breast cancer of patients diagnosed at the Institute of Surgical Pathology (University Hospital, Zurich, Switzerland), as described (28). Tumor histology was determined according to the criteria of the World Health Organization (2003), staging the disease followed UICC guidelines (2002). Tumors were graded according to Bloom and Richardson, as modified by Elston and Ellis (55). Clinico-pathological characteristics of the patients/tumors are given in Table 1. For statistical analysis, only cases with clinical follow-up data were considered. The median observation time for overall survival was 59 months for patients still alive at the time of analysis. Two-hundred-and-twenty-five patients (24%) died during follow-up. Data on adjuvant therapy was not available.

5.2 Cell lines

The human mammary epithelial cell line MCF12A as well as the breast cancerous cell lines BT20, BT474, Cal51, EFM19, HBL100, Hs578T, MDA-MB231, MDA-MB361, MDA-MB453, MDA-MB415, MDA-MB436, MDA-MB-468, MCF7, SKBR3, T47-D and ZR75-1 were obtained from the ATCC (Rockville, MD, USA) and cultured under recommended conditions.

5.3 Hypoxia experiments

The benign breast cell line MCF12A and the breast cancer cell lines MDA-MB231, MDA-MB-468 and MCF7 were used for hypoxic exposures. Culture conditions included: normoxia = ventilated room air in incubator in water-saturated, 5% CO_2 atmosphere at sea level and 37°C = 141.6 mmHg or 18.6% O_2; hypoxia: water-saturated 1% O_2 / 5% CO_2 / balance N_2 atmosphere at 37°C for 4, 8, 24, 48 and 72h respectively. Albeit we approximated the normoxic concentration of O_2 with 20% in some figures (e.g. Fig. 3), we are fully aware that the calculated tension in incubators is slightly lower. We used Hera cell240 incubators (MultiTemp Scientific AG, Kloten, Switzerland) or an Invivo$_2$ 400 Hypoxia Workstation (Ruskinn Technology Ltd, Leeds, UK) for hypoxic exposures.

5.4 Quantitative real-time reverse transcription PCR

At RWTH Aachen qPCR experiments used the LightCycler® system (Roche Diagnostics, Germany) as recently described (54). At the Universities of Zurich and Mainz qPCR experiments used the ABI Prism 7500 Fast SDS (Applied Biosystems, Darmstadt, Germany) (see (56) for details).

Mean (±SD) expression levels of standard (NM_005368, Mb-s) and alternative (NM_203377, Mb-a)

Mb transcript were calculated by the standard-curve approach measuring Ct-values for hypoxic and normoxic samples (Fig. 6B; n=2 experiments, triplicate assays). Differences in relative abundance between Mb-s and Mb-a transcripts in normoxic MDA-MB-468 cells were calculated using the standard-curve method and a standard plasmid construct harbouring both amplicons, Mb-s and Mb-a (Fig. 6B, n=4 experiments, duplicate assays).

5.5 Western blots

Following normoxic exposure for 72h and hypoxic (1% O_2) exposure for 4, 8, 24, 48 and 72h, MDA-MB-468 and MCF7 were harvested with a lysis buffer containing 0.1% NP-40, 400mM NaCl, 1mM EDTA (pH8.0), 10mM Tris-HCl (pH8.0) and protease inhibitors. Protein extracts were electrophoresed on a 15% SDS-PAGE gel. Monoclonal antibody mouse anti-myoglobin (No. 113-0533, Zytomed Systems GmbH, Berlin, Germany) was used for immunoblotting (1:1000 dilution). For equal loading control, blots were stripped and re-probed by monoclonal antibody mouse anti-β-actin at a 1:5000 dilution (A5441 Sigma-Aldrich, Basel, Switzerland). For HIF-1α and -2α immunoblots, mouse monoclonal anti-HIF-1α (mgc3) and rabbit polyclonal anti-HIF-2α (NB100-480, Novus Biologicals, LLC, Littleton, USA) were used at 1:500 and 1:750 dilutions, respectively**.**

5.6 Immunohistochemistry and immunofluorescence

Tissue sections were processed using automated immunohistochemistry platforms (BOND, Labvision; Benchmark, Ventana). Validation of the specificity of used Mb antibodies (Supplement Fig. S1) and a summary of employed immunohistochemical (Supplement Tab. ST1) are given as indicated. Intensity of Mb, Cgb, GLUT1, CAIX and FASN immunohistochemistry was evaluated by two clinical pathologists (GK, FFR) and semiquantitatively scored as negative, weakly, moderately or strongly positive (0 to 3+). ER, HIF-1α/-2α was evaluated in percent of positive nuclei. Double Immunofluorescence was performed as recently described (57).

5.7 Identification of candidate transcription factor binding sites

Genomic sequences covering the analyzed gene loci were extracted from the NCBI database (www.ncbi.nlm.nih.gov): human MB (NC_000022), mouse *Mb* (NC_000081) and human HSP27 (NC_000007). For the identification of putative transcription factor binding sites conserved across different species, the rVISTA program was used (58) (http://rvista.dcode.org). A global sequence alignment file as prepared by the program Mulan (http://mulan.dcode.org/) was used as input. Transcription factor binding site searches in rVISTA are based on the TRANSFAC database (http://transfac.gbf.de/TRANSFAC/) (59). The default program values (core similarity: 0.9; matrix similarity: 0.85) were used in the sequence motif search.

5.8 Stable and transient RNA interference

5.8.1 Targeting HIF

To target nucleotides 1380-1400 of human HIF-1α mRNA (accession no. AF304431.1), HIF-1α RNA oligonucleotides were synthesized as sense 5'-CUGAUGACCAGCAACUUGAdTdT-3' and antisense UCAAGUUGCUGGUCAUCAGdTdT-3' sequences. HIF-2α specific siRNA oligonucleotides were synthesized as sense 5'-CAGCAUCUUUGAUAGCAGUdTdT-3'; and antisense 5'-ACUGCUAUCAAAGAUGCUGdTdT-3' sequences to target nucleotides 1260-1280 of human HIF-2α (accession no. NM_001430). Both siRNAs, and the Si*CONTROL* non-targeting pool #2 of scrambled siRNAs, were purchased from Dharmacon Research Inc (Lausanne, Switzerland). Oligofectamine transfections (Invitrogen, Basel, Switzerland) of siRNAs used final concentrations of 200nM of either HIF-1α or -2α single siRNA, and 100nM each of HIF-1α and -2α siRNA in combined transfections. MDA468 cells were transfected as a pool in 6-well plates and divided into 6cm plates after 3-4 h post-transfection. At 18 h post-transfection, cells were exposed to 1% oxygen for 52, 56, 72 or 96 h. Cells were lysed in the 0.1% NP-40 lysis buffer.

5.8.2 Targeting Mb

Short hairpin RNAs (shRNA) were used for targeting of the human myoglobin mRNA (GenBank™ accession number NM_203377) at nucleotides 284-304 (construct #83), 483-503 (#84), 340-360 (#85) and 415-435 (#86). Inserted into the mammalian expression vector pLKO.1-puro, these four shRNA constructs, were purchased as bacterial glycerol stock from Sigma-Aldrich (Basel, Switzerland). Stable shRNA Mb knockdown MDA-MB-468 cells were established by overnight calcium phosphate transfection followed by selection and maintenance in 0.75μg/ml puromycin containing medium. Mb protein levels in knockdown and control cells were analyzed by Western blot as described above**.**

For transient knockdown, MDA-MB-468 cells were transfected with 10nM siRNA solutions (#6, #8 and allStars negative control, Qiagen, Hilden, Germany) immediately after seeding using Lipofectamine 2000 (Invitrogen, Carlsbad, California). 24h post-transfection the medium was changed. Knockdown efficiency was confirmed on protein and RNA level in a Western Blot analysis and real-time qPCR, respectively.

5.9 High-resolution respirometry

Oxygen kinetics of trypsinized, suspended and heavily stirred MDA-MB-468 cells, both of Mb control and knockdown make-up, were measured at ~1x10^6/ml densities in twin-chamber Oroboros® Oxygraph-2k respirometers. Each chamber was filled with cells suspended in 2 ml culture medium (glucose-free DMEM + 10%FBS + penicillin /streptomycin + 0.75 μg/ml puromycin). Details regarding the deconvolution of the oxygen signal (60), instrumental design and data analysis (45, 60, 61) are summarized in earlier publications. The systems inherent high signal stability and dynamic background correction for oxygen consumption of the oxygen sensor and oxygen back-diffusion

provide the basis for high resolution of oxygen flux (<2 pmol.s^{-1}.cm^{-3}). To measure routine respiration, the medium was initially free of glucose, but contained 280 IU/ml of catalase. Later, 25 mM of glucose were added to measure the extent of its inhibition on respiration (Crabtree effect). In addition, injection of 40 μM H_2O_2 triggered the catalase-driven release of controlled amounts of oxygen to record additional oxy-regulated/oxy-conform transitions of respiratory activity of MDA-MB-468 cells (see Fig. 7B). Alternatively, 400 μM H_2O_2 were added to achieve full reoxygenation via the catalase reaction. For the recording of electron transport saturated (ETS) oxygen flows, oxidative phosphorylation was uncoupled with increasing doses (4.0 - 5.5 μM) of the protonophore carbonylcyanide-4-(trifluoromethoxy)-phenylhydrazone (FCCP). Finally, mitochondria were poisoned through injection of 0.5 μM of myxothiazol to obtain the residual O_2-consumption (ROX).

5.10 In vitro proliferation and migration assays

Proliferation rates of wildtype (wt) and selected stable Mb-control (con) or Mb-knockdown (kd) MDA-MB-468 cells was determined over a 96h time course in normoxic and hypoxic atmospheres either by direct counting of viable cells (Trypan Blue exclusion assay, dotted lines) or by using the MTT assay (continuous lines), which correlates cellular growth indirectly with a colorimetric determination of the activities of mitochondrial enzymes (n=4 independent measurements/assay; data as mean rate ± SD, relative to 0h time point = 1x). To extract the impact of the Mb knockdown on cellular growth, 96h proliferation ratios (wt/kd, con/kd) were calculated relative to the growth of kd cells (=1) at high and low oxygen tensions.

The *in vitro* motility of MDA-MB-468 cells was assessed for stable Mb kd clones as well as for transiently siRNA transfected cells by performing a monolayer scratch wound assay (62). Once 3 x 10^5 plated MDA cells had reached 100% confluence, the monolayer was linearly scratched with a 100μl pipette tip, washed twice gently with PBS and cultured further with complete (10% FBS) medium. Pictures of the wound were taken with a Canon digital camera fitted to a light microscope at 0, 24, 48 and 72h after scratching. The wound closure dynamics was determined as "percentage of remaining wound size" by evaluation the acellular gap width in relation to the initial wound width at three different sites for each wound in each picture (data as mean relative wound size ± SD of triplicate measurements/clone).

5.11 Electron Microscopy (EM)

Tissues from two breast tumors were fixed with 2.5% glutaraldehyde, postfixed with osmium tetroxide, embedded in epoxy resin, cut with an ultramicrotome, mounted on 200 mesh copper grids, stained with uranyl acetate and lead citrate and examined with a Zeiss EM10 transmission electron microscope (Zeiss, Oberkochen, Germany) at 60 kV.

5.12 Expression of Mb gene after incubation of MCF-7 cells with ß-Estradiol

MCF7 cells ($8x10^5$) were seeded into a 10cm culture dish and 24h later ß-Estradiol (Sigma-Aldrich, Deisenheim, Germany) dissolved in 5 µl ethanol abs., was applied to the cells at a final concentration of 0 pM, 20 pM, 40 pM and 60 pM. Cells without ß-Estradiol and Ethanol served as internal control. PCR primers used are shown in Table 2.

5.13 Expression of Mb gene after incubation of MDA-MB-468 cells with the FASN inhibitor C75

$3x10^5$ MDA-MB-468 cells were seeded into 6 well-plates and exposed to 10 µg/ml final concentration of the FASN inhbitor C75 (Sigma-Aldrich, St. Louis, MO, USA) for 8, 24 and 48h. RNA and proteins were isolated following standard procedures.

5.14 Statistical Analysis

Expression data were analyzed with the software package SPSS, version 16.0 (SPSS Inc., Chicago, USA). Comparison of the delta CT values of the real time qPCR results between specific groups used the non-parametric Mann-Whitney-U-test. Fisher's exact and chi-square tests for trends were used to asses the statistical significance of associations between Mb expression and clinico-pathological parameters (Tab. 1). Bivariate correlations according to Spearman were applied to the immuno-intensity of normal tissue, intraductal and invasive carcinomas. Univariate survival analysis was performed with univariate Cox analyses and Kaplan-Meier curves (Log rank test).

SiRNA and respirometry results were analyzed with the software package STATA 10.0 (Stata™ 10.0; StataCorp, College Station, USA). Extent of Mb induction was compared for corresponding time points between siControl versus siHIF-1α or siHIF-2α or the combined siHIF-1α/-2α treatments. Mean O_2 consumption rates or p50 measurements were compared pairwise between pooled Mb control (con) and knockdown (kd) samples. Statistical significance was calculated in accordance with prior testing for variance equality between compared data, i.e. by standard Student t-tests when variance equality was ascertained (e.g. R(-G), R(G), ROX O_2 consumption rates, all p50 data) or by a Welch-approximated t-test that takes unequal variances into account and (e.g. siRNA 72h hypoxia time point comparison; ETS consumption rate). For all analyses, p values < 0.05 were considered significant.

References

1. Kendrew, J.C. 1958. Architecture of a protein molecule. *Nature* 182:764-767.
2. Ordway, G.A., and Garry, D.J. 2004. Myoglobin: an essential hemoprotein in striated muscle. *J Exp Biol* 207:3441-3446.
3. Wittenberg, J.B. 1970. Myoglobin-facilitated oxygen diffusion: role of myoglobin in oxygen entry into muscle. *Physiol Rev* 50:559-636.
4. Jurgens, K.D., Peters, T., and Gros, G. 1994. Diffusivity of myoglobin in intact skeletal muscle cells. *Proc Natl Acad Sci U S A* 91:3829-3833.
5. Garry, D.J., Ordway, G.A., Lorenz, J.N., Radford, N.B., Chin, E.R., Grange, R.W., Bassel-Duby, R., and Williams, R.S. 1998. Mice without myoglobin. *Nature* 395:905-908.
6. Godecke, A., Flogel, U., Zanger, K., Ding, Z., Hirchenhain, J., Decking, U.K., and Schrader, J. 1999. Disruption of myoglobin in mice induces multiple compensatory mechanisms. *Proc Natl Acad Sci U S A* 96:10495-10500.
7. Flogel, U., Merx, M.W., Godecke, A., Decking, U.K., and Schrader, J. 2001. Myoglobin: A scavenger of bioactive NO. *Proc Natl Acad Sci U S A* 98:735-740.
8. Hendgen-Cotta, U.B., Merx, M.W., Shiva, S., Schmitz, J., Becher, S., Klare, J.P., Steinhoff, H.J., Goedecke, A., Schrader, J., Gladwin, M.T., et al. 2008. Nitrite reductase activity of myoglobin regulates respiration and cellular viability in myocardial ischemia-reperfusion injury. *Proc Natl Acad Sci U S A* 105:10256-10261.
9. Brunori, M. 2001. Nitric oxide moves myoglobin centre stage. *Trends Biochem Sci* 26:209-210.
10. Khan, K.K., Mondal, M.S., Padhy, L., and Mitra, S. 1998. The role of distal histidine in peroxidase activity of myoglobin--transient-kinetics study of the reaction of H2O2 with wild-type and distal-histidine-mutanted recombinant human myoglobin. *Eur J Biochem* 257:547-555.
11. Flogel, U., Godecke, A., Klotz, L.O., and Schrader, J. 2004. Role of myoglobin in the antioxidant defense of the heart. *FASEB J* 18:1156-1158.
12. Masuda, K., Truscott, K., Lin, P.C., Kreutzer, U., Chung, Y., Sriram, R., and Jue, T. 2008. Determination of myoglobin concentration in blood-perfused tissue. *Eur J Appl Physiol* 104:41-48.
13. Smith, T.W., and Davidson, R.I. 1984. Medullomyoblastoma. A histologic, immunohistochemical, and ultrastructural study. *Cancer* 54:323-332.
14. Iseki, M., Tsuda, N., Kishikawa, M., Shimada, O., Hayashi, T., Kawahara, K., and Tomita, M. 1990. Thymolipoma with striated myoid cells. Histological, immunohistochemical, and ultrastructural study. *Am J Surg Pathol* 14:395-398.
15. Ruck, P., Horny, H.P., Greschniok, A., Wehrmann, M., and Kaiserling, E. 1995. Nonspecific immunostaining of blast cells of acute leukemia by antibodies against nonhemopoietic antigens. *Hematol Pathol* 9:49-56.
16. Zhang, P.J., Goldblum, J.R., Pawel, B.R., Fisher, C., Pasha, T.L., and Barr, F.G. 2003. Immunophenotype of desmoplastic small round cell tumors as detected in cases with EWS-WT1 gene fusion product. *Mod Pathol* 16:229-235.
17. Farmer, P., Bonnefoi, H., Becette, V., Tubiana-Hulin, M., Fumoleau, P., Larsimont, D., Macgrogan, G., Bergh, J., Cameron, D., Goldstein, D., et al. 2005. Identification of molecular apocrine breast tumours by microarray analysis. *Oncogene* 24:4660-4671.
18. Weller, P., Jeffreys, A.J., Wilson, V., and Blanchetot, A. 1984. Organization of the human myoglobin gene. *EMBO J* 3:439-446.
19. Wenger, R.H., Stiehl, D.P., and Camenisch, G. 2005. Integration of oxygen signaling at the consensus HRE. *Sci STKE* 2005:re12.
20. Coser, K.R., Chesnes, J., Hur, J., Ray, S., Isselbacher, K.J., and Shioda, T. 2003. Global analysis of ligand sensitivity of estrogen inducible and suppressible genes in MCF7/BUS breast cancer cells by DNA microarray. *Proc Natl Acad Sci U S A* 100:13994-13999.
21. Gloster, J., and Harris, P. 1977. Fatty acid binding to cytoplasmic proteins of myocardium and red and white skeletal muscle in the rat. A possible new role for myoglobin. *Biochem Biophys Res Commun* 74:506-513.
22. Yackzan, K.S., and Wingo, W.J. 1982. Transport of fatty acids by myoglobin- a hypothesis. *Med Hypotheses* 8:613-618.
23. Menendez, J.A., and Lupu, R. 2007. Fatty acid synthase and the lipogenic phenotype in cancer pathogenesis. *Nat Rev Cancer* 7:763-777.
24. Kuhajda, F.P., Pizer, E.S., Li, J.N., Mani, N.S., Frehywot, G.L., and Townsend, C.A. 2000. Synthesis and antitumor activity of an inhibitor of fatty acid synthase. *Proc Natl Acad Sci U S A* 97:3450-3454.
25. Eusebi, V., Bondi, A., and Rosai, J. 1984. Immunohistochemical localization of myoglobin in nonmuscular cells. *Am J Surg Pathol* 8:51-55.

26. Jamieson, S., and Rudland, P.S. 1990. Identification of metaplastic variants generated by transfection of a nonmetastatic rat mammary epithelial cell line with DNA from a metastatic rat mammary cell line. *Am J Pathol* 137:629-641.
27. Yang, G.C., Yee, H.T., and Waisman, J. 2003. Metaplastic carcinoma of the breast with rhabdomyosarcomatous element: aspiration cytology with histological, immunohistochemical, and ultrastructural correlations. *Diagn Cytopathol* 28:153-158.
28. Theurillat, J.P., Ingold, F., Frei, C., Zippelius, A., Varga, Z., Seifert, B., Chen, Y.T., Jager, D., Knuth, A., and Moch, H. 2007. NY-ESO-1 protein expression in primary breast carcinoma and metastases: correlation with CD8+ T-cell and CD79a+ plasmacytic/B-cell infiltration. *Int J Cancer* 120:2411-2417.
29. Flonta, S.E., Arena, S., Pisacane, A., Michieli, P., and Bardelli, A. 2009. Expression and functional regulation of myoglobin in epithelial cancers. *Am J Pathol* 175:201-206.
30. Perou, C.M., Sorlie, T., Eisen, M.B., van de Rijn, M., Jeffrey, S.S., Rees, C.A., Pollack, J.R., Ross, D.T., Johnsen, H., Akslen, L.A., et al. 2000. Molecular portraits of human breast tumours. *Nature* 406:747-752.
31. Wittenberg, B.A., Wittenberg, J.B., and Caldwell, P.R. 1975. Role of myoglobin in the oxygen supply to red skeletal muscle. *J Biol Chem* 250:9038-9043.
32. Gray, L.H., Conger, A.D., Ebert, M., Hornsey, S., and Scott, O.C. 1953. The concentration of oxygen dissolved in tissues at the time of irradiation as a factor in radiotherapy. *Br J Radiol* 26:638-648.
33. Thomlinson, R.H., and Gray, L.H. 1955. The histological structure of some human lung cancers and the possible implications for radiotherapy. *Br J Cancer* 9:539-549.
34. Vaupel, P., Schlenger, K., Knoop, C., and Hockel, M. 1991. Oxygenation of human tumors: evaluation of tissue oxygen distribution in breast cancers by computerized O2 tension measurements. *Cancer Res* 51:3316-3322.
35. Thews, O., Koenig, R., Kelleher, D.K., Kutzner, J., and Vaupel, P. 1998. Enhanced radiosensitivity in experimental tumours following erythropoietin treatment of chemotherapy-induced anaemia. *Br J Cancer* 78:752-756.
36. Brown, J.M. 1999. The hypoxic cell: a target for selective cancer therapy--eighteenth Bruce F. Cain Memorial Award lecture. *Cancer Res* 59:5863-5870.
37. Brown, J.M., and Wilson, W.R. 2004. Exploiting tumour hypoxia in cancer treatment. *Nat Rev Cancer* 4:437-447.
38. Vaupel, P., Schlenger, K.H., Hoeckel, M., and Okunieff, P. 1992. Oxygenation of mammary tumors: from isotransplanted rodent tumors to primary malignancies in patients. *Adv Exp Med Biol* 316:361-371.
39. Arcasoy, M.O., Amin, K., Karayal, A.F., Chou, S.C., Raleigh, J.A., Varia, M.A., and Haroon, Z.A. 2002. Functional significance of erythropoietin receptor expression in breast cancer. *Lab Invest* 82:911-918.
40. Blanchetot, A., Price, M., and Jeffreys, A.J. 1986. The mouse myoglobin gene. Characterisation and sequence comparison with other mammalian myoglobin genes. *Eur J Biochem* 159:469-474.
41. Wystub, S., Ebner, B., Fuchs, C., Weich, B., Burmester, T., and Hankeln, T. 2004. Interspecies comparison of neuroglobin, cytoglobin and myoglobin: sequence evolution and candidate regulatory elements. *Cytogenet Genome Res* 105:65-78.
42. Whitlock, N.A., Agarwal, N., Ma, J.X., and Crosson, C.E. 2005. Hsp27 upregulation by HIF-1 signaling offers protection against retinal ischemia in rats. *Invest Ophthalmol Vis Sci* 46:1092-1098.
43. Massaad-Massade, L. 2004. [Hypoxia, HIF1alpha and estrogen receptor]. *Bull Cancer* 91:677-683.
44. Kurebayashi, J. 2003. Endocrine-resistant breast cancer: underlying mechanisms and strategies for overcoming resistance. *Breast Cancer* 10:112-119.
45. Steinlechner-Maran, R., Eberl, T., Kunc, M., Margreiter, R., and Gnaiger, E. 1996. Oxygen dependence of respiration in coupled and uncoupled endothelial cells. *Am J Physiol* 271:C2053-2061.
46. Hutter, E., Renner, K., Pfister, G., Stockl, P., Jansen-Durr, P., and Gnaiger, E. 2004. Senescence-associated changes in respiration and oxidative phosphorylation in primary human fibroblasts. *Biochem J* 380:919-928.
47. Nisoli, E., Clementi, E., Carruba, M.O., and Moncada, S. 2007. Defective mitochondrial biogenesis: a hallmark of the high cardiovascular risk in the metabolic syndrome? *Circ Res* 100:795-806.
48. Nitta, T., Xundi, X., Hatano, E., Yamamoto, N., Uehara, T., Yoshida, M., Harada, N., Honda, K., Tanaka, A., Sosnowski, D., et al. 2003. Myoglobin gene expression attenuates hepatic ischemia reperfusion injury. *J Surg Res* 110:322-331.
49. Galluzzo, M., Pennacchietti, S., Rosano, S., Comoglio, P.M., and Michieli, P. 2009. Prevention of hypoxia by myoglobin expression in human tumor cells promotes differentiation and inhibits metastasis. *J Clin Invest* 119:865-875.
50. Mashima, T., Seimiya, H., and Tsuruo, T. 2009. De novo fatty-acid synthesis and related pathways as molecular targets for cancer therapy. *Br J Cancer* 100:1369-1372.

51. Lewis, U.J., Cheever, E.V., and Seavey, B.K. 1968. Influence of fatty acids on the electrophoretic behavior of proteins with special reference to pituitary hormone and thyroglobulin. *J Biol Chem* 243:260-267.
52. Sriram, R., Kreutzer, U., Shih, L., and Jue, T. 2008. Interaction of fatty acid with myoglobin. *FEBS Lett* 582:3643-3649.
53. Flogel, U., Laussmann, T., Godecke, A., Abanador, N., Schafers, M., Fingas, C.D., Metzger, S., Levkau, B., Jacoby, C., and Schrader, J. 2005. Lack of myoglobin causes a switch in cardiac substrate selection. *Circ Res* 96:e68-75.
54. Veeck, J., Niederacher, D., An, H., Klopocki, E., Wiesmann, F., Betz, B., Galm, O., Camara, O., Durst, M., Kristiansen, G., et al. 2006. Aberrant methylation of the Wnt antagonist SFRP1 in breast cancer is associated with unfavourable prognosis. *Oncogene* 25:3479-3488.
55. Elston, E.W., and Ellis, I.O. 1993. Method for grading breast cancer. *J Clin Pathol* 46:189-190.
56. Wirthner, R., Wrann, S., Balamurugan, K., Wenger, R.H., and Stiehl, D.P. 2008. Impaired DNA double-strand break repair contributes to chemoresistance in HIF-1 alpha-deficient mouse embryonic fibroblasts. *Carcinogenesis* 29:2306-2316.
57. Kristiansen, G., Fritzsche, F.R., Wassermann, K., Jager, C., Tolls, A., Lein, M., Stephan, C., Jung, K., Pilarsky, C., Dietel, M., et al. 2008. GOLPH2 protein expression as a novel tissue biomarker for prostate cancer: implications for tissue-based diagnostics. *Br J Cancer* 99:939-948.
58. Loots, G.G., and Ovcharenko, I. 2004. rVISTA 2.0: evolutionary analysis of transcription factor binding sites. *Nucleic Acids Res* 32:W217-221.
59. Wingender, E., Chen, X., Hehl, R., Karas, H., Liebich, I., Matys, V., Meinhardt, T., Pruss, M., Reuter, I., and Schacherer, F. 2000. TRANSFAC: an integrated system for gene expression regulation. *Nucleic Acids Res* 28:316-319.
60. Gnaiger, E., Steinlechner-Maran, R., Mendez, G., Eberl, T., and Margreiter, R. 1995. Control of mitochondrial and cellular respiration by oxygen. *J Bioenerg Biomembr* 27:583-596.
61. Gnaiger, E. 2001. Bioenergetics at low oxygen: dependence of respiration and phosphorylation on oxygen and adenosine diphosphate supply. *Respir Physiol* 128:277-297.
62. Rosman, D.S., Phukan, S., Huang, C.C., and Pasche, B. 2008. TGFBR1*6A enhances the migration and invasion of MCF-7 breast cancer cells through RhoA activation. *Cancer Res* 68:1319-1328.

Table 1 Clinico-pathological parameters of invasive breast cancer cases and relation to myoglobin expression

Characteristic	Number of cases (%)	MB negative	MB weak	MB moderate	MB strong	p-value
	917 (100%)					
<60 years	416 (45.4%)	125	132	130	29	0.170#
>=60 years	501 (54.6%)	142	157	142	60	
Pre-menopausal	198 (21.5%)	67	64	60	7	0.007#
Post-menopausal	719 (78.5%)	200	225	212	82	
Invasive ductal	739 (80.6%)	214	221	228	76	0.375*
Invasive lobular	125 (13.6%)	39	49	29	8	
NOS	53 (5.8%)	14	19	15	5	
pT1	335 (36.5%)	91	108	106	30	0.479#
pT2	410 (44.7%)	115	134	119	42	
pT3	66 (7.2%)	27	19	17	3	
pT4	106 (11.6%)	34	28	30	14	
pN0	346 (42.5%)	92	107	111	36	0.355#
pN1	369 (45.3%)	113	120	105	31	
pN2	69 (8.5%)	21	20	16	12	
pN3	31 (3.8%)	10	8	12	1	
G1	126 (13.7%)	30	40	46	10	0.001#
G2	460 (50.2%)	112	155	141	52	
G3	331 (36.1%)	125	94	85	27	
ER-negative	163 (18.7%)	78	45	34	6	0.001#
ER-Positive	709 (81.3%)	171	226	231	81	
PR-negative	314 (34.8%)	114	104	82	14	0.001#
PR-positive	588 (65.2%)	145	183	187	73	
HER2 0, 1+,2+,	776 (88.1%)	223	241	239	73	0.346#
HER2 3+	105 (11.9%)	33	37	25	10	

* Pearson Chi-Square, # Chi-Square for trends

Table 2 Primers used for real time PCR.

Gene	Primer sequence	Product size
Myoglobin	5´- GGCATCATGAGGCAGAGATT – 3´	111 bp
	5´- TCTGCAGAACCTGGATGATG – 3`	
GAPDH	5'-GAAGGTGAAGGTCGGAGTCA-3'	289 bp
	5'-TGGACTCCACGACGTACTCA-3'	
ß-Actin	5'- GGACGACATGGAGAAAATC-3'	185 bp
	5'- ATAGCACAGCCTGGATAGC-3'	
HsaMb NM_005368	5´- CCCAGTGAGCCCATACTTGC -3´	219 bp
	5´- GTCAGAGGACGAGATGAAGGC -3´	
HsaMb NM_203377	5´- GCATGTTGGCCTGGTCCTTTGC -3´	275 bp
	5´- GTCCTCATCAGGCTCTTTAAG -3´	
L28 NM_000991	5´-GCAATTCCTTCCGCTACAAC-3´	198 bp
	5´- TGTTCTTGCGGATCATGTGT -3´	

Table 3 Univariate Cox analysis of clinicopathological variables and markers of hypoxia including myoglobin expression

Parameter	Relative risk	95%-Confidence interval	p-value
Age (<= 60 *vs.* >)	1.881	1.495-2.367	0.001
Menopausal status	1.569	1.172-2.100	0.002
pT (1-4)	1.699	1.537-1.877	0.001
pN (0-3)	1.610	1.403-1.846	0.001
G (1-3)	1.616	1.360-1.920	0.001
ER (neg. *vs.* pos.)	0.549	0.425-0.709	0.001
PR (neg. vs. pos.)	0.527	0.408-0.680	0.001
HER2 (0-2+ *vs.* 3+)	1.839	1.372-2.465	0.001
CK5/6 (neg *vs.* pos)	1.669	1.166-2.390	0.005
Hif1α*	0.860	0.504-1.468	0.580
Hif2α*	0.426	0.239-0.760	0.004
GLUT1*	1.650	1.026-2.654	0.039
CAIX*	0.619	0.345-1.111	0.108
MB*	0.686	0.516-0.913	0.010

dichotomized by the median

Fig. 1 Detection of Mb mRNA in clinical breast cancer samples and cell lines

A

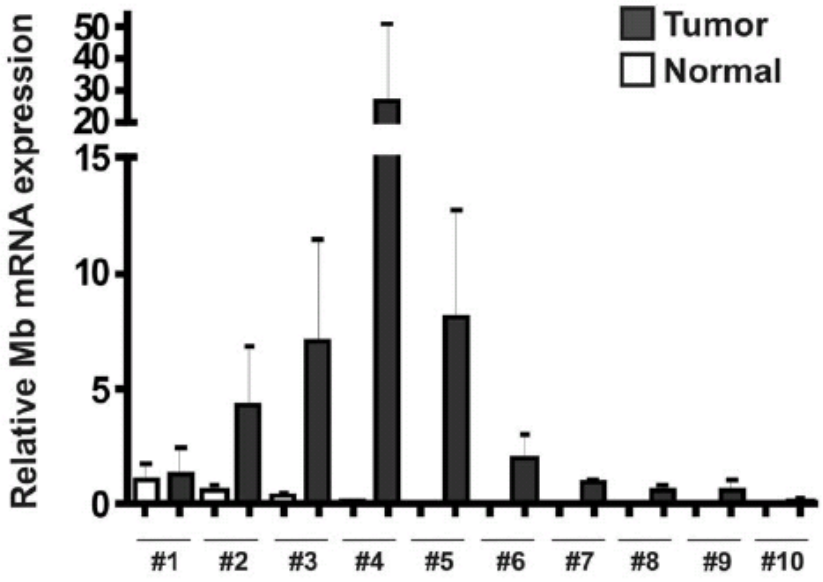

A) Myoglobin mRNA expression in ten randomly chosen samples of human breast cancer and corresponding normal breast tissues (#1 to #10) as measured by quantitative RT-PCR. Calculation of error bars according to Applied Biosystems user manual. Median myoglobin expression was up to 352-fold up-regulated in breast tumors (gray) compared to matching normal breast tissues (white).

B

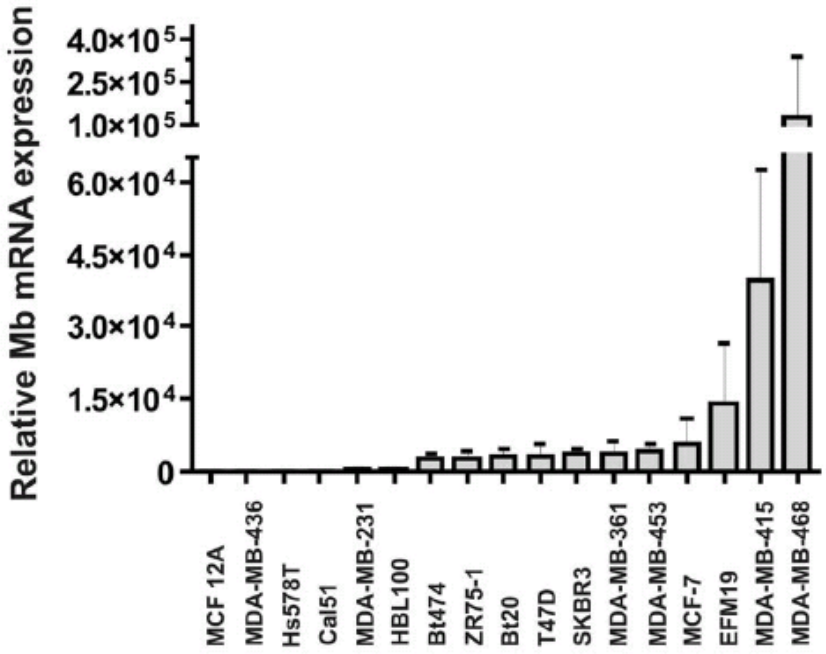

B) Myoglobin mRNA expression in benign MCF12A breast cells (used for normalisation) and various breast cancer cell lines.

Fig. 2 Myoglobin immunohistochemistry (clone Z001) in breast tissues

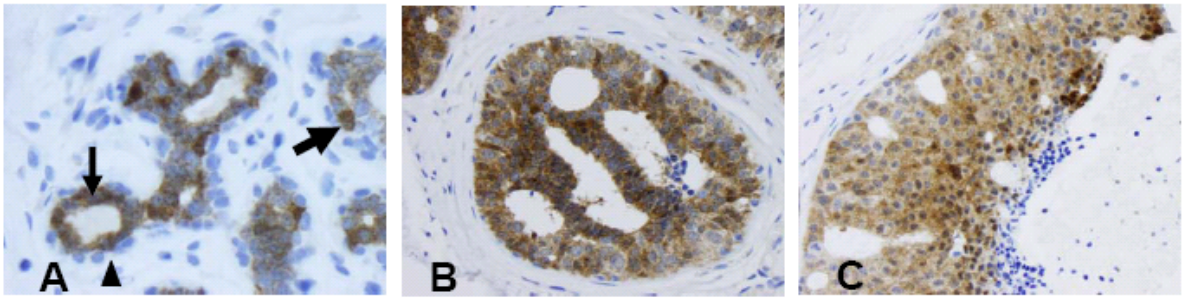

A) Normal lobular parenchyma of the breast, illustrating a mild Mb immunoreactivity in luminal epithelial cells (inner layer, thin arrow), whereas myoepithelial cells (outer cell layer, arrowhead) are negative. Note, that single luminal cells (bold arrow) are highlighted by a stronger Mb immunostaining (400x).
B) Strong myoglobin positivity in a ductal carcinoma *in situ* (DCIS), low grade, showing a slight accentuation of staining in the center (200x).
C) DCIS, high grade, again with a zonal pronunciation of Mb expression, which is most abundant in vital cells close to the central zone of necrosis and macrophages (200x).

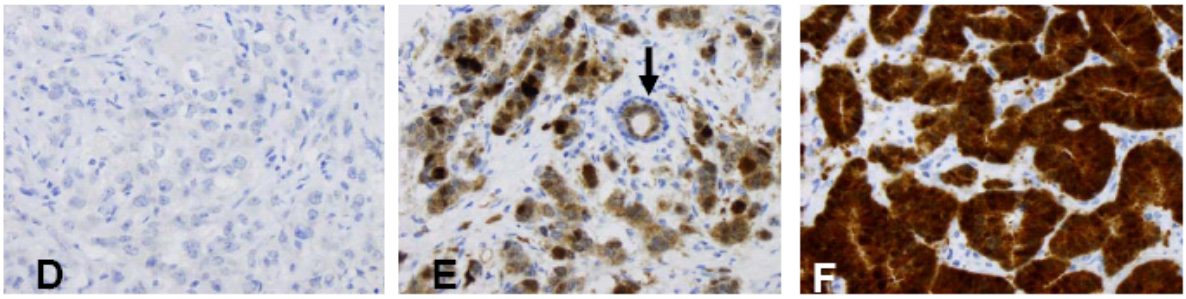

D-F) Examples of invasive ductal carcinoma of the breast (all 200x).
D) Poorly differentiated and Mb negative.
E) Moderately differentiated with a moderate to strong and patchy Mb expression. Note also the central normal duct (arrow) with the Mb-positive secretory cell layer and the Mb negative myoepithelial layer.
F) Strong Mb immunoreactivity in a well differentiated carcinoma.

Fig. 3 Kaplan Meier-Analysis of Overall Survival Times in a large cohort (n=917) of invasive breast cancer cases (n=917= stratified according to Mb

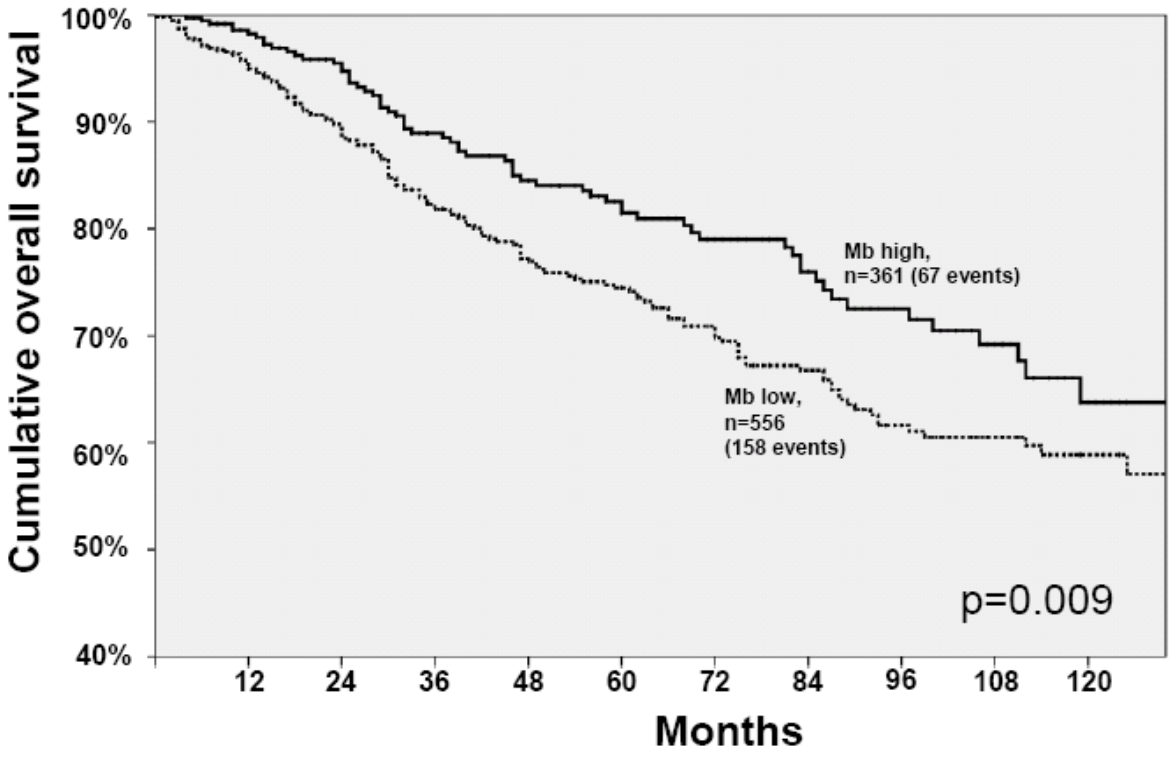

Tumors with high Mb expression demonstrate a significant prognostic value for the patient of an improved cumulative overall survival compared to cases with low Mb expression.

Fig. 4 Myoglobin mRNA and protein expression and HIF-dependence of induction in tumor-versus-healthy breast tissues and benign or malignant breast cancer cell lines

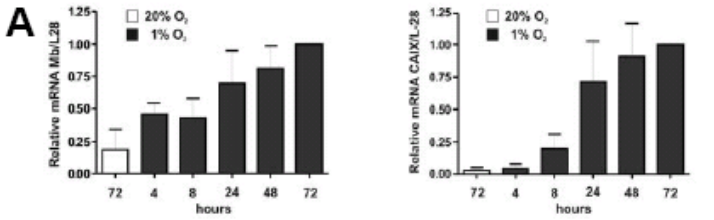

A) Myoglobin and CaIX mRNA induction in MCF7 cells, normalized to ribosomal L28 mRNA, are shown for indicated times during the course of hypoxia (1% O2). Data are given as mean ± SEM of relative expression ratios (Mb/L28 or CaIX/L28), obtained from three independent experiments. Highest hypoxic expression levels at 72h were arbitrarily defined as 1.

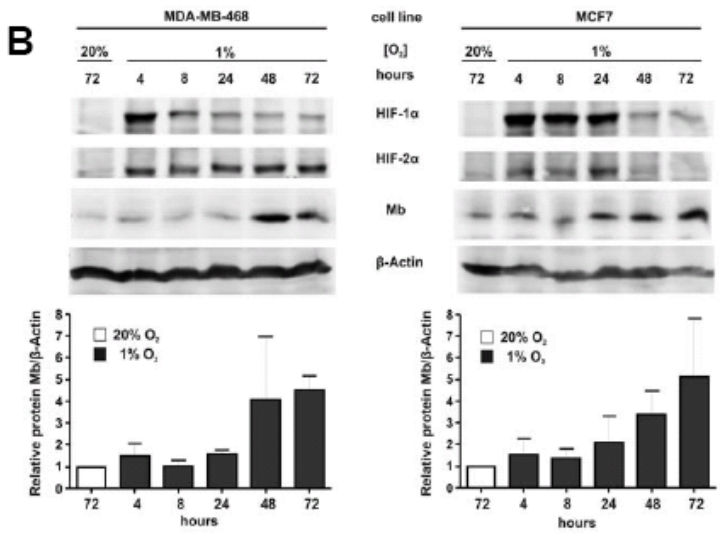

B) Protein expression in MDA-MD468 (left) and MCF7 (right) of (top-bottom) HIF-1α, HIF-2 α, Mb and β-Actin (loading control). Cells were subjected to 72h normoxia and 4, 8, 24, 48, 72h hypoxia (1% O2), respectively.

Lower graphics summarizes densitometry of three independent immunoblot determinations of Mb protein induction during 1% O2, relative to its normoxic abundance (=1), in MDA-MD468 (left) and MCF7 (right) cells.

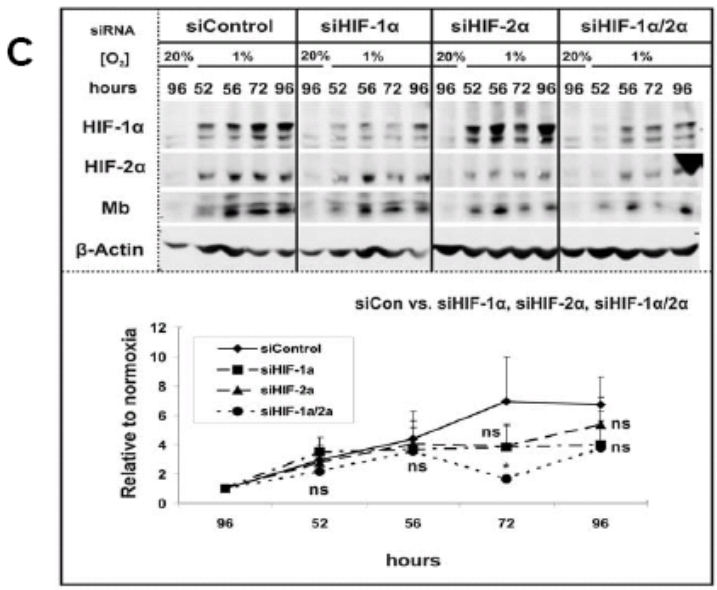

C) siRNA transfections of MDA-MB468 cells for, relative to scrambled siRNA control transfections (siControl, 200nM siRNA oligonucleotides), specific knockdown of HIF-1α (siHIF-1α, 200nM), HIF-2α (siHIF-2α, 200nM) and both transcription factors (siHIF-1α/2α, 100nM each).
Representative Western blot of three independent experiments shows (top-bottom): HIF-1α, HIF-2α, Mb and β-Actin (loading control) abundance for 96h normoxia versus 52, 56, 72 and 96h of hypoxia (1% O2).

Bottom graph: Mb protein induction during indicated hypoxia time course (96h normoxia data set to 1) as function of siControl (line continuous with diamond symbols), siHIF-1α (line hatched-squares), siHIF-2α (line hatched-triangles) and combined siHIF-1α/2α (line dotted-circles) transfections.
Relative to siControl (siCon) value at given time point, siHIF-1α, siHIF-2α and siHIF-1α/2α values of Mb content were non-significantly (ns) or significantly ($p<0.05$) different (3 independent experiments).

Fig. 5 DCIS as an *in vivo* model for tissue hypoxia – patterns of marker expression

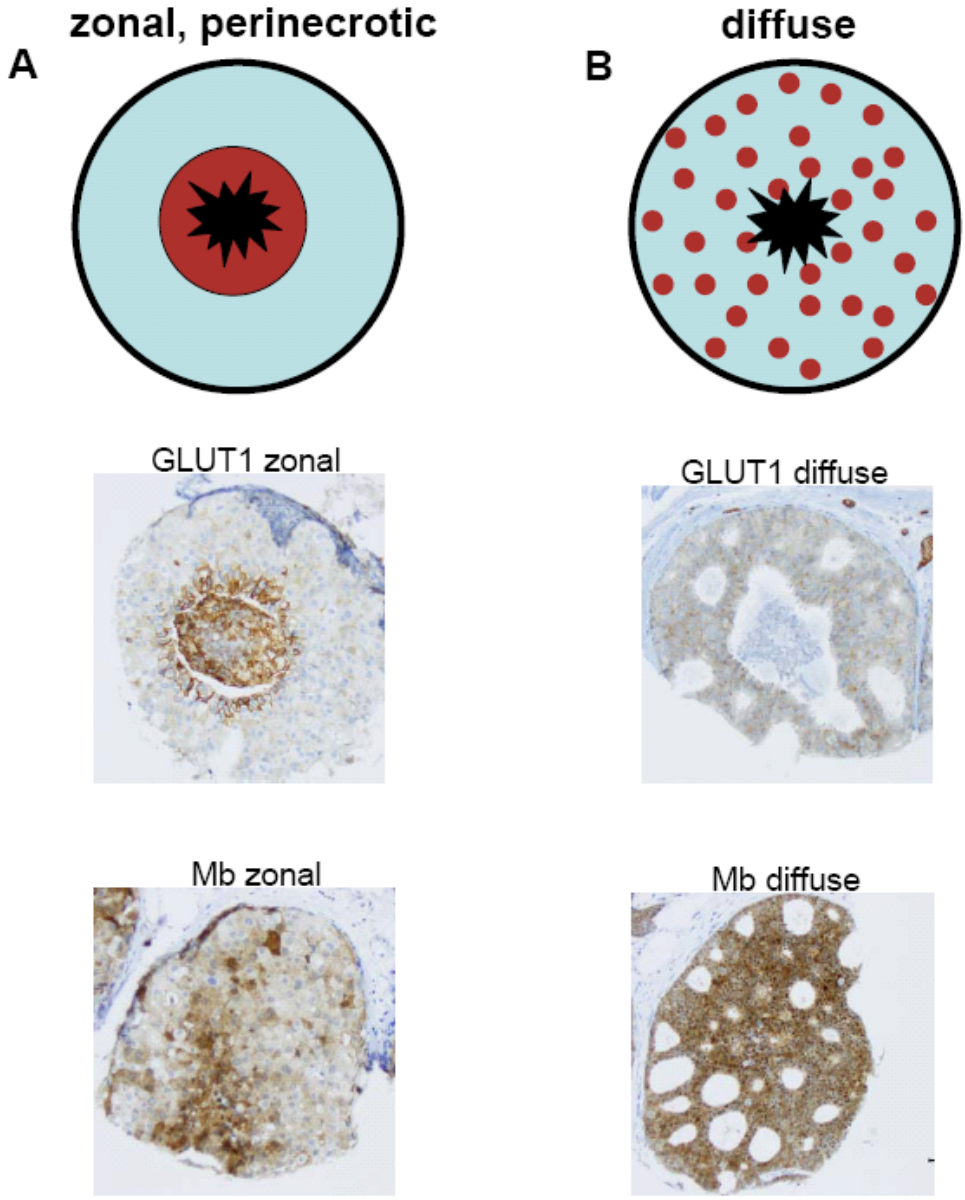

In the upper panel (A) a schematic image of *Ductal Carcinoma in Situ* (DCIS) is depicted, with a black outer rim, that constitutes the basal membrane, an inner zone (light blue) of atypical epithelial proliferates and a central necrosis (black star). Since DCIS are non-vascularized, oxygen is supplied to the intraductal cells only via diffusion from the exterior milieu. This leads to an increasing gradient of tissue hypoxia (red rim) towards the anoxic zone in the center. Expression of the established hypoxia marker GLUT1 follows this gradient in the majority of DCIS cases (**A**, middle). However, also diffuse GLUT1 staining can be seen (**B**, middle, schematic image in upper **B**). Mb expression can show a typical hypoxia related pattern (**A**, bottom), but mostly displays a diffuse staining (**B**, bottom).

Fig. 6 Standard and variant transcripts of the Mb gene

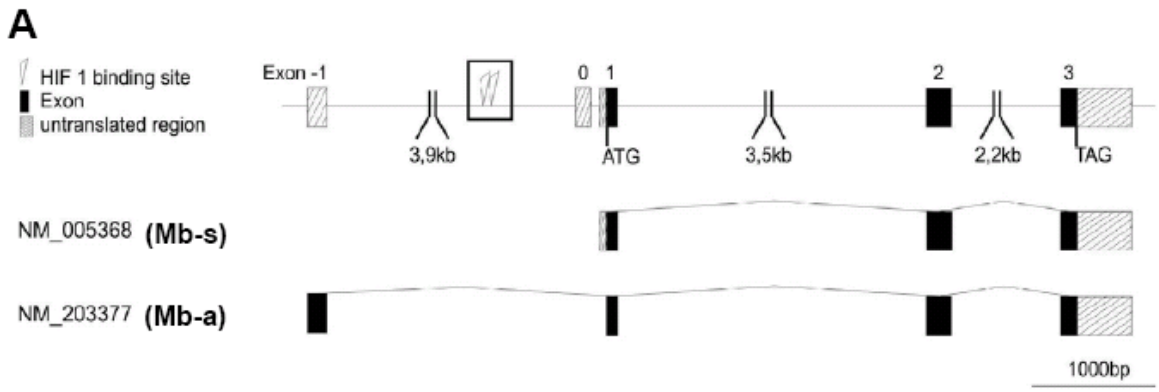

A) Schematic overview of human *MB* gene structure and the two transcript variants NM_005368 ("Mb-s") and NM_203377 ("Mb-a"). Coding parts of exons are shown by black boxes with translational start and stop codons indicated, untranslated exonic regions are hatched. A putative HRE conserved between human and mouse, containing two HIF-1 binding sites in inverted orientation (triangles), is highlighted (open frame).

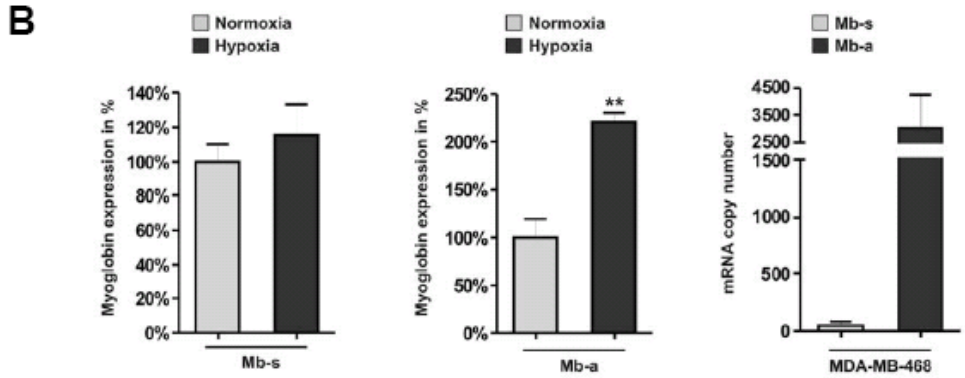

B) Differential expression of human *MB* transcript variants Mb-s (left) and Mb-a (middle) in MDA-MB-468 cells after hypoxia treatment. mRNA levels (bars) are shown relative to the gene expression at normoxia. Results indicate hypoxic upregulation only of transcript Mb-a (**p < 0.01). Chart on the right site shows difference in the relative abundance of transcripts Mb-s and Mb-a in MDA-MB-468 cells cultured under normoxic conditions.
Bars represent absolute mRNA copy numbers.

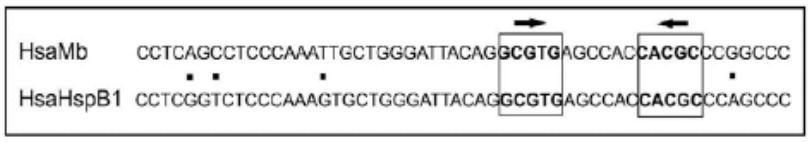

C) Sequence alignment of the 53 bp region (see frame in (A)) which is conserved in human (HsaMB) and mouse (MmuMb). The two potential HIF-1 binding sites, corresponding to the consensus 5'-RCGTG-3', are printed bold. Their inverted orientation is indicated by arrows. The putative myoglobin HRE almost perfectly matches a sequence upstream of the HSPB1 in human.

Fig. 7 High resolution respirometry of Mb control and knockdown MDA-MB468 cells

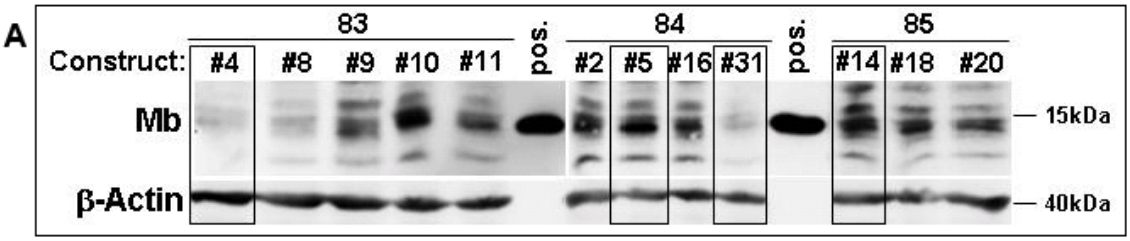

A) Mb and b-Actin Western blot of 12 MDA-MB-468 shRNA clones, derived from RNA constructs 83, 84, 85, together with positive (pos.) Mb control extractions from a human skeletal muscle biopsy. Mb control (84#5, 85#14) and knockdown (83#4, 84#31) clones used for respirometry are boxed.

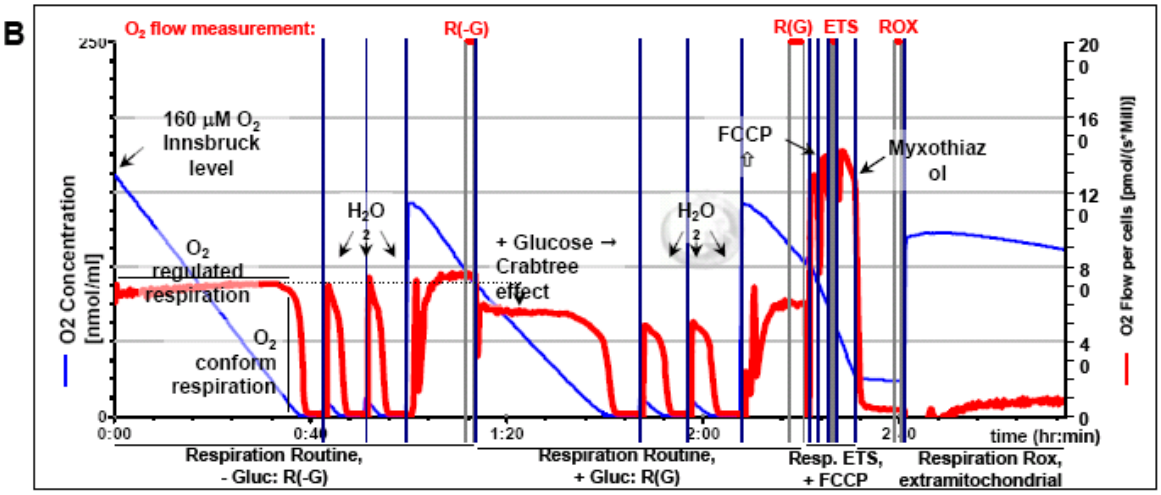

B) Original MDA-MB-468 cell respirometry recording at bottom of figure shows O2 flow per second and million cells (red trace) as a function of oxygen concentration (blue trace). For annotation, see text.

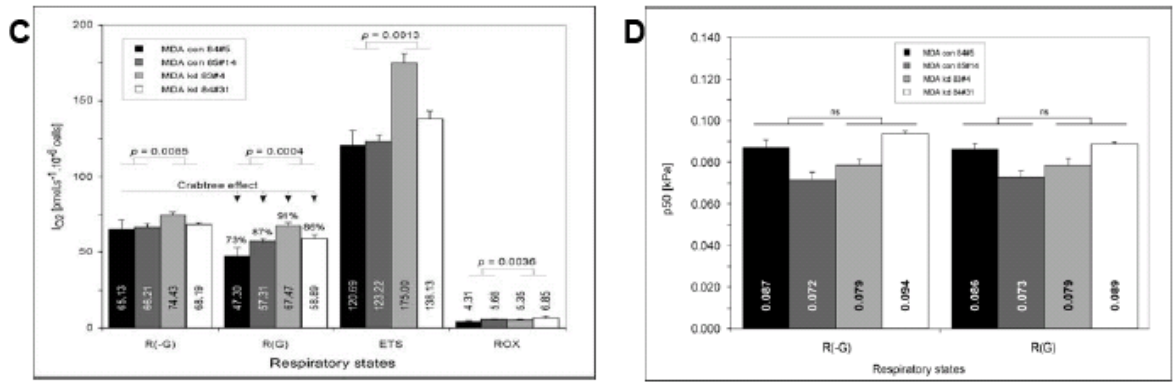

C) O2 consumption rates of Mb con (black + dark gray column) and Mb kd clones (light gray + white column) for i) routine respiration without glucose [= R(-G)]; ii) routine respiration with 25 mM glucose added [= R(G)]; iii) maximal respiration through uncoupling of oxidative phosphorylation by FCCP [= ETS]; iv) residual O2 consumption subsequent to poisoning of mitochondria with myxothiazol [=ROX]. R(-G) and R(G) states indicate oxygen consumption at higher versus lower fluxes, respectively (Crabtree effect). **D)** Cytochrome c oxidase (Cox) p50(O2) data of Mb con (black + dark gray column) and Mb kd clones (light gray + white column) for R(-G) and R(G) states. Mean p50 data highlighted within respective column. Results indicate the significant activation of respiration in Mb kd cells compared to con cells across all mitochondrial (R(-G), R(G), ETS) and residual (ROX) O2 fluxes. In contrast, mean Cox p50(O2) values were statistically indistinguishable (ns: non-significant) in con versus kd comparisons for either glucose-deficient or -proficient respiration.

Fig. 8 Functional Analysis of Mb-knock down cell lines

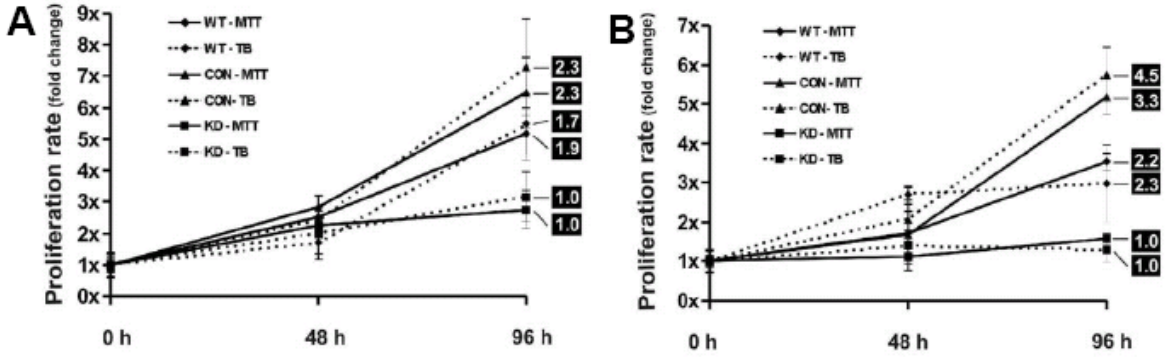

A/B) Proliferation Assay. MTT (continuous lines) and Trypan Blue exclusion assays (dotted lines) were utilized to compare proliferation rates over a 0-48-96h time course of wildtype (WT, diamond symbols) MDA-MB-468 cells and stable Mb-control (CON, triangles) and Mb-knockdown (KD, squares) clones thereof under normoxic (air, Fig. 8A) and hypoxic (1% O2, Fig. 8B) atmospheres. Data are given as mean fold-change (± SD), relative to 0 h time point = 1x (n=4 independent measurements/assays). 96 h proliferation ratios (wt/kd, con/kd; inverted numbers) are shown relative to the growth of KD cells (=1).

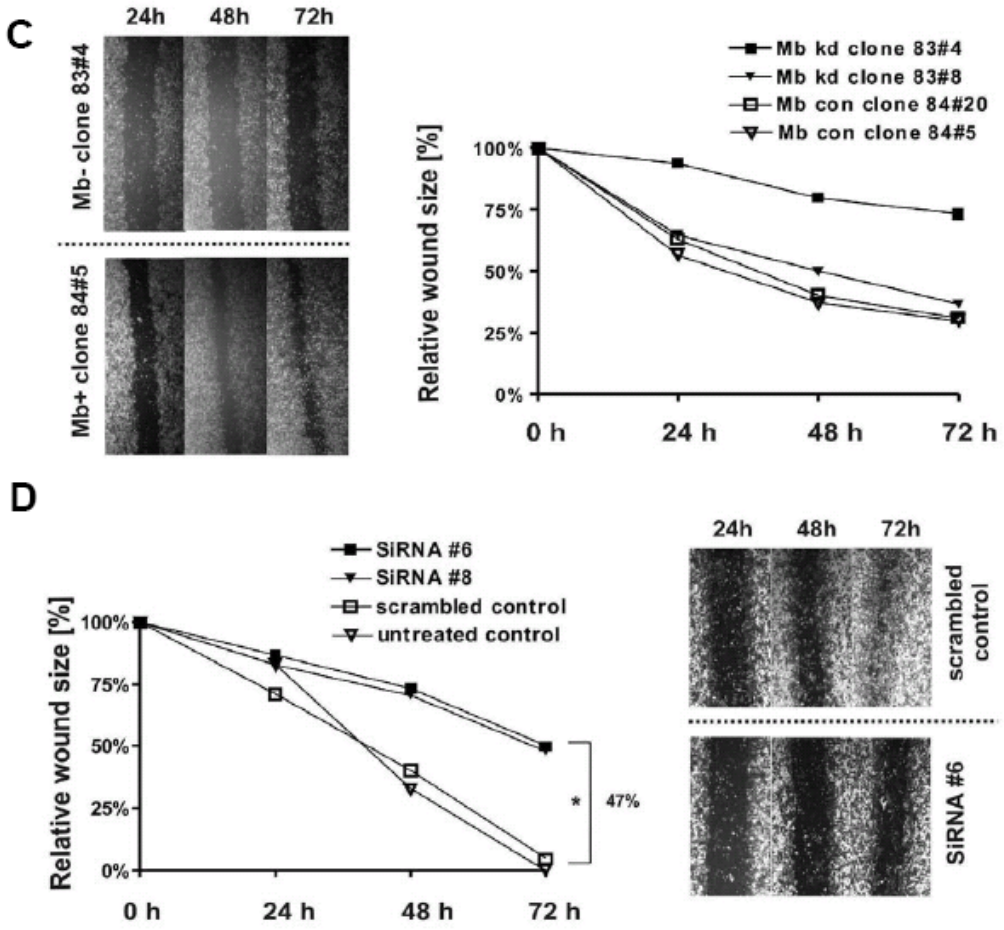

C/D) Scratch Assay. *Left*: Confluent MDA-MB-468 cells were scratched with a 100µl pipette tip and the size of the gap was evaluated 24, 48 and 72h later. *Right:* Diagram of wound closure over time indicating cell migration capacity. Control cells (Mb con clones) were able to reconstitute the gap notably faster than one stable Mb knockdown clone (Mb KD clone 83#4). Results are averages of triplicate experiments for each clone.

Fig. 9 Regulation of Mb by estrogen

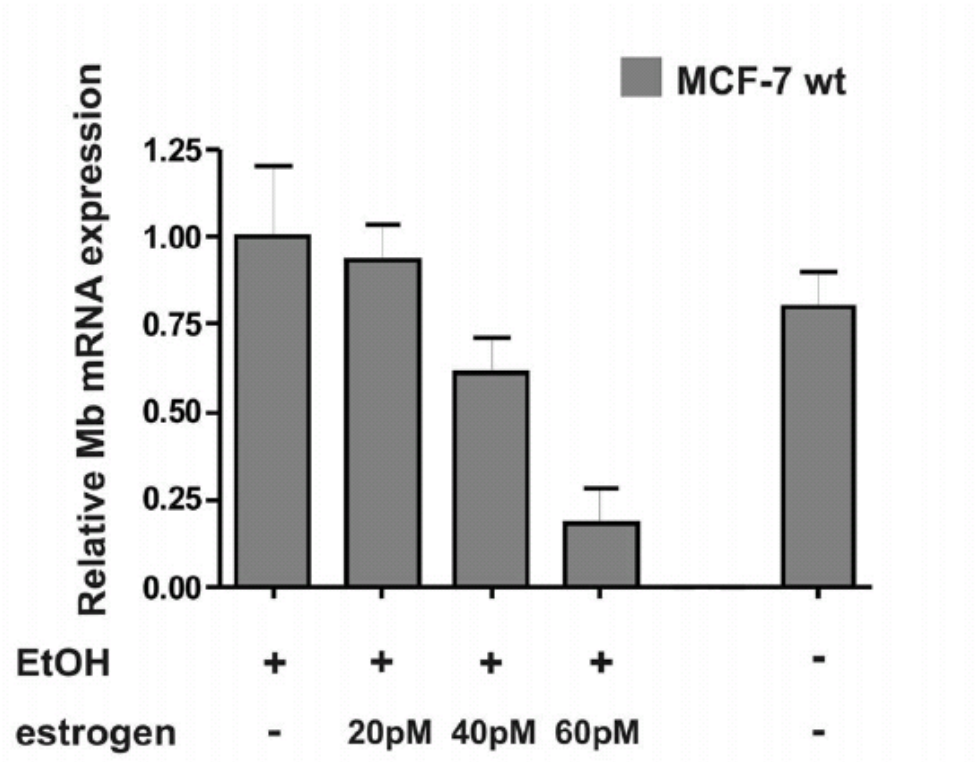

Myoglobin expression in MCF7 breast cancer cells is repressed by increasing concentrations of estrogen (ß-Estradiol, dissolved in ethanol) as measured by quantitative RT-PCR.

Fig. 11 Double immunofluorescence (Mb/FASN) staining of breast tissues

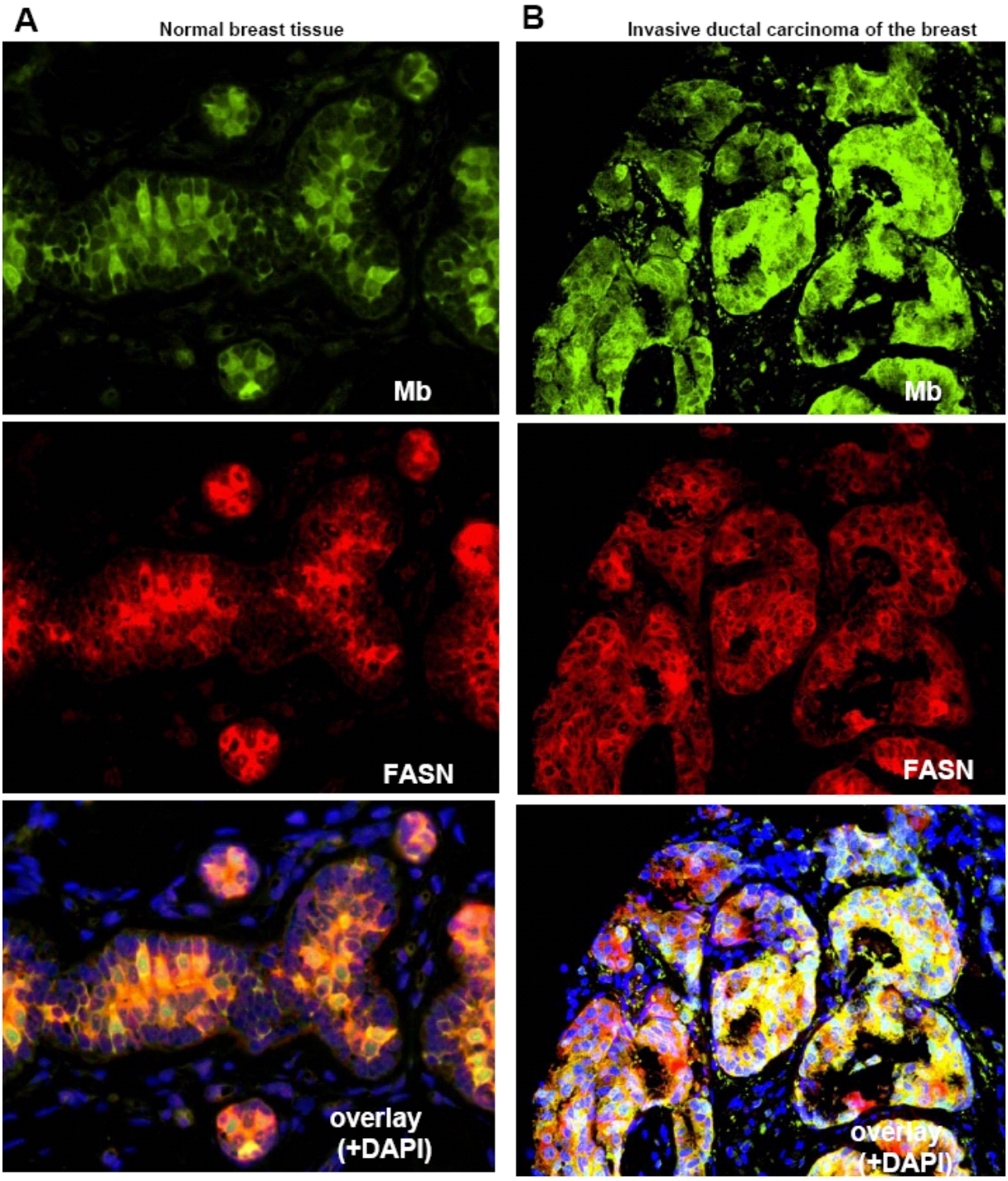

A) Normal breast tissue shows weak immunofluorescence for Mb in the secretory cell layer, along with some stronger staining cells are intermingled. The immunofluorescence for FASN (middle) shows strong cytoplasmic staining.
The overlay Figure (bottom) illustrates high degree of correspondence (yellow) between cells expressing Mb and FASN (all 400x).

B) In invasive carcinomas, a greater variation is seen and co-expression of Mb and FASN is only preserved in a subset of cells as the overlay illustrates. In general, the FASN expression exceeds Mb immunoreactivity (all 200x).

Fig. 12 Regulation of Mb by C75-induced FASN inhibition

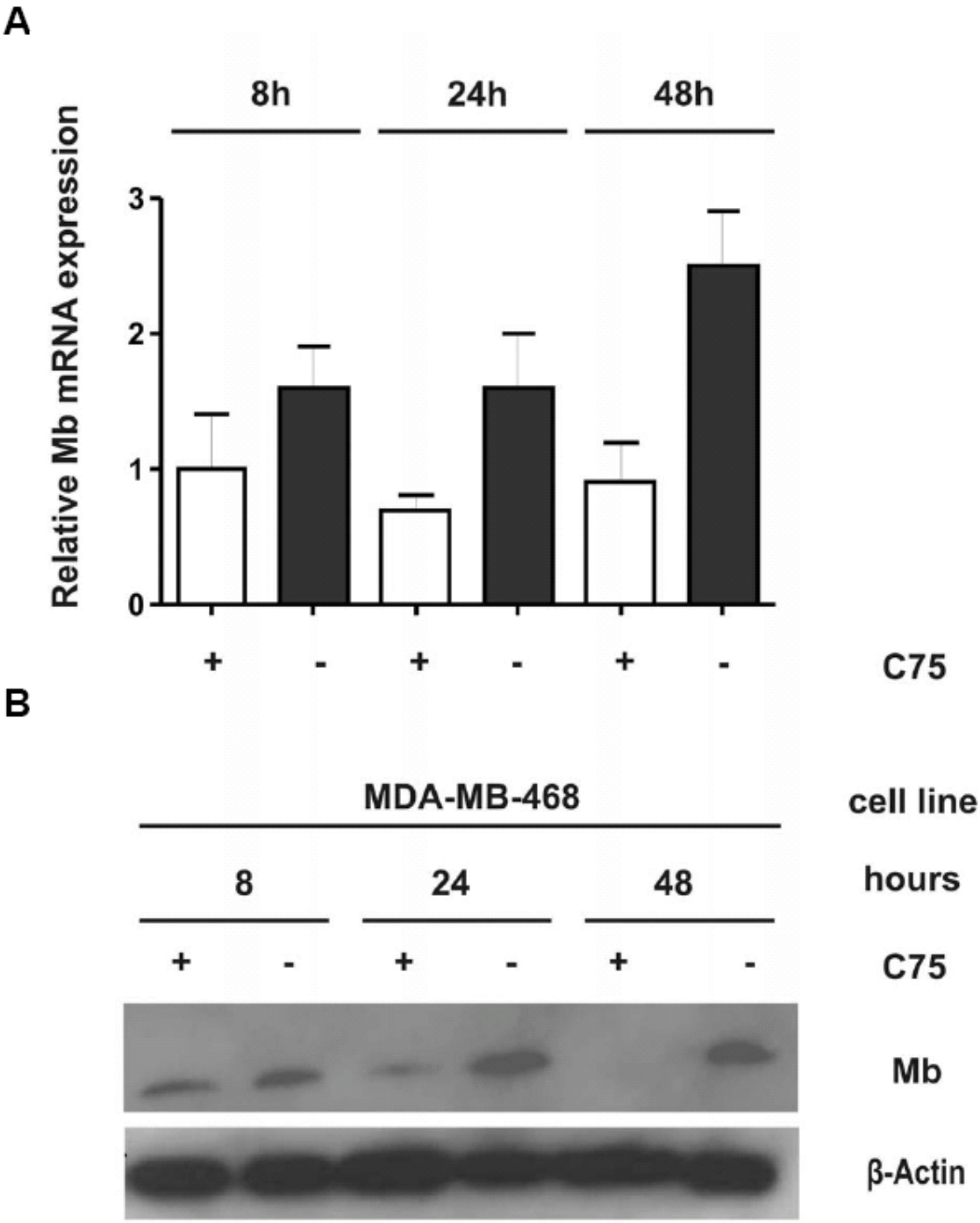

A) RT-PCR evidence for C75-mediated downregulation of Mb mRNA.
B) Western blot evidence for C75-mediated downregulation of Mb protein.

Supplemental Table

Table S1 Immunohistochemistry Protocols and Antibodies

Antibody	Clone	Dilution	Supplier	Platform	Protocol	Detection System
Myoglobin	Z001	1:300	ZYMED Laboratories Inc.	Bond	H2(60)	ADVANCE HRP
HIF-1α	mgc3	1:400	Abcam Limited	Bond	H2(60)	Refine 30'/30'
HIF-2α	polyclonal	1:150	Novus Biologicals, Inc	Bond	H1(60)	Refine enh. HRP
GLUT-1	polyclonal	1:1000	CHEMICON international, Inc.	Ventana	CC1m	UView HRP
CA IX	polyclonal	1:300	Abcam Limited	Bond	H2 30/95°	Refine 30'/30'
ER-α	SP1	prediluted	Ventana	Ventana	CC1m	UView mono HRP
Pimonidazole	polyclonal	1:300	CHEMICON international, Inc.	Ventana	CC1m	iVIEW-FITC HRP
CD34	QBEND/10	1:800	Serotec Ltd	Ventana	-	UView HRP
FASN	3F2-1F3	1:2000	Abnova (Taiwan) Corporation	Bond	H2(20)	Refine 30'/30'
HER2	10A7	1:50	Novocastra Laboratories Ltd	Ventana	CC1m	UView HRP
Cygb	polyclonal	1:50	T Hankeln	Bond	H2(60)	Refine enh. HRP
E-Cadherin	ECH-6	1:10	Cell Marque Lifescreen Ltd.	Ventana	CC1m	UView mono HRP

Fig. S1 Establishment of a sensitive and specific immunohistochemistry protocol to detect myoglobin

Blocking Mb immunoreactivity in human breast cancer after pre-incubation of clone Z001 with an excess (1:10 mol) of purified human Mb:

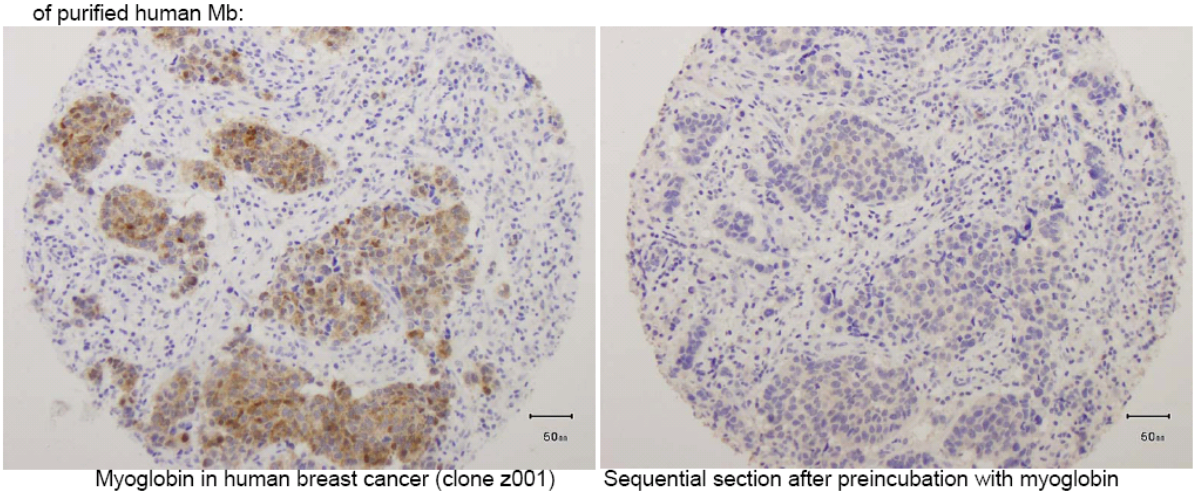

Myoglobin in human breast cancer (clone z001) Sequential section after preincubation with myoglobin

Three different myoglobin antibodies were compared for their suitability to detect myoglobin in formalin fixed paraffin embedded (FFPE) tissues, i.e. mouse monoclonal clone z001, Zymed, USA; mouse monoclonal clone MG1, Neomarkers, USA and rabbit polyclonal anti-human myoglobin, DAKO, Denmark.
All three antibodies yielded comparable results with clone z001 showing the cleanest immunoreactivity. To further enhance sensitivity a heat induced epitope retrieval (HIER) was included in the z001 detection protocol (Advance ™, DAKO, Denmark).
A blocking experiment with purified human myoglobin confirmed the specificity of the immunoreaction (shown above).

Fig. S2 Transmission electron microscopy of two Mb positive breast cancer specimens

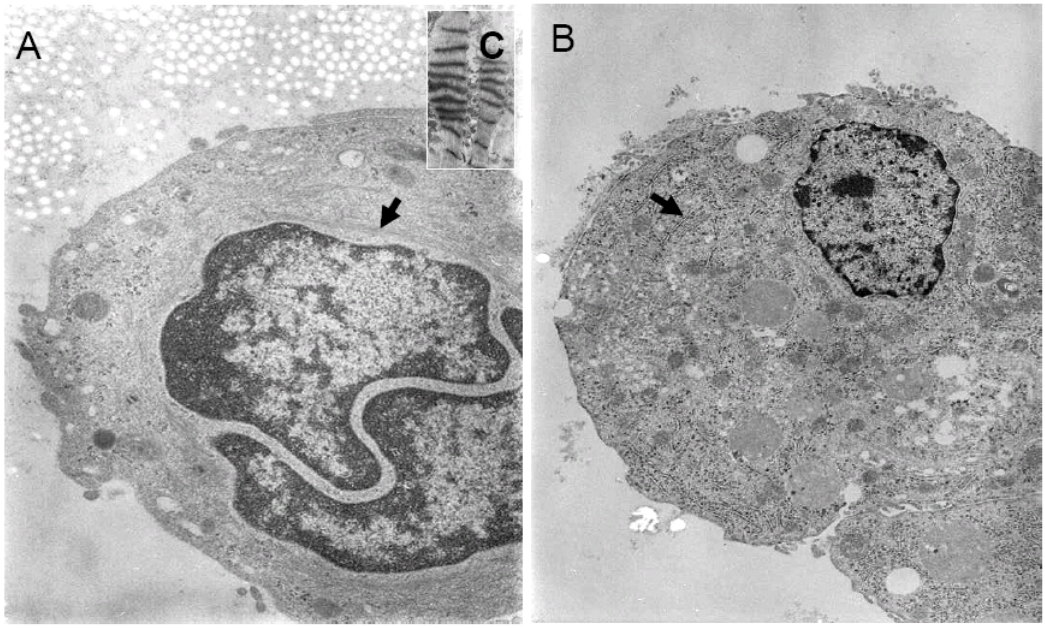

Since myoglobin has been described as a marker of rhabdomyoid differentiation, two breast tumors with strong myoglobin immunoreactivity were analysed by transmission electron microscopy.
A) Cell of an invasive lobular carcinoma with broad bundles of intermediate filaments (arrow).
B) Cell of an invasive ductal carcinoma exhibiting a plethora of endoplasmatic reticulum. No striated muscle elements as exemplified in **C)** (human heart muscle) were noted.

Fig. S3 Endogenous markers of hypoxia in a cases of invasive ductal breast cancer

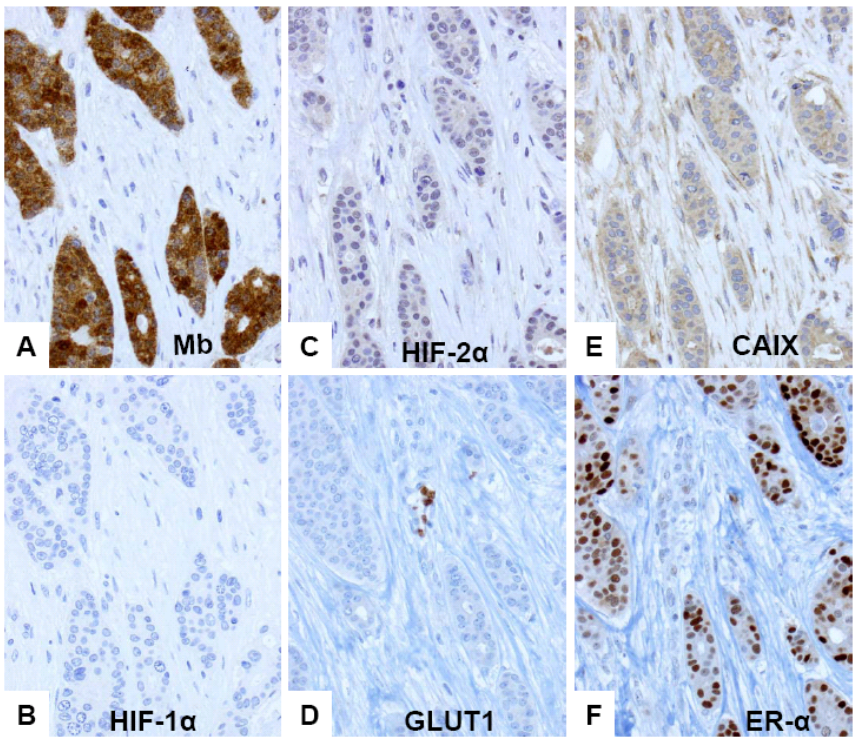

A) Abundant cytoplasmic Mb expression.

B) HIF-1α staining is completely negative.

C) HIF-2α staining is moderately positive (nuclear staining).

D) GLUT1 staining is negative (note the positive erythrocytes in the center as internal positive control).

E) CAIX is moderately positive, showing a cytoplasmic staining pattern.

F) Strong expression of the estrogen receptor-α in more than 90% of tumor cells.

Fig. S4 Comparison of Mb with the exogenous hypoxia marker Pimonidazole

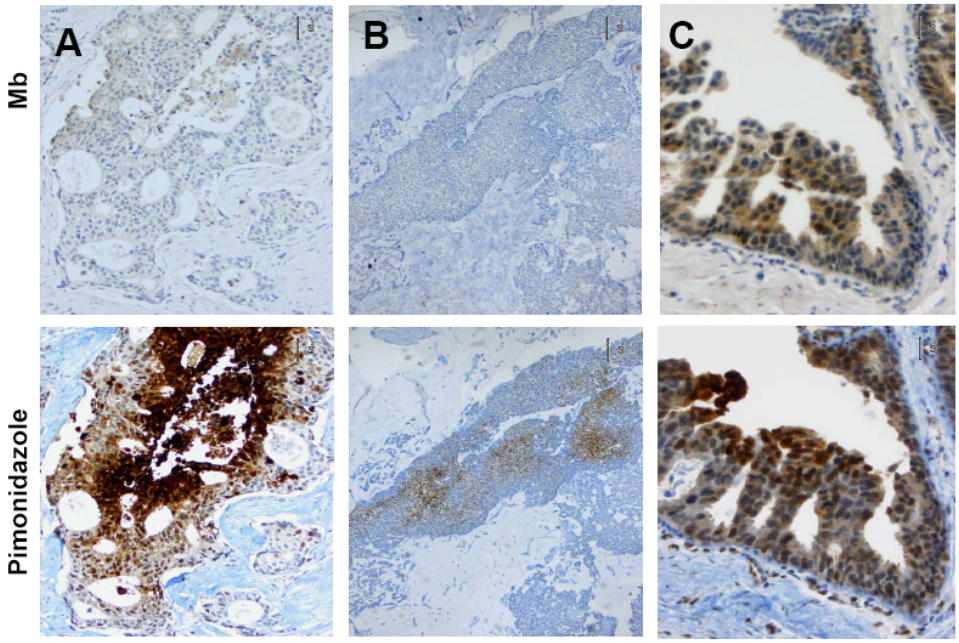

Two sequential sections of three breast cancer cases were immunostained for pimonidazole and Mb (A-C).
Although all three cases were strongly positive for pimonidazole, only one of these cases (C), a DCIS, showed a co-localization with Mb.
This indicates that hypoxia alone is not sufficient to upregulate Mb in breast cancer.

Fig. S5 *In silico* analysis of E2 and Mb in MCF7 cells

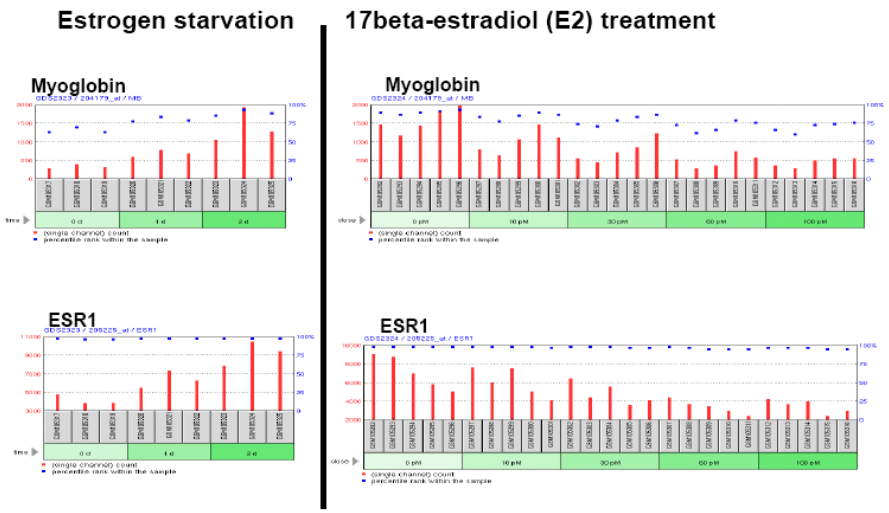

Retrieving the array datasets of Coser *et al.* (2003) via the web based data mining tool GEO Profiles, two experiments were analysed.

On the left, the influence of estrogen starvation on the expression of Mb and ESR1 (=ERa) is illustrated. Clearly, a concomitant up-regulation of both transcripts (single channel counts, red bars) during 48h is apparent. Conversely, the profiles of MCF-7 cells that were treated with 17β-estradiol (on the right) show a dose dependent down-regulation of Mb and ESR1.

Note, however, that the amplitude of either ESR1 regulation (red bars) is artificially enhanced due to the start of Y-axis labels at non-zero values (explains poor correspondence with blue percentile rank data in ESR1 profiles).

16 Curriculum Vitae

Personal Information

Last name:	Hu
First name:	Junmin
Date of birth:	11 October 1973
Nationality:	Chinese

University Education

Since May 2006	PhD studies at the Institute of Veterinary Physiology, University of Zurich
Oct 2000 - Dec 2005	Molecular Biology and Biochemistry studies with Master degree at ETH Zurich
1992 - 1997	Biology studies with Bachelor degree at Shanghai Teachers' University, China

Work experience

Nov 2008	Exchange student at Karolinska Institute, Stockholm, Sweden (Group of Prof. Dr. L. Poellinger)
Jan - Apr 2006	Internship at 4-Antibody AG in Basel
Jul 1997 - Jul 2000	Biology teacher: High School in Shanghai, China

Publications

Hu J, Stiehl DP, Setzer C, Hradecky P, Gassmann M and Gorr TA. Interaction of HIF and USF signaling pathways onto human genes flanked by hypoxia-response elements and E-box palindromes; Mol. Cell. Biol. (2009); submitted

Kristiansen G, **Hu J**, Stiehl DP, Rose M, Geisler C, Gerhardt J, Fritzsche FR, Lüke C, Ladhoff AM, Knüchel R, Dietel M, Moch H, Varg Z, Theurillat J-P, Raleigh J, Varia MA, Subarsky P, Scandurra FM, Gnaiger E, Hankeln T, Gleixner E, Gassmann M, Gorr TA and Dahl E. Endogenous myoglobin in human breast cancer: Novel insights into regulation, function and clinical relevance; J. Clin. Invest. (2009); submitted.

Posters and Presentations

1) *Oral presentation:* Convergence of HIF and USF signaling pathways onto bibox genes in human cancer cells.
   Euroxy meeting "Tumor hypoxia: from biology to therapy II" October 22nd-25th, 2008, Tuscany, Italy
2) *Oral presentation:* Characterization of HIF interfering transcription factor USFs in human cancer cells.
   Meeting "3rd Cancer Research Retreat" January 13th-16th, 2008, Fiesch, Wallis, Switzerland
3) *Poster presentation:* Characterization of HIF interfering transcription factor USFs in human cancer cells.
   International conference "Hypoxia, from integrative Biology to Human Disease" November 25th-30th, 2007, Monte Verita, Ascona, Switzerland
4) *Oral presentation:* Hydroxylation-independent control of HIF signaling in hypoxic cancer cells.
   Euroxy meeting "Tumor hypoxia from biology to therapy I", February 26th-28th, 2007, Maastricht, Netherlands

17 Acknowledgements

First of all, I would like to thank Prof. Max Gassmann for providing me the opportunity to work on my PhD project in his lab.

I am grateful to my supervisor Dr. Thomas Gorr for his invaluable support and critical input throughout these four years.

I thank Prof. Michael Hengartner and Dr. Gieri Camenisch as members of my PhD thesis committee for their invaluable comments during my PhD work.

Special thanks go to Dr. Benoit Viollet (Institut Cochin INSERM, Universite Paris Descartes Dpt Endocrinology, Metabolism and Cancer, Paris France) not only for his materials (USF antibodies and plasmids) but also for his unwavering willingness to act as expert sounding board throughout the project.

Further thanks go to Dr. Daniel Stiehl and Ms Kristin Wollenick (Institute of Physiology, University of Zurich) for kindly providing stable knockdown HIF-1α MCF7 cells and the short version of PHD2 luciferase reporter plasmid, respectively.

Many thanks to all members of Gassman's group: Dr. Lara Ogunshola, Dr. Anna Bogdanova, Prof. Johannes Vogel, Dr. Louise Ostergaard, Dr. Jorge Soliz, Dr. Beat Schuler, Dr. Abraham Al Ahmad, Dr. Mihov Deyan, Dr. Arezoo Daryadel, Mikola Bogdanov and all my PhD fellows Milena Segato Komniski, Sergey Yakushev, Elena Gammella, Robert Jacobs, Thomas Haider, Asya Makhro, Carole Bürgi-Taboada, Zhenghui Wang for the scientific support and friendly atmosphere in the group.

I would like to thank my husband Thomas for his strong support in good and hard times during the last four years.